NEUROIMAGING OF COGNITIVE AND NEUROPSYCHIATRIC SYMPTOMS IN MOVEMENT DISORDERS

EDITED BY: Frederic Sampedro, Estela Camara and Jaime Kulisevsky
PUBLISHED IN: Frontiers in Neurology

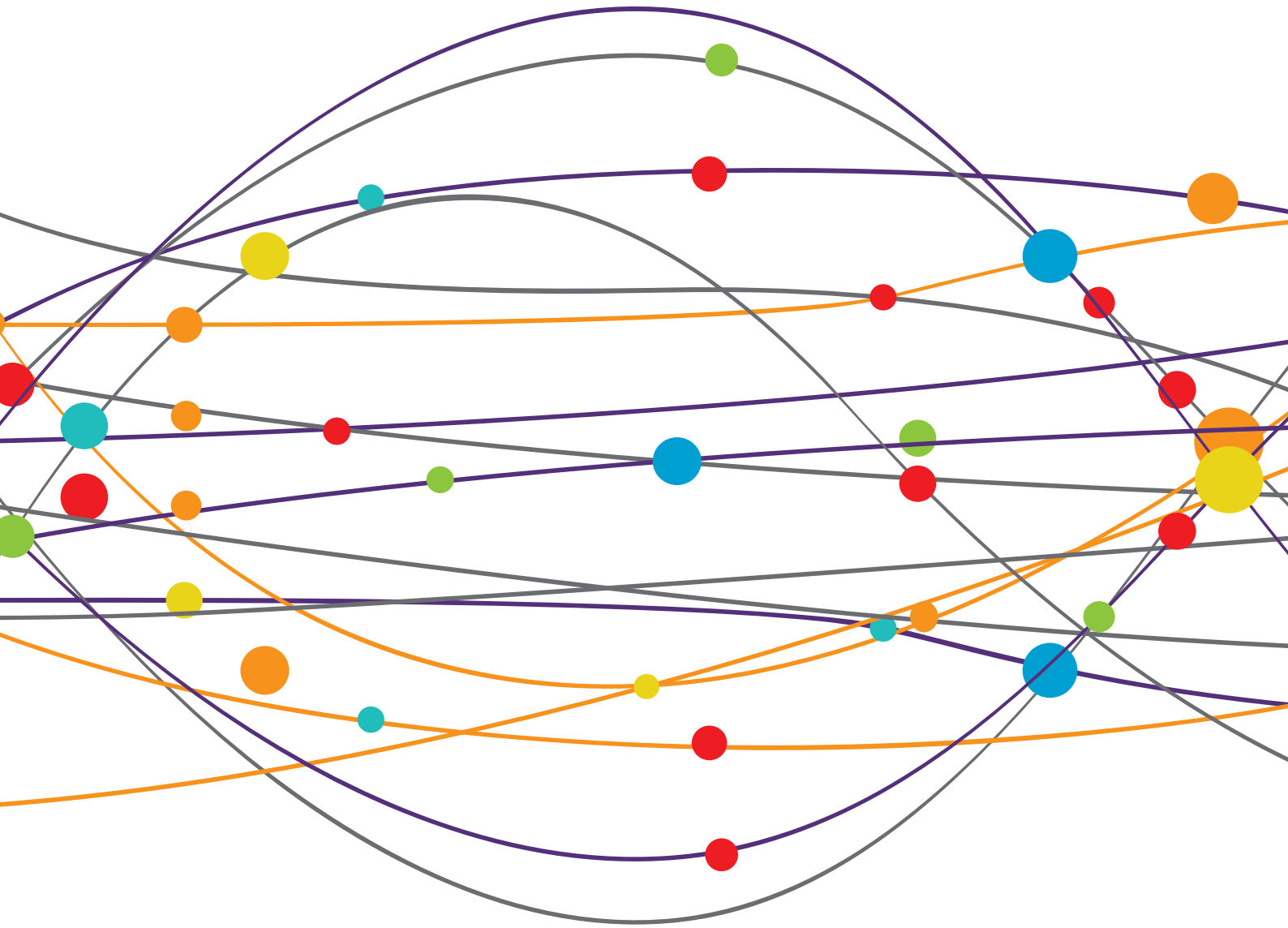

frontiers Research Topics

frontiers

ISSN 1664-8714
ISBN 978-2-88974-548-7
DOI 10.3389/978-2-88974-548-7

About Frontiers

Frontiers is more than just an open-access publisher of scholarly articles: it is a pioneering approach to the world of academia, radically improving the way scholarly research is managed. The grand vision of Frontiers is a world where all people have an equal opportunity to seek, share and generate knowledge. Frontiers provides immediate and permanent online open access to all its publications, but this alone is not enough to realize our grand goals.

Frontiers Journal Series

The Frontiers Journal Series is a multi-tier and interdisciplinary set of open-access, online journals, promising a paradigm shift from the current review, selection and dissemination processes in academic publishing. All Frontiers journals are driven by researchers for researchers; therefore, they constitute a service to the scholarly community. At the same time, the Frontiers Journal Series operates on a revolutionary invention, the tiered publishing system, initially addressing specific communities of scholars, and gradually climbing up to broader public understanding, thus serving the interests of the lay society, too.

Dedication to Quality

Each Frontiers article is a landmark of the highest quality, thanks to genuinely collaborative interactions between authors and review editors, who include some of the world's best academicians. Research must be certified by peers before entering a stream of knowledge that may eventually reach the public - and shape society; therefore, Frontiers only applies the most rigorous and unbiased reviews.
Frontiers revolutionizes research publishing by freely delivering the most outstanding research, evaluated with no bias from both the academic and social point of view. By applying the most advanced information technologies, Frontiers is catapulting scholarly publishing into a new generation.

What are Frontiers Research Topics?

Frontiers Research Topics are very popular trademarks of the Frontiers Journals Series: they are collections of at least ten articles, all centered on a particular subject. With their unique mix of varied contributions from Original Research to Review Articles, Frontiers Research Topics unify the most influential researchers, the latest key findings and historical advances in a hot research area! Find out more on how to host your own Frontiers Research Topic or contribute to one as an author by contacting the Frontiers Editorial Office: frontiersin.org/about/contact

NEUROIMAGING OF COGNITIVE AND NEUROPSYCHIATRIC SYMPTOMS IN MOVEMENT DISORDERS

Topic Editors:
Frederic Sampedro, Sant Pau Institute for Biomedical Research, Spain
Estela Camara, Institut d'Investigacio Biomedica de Bellvitge (IDIBELL), Spain
Jaime Kulisevsky, Hospital de la Santa Creu i Sant Pau, Spain

Citation: Sampedro, F., Camara, E., Kulisevsky, J., eds. (2022). Neuroimaging of Cognitive and Neuropsychiatric Symptoms in Movement Disorders. Lausanne: Frontiers Media SA. doi: 10.3389/978-2-88974-548-7

Table of Contents

frontiers in Neurology

EDITORIAL
published: 31 January 2022
doi: 10.3389/fneur.2022.843440

Editorial: Neuroimaging of Cognitive and Neuropsychiatric Symptoms in Movement Disorders

Frederic Sampedro[1,2,3]*, *Estela Camara*[4,5] *and Jaime Kulisevsky*[1,2,3]

[1] Movement Disorders Unit, Neurology Department, Hospital de la Santa Creu i Sant Pau, Barcelona, Spain, [2] Biomedical Research Institute (IIB-Sant Pau), Barcelona, Spain, [3] Centro de Investigación en Red-Enfermedades Neurodegenerativas (CIBERNED), Barcelona, Spain, [4] Cognition and Brain Plasticity Unit, Institut d'Investigació Biomèdica de Bellvitge (IDIBELL), Barcelona, Spain, [5] Cognition, Development and Educational Psychology, University of Barcelona, Barcelona, Spain

Keywords: neuroimaging, movement disorders, cognitive symptoms, neuropsychiatric symptoms, genetic modifiers

Editorial on the Research Topic

Neuroimaging of Cognitive and Neuropsychiatric Symptoms in Movement Disorders

Movement disorders are relatively frequent neurological disorders that can have a profound impact on the patients' quality of life. Examples of movement disorders are Parkinson's disease (PD) and Huntington's disease (HD). Even though they are best known for its cardinal motor symptoms, most of the patients show concomitant cognitive or neuropsychiatric disturbances, which can be as debilitating as motor symptoms and have, unfortunately very limited therapeutic options.

The pathological hallmarks of PD and HD are, respectively, subcortical dopaminergic depletion due to substantia nigra degeneration and caudate atrophy due to aggregation of mutant huntingtin. These are responsible for the characteristic motor symptoms observed in the patients. Conversely, the origin of non-motor symptoms in PD or HD is not fully understood. For many years, it was assumed that they were a mere consequence of the inherent subcortical damage occurring in these disorders.

However, it is now clear that early cortical—and not only subcortical—damage occurs in these disorders, playing in turn a key role in the development and severity of cognitive and behavioral disturbances. Nonetheless, the neuropathological processes leading to cortical degeneration in movement disorders remain elusive, and are likely to differ from those leading to subcortical damage. Therefore, a precise understanding of these processes and its association with non-motor symptoms is urgently needed to design optimal therapeutic strategies.

In this context, neuroimaging techniques have played a key role in unraveling not only the presence of cortical damage and its association with non-motor symptoms, but also contributing to our understanding of its pathological origin. This Research Topic succeeded at providing high quality contributions in this research field. Here, a brief introduction to the 11 accepted papers is given. We refer the readers to the papers in this topic and the references therein for more details.

Martín-Bastida et al. provided an excellent review of the imaging alterations underlying cognitive impairment and impulse control disorders in PD, highlighting its potential use as diagnostic, prognostic or monitoring indicators.

In PD, beta-amyloid aggregation has been suggested to be one of the possible pathological entities contributing to cortical damage and cognitive decline. However, whether amyloid pathology is an inherent process in PD or rather reflects concurrent co-morbid Alzheimer's disease (AD) pathology, has not been fully elucidated. In fact, contradictory results have been published in this context. The fact that Melzer et al. were unable to find an association between amyloid PET and cognitive performance in a PD sample suggest that, at least, that amyloid pathology would not

OPEN ACCESS

Edited and reviewed by:
Alberto Albanese, Catholic University of the Sacred Heart, Italy

***Correspondence:**
Frederic Sampedro
fredsampedro@gmail.com

Specialty section:
This article was submitted to Movement Disorders, a section of the journal Frontiers in Neurology

Received: *25 December 2021*
Accepted: *10 January 2022*
Published: *31 January 2022*

Citation:
Sampedro F, Camara E and Kulisevsky J (2022) Editorial: Neuroimaging of Cognitive and Neuropsychiatric Symptoms in Movement Disorders. Front. Neurol. 13:843440. doi: 10.3389/fneur.2022.843440

be the primary driver of cognitive impairment and dementia in most PD patients. This hypothesis was further reinforced by the findings of Antonini et al.

Genetic risk factors such as the MAPT H1H1 haplotype have also been related to cognitive impairment in PD, and Sampedro et al. showed that this genetic variant is also associated with cortical gray matter loss. It should not be overlooked that age is a constant and strong risk factor cognitive disturbances in PD. The specific mechanisms involved in this association were assessed by Nagano-Saito et al. using resting-state fMRI data, unraveling the a pattern of hub alterations and compensatory mechanisms associated with age in PD. Resting-state data also revealed an important contribution of cerebelo-cortical connectivity to cognitive dysfunction in PD (Palmer et al.). Motor symptom lateralization in PD also appeared to modulate cortico-striatal connectivity (Su et al.), which is known to influence the development and severity of cognitive and behavioral symptoms in PD.

Neuropsychiatric disturbances such as depression, apathy, hallucinations, impulse control disorders or irritability are also very common in movement disorders. They are especially frequent and severe in Lewy body dementia (DLB), which presents with the prototypical motor symptoms of PD but accompanied by severe and concomitant neuropsychiatric and cognitive dysfunction. Jaramillo-Jimenez et al. highlighted the important role of the amygdala in the development and trajectories of neuropsychiatric symptoms in DLB patients.

Subcortical deep brain stimulation in the subthalamic nucleus (STN) has been established as a highly-effective therapy for advanced Parkinson's disease. However, as Liu et al. showed, even though STN stimulation has shown clear benefits in terms of improving motor symptoms, they have also a detrimental impact on non-motor symptoms with significant impact in quality of life.

HD is a genetic neurological disorder in which patients experience progressive motor, cognitive, and neuropsychiatric alterations, resulting in a devastating loss of functional independence around the fourth decade of life. Even though the genetic alteration underlying HD is well-known, there is significant heterogeneity in the symptomatic trajectories across patients. For instance, it is currently unknown why some HD patients present with early and severe cognitive and neuropsychiatric disturbances, even in the absence of pronounced motor symptoms. Whereas, Zhang et al. reinforced the importance and heterogeneity of cognitive impairment in HD, Liu et al. showed that this heterogeneity is not explained by the inherent genetic burden, suggesting the involvement of additional pathological pathways whose characterization may reveal new therapeutic targets.

To conclude, through the use of neuroimaging, this Research Topic has contributed to advancing our understanding of cognitive and neuropsychiatric disturbances in Parkinson's disease and to disentangle cognitive heterogeneity in Huntington's disease. We thank the authors, the reviewers and the journal for their efforts leading to this collection.

AUTHOR CONTRIBUTIONS

All authors listed have made a substantial, direct, and intellectual contribution to the work and approved it for publication.

Conflict of Interest: The authors declare that the research was conducted in the absence of any commercial or financial relationships that could be construed as a potential conflict of interest.

Publisher's Note: All claims expressed in this article are solely those of the authors and do not necessarily represent those of their affiliated organizations, or those of the publisher, the editors and the reviewers. Any product that may be evaluated in this article, or claim that may be made by its manufacturer, is not guaranteed or endorsed by the publisher.

frontiers in Neurology

ORIGINAL RESEARCH
published: 29 March 2018
doi: 10.3389/fneur.2018.00190

Genetics Modulate Gray Matter Variation Beyond Disease Burden in Prodromal Huntington's Disease

Jingyu Liu[1,2†], Jennifer Ciarochi[3,4†], Vince D. Calhoun[1,2], Jane S. Paulsen[5,6,7], H. Jeremy Bockholt[5,6,7], Hans J. Johnson[5,8], Jeffrey D. Long[5,9], Dongdong Lin[1], Flor A. Espinoza[1], Maria B. Misiura[3,4], Arvind Caprihan[1], Jessica A. Turner[1,3,4] and PREDICT-HD Investigators and Coordinators of the Huntington Study Group*

[1]*The Mind Research Network & Lovelace Biomedical and Environmental Research Institute (LBERI), Albuquerque, NM, United States,* [2]*Department of Electrical and Computer Engineering, University of New Mexico, Albuquerque, NM, United States,* [3]*Department of Psychology, Georgia State University, Atlanta, GA, United States,* [4]*Department of Neuroscience, Georgia State University, Atlanta, GA, United States,* [5]*Department of Psychiatry, University of Iowa, Iowa City, IA, United States,* [6]*Department of Neurology, University of Iowa, Iowa City, IA, United States,* [7]*Department of Psychological and Brain Sciences, University of Iowa, Iowa City, IA, United States,* [8]*Department of Electrical and Computer Engineering, University of Iowa, Iowa City, IA, United States,* [9]*Department of Biostatistics, University of Iowa, Iowa City, IA, United States*

OPEN ACCESS

Edited by:
Huifang Shang, Sichuan University, China

Reviewed by:
Zhong Pei, Sun Yat-Sen University, China
Christian Dresel, Universitätsmedizin der Johannes Gutenberg-Universität Mainz, Germany

***Correspondence:**
Jingyu Liu
jliu@mrn.org

[†]*These authors have contributed equally to this work.*

Specialty section:
This article was submitted to Movement Disorders, a section of the journal Frontiers in Neurology

Received: *06 January 2018*
Accepted: *12 March 2018*
Published: *29 March 2018*

Citation:
Liu J, Ciarochi J, Calhoun VD, Paulsen JS, Bockholt HJ, Johnson HJ, Long JD, Lin D, Espinoza FA, Misiura MB, Caprihan A, Turner JA and PREDICT-HD Investigators and Coordinators of the Huntington Study Group (2018) Genetics Modulate Gray Matter Variation Beyond Disease Burden in Prodromal Huntington's Disease. Front. Neurol. 9:190. doi: 10.3389/fneur.2018.00190

Huntington's disease (HD) is a neurodegenerative disorder caused by an expansion mutation of the cytosine–adenine–guanine (CAG) trinucleotide in the *HTT* gene. Decline in cognitive and motor functioning during the prodromal phase has been reported, and understanding genetic influences on prodromal disease progression beyond CAG will benefit intervention therapies. From a prodromal HD cohort ($N = 715$), we extracted gray matter (GM) components through independent component analysis and tested them for associations with cognitive and motor functioning that cannot be accounted for by CAG-induced disease burden (cumulative effects of CAG expansion and age). Furthermore, we examined genetic associations (at the genomic, HD pathway, and candidate region levels) with the GM components that were related to functional decline. After accounting for disease burden, GM in a component containing cuneus, lingual, and middle occipital regions was positively associated with attention and working memory performance, and the effect size was about a tenth of that of disease burden. Prodromal participants with at least one dystonia sign also had significantly lower GM volume in a bilateral inferior parietal component than participants without dystonia, after controlling for the disease burden. Two single-nucleotide polymorphisms (SNPs: rs71358386 in *NCOR1* and rs71358386 in *ADORA2B)* in the HD pathway were significantly associated with GM volume in the cuneus component, with minor alleles being linked to reduced GM volume. Additionally, homozygous minor allele carriers of SNPs in a candidate region of ch15q13.3 had significantly higher GM volume in the inferior parietal component, and one minor allele copy was associated with a total motor score decrease of 0.14 U. Our findings depict an early genetical GM reduction in prodromal HD that occurs irrespective of disease burden and affects regions important for cognitive and motor functioning.

Keywords: genetic modifier, gray matter, Huntington's disease, cognition, prodromal disease progression

INTRODUCTION

Huntington's disease (HD) is a neurodegenerative disorder characterized by deterioration of motor, cognitive, and psychiatric functioning. Abnormal cytosine–adenine–guanine (CAG) repeat expansion (>35 repeats) in the huntingtin gene (*HTT*) causes this progressive disorder, and age of clinical diagnosis is inversely correlated with CAG expansion length (i.e., greater expansion is associated with more rapid progression) (1). Although CAG repeat number is the primary determinant of the rate of pathogenesis (explaining about 56% of the variation in onset age), overall onset time is highly variable, especially in patients with lower CAG repeat numbers (1–3). Other genetic and environmental factors likely account for additional onset variation (4–6), as illustrated by an HD pedigree study showing that approximately 40% of the variation in onset age (after accounting for CAG effects) was due to non-*HTT* genetic factors (7).

Up to a decade prior to clinical diagnosis, individuals with the abnormal CAG expansion already differ from healthy controls in brain structure as well as cognitive and motor functioning (3, 8, 9). Investigating early prodromal changes may be necessary for identifying optimal targets for disease prevention or delay (10). This is a major goal of PREDICT-HD, a multisite prodromal HD study that has characterized many features of the HD prodrome (10–12), including widespread gray matter (GM) concentration reductions [even at the earliest prodromal stage (13)], robust annual changes in putamen, caudate, and nucleus accumbens volumes, as well as metrics of motor and cognitive functioning (3), resting state functional connectivity changes (14), and subcortical brain volume variations associated with motor symptom severity, cognitive control, and verbal learning (8, 9, 15). The extensiveness of brain structural and functional changes in this population supports the suitability of brain-based phenotypes for probing early genetic effects on prodromal disease progression.

To date, several promising non-*HTT* genetic modulators, including *ADORA2A* (16, 17) and *GRIN2A-2B* (18), among others (5, 6, 19–22), have been highlighted as potential modifiers of disease onset or progression. The GeM-HD (genetic modifiers of HD) consortium conducted the largest such study, compiling genetic data from multiple projects and investigating genetic factors associated with residual variance in onset time (after controlling for CAG influence). This study identified two genomic significant loci in chromosome 15 that accelerated or delayed onset by 6.1 and 1.4 years, respectively (20). Another new study of disease progression in both prodromal and diagnosed HD patients reported an association between single-nucleotide polymorphisms (SNPs) in chromosome 5 and a reduced rate of change in motor and functional capacity scores (23). However, no study has examined genetic modulation of brain-based phenotypes during the HD prodrome.

The CAG age product (CAP), computed as age × (CAG repeat − constant), captures the cumulative effect of CAG expansion on the duration of exposure, and is a validated index of disease burden in HD (24, 25). During the prodromal phase, CAP significantly and reliably associated with brain volumetric changes and cognitive and motor decline (24), yet it cannot explain all the variation in these measures (or in clinical onset age) (3). Thus, to pinpoint non-*HTT* genetic factors that influence prodromal brain-based phenotypes, we intentionally removed CAP influence on GM variation through regression; this is analogous to the residual variance in onset time implemented in the GeM-HD study. We then identified GM networks associated with cognitive or motor decline in prodromal individuals and tested these for genetic effects.

MATERIALS AND METHODS

Participants

715 (447 female and 268 male) PREDICT-HD prodromal individuals from 33 sites were analyzed. These participants were gene positive (with >36 CAG repeats) independent samples, and did not convert to HD during the study. All participants provided written, informed consent and were treated in accordance with protocols approved by each participating institution's internal review board. Detailed enrollment and exclusion criteria can be found in previous publications (12). Participant demographic information is provided in **Table 1**. There were no differences in age, CAG repeats, or education years between males and females. 54 participants had fewer than 40 CAG repeats; even though these participants may or may not develop HD in their lifetimes, the large variability in their prodromal disease progression (which partially contributes to the uncertainty of onset) makes it more appealing to include them in the prodromal analysis.

Cognitive and Motor Functioning Assessments

Motor variables included total motor score (TMS) from the Unified Huntington's Disease Rating Scale and the chorea, bradykinesia, oculomotor, and dystonia subdomains from the 15-item standardized motor assessment (26, 27). Many participants had low or 0 scores on the motor variables, skewing the data toward a negative exponential distribution. Cognitive variables included the Symbol Digit Modalities Test (SDMT) (27, 28), Stroop Color,

TABLE 1 | Demographic information of participants.

	715 prodromal HD	Female (*N* = 447, 62.5%)	Male (*N* = 268, 37.5%)
Age	42.55 ± 10.53 (19–83)	42.6 ± 10.5	43.5 ± 10.7
Cytosine adenine guanine repeats	42.47 ± 2.54 (37–61)	42.43 ± 2.57	42.53 ± 2.50
Education years	14.50 ± 2.61 (8–20)	14.36 ± 2.55	14.73 ± 2.69
Race (self-reported)	694 (97.06%) White 1 American Indian 3 Asians 14 intermixed 7 unknown	96.64% White 1 American Indian 2 Asians 11 intermixed 5 unknown	97.76% White 1 Asians 3 intermixed 2 unknown
Race (genetic estimated)	97.34% Caucasian 1 Asian 2 intermixed 17 Mexican/Indians	97.09% Caucasian 1 Asian 12 Mexican/Indians	97.76% Caucasian 2 intermixed 5 Mexican/Indians

Stroop Word, and Stroop Interference tests (27, 29), and Trail Making Tests A (TMTA) and B (TMTB) (27, 30, 31). Cognitive variables had approximately normal distributions. More details for each variable are available in the Supplementary Material.

Total motor score, oculomotor, bradykinesia, and chorea were highly correlated (e.g., TMS correlated with oculomotor, bradykinesia and chorea at $r = 0.79$, 0.83, and 0.70, respectively; Figure S1 in Supplementary Material). Thus, we used principal component analysis (PCA) to extract the first PC (89% of the total variance) as the representative variable for overall motor function; higher scores indicate more abnormal motor control, and the most weighted variable is TMS. Similarly, SDMT and Stroop scores were highly correlated ($r = 0.53$–0.78), and we obtained the first PC (76% of the total variance) as the representative variable for attention and working memory; higher scores indicate better performance, and the most weighted variable is Stroop Word. TMTA and TMTB were grouped and the first PC (95% of the total variance) was obtained as the representative variable for problem solving; higher scores indicate slower processing, and the most weighted variable is TMTB. For dystonia, which was not highly correlated with the other motor variables, 639 participants had scores of 0, 37 had scores of 1, 24 had scores of 2, and 5 had scores higher than 2. The low scores on dystonia are in line with the prodromal status of the participants, as dystonia is usually a sign of disease manifestation. We converted dystonia score into a binary variable representing presence or absence of dystonia signs.

Genetic Data Preprocessing

Genomic SNP data were downloaded from dbGAP (Study Accession: phs000222.v4.p2). We removed problematic loci in accordance with PREDICT-HD quality control recommendations, and filtered SNPs for a missingness rate of 5% per sample and 5% per SNP and a minor allele frequency of 5%. Family relatedness was determined using PLINK identity-by-descent analysis, and only one member per family was included. The top 10 multidimensional scaling (MDS) factors from PLINK were used to correct for population structure. A total of 1,160,231 SNPs across the genome were investigated. In parallel, we also investigated an HD pathway derived from the Ingenuity Pathway Analysis knowledgebase and the KEGG database. The HD pathway from the two combined databases included 310 genes and 3,404 SNPs after pruning with $r^2 > 0.5$ (see Table S1 in Supplementary Material).

Candidate Selection

Since only prodromal patients were investigated and prodromal functional decline is more relevant to symptom onset than to disease progression [which accelerates significantly faster after onset compared to during the prodrome (23)], we selected candidate SNPs for modifying onset time; these were from the GeM-HD study, and included two regions (chr15q13.2-3: rs146353869, rs2140734; chr8: rs1037699) with significant influences on age of motor diagnosis and nominal associations with cognitive and psychiatric symptom onset (20). We tested SNPs within these regions for effects on prodromal progression. Although our data did not include these exact three SNPs, we identified seven nearby SNPs in high linkage disequilibrium (LD) with rs2140734 ($r > 0.98$ based on NIH LDlink web[1]): rs11293, rs11629793, rs8034856, rs7176569, rs35784593, rs1474380, and rs61997138. These SNPs were highly correlated in our data ($r > 0.99$), exhibiting almost identical genotype patterns. There were also three SNPs in our data with identical genotype patterns that were in high LD with rs1037699 ($r > 0.85$): rs16869295, rs11777942, and rs11778107.

Imaging Data Processing

T1-weighted images from the earliest available MRI scans were segmented into GM, modulated, normalized to MNI space, and smoothed with an 8 mm × 8 mm × 8 mm Gaussian kernel using the statistical parametric mapping 8 software package.[2] Images less than 80% correlated with the averaged GM were removed, and a >0.2 GM volume mask was generated to include only GM relevant voxels. Since these imaging data were collected from 50 site and scanner field strength (1.5 or 3 T) combinations, known influences of site scanner, age, sex, and disease burden on GM were removed by applying a linear regression model to each GM voxel. Site scanners were coded as 49 dummy variables, and disease burden was calculated using the formula suggested by PREDICT-HD: CAP = age × (CAG − 33.66) (24).

Source-Based Morphometry

We then applied independent component analysis (ICA) to whole-brain GM voxels using the source-based morphometry toolbox within the GIFT software package (http://mialab.mrn.org/software/gift). ICA decomposes the brain imaging data into maximally independent GM components, often comprised of multiple brain regions, with each component/network grouping voxels that covary among subjects (32). The model can be described simply as $X = A \times S$, where X is the measured data, S contains the extracted components, and A is the loading matrix. A participant's loading coefficient for a given component indicates how strongly that component manifests in the participant's imaging data [see Ref. (32–35) for details]. Fifteen GM components were estimated, as determined by the minimum description length criteria (36).

Statistical Analyses

We first tested whether the cognitive and motor variables were significantly associated with disease burden in our prodromal sample. PCA-derived representative variables and original variables were tested one by one, separately. A regression model (cognitive or motor variable = age + sex + CAP) was used for each variable. Due to different distributions for motor versus cognitive variables, a linear regression model was used for cognitive variables, a logistic regression model was used for the converted binary dystonia variable, and a Poisson regression model was applied to the other motor variables.

Next, we tested for associations between the extracted GM components and cognitive and motor functioning variables using a regression model in which the cognitive or motor functioning variable = age + sex + GM loadings + CAP. Similarly, linear, Poisson, and logistic models were used accordingly. The GM

[1] https://analysistools.nci.nih.gov/LDlink/ (Accessed: April, 2017).
[2] http://www.fil.ion.ucl.ac.uk/spm/software/spm8/.

components significantly contributing to motor or cognitive functioning after adjusting for CAP were our primary components of interest for genetic associations. For any GM component of interest, a regression model (GM loading = SNP + top 10 MDS scores) was used to test for SNP associations at the genomic, pathway and candidate levels. We also tested for associations between clinical (motor or cognitive) variables and SNPs using the following regression model: motor or cognitive variable = age + sex + CAP + SNP + top 10 MDS scores. All tests, genomic level and pathway level, were false discovery rate (FDR) corrected at $p < 0.05$ for the number of tested SNPs.

RESULTS

Disease Burden and Clinical Functioning

Individual motor and cognitive variables and derived representative variables were all associated with CAP after controlling for age and sex ($p = 0.04$ for the converted binary dystonia score, $p = 0.01$ for the original dystonia score, and $p < 1 \times 10^{-11}$ for all other variables). Due to highly consistent results among representative variables and original individual variables, hereafter we report the results from representative measures. Results from individual variables are provided in the Supplementary Material. The total variance explained by the regression model was 19% for overall motor function (9–18% for individual variables), 18% for working memory/attention (12–21% for individual variables), and 15% for problem solving (13 and 15% for TMTA and TMTB, respectively). The pseudo R^2 for dystonia was 1.3% (2% for the original dystonia score).

GM and Clinical Functioning

Fifteen GM components were extracted (see Supplementary Material), one of which was a typical artifact forming a ring around brain [as demonstrated by Chen et al. (37)]. This component was thus removed from further analyses. As expected, none of the GM components were related to CAP. The association tests with cognitive and motor functioning revealed a GM component (**Figure 1A**), mainly in cuneus, lingual gyrus, and middle occipital gyrus, that was significantly related to working memory and attention ($p = 1.39 \times 10^{-4}$ uncorrected, passing FDR correction). Higher GM volume in this component was related to better attention and working memory performance, explaining 1.7% of the variance after controlling for age, sex and CAP, as shown in **Figure 1A** (CAP explained 15.7%). Another GM component, mainly in bilateral inferior parietal and superior/middle temporal regions, was significantly related to dystonia (**Figure 1B**; logistic regression $p = 2.34 \times 10^{-4}$ uncorrected); prodromal participants with at least one dystonia sign had significantly lower GM volume in this network (Cohen's $d = 0.47$, $p = 2.37 \times 10^{-4}$).

GM and SNPs (Full Genomic Data and HD Pathway)

Over one million SNPs were tested for associations with GM variation in the aforementioned two components, and none exhibited a genomic significant association passing FDR correction. Similarly, no significant genomic associations with cognitive or motor functioning variables were observed. In our separate analysis of SNPs in 310 HD pathway genes, only one SNP (rs71358386 in *NCOR1)* was significantly associated with GM in the cuneus component ($p = 2.38 \times 10^{-5}$, passing FDR), with minor allele G being negatively linked to GM volume. For this SNP, 636 participants were homozygous major allele (A) carriers, 77 were heterozygous, and 2 were homozygous minor allele (G) carriers. We pooled the heterozygous and homozygous minor allele carriers together and computed the difference

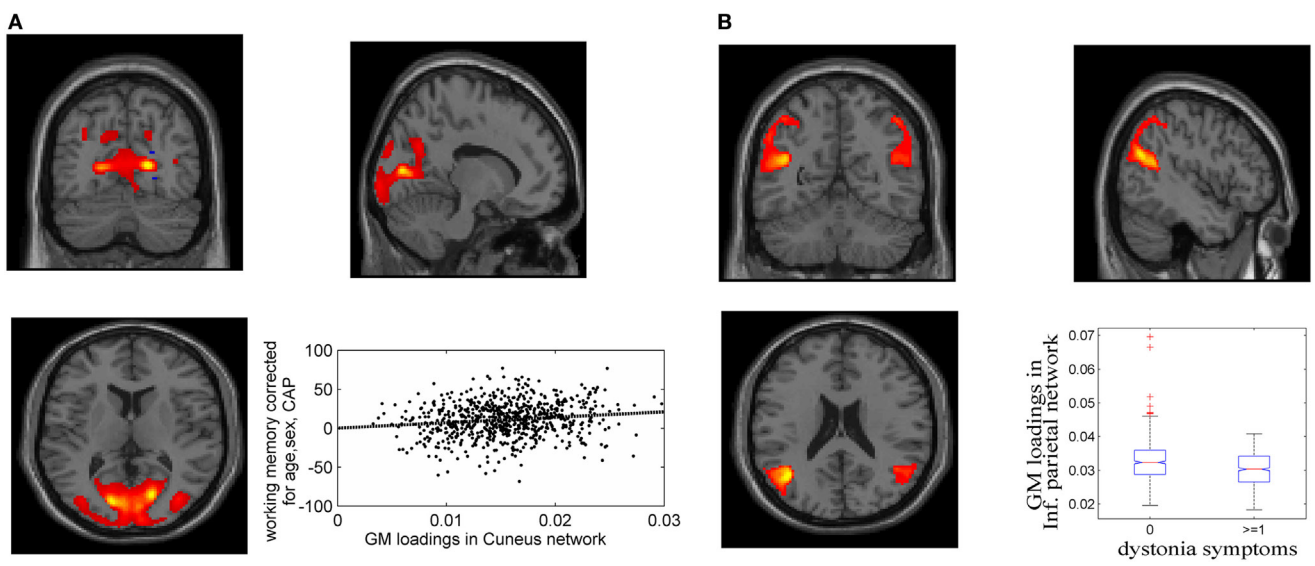

FIGURE 1 | Gray matter (GM) components associated with working memory/attention and dystonia after controlling for disease burden. **(A)** GM component containing cuneus, lingual gyrus, and middle occipital gyrus, and its association with working memory/attention. **(B)** GM component highlighting bilateral inferior parietal and superior/middle temporal gyri, and its association with dystonia. The GM loadings are relative values without unit.

between minor allele carriers and homozygous major allele carriers. The difference was significant ($p < 1.56 \times 10^{-5}$ for the two-sample t-test and $p < 6.42 \times 10^{-6}$ for the Wilcoxon rank test), with a Cohen's d of 0.53 (**Figure 2**). Interestingly, another SNP (rs78804732 in *ADORA2B*) was in strong LD with rs71358386 ($r = 0.91$). This SNP was also significantly associated with GM in the cuneus component ($p = 1.51 \times 10^{-5}$), with minor allele A being linked to lower GM volume and A carriers having significantly lower GM volume than major allele C carriers (Cohen's $d = 0.59$; $p < 8.0 \times 10^{-6}$ for the two-samples t-test; $p < 3.48 \times 10^{-6}$ for the Wilcoxon rank test; **Figure 2**). These two SNPs were also nominally associated with GM in the inferior parietal component ($p = 0.02$ and $p = 0.04$, respectively), with minor alleles being linked to lower GM volume. An extended analysis on these two SNPs provided some promising but not strictly significant results, and we reported them in the Supplementary Material for the interest of readers. At the pathway level, no SNPs were significantly associated with motor or cognitive functioning, though these two SNPs were marginally associated with overall motor functioning ($p = 0.05$, not passing FDR correction), with more minor alleles being linked to greater motor dysfunction. To obtain an intuitive effect size, we assessed these SNPs' effects on TMS and found that one minor allele copy was associated with an increase of 0.20 U in TMS score after controlling for age, sex, CAP, and MDS.

Candidate SNP Analyses

Seven SNPs in LD with rs2140734 in chromosome 15 showed a marginal connection to GM in the inferior parietal network in the regression model ($p = 0.06$–0.09, not significant); greater minor allele number was linked to increased GM in the network. Further ANOVA tests revealed that the main driver of the association was the homozygous minor allele carrier group. As shown in **Figure 3** using the example of rs11293, there was no difference between homozygous major allele G carriers and heterozygous carriers ($p = 0.75$), but homozygous minor allele A carriers had significantly higher GM than the other groups ($p = 0.01$, no multiple comparison correction was applied due to near identical patterns among the seven SNPs). This SNP was also negatively related to overall motor function ($p = 0.01$), indicating an association with better motor performance. To obtain an intuitive effect size, we assessed its effect on TMS, and found that one minor allele copy was associated with a TMS score decrease of 0.14 U after controlling for age, sex, CAP, and MDS. No connections with GM, cognition or motor functioning were observed for SNPs in LD with rs1037699 on chromosome 8.

DISCUSSION

Gray matter and motor and cognitive functioning show significant prodromal decline in HD (11, 15, 25, 38–41). Our results first confirmed that variation in these domains relates significantly to CAP, a metric reflecting disease burden and based on CAG mutation and exposure time (age) (13, 42). Individuals with more CAG repeats are likely to develop symptoms more rapidly and be diagnosed at younger ages. However, our results agree with previous work showing that a considerable amount of variance in prodromal functional decline is beyond this disease burden (3, 20). After regressing out CAP effects, two GM components yielded significant associations with working memory/attention and dystonia, respectively, though the variance accounted for was relatively small compared to CAP influence (about one

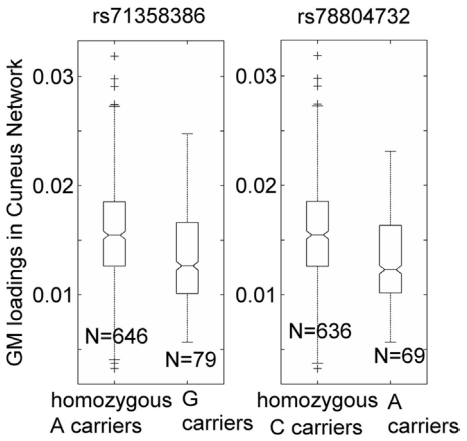

FIGURE 2 | Association of two single-nucleotide polymorphisms, rs71358386 and rs78804732, with a cuneus gray matter (GM) component. GM loadings are relative values without unit. In the box plots, the middle line is the median value, the top and bottom of each box are the 25th and 75th percentile values, the whiskers extend from the ends of the interquartile to the further values within 1.5 times the interquartile, and plus (+) signs show values that are more than 1.5 times the interquartile range away from the top or bottom of the box. The plot of medium and 25/75th percentile presents a similar overall pattern as the mean and standard deviation in these data.

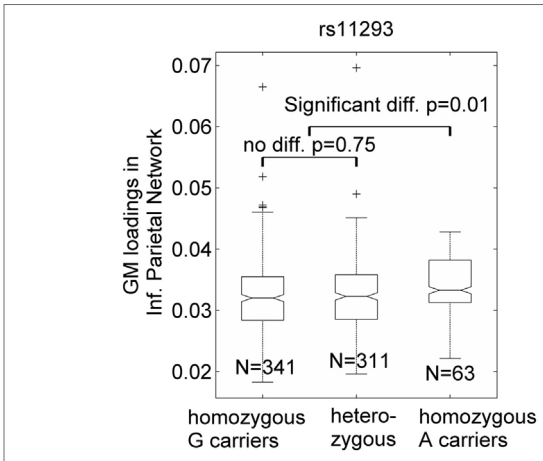

FIGURE 3 | Single-nucleotide polymorphism rs11293's association with an inferior parietal gray matter (GM) component. GM loadings are relative values without unit. In the box plots, the middle line is the median value, the top and bottom of each box are the 25th and 75th percentile values, the whiskers extend from the ends of the interquartile to the further values within 1.5 times the interquartile, and plus (+) signs show values that are more than 1.5 times the interquartile range away from the top or bottom of the box. The plot of medium and 25/75th percentile presents a similar overall pattern as the mean and standard deviation in these data.

tenth). Nonetheless, this is an exciting finding; the *HTT* CAG expansion is a causal mutation associated with HD, and age has widely known effects on GM variation and clinical functioning in both prodromal/HD patients and healthy individuals. Thus, modest residual effects are to be expected. As modifiers of disease progression, symptoms, and onset continue to be discovered, the potential for promising gene therapies increases as well. Such therapies could eventually target multiple modifiers with modest individual effects but substantial combined influence on progression. These findings reinforce evidence that the disease burden from CAG mutation and age does not explain all observed variance in prodromal disease progression and clinical onset (3, 20), and further suggest that GM variability may be a useful phenotype for examining genetic factors that account for unexplained variability in HD progression and onset.

Better performance on *working memory and attention* tasks was associated with higher GM volume in a component that included *cuneus*, *lingual gyrus*, and *middle occipital gyrus*. Structural changes in occipital regions have been consistently documented in prodromal and diagnosed HD, albeit overshadowed by caudate and putamen effects (8, 40, 43–46). Our findings are mirrored by a study staging cortical thinning across the prodrome, in which visual cortical regions were among the earliest and most severely affected regions, and cortical thinning in these regions was associated with lower scores on Stroop Color, Stroop Word, and SDMT (45). Similarly, a PREDICT-HD study investigating neuroanatomical correlates of five cognitive functions also reported that occipital cortical thickness was associated with letter-number sequencing working memory, as well as SDMT performance (8). In prodromal and diagnosed patients (relative to controls), TRACK-HD also reported reduced occipital cortical thickness, which was associated with poorer performance on the SDMT, Stroop Word test, and TMTA (44). Taken together, these findings highlight cuneus, lingual, and occipital abnormalities in prodromal and diagnosed patients, and indicate that these aberrations may influence cognitive performance. Our findings support these previous associations, and further suggest that they may be partially modulated by factors outside of *HTT* CAG repeat number and age.

Dystonia is a common symptom of HD manifesting at varying degrees of severity (47). In our cohort, dystonia signs were associated with reduced GM in a component containing *inferior parietal* and *middle and superior temporal* regions, after controlling for CAP. Inferior parietal areas interface with other sensorimotor regions to promote motor planning and initiation (48), and show increased activation before self-initiated movements (49). Inferior parietal GM loss has been reported in prodromal patients and is consistently observed in diagnosed HD (45, 46, 50), and has been further linked to abnormal eye movement (50). A meta-analysis of HD voxel-based morphometry studies identified brain clusters associated with motor symptoms, grouping inferior parietal together with precentral gyrus, primary motor, postcentral gyrus, and somatosensory cortex; these regions were more strongly related to motor functioning than the caudate (46). As for superior temporal gyrus, a smaller prodromal study ($N = 325$) associated bilateral superior temporal cortex with motor timing precision, and found that it was the greatest structural contributor to performance outside of the striatum and middle frontal cortex (8). These studies emphasize the importance of temporal and parietal regions in movement-related tasks in both healthy controls and prodromal and diagnosed HD patients. Our results reinforce these findings, and the removal of CAP effects in our analyses further suggests that a portion of these effects relates to factors outside of the disease-determining *HTT* mutation.

Frontal and striatal abnormalities are the most robust and commonly reported effects in HD, and these regions are heavily involved in cognitive and motor functioning. Our findings reflect brain structural influences on cognition and movement that are not accounted for by disease burden. It is thus unsurprising that the striatum and frontal lobe were not key contributors to the effects we report. Alternatively, our results pinpoint occipital, parietal, and temporal regions of the brain that comprise networks important for attention, working memory, and planned movement. These areas often work in concert with the frontal lobe and striatum to promote cognitive and motor functioning. In this large prodromal cohort, these regions appear to contribute to prodromal clinical functioning in a manner that is independent of *HTT* CAG influence.

The genome-wide association test did not produce significant results, which is not particularly surprising since HD is a rare disorder and genomic tests require very large sample sizes to balance multiple comparison corrections and small effect sizes. Similar to studies of genetic modifiers of motor onset time (5, 20), some true genetic effects may be missed due to strict genome-wide significance thresholds. The HD pathway-based genetic association analysis leveraged prior knowledge of gene functions and their involvement in HD. Therefore, these findings fit into the double-hit phenomena in which gene functions are known to contribute to disease pathogenesis, and changes in these genes are also related to GM variation that contributes to prodromal symptoms and cognitive decline. Thus, these genetic variants have an increased likelihood of affecting disease progression.

We observed two SNPs in strong LD but located in two different genes (*NCOR1* and *ADORA2B*, 54k base pairs apart) that were associated with GM variations. In fact, SNP rs71358386 in *NCOR1* regulates expression of *ADORA2B* in various tissues based on the GTEx database[3] (51). In our cohort, minor allele carriers of the two SNPs showed significant occipital GM reduction and some level of reduction in inferior parietal regions, as well as marginally higher motor dysfunction. *NCOR1* is part of the HD pathway and encodes the protein nuclear receptor corepressor 1, which mediates transcriptional repression of thyroid-hormone and retinoic acid receptors. This protein reportedly interacts with mutant HTT (52, 53) to alter nuclear receptor function and is also differentially located in patient brain tissue (53, 54). *ADORA2B* encodes adenosine receptor subtype A2B, a protein that interacts with netrin-1, which is involved in axon elongation. Currently, *ADORA2B* is not part of the HD pathway, although *ADORA2A* is (55–57). *ADORA2A* and *ADORA2B* are two of four human genes that encode adenosine receptors that increase cyclic adenosine monophosphate (58), which is important for signal transduction

[3]https://gtexportal.org (Accessed: April, 2017).

and other biochemical processes (59). We cannot currently establish these SNPs as true causal mutations, and further investigation of the molecular, cellular, and functional impact of these genes is warranted.

In addition, within two candidate regions selected based on their significant effects on clinical onset time (20), our results revealed that SNPs in ch15q13.3 (*MTMR10* and *FAN1* genes) affected GM in prodromal participants; homozygous minor allele carriers had higher GM densities in the inferior parietal component. Given the negative link between GM volume in this component and dystonia symptoms and overall motor functioning, this minor allele has a protective effect on prodromal dystonia and motor dysfunction, with one minor allele copy being associated with a TMS score decrease of 0.14. Excitingly, this finding is in total agreement with the reported clinical onset delay attributed to these SNPs [the minor allele was associated with a 1.4-year onset delay (20)]. The possible mechanisms through which these genes influence disease progression have been elaborated upon by the GeM-HD study. Our results suggest that genetic variations outside of *HTT* are already altering GM in the prodromal phase, before the emergence of diagnosis-associated motor symptoms.

This investigation of extra-*HTT* genetic modifiers before clinical diagnosis represents a new direction for the development of treatments to prevent or delay this devastating disorder. Leveraging brain structural variation, which is likely more precise and subtle than clinical outcome changes, enhances power for identifying genetic modifiers. The findings of this study demonstrate that: (1) GM variation beyond CAG influence is associated with disease progression and manifests as early as the prodrome; (2) genetic modifiers of biologically measured GM volume are already exerting their effects during the prodromal phase; and (3) the accumulation of these effects across disease progression ultimately alters clinical onset time. Replication using an independent sample and follow-up studies manipulating cell lines or animal strains should be carried out to fully illuminate the mechanisms of these genetic modifiers. As a proof of concept, our findings suggest that studying brain structural variation beyond disease burden can be a very promising method for identifying genetic modifiers of HD progression. The limitations of this study include the following: (1) inclusion of some gene positive participants who may never be diagnosed with HD and thus may be healthy participants; (2) only linear relationships between GM, cognition, motor functioning, and genetic variations were tested; and (3) a longitudinal study on changes in GM, cognition, and motor functioning, as well as a carefully designed comparison with healthy controls, would help confirm the genetic effects reported here.

ETHICS STATEMENT

All participants provided written, informed consent and were treated in accordance with protocols approved by each participating institution's internal review board.

AUTHOR CONTRIBUTIONS

JL, JT, and VC have designed this study; JL, JC, and DL have conducted data analyses; JL and JC were involved in writing the first draft, and all authors contributed to reviewing and editing the final manuscript.

ACKNOWLEDGMENTS

The PREDICT-HD study was supported by NIH/NINDS grant 5R01NS040068, CHDI Foundation, Inc., A3917 and 6266, Cognitive and Functional Brain Changes in Preclinical Huntington Disease 5R01NS054893, awarded to Jane S. Paulsen. We thank the PREDICT-HD sites, the study participants, the National Research Roster for Huntington's Disease Patients and Families, the Huntington's Disease Society of America and the Huntington's Study Group.

FUNDING

This project is supported by NIH U01NS082074 (VC and JT, co-PIs) from National Institute of Neurological Disorders and Stroke.

SUPPLEMENTARY MATERIAL

The Supplementary Material for this article can be found online at https://www.frontiersin.org/articles/10.3389/fneur.2018.00190/full#supplementary-material.

REFERENCES

1. Ross CA, Aylward EH, Wild EJ, Langbehn DR, Long JD, Warner JH, et al. Huntington disease: natural history, biomarkers and prospects for therapeutics. *Nat Rev Neurol* (2014) 10(4):204–16. doi:10.1038/nrneurol.2014.24
2. Gusella JF, MacDonald ME, Lee JM. Genetic modifiers of Huntington's disease. *Mov Disord* (2014) 29(11):1359–65. doi:10.1002/mds.26001
3. Paulsen JS, Long JD, Ross CA, Harrington DL, Erwin CJ, Williams JK, et al. Prediction of manifest Huntington's disease with clinical and imaging measures: a prospective observational study. *Lancet Neurol* (2014) 13(12):1193–201. doi:10.1016/S1474-4422(14)70238-8
4. Djousse L, Knowlton B, Hayden M, Almqvist EW, Brinkman R, Ross C, et al. Interaction of normal and expanded CAG repeat sizes influences age at onset of Huntington disease. *Am J Med Genet A* (2003) 119A(3):279–82. doi:10.1002/ajmg.a.20190
5. Correia K, Harold D, Kim KH, Holmans P, Jones L, Orth M, et al. The genetic modifiers of motor OnsetAge (GeM MOA) website: genome-wide association analysis for genetic modifiers of Huntington's disease. *J Huntingtons Dis* (2015) 4(3):279–84. doi:10.3233/JHD-150169
6. Cowin RM, Bui N, Graham D, Green JR, Yuva-Paylor LA, Weiss A, et al. Genetic background modulates behavioral impairments in R6/2 mice and suggests a role for dominant genetic modifiers in Huntington's disease pathogenesis. *Mamm Genome* (2012) 23(5–6):367–77. doi:10.1007/s00335-012-9391-5
7. Wexler NS, Lorimer J, Porter J, Gomez F, Moskowitz C, Shackell E, et al. Venezuelan kindreds reveal that genetic and environmental factors modulate Huntington's disease age of onset. *Proc Natl Acad Sci U S A* (2004) 101(10):3498–503. doi:10.1073/pnas.0308679101
8. Harrington DL, Liu D, Smith MM, Mills JA, Long JD, Aylward EH, et al. Neuroanatomical correlates of cognitive functioning in prodromal Huntington disease. *Brain Behav* (2014) 4(1):29–40. doi:10.1002/brb3.185

9. Aylward EH, Harrington DL, Mills JA, Nopoulos PC, Ross CA, Long JD, et al. Regional atrophy associated with cognitive and motor function in prodromal Huntington disease. *J Huntingtons Dis* (2013) 2(4):477–89. doi:10.3233/JHD-130076
10. Paulsen JS, Hayden M, Stout JC, Langbehn DR, Aylward E, Ross CA, et al. Preparing for preventive clinical trials: the Predict-HD study. *Arch Neurol* (2006) 63(6):883–90. doi:10.1001/archneur.63.6.883
11. Long JD, Paulsen JS; PREDICT-HD Investigators and Coordinators of the Huntington Study Group. Multivariate prediction of motor diagnosis in Huntington's disease: 12 years of PREDICT-HD. *Mov Disord* (2015) 30(12):1664–72. doi:10.1002/mds.26364
12. Paulsen JS, Langbehn DR, Stout JC, Aylward E, Ross CA, Nance M, et al. Detection of Huntington's disease decades before diagnosis: the Predict-HD study. *J Neurol Neurosurg Psychiatry* (2008) 79(8):874–80. doi:10.1136/jnnp.2007.128728
13. Ciarochi JA, Calhoun VD, Lourens S, Long JD, Johnson HJ, Bockholt HJ, et al. Patterns of co-occurring gray matter concentration loss across the Huntington disease prodrome. *Front Neurol* (2016) 7:147. doi:10.3389/fneur.2016.00147
14. Espinoza FA, Turner JA, Vergara VM, Miller RL, Mennigen E, Liu J, et al. Whole-brain connectivity in a large study of Huntington's disease gene mutation carriers and healthy controls. *Brain Connect* (2018). doi:10.1089/brain.2017.0538
15. Misiura MB, Lourens S, Calhoun VD, Long J, Bockholt J, Johnson H, et al. Cognitive control, learning, and clinical motor ratings are most highly associated with basal ganglia brain volumes in the premanifest Huntington's disease phenotype. *J Int Neuropsychol Soc* (2017) 23(2):159–70. doi:10.1017/S1355617716001132
16. Li W, Silva HB, Real J, Wang YM, Rial D, Li P, et al. Inactivation of adenosine A2A receptors reverses working memory deficits at early stages of Huntington's disease models. *Neurobiol Dis* (2015) 79:70–80. doi:10.1016/j.nbd.2015.03.030
17. Taherzadeh-Fard E, Saft C, Wieczorek S, Epplen JT, Arning L. Age at onset in Huntington's disease: replication study on the associations of ADORA2A, HAP1 and OGG1. *Neurogenetics* (2010) 11(4):435–9. doi:10.1007/s10048-010-0248-3
18. Arning L, Saft C, Wieczorek S, Andrich J, Kraus PH, Epplen JT. NR2A and NR2B receptor gene variations modify age at onset in Huntington disease in a sex-specific manner. *Hum Genet* (2007) 122(2):175–82. doi:10.1007/s00439-007-0393-4
19. Gusella JF, MacDonald ME. Huntington's disease: the case for genetic modifiers. *Genome Med* (2009) 1(8):80. doi:10.1186/gm80
20. Genetic Modifiers of Huntington's Disease (GeM-HD) Consortium. Identification of genetic factors that modify clinical onset of Huntington's disease. *Cell* (2015) 162(3):516–26. doi:10.1016/j.cell.2015.07.003
21. Campesan S, Green EW, Breda C, Sathyasaikumar KV, Muchowski PJ, Schwarcz R, et al. The kynurenine pathway modulates neurodegeneration in a *Drosophila* model of Huntington's disease. *Curr Biol* (2011) 21(11):961–6. doi:10.1016/j.cub.2011.04.028
22. Li JL, Hayden MR, Warby SC, Durr A, Morrison PJ, Nance M, et al. Genome-wide significance for a modifier of age at neurological onset in Huntington's disease at 6q23-24: the HD MAPS study. *BMC Med Genet* (2006) 7:71. doi:10.1186/1471-2350-7-71
23. Hensman Moss DJ, Pardinas AF, Langbehn D, Lo K, Leavitt BR, Roos R, et al. Identification of genetic variants associated with Huntington's disease progression: a genome-wide association study. *Lancet Neurol* (2017) 16(9):701–11. doi:10.1016/S1474-4422(17)30161-8
24. Zhang Y, Long JD, Mills JA, Warner JH, Lu W, Paulsen JS, et al. Indexing disease progression at study entry with individuals at-risk for Huntington disease. *Am J Med Genet B Neuropsychiatr Genet* (2011) 156B(7):751–63. doi:10.1002/ajmg.b.31232
25. Harrington DL, Rubinov M, Durgerian S, Mourany L, Reece C, Koenig K, et al. Network topology and functional connectivity disturbances precede the onset of Huntington's disease. *Brain* (2015) 138(Pt 8):2332–46. doi:10.1093/brain/awv145
26. Huntington Study Group. Unified Huntington's disease rating scale: Reliability and consistency. *Mov Disord* (1996) 11(2):136–42. doi:10.1002/mds.870110204
27. Paulsen JS, Long JD, Johnson HJ, Aylward EH, Ross CA, Williams JK, et al. Clinical and biomarker changes in premanifest Huntington disease show trial feasibility: a decade of the PREDICT-HD study. *Front Aging Neurosci* (2014) 6:78. doi:10.3389/fnagi.2014.00078
28. Smith A. *Symbol Digit Modalities Test (SDMT) Manual (Revised)*. Los Angeles, CA: Western Psychological Services (1982).
29. Stroop JR. Studies of interference in serial verbal reactions. *J Exp Psychol* (1935) 18(6):643–62. doi:10.1037/h0054651
30. O'Rourke JJ, Beglinger LJ, Smith MM, Mills J, Moser DJ, Rowe KC, et al. The trail making test in prodromal Huntington disease: contributions of disease progression to test performance. *J Clin Exp Neuropsychol* (2011) 33(5):567–79. doi:10.1080/13803395.2010.541228
31. Reitan RM. Validity of the trail making test as an indicator of organic brain damage. *Percept Mot Skills* (1958) 8:271–6. doi:10.2466/PMS.8.7.271-276
32. Xu L, Groth KM, Pearlson G, Schretlen DJ, Calhoun VD. Source-based morphometry: the use of independent component analysis to identify gray matter differences with application to schizophrenia. *Hum Brain Mapp* (2009) 30(3):711–24. doi:10.1002/hbm.20540
33. Cardoso JF. Infomax and maximum likelihood for blind source separation. *IEEE Signal Process Lett* (1997) 4(4):112–4. doi:10.1109/97.566704
34. Calhoun VD, Adali T. Unmixing fMRI with independent component analysis. *IEEE Eng Med Biol Mag* (2006) 25(2):79–90. doi:10.1109/MEMB.2006.1607672
35. Calhoun V, Adali T, Liu J. A feature-based approach to combine functional MRI, structural MRI and EEG brain imaging data. *Conf Proc IEEE Eng Med Biol Soc* (2006) 1:3672–5. doi:10.1109/IEMBS.2006.259810
36. De Ridder F, Pintelon R, Schoukens J, Gillikin DP. Modified AIC and MDL model selection criteria for short data records. *IEEE Trans Instrum Meas* (2005) 54(1):144–50. doi:10.1109/TIM.2004.838132
37. Chen J, Liu J, Calhoun VD, Arias-Vasquez A, Zwiers MP, Gupta CN, et al. Exploration of scanning effects in multi-site structural MRI studies. *J Neurosci Methods* (2014) 230:37–50. doi:10.1016/j.jneumeth.2014.04.023
38. Wu D, Faria AV, Younes L, Mori S, Brown T, Johnson H, et al. Mapping the order and pattern of brain structural MRI changes using change-point analysis in premanifest Huntington's disease. *Hum Brain Mapp* (2017) 38:5035–50. doi:10.1002/hbm.23713
39. Shaffer JJ, Ghayoor A, Long JD, Kim RE, Lourens S, O'Donnell LJ, et al. Longitudinal diffusion changes in prodromal and early HD: evidence of white-matter tract deterioration. *Hum Brain Mapp* (2017) 38(3):1460–77. doi:10.1002/hbm.23465
40. Harrington DL, Long JD, Durgerian S, Mourany L, Koenig K, Bonner-Jackson A, et al. Cross-sectional and longitudinal multimodal structural imaging in prodromal Huntington's disease. *Mov Disord* (2016) 31(11):1664–75. doi:10.1002/mds.26803
41. Epping EA, Kim JI, Craufurd D, Brashers-Krug TM, Anderson KE, McCusker E, et al. Longitudinal psychiatric symptoms in prodromal Huntington's disease: a decade of data. *Am J Psychiatry* (2016) 173(2):184–92. doi:10.1176/appi.ajp.2015.14121551
42. Faria AV, Ratnanather JT, Tward DJ, Lee DS, van den Noort F, Wu D, et al. Linking white matter and deep gray matter alterations in premanifest Huntington disease. *Neuroimage Clin* (2016) 11:450–60. doi:10.1016/j.nicl.2016.02.014
43. Wolf RC, Sambataro F, Vasic N, Baldas EM, Ratheiser I, Bernhard Landwehrmeyer G, et al. Visual system integrity and cognition in early Huntington's disease. *Eur J Neurosci* (2014) 40(2):2417–26. doi:10.1111/ejn.12575
44. Johnson EB, Rees EM, Labuschagne I, Durr A, Leavitt BR, Roos RA, et al. The impact of occipital lobe cortical thickness on cognitive task performance: an investigation in Huntington's disease. *Neuropsychologia* (2015) 79(Pt A):138–46. doi:10.1016/j.neuropsychologia.2015.10.033
45. Rosas HD, Salat DH, Lee SY, Zaleta AK, Pappu V, Fischl B, et al. Cerebral cortex and the clinical expression of Huntington's disease: complexity and heterogeneity. *Brain* (2008) 131(Pt 4):1057–68. doi:10.1093/brain/awn025
46. Dogan I, Eickhoff SB, Schulz JB, Shah NJ, Laird AR, Fox PT, et al. Consistent neurodegeneration and its association with clinical progression in Huntington's disease: a coordinate-based meta-analysis. *Neurodegener Dis* (2013) 12(1):23–35. doi:10.1159/000339528
47. van de Zande NA, Massey TH, McLauchlan D, Pryce Roberts A, Zutt R, Wardle M, et al. Clinical characterization of dystonia in adult patients with Huntington's disease. *Eur J Neurol* (2017) 24:1140–7. doi:10.1111/ene.13349

48. Mattingley JB, Husain M, Rorden C, Kennard C, Driver J. Motor role of human inferior parietal lobe revealed in unilateral neglect patients. *Nature* (1998) 392(6672):179–82. doi:10.1038/32413
49. Boecker H, Jankowski J, Ditter P, Scheef L. A role of the basal ganglia and midbrain nuclei for initiation of motor sequences. *Neuroimage* (2008) 39(3):1356–69. doi:10.1016/j.neuroimage.2007.09.069
50. Rupp J, Dzemidzic M, Blekher T, West J, Hui S, Wojcieszek J, et al. Comparison of vertical and horizontal saccade measures and their relation to gray matter changes in premanifest and manifest Huntington disease. *J Neurol* (2012) 259(2):267–76. doi:10.1007/s00415-011-6172-0
51. GTEx-Consortium. Human genomics. The genotype-tissue expression (GTEx) pilot analysis: multitissue gene regulation in humans. *Science* (2015) 348(6235):648–60. doi:10.1126/science.1262110
52. Yohrling GJ, Farrell LA, Hollenberg AN, Cha JH. Mutant huntingtin increases nuclear corepressor function and enhances ligand-dependent nuclear hormone receptor activation. *Mol Cell Neurosci* (2003) 23(1):28–38. doi:10.1016/S1044-7431(03)00032-0
53. Boutell JM, Thomas P, Neal JW, Weston VJ, Duce J, Harper PS, et al. Aberrant interactions of transcriptional repressor proteins with the Huntington's disease gene product, huntingtin. *Hum Mol Genet* (1999) 8(9):1647–55. doi:10.1093/hmg/8.9.1647
54. Jones AL. The localization and interactions of huntingtin. *Philos Trans R Soc Lond B Biol Sci* (1999) 354(1386):1021–7. doi:10.1098/rstb.1999.0454
55. Vital M, Bidegain E, Raggio V, Esperon P. Molecular characterization of genes modifying the age at onset in Huntington's disease in Uruguayan patients. *Int J Neurosci* (2016) 126(6):510–3. doi:10.3109/00207454.2015.1036422
56. Chiu FL, Lin JT, Chuang CY, Chien T, Chen CM, Chen KH, et al. Elucidating the role of the A2A adenosine receptor in neurodegeneration using neurons derived from Huntington's disease iPSCs. *Hum Mol Genet* (2015) 24(21):6066–79. doi:10.1093/hmg/ddv318
57. Villar-Menendez I, Blanch M, Tyebji S, Pereira-Veiga T, Albasanz JL, Martin M, et al. Increased 5-methylcytosine and decreased 5-hydroxymethylcytosine levels are associated with reduced striatal A2AR levels in Huntington's disease. *Neuromolecular Med* (2013) 15(2):295–309. doi:10.1007/s12017-013-8219-0
58. Raskovalova T, Huang X, Sitkovsky M, Zacharia LC, Jackson EK, Gorelik E. Gs protein-coupled adenosine receptor signaling and lytic function of activated NK cells. *J Immunol* (2005) 175(7):4383–91. doi:10.4049/jimmunol.175.7.4383
59. Cooper GM. Pathways of intracelluar signal transduction. 2nd ed. *The Cell: A Molecular Approach*. Sunderland, MA: Sinauer Associates Inc (2000).

Conflict of Interest Statement: The authors declare that the research was conducted in the absence of any commercial or financial relationships that could be construed as a potential conflict of interest.

frontiers in Neurology

BRIEF RESEARCH REPORT
published: 30 May 2018
doi: 10.3389/fneur.2018.00394

Early Gray Matter Volume Loss in MAPT H1H1 *de Novo* PD Patients: A Possible Association With Cognitive Decline

Frederic Sampedro[1,2,3], *Juan Marín-Lahoz*[1,2,3], *Saul Martínez-Horta*[1,2,3], *Javier Pagonabarraga*[1,2,3] *and Jaime Kulisevsky*[1,2,3]*

[1] Movement Disorders Unit, Neurology Department, Hospital de la Santa Creu i Sant Pau, Barcelona, Spain, [2] Biomedical Research Institute (IIB-Sant Pau), Barcelona, Spain, [3] Centro de Investigación Biomédica en Red Enfermedades Neurodegenerativas, Madrid, Spain

The MAPT H1 haplotype has been identified as a predictor of cognitive decline in Parkinson's disease (PD). However, its underlying pathological mechanisms have not been fully established. In this work, using a cohort of 120 *de novo* PD patients with preserved cognition from the Parkinson's Progression Markers Initiative (PPMI) database, we found that patients who were homozygous for MAPT H1 had less gray matter volume (GMV) and greater 1-year GMV loss than patients without this genetic profile. Importantly, these changes were associated with a longitudinal worsening of cognitive indicators. Our findings suggest that early GMV loss in MAPT H1H1 PD patients increases their risk to develop cognitive decline.

Keywords: MAPT, T1-MRI, cognitive decline, Parkinson's disease, gray matter volume

OPEN ACCESS

Edited by:
Christian Gaser, Friedrich-Schiller-Universität-Jena, Germany

Reviewed by:
Cristoforo Comi, Università degli Studi del Piemonte Orientale, Italy
Tien K. Khoo, Griffith University, Australia
Bogdan O. Popescu, Carol Davila University of Medicine and Pharmacy, Romania

***Correspondence:**
Jaime Kulisevsky
jkulisevsky@santpau.cat

Specialty section:
This article was submitted to Applied Neuroimaging, a section of the journal Frontiers in Neurology

Received: *18 April 2018*
Accepted: *14 May 2018*
Published: *30 May 2018*

Citation:
Sampedro F, Marín-Lahoz J, Martínez-Horta S, Pagonabarraga J and Kulisevsky J (2018) Early Gray Matter Volume Loss in MAPT H1H1 de Novo PD Patients: A Possible Association With Cognitive Decline. Front. Neurol. 9:394. doi: 10.3389/fneur.2018.00394

INTRODUCTION

Cognitive decline is a core non-motor symptom of Parkinson's disease (PD). Given its high prevalence and negative impact on the patient's quality of life, identifying early prognostic markers of cognitive impairment in this population can help develop a person-centered care plan and achieve optimal clinical management (1).

Several genetic variants have been linked to cognitive impairment in PD. In particular, the MAPT H1 haplotype has been associated with an increased risk for the development of dementia in this population (2). The microtubule-associated protein tau (MAPT) gene is located on chromosome 17q21, where an inversion polymorphism of approximately 900 kb defines two haplotypes, H1 and H2. However, the underlying pathological mechanisms responsible for the association of this genetic variant and cognitive decline in PD remain poorly understood.

Here we hypothesize that, among recently diagnosed PD patients with preserved cognition, those with MAPT H1 homozygosis will exhibit a differential cross-sectional or longitudinal gray matter volume (GMV) pattern that could make them more prone to develop cognitive decline than patients without this genetic condition.

Using the data from the Parkinson's Progression Markers Initiative (PPMI), we aimed to validate our hypothesis using structural MRI and MAPT genotyping from *de-novo*, untreated and cognitively preserved PD patients. The PPMI is a large observational study that offers a superb framework to analyze cross-sectional and longitudinal biomarker interactions in early PD patients (3).

MATERIALS AND METHODS

Sample

A hundred and twenty PD patients were considered for this study. The inclusion criteria were: *de novo*, untreated, cognitively preserved [MoCA $\geq$ 26 (4)] and non-depressed [GDS-15 $\leq$ 7 (5)] PD patients who had a baseline T1-MRI and MAPT H1 haplotype status (rs17649553, which is in linkage disequilibrium with the H1 haplotype). We defined two groups of patients: those with MAPT H1 homozygosis ($N = 79$) and MAPT H2 carriers ($N = 41$). A 1-year follow-up T1-MRI scan was also available for 96 (64 MAPT H1H1) participants.

Assessments

To isolate the possible effects of the MAPT H1 homozygosis on brain structure and cognitive decline, we considered the presence of other demographic, clinical, neuropsychological, and biological variables that could act as confounding factors known to affect brain structure and cognition (**Table 1**).

We also investigated whether the MAPT haplotype was related to the longitudinal development of cognitive decline, which was defined as showing a MoCA score <26 (5) throughout a 4-year follow-up period.

Details about the considered clinical scales, genotyping, image acquisition, and other biological variables are available at http://www.ppmi-info.org/.

T1-MRI Neuroimaging Methods

To study baseline gray matter volume (GMV) differences related to the MAPT H1H1 profile, we applied a standard GMV voxel-based morphometry (VBM) pipeline using SPM12 (http://www.fil.ion.ucl.ac.uk/spm/). T1-MRI scans were segmented and their associated GMV maps were then spatially normalized to the Montreal Neurological Institute (MNI) space using DARTEL. A Gaussian smoothing of 8 mm FWHM was applied to the resulting images.

To analyze differences in 1-year gray matter volume loss across groups, we used the SPM12 longitudinal VBM pipeline. Processing steps were pairwise registration, computation of Jacobian difference images (restricted to gray matter), and subsequent normalization to MNI space using DARTEL.

The resulting set of preprocessed GMV and GMV loss maps were entered into a voxelwise two-sample *t*-test analysis to study differential patterns related to MAPT H1 homozygosis. Age, sex, education, and total intracranial volume (TIV) were used as covariates of no interest. Results were considered significant at $p < 0.005$, uncorrected with a minimum cluster size of 50 voxels. Only cerebral regions in the MNI space with an a priori GM probability greater than 0.4 were considered.

Finally, aiming to study whether the obtained imaging results were related to cognitive progression, we correlated GMV and GMV-loss values at the identified clusters with the 4-year decrease in total MoCA score.

RESULTS

As seen in **Table 1**, no significant basal differences between MAPT groups were found ($p < 0.05$), ruling out the presence of confounding factors that could indirectly compromise brain integrity in the H1H1 group. Ninety-five percentage of the sample is Caucasian.

In terms of cognitive progression, we found that 58% of patients with MAPT H1 homozygosis developed cognitive decline over a 4-year follow-up period. This percentage was 36% for MAPT H2 carriers. Therefore, H1 homozygotes had an increased relative risk of 1.6 (CI 95%; 0.7–3.6) to develop cognitive decline with respect to H2 carriers. In this sample, the Delayed Recall and Visuospatial domains were the ones that became most commonly compromised in the set of patients that converted to cognitive impairment.

Figure 1 shows the brain areas where MAPT H1 homozygotes showed cross-sectional and longitudinal gray matter volume differences with respect to the other genotypes.

Significant correlations were found between the GMV values at the identified clusters and the 4-year decrease in total MoCA score: left superior temporal GMV ($r = -0.23$, $p = 0.025$), left middle frontal gyrus GMV ($r = -0.24$, $p = 0.021$), right frontal inferior operculum GMV ($r = -0.26$, $p = 0.014$), and left parahippocampal GMV loss ($r = 0.29$, $p = 0.011$).

DISCUSSION

Here we investigated whether an early reduction in cerebral GMV could be a mechanism by which PD patients with MAPT H1 homozygozis have an increased risk to develop cognitive decline. In this group, we found a cross-sectional GMV reduction and an increased GMV loss over a 1-year period. Frontal and parieto-temporal areas were involved. These areas are known to play a major role in the emergence of mild cognitive impairment and its progression to dementia in PD (6).

The observed GMV compromise was associated in a unidirectional manner with the H1H1 group, without evidence of structural compensatory mechanisms. Importantly, GMV values in several of the obtained clusters were associated with a longitudinal decrease in MoCA scores.

Our results suggest that in PD, harboring the MAPT H1H1 genotype is associated with an early decrease in GMV, even in cognitively preserved patients, possibly making this population more prone to cognitive decline. A biological explanation for this observation could be related to an increased 4-repeat tau transcription associated with the H1 haplotype in PD brains, since this isoform has been suggested as the pathogenic driver (7, 8).

The effect of the MAPT H1 haplotype on brain function in PD patients and in control subjects has been addressed previously using functional MRI (9, 10). It was observed that subjects in the PD group and those in the control group with H1 homozygotes had an altered activation pattern while

TABLE 1 | Demographic, clinical, neuropsychological, and biomarker values for the two MAPT groups at baseline.

	MAPT H1H1 ($n = 79$)	MAPT H1H2/H2H2 ($n = 41$)	Significance (p-value)
Age [years]	60.1 ± 9.5	61.5 ± 9.9	0.45
Sex [Female/Male]	30/49	17/24	0.71 X^2
Education [years]	15.35 ± 2.9	15.68 ± 2.9	0.57
Months since PD diagnosis	7.2 ± 7.7	6.5 ± 6.7	0.61
UPDRS-III	20.2 ± 9.2	19.9 ± 7.2	0.84
GDS-15	4.99 ± 1.1	5.1 ± 1.4	0.64
MoCA	28.3 ± 1.4	28.4 ± 1.2	0.67
BJLO	13.04 ± 2.1	12.6 ± 2.1	0.32
HVLT Delayed free recall	8.6 ± 2.8	9.5 ± 1.7	0.08
HVLT Total recall	25.2 ± 5.1	26.7 ± 4.3	0.09
Numbers and Letters	11.3 ± 2.5	10.5 ± 2.8	0.11
Semantic Fluency	21.6 ± 5.1	20.9 ± 4.7	0.47
SDMT	43.1 ± 9.8	41.4 ± 8.9	0.37
Phonetic Verbal Fluency	13.3 ± 4.4	12.6 ± 4.3	0.38
DATSCAN	1.3 ± 0.4	1.3 ± 0.4	0.73
CSF Aβ42 [pg/ml]	366.9 ± 93.9	370.3 ± 105.5	0.87
CSF tau [pg/ml]	44.7 ± 18.2	46.5 ± 18.8	0.61
CSF p-tau [pg/ml]	16.5 ± 10.2	16.9 ± 9.9	0.83
CSF α-Synuclein [pg/ml]	1774.7 ± 617.9	1927.5 ± 834.6	0.31
APOE4 (APOE4+/APOE4−)	24/46	10/27	0.44 X^2

To examine differences across groups, t-test analyses were used for continuous variables and X^2 for categorical measures. UPDRS-III: total motor score for the Unified Parkinson's disease rating scale GDS-15: Geriatric Depression Scale (15-item), MoCA, Montreal Cognitive Assessment (MoCA) [total score]; BJLO, Benton Judgment of Line Orientation [total score]; HVLT, Hopkins Verbal Learning Test; SDMT, Symbol Digit Modality Test [total score]; DATSCAN, average striatal binding ratios of the caudate and putamen regions. BJLO, HVLT, DLY, HVLT SUM, LETNUM, SEMFLU, SDMT data were available for 119 participants. CSF Aβ42 and CSF α-Synuclein for 118 participants, CSF tau and p-tau for 116 participants, DATSCAN for 112 participants, and APOE4 status for 107 participants.

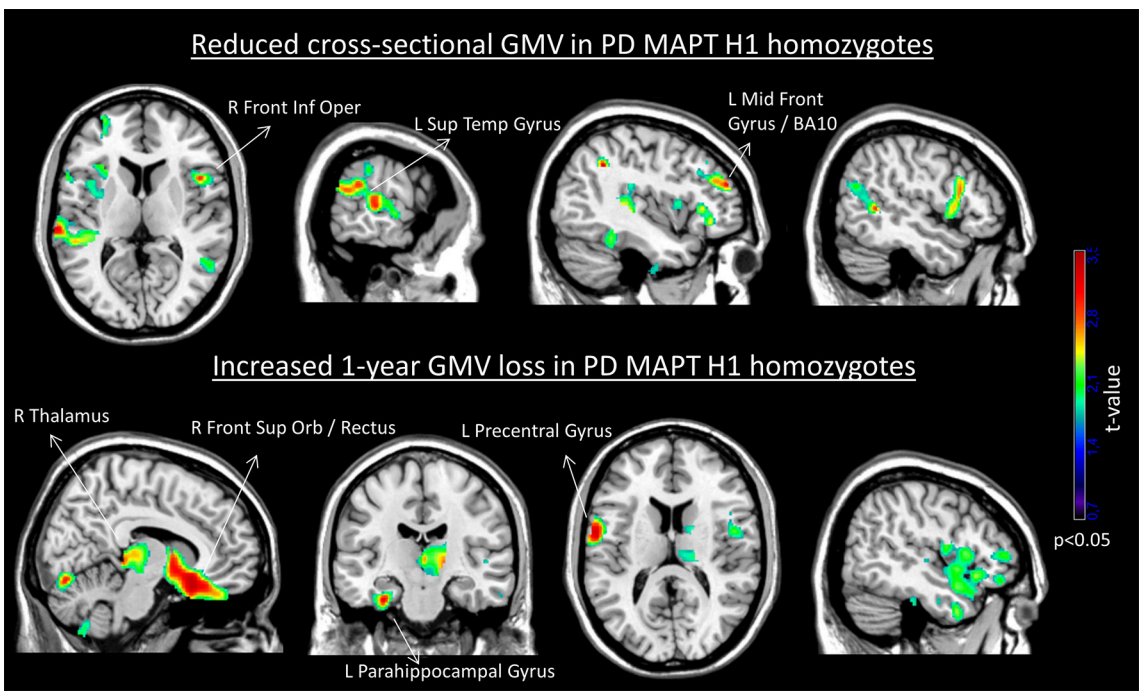

FIGURE 1 | Cross-sectional reduced gray matter volume **(Top)** and increased 1-year GMV loss **(Bottom)** in the MAPT H1H1 group. For depiction purposes, results are displayed using $p < 0.05$ uncorrected and minimum cluster size (k) of 500 voxels. The set of labeled clusters survived a significance of $p < 0.005$ uncorrected and $k = 50$ voxels. No significant regions of increased gray matter volume or lower GMV loss were obtained in the H1H1 group.

performing cognitive tasks. Furthermore, in line with our results, structural brain differences were found in healthy H1H1 subjects (11). Hence, our findings suggest that the potential underlying pathological mechanism of this genetic variant is shared across the spectrum of healthy subjects, individuals with Parkinson's disease, and people with other types of dementia (12).

Limitations of this work include the absence of a control sample and the use of MoCA scores to evaluate cognitive status. Even though this tool has shown some performance limitations in cognitive testing (4), it is commonly used in PD and is the only global and quantitative cognitive assessment available in PPMI. Additionally, in the light of the imaging results described here, further study into the particular relationship of this genetic variant and the worsening of specific cognitive domains and neuropsychological functions in PD could establish more specific clinical implications related to these findings.

To conclude, the present work reports a set of structural brain changes associated with MAPT H1 homozygosis in PD which may increase the risk of developing cognitive decline in this population. This observation sparks the need to further study the mechanisms by which tau transcription schemes could be responsible for a brain structural compromise in the early stages of PD.

AUTHOR CONTRIBUTIONS

FS, JP, and JK conception or design of the work. FS, JM-L, and SM-H data analysis and interpretation. FS, JM-L, and SM-H drafting the article. JP and JK critical revision of the article.

FUNDING

This work was partially supported by CERCA and CIBERNED funding, and grants from la Marató de TV3 (2014/U/477 and 20142910) and Fondo de Investigaciones Sanitarias del Ministerio de Sanidad y Consumo (PI15/00962 and PI14/02058).

ACKNOWLEDGMENTS

Data used in the preparation of this article were obtained from the Parkinson's Progression Markers Initiative (PPMI) database (www.ppmi-info.org/data). For up-to-date information on the study, visit www.ppmi-info.org.

PPMI—a public-private partnership—is funded by the Michael J. Fox Foundation for Parkinson's Research and funding partners, including Abbvie, Avid Radiopharmaceuticals, Biogen Idec, BioLegend, Bristol-Myers Squibb, Eli Lilly & Co., GE Healthcare, Genentech, GlaxoSmithKline, Lundbeck, Merck, MesoScale Discovery, Pfizer, Piramal, Roche, Sanofi Genzyme, Servier, Takeda, Teva, and UCB.

REFERENCES

1. Aarsland D, Larsen JP, Tandberg E, Laake K. Predictors of nursing home placement in Parkinson's disease. *J Am Geriatr Soc*. (2000) **48:**938–42. doi: 10.1111/j.1532-5415.2000.tb06891.x
2. Setó-Salvia N, Clarimón J, Pagonabarraga J, Pascual-Sedano B, Campolongo A, Combarros O, et al. Dementia risk in Parkinson disease: disentangling the role of MAPT haplotypes. *Arch Neurol*. (2011) **68:**359–64. doi: 10.1001/archneurol.2011.17
3. Marek K, Jennings D, Lasch S, Siderowf A, Tanner C, Simuni T, et al. The Parkinson Progression Marker Initiative (PPMI). *Prog Neurobiol*. (2011) **95:**629–35. doi: 10.1016/j.pneurobio.2011.09.005
4. Dalrymple-Alford J, MacAskill M, Nakas C, Livingston L, Graham C, Crucian G, et al. The MoCA: wellsuited screen for cognitive impairment in Parkinson disease. *Neurology* (2010) **75:**1717–25. doi: 10.1212/WNL.0b013e3181fc29c9
5. Weintraub D, Oehlberg KA, Katz IR, Stern MB. Test characteristics of the 15-item geriatric depression scale and hamilton depression rating scale in Parkinson disease. *Am J Geriatr Psychiatry* (2006) **14:**169–75. doi: 10.1097/01.JGP.0000192488.66049.4b
6. Pagonabarraga J, Kulisevsky J. Cognitive impairment and dementia in Parkinson's disease. *Neurobiol Dis*. (2012) **46:**590–96. doi: 10.1016/j.nbd.2012.03.029
7. Williams-Gray CH, Evans JR, Goris A, Foltynie T, Ban M, Robbins TW, et al. The distinct cognitive syndromes of Parkinson's disease: 5 year follow-up of the CamPaIGN cohort. *Brain* (2009) **132:**2958–69. doi: 10.1093/brain/awp245
8. Myers AJ, Pittman AM, Zhao AS, Rohrer K, Kaleem M, Marlowe L, et al. The MAPT H1c risk haplotype is associated with increased expression of tau and especially of 4 repeat containing transcripts. *Neurobiol Dis*. (2007) **25:**561–70. doi: 10.1016/j.nbd.2006.10.018
9. Nombela C, Rowe J, Winder-Rhodes S, Hampshire A, Owen AM, Breen DP, et al. Genetic impact on cognition and brain function in newly diagnosed Parkinson's disease: ICICLE-PD study. *Brain* (2014) **137:**2743–58. doi: 10.1093/brain/awu201
10. Winder-Rhodes SE, Hampshire A, Rowe JB, Peelle JE, Robbins TW, Owen AM, et al. Association between MAPT haplotype and memory function in patients with Parkinson's disease and healthy aging individuals. *Neurobiol Aging* (2015) **36:**1519–28. doi: 10.1016/j.neurobiolaging.2014.12.006
11. Canu E, Boccardi M, Ghidoni R, Benussi L, Testa C, Pievani M, et al. H1 haplotype of the MAPT gene is associated with lower regional gray matter volume in healthy carriers. *Eur J Hum Genet*. (2009) **17:**287–94. doi: 10.1038/ejhg.2008.185
12. Pastor P, Moreno F, Clarimón J, Ruiz A, Combarros O, Calero M, et al. MAPT H1 Haplotype is Associated with Late-Onset Alzheimer's Disease Risk in APOE?4 Noncarriers: results from the dementia genetics spanish consortium. *J Alzheimers Dis*. (2016) **49:**343–52. doi: 10.3233/JAD-150555

Conflict of Interest Statement: The authors declare that the research was conducted in the absence of any commercial or financial relationships that could be construed as a potential conflict of interest.

frontiers in Neurology

ORIGINAL RESEARCH
published: 22 March 2019
doi: 10.3389/fneur.2019.00267

Why Is Aging a Risk Factor for Cognitive Impairment in Parkinson's Disease?—A Resting State fMRI Study

Atsuko Nagano-Saito[1,2], Pierre Bellec[1,3], Alexandru Hanganu[1,3,4,5], Stevan Jobert[1], Béatriz Mejia-Constain[1], Clotilde Degroot[1,2], Anne-Louise Lafontaine[2,6,7,8], Jennifer I. Lissemore[2], Kelly Smart[2], Chawki Benkelfat[2] and Oury Monchi[1,2,3,4,5,8]**

[1] Centre de Recherche, Institut Universitaire de Gériatrie de Montréal, Montreal, QC, Canada, [2] Department of Neurology & Neurosurgery, and Psychiatry, McGill University, Montreal, QC, Canada, [3] Université de Montréal, Montreal, QC, Canada, [4] Cumming School of Medicine, Hotchkiss Brain Institute, Calgary, AB, Canada, [5] Department of Clinical Neurosciences and Department of Radiology, University of Calgary, Calgary, AB, Canada, [6] Movement Disorders Unit, McGill University Health Center, Montreal, QC, Canada, [7] Department of Neurology, Montreal Neurological Hospital, Montreal, QC, Canada, [8] Centre Hospitalier de l'Université de Montréal, Montreal, QC, Canada

OPEN ACCESS

Edited by:
Huifang Shang,
Sichuan University, China

Reviewed by:
Ruey-Meei Wu,
National Taiwan University, Taiwan
Matteo Bologna,
Sapienza University of Rome, Italy

***Correspondence:**
Atsuko Nagano-Saito
atsuko.nagano@gmail.com
Oury Monchi
oury.monchi@ucalgary.ca

Specialty section:
This article was submitted to Movement Disorders, a section of the journal Frontiers in Neurology

Received: 01 October 2018
Accepted: 27 February 2019
Published: 22 March 2019

Citation:
Nagano-Saito A, Bellec P, Hanganu A, Jobert S, Mejia-Constain B, Degroot C, Lafontaine A-L, Lissemore JI, Smart K, Benkelfat C and Monchi O (2019) Why Is Aging a Risk Factor for Cognitive Impairment in Parkinson's Disease?—A Resting State fMRI Study. Front. Neurol. 10:267. doi: 10.3389/fneur.2019.00267

Using resting-state functional MRI (rsfMRI) data of younger and older healthy volunteers and patients with Parkinson's disease (PD) with and without mild cognitive impairment (MCI) and applying two different analytic approaches, we investigated the effects of age, pathology, and cognition on brain connectivity. When comparing rsfMRI connectivity strength of PD patients and older healthy volunteers, reduction between multiple brain regions in PD patients with MCI (PD-MCI) compared with PD patients without MCI (PD-non-MCI) was observed. This group difference was not affected by the number and location of clusters but was reduced when age was included as a covariate. Next, we applied a graph-theory method with a cost-threshold approach to the rsfMRI data from patients with PD with and without MCI as well as groups of younger and older healthy volunteers. We observed decreased hub function (measured by degree and betweenness centrality) mainly in the medial prefrontal cortex (mPFC) in older healthy volunteers compared with younger healthy volunteers. We also found increased hub function in the posterior medial structure (precuneus and the cingulate cortex) in PD-non-MCI patients compared with older healthy volunteers and PD-MCI patients. Hub function in these posterior medial structures was positively correlated with cognitive function in all PD patients. Together these data suggest that overlapping patterns of hub modifications could mediate the effect of age as a risk factor for cognitive decline in PD, including age-related reduction of hub function in the mPFC, and recruitment availability of the posterior medial structure, possibly to compensate for impaired basal ganglia function.

Keywords: Parkinson's disease, mild cognitive impairment, age, functional connectivity, cognition, neuroimaging (functional)

INTRODUCTION

In Parkinson's disease (PD), cognitive deficits are frequently present even in the early course of disease development (1). It has been reported that up to 40% of patients with PD have mild cognitive impairment (MCI) (2). Furthermore, patients with PD and MCI have a higher risk of developing dementia compared with patients who do not have MCI (3). In patients with MCI, deficits are neither severe enough to interfere considerably with daily life nor reach criteria for dementia (recent guidelines for MCI diagnosis in PD) (4), but the early presence of MCI in PD has a significant effect on the incidence of dementia at later stages of PD (5, 6). Aging is a risk factor for MCI in PD. Having MCI in PD was associated with older age at assessment and at disease onset (7). Aging is also the strongest predictive factor of dementia in PD patients (2). Untangling the effect of the neuro-degeneration of PD from the effects of regular aging is important for further understanding the functional connectivity in PD patients associated with cognitive deficits. A recent study support this, showing a strong effect of aging on PD patients' cognition (8).

Various studies related to resting-state functional MRI (rs-fMRI) involving PD patients have been published to date (9–11), but discrepancies in brain connectivity findings have been frequently observed. For example, in PD patients, both decreased (12–14) and increased (12, 15–17) cortico-striatal connectivity have been observed. The discrepancy could be related to clinical differences in the patient samples (e.g., cognitive, emotional, motor dysfunctional states, but also age). However, methodological differences might also induce discrepancies. Moreover, even when using the same approach (e.g., comparison of the connectivity strength between brain regions), selection of the brain regions (location and number) could affect the results (18).

The application of graph theory methods to brain imaging data is a simple and powerful mathematical framework for the characterization of topological features of brain networks (19, 20). Intrinsic patterns of functional connectivity in the human have been established, such as in the visual, auditory, somatosensory-motor, task-control, attention, and default mode networks (21–23). When the brain network is designed to be calculated on binary graphs with graph theory approaches, highly connected regions in networks with other regions in the brain are defined as hubs, including the "provincial hubs" (indicating more local connectivity) and "connector hubs" (indicating long range connectivity between different brain networks). A previous study with younger people using graph theory revealed that each intrinsic network (or module) connects each other via specific connector hubs, including medial structures such as the medial prefrontal cortex (mPFC), anterior and posterior cingulate cortex, and medial posterior parietal cortex (24–26). The connectivity between the anterior and posterior medial cortices, and connector hub function of the prefrontal cortex is lowered in older people (27, 28).

The basal ganglia is known to receive many connections from most of the cortex (29), and considered to function by integrating different modules (30, 31). Therefore, one might think that the basal ganglia can act as connector hubs, which have many numbers of the connectivity during resting-state. However, in a previous analysis the basal ganglia did not emerge as a hub in both younger and older healthy individuals, with only limited number of connectivity with other brain regions (28), although this region acts as a "module connector," supporting connectivity between different networks. Our previous studies indicated that the cortico-striatal connectivity increased significantly while performing a cognitive task (32), plausibly acting to link separate networks in a task-dependent manner (33). The nigrostriatal dopaminergic pathology in PD patients (34) could result in impairments of this network-integration function (33). In our longitudinal study with PD patients, increased activation in medial cortical structures (e.g., the mPFC and the precuneus) during a cognitive task was observed both in PD-non-MCI and PD-MCI when they performed an executive task at the second time, compared to the first time point (35). One possibility is that these medial regions are recruited in PD patients to compensate for the loss of "module connector" function of the basal ganglia seen in healthy people.

Here, we aimed to investigate the connectivity change PD patients associated with MCI and aging, in two steps. In the first step, we analyzed rs-fMRI data of three groups, Older healthy volunteers (OHV), PD-non-MCI, and PD-MCI, which were collected with the same scanning protocol. The bootstrap analysis of stable cluster (BASC) method (36) was applied in a data-driven way, to see the impact of selection of "*clusters,*" in the brain. Then, the connectivity strength of each cluster between groups were compared. This allowed to compare the effect of clusters selection at different resolutions and locations. In a second step, using a set of clusters from step 1, we applied a graph-theory approach to data from four groups of interest: PD-non-MCI, PD-MCI, OHV, and young healthy volunteers (YHV), and investigated differences in regional hub function in the brain. We applied the cost-threshold approach adjusting the number of connections in all the participants, rather than connectivity strength-threshold approach, because the former is more stable and relevant in the analysis of connectivity "patterns" between different populations (33, 37, 38). Together these analyses allowed us to explore the independent and overlapping relationships among aging, pathology, cognitive capability, and brain connectivity in PD. We predicted that the connectivity results would reflect the importance of age as an important factor for cognitive deficits in PD.

METHODS

Subjects

Thirty-five non-demented PD patients at stages I and II of Hoehn and Yahr (mean age ± SD, 66.2 ± 7.6 years; range, 50–85; 20 male and 15 female patients) were recruited and subsequently divided into two groups: those with MCI (PD-MCI; $n = 15$) and those cognitively intact (PD-non-MCI, $n = 20$). The sample size was determined based on our previous study of functional MRI, comparing the PD-non-MCI vs. PD-MCI (19 vs. 14) (39). Inclusion criteria for MCI were based on the Movement Disorder Society Task Force guideline for PD (6),

based on five cognitive domains (**Table 1**). Objective evidence of cognitive decline defined as performance (1) standard deviation below the standardized mean (taking into account age and sex) in at least two measures within the same cognitive domain of the neuropsychological assessment. (2) Subjective complaint about cognitive decline by the patient or accompanying person; (3) Absence of significant decline in daily living activities; and (4) Absence of dementia. PD patients underwent cognitive assessment and fMRI and took their usual level of dopaminergic medication during these sessions. As a control group, 21 non-MCI older volunteers (mean age ± SD, 70.0. ± 5.4 years; range, 62–78; 5 male and 16 female patients) were recruited, and also underwent cognitive assessment and MRI within 2 weeks of each other. The same criteria were used in the control group, including a neuropsychological assessment to exclude the presence of MCI.

Demographic details are given in **Table 2**. A significant difference in age occurred between the PD-non-MCI and PD-MCI (**Table 2**). Matching for age of PD-non MCI and PD-MCI, however, might induce a recruitment bias, as many studies indicate that PD patients with MCI are generally older than PD-non MCI (2, 7, 8). Here, we opted for another strategy to investigate the effect of age, we added a young healthy group allowing us to investigate of age vs. the effect of disease. Of note, UPDRS scores for six PD patients (PD-non-MCI; 3, PD-MCI; 3) were missing.

rsfMRI data from 30 young participants (mean age ± SD, 23.8 ± 3.17 years; range, 20–30; 14 male and 16 female) were obtained. The data was collected for two other studies [Transcranial magnetic stimulation, $n = 16$, (not published), and positron emission tomography (PET), $n = 14$ (40)].

Resting-State fMRI Acquisition

All participants were scanned with 3T Siemens TIM MRI scanners at the Institut Universitaire de Gériatrie de Montréal (OHV, PD-non-MCI, PD-MCI, and YHV-TBS), and at the McConnell Brain Imaging Center, Montreal Neurological Institute, McGill University (YHV-PET). Sessions began with high-resolution, T1-weighted, 3D volume acquisition for anatomic localization (voxel size 1 mm^3), followed by "resting-state" echo-planar T2*-weighted image acquisitions with BOLD contrast. The parameters for echo-planar T2*-weighted images were different; for OHV, PD-non-MCI, and PD-MCI, TR = 2.6 s, echo time, 30 ms; flip angle, 90°, volume number 150, slice number, 42, matrix size, 64 × 64 pixels; voxel size, 3.4 × 3.4 × 3.4 mm^3; for YHV in TBS study, TR = 2.5 s, echo time, 30 ms; flip angle, 90°, 252 volumes, slice number, 41, matrix size, 64 × 64 pixels; voxel size, 3.5 × 3.5 × 3.5 mm^3; and for YHV in PET study, TR = 2.11 s, echo time, 30 ms; flip angle, 90°, 180 volumes, slice number, 40, matrix size, 64 × 64 pixels; voxel size, 3.5 × 3.5 × 3.5 mm^3. The OHV and PD participants had three runs of T2*-weighted image acquisitions. All scans were used for the first step analysis of comparison of the connectivity strength among the OHV, PD-non-MCI, and PD-MCI groups, but only the first run was used in order to make comparisons with the YHV (who were scanned only once) for the second step analysis using the graph theory approach. During rsfMRI, OHV, PD-non-MCI, PD-MCI, and YHV-TBS groups were presented with a white screen and a black cross in the middle, and YHV-PET participants were presented with a white screen. They were instructed to keep their eyes open (to avoid falling asleep), focus on the cross or white screen, and relax.

Of note, we confirmed that there were no significant differences in network properties (e.g., global and local efficiency, degrees and betweenness centrality of all the clusters, using the methods described below in Step 2) between the two sets of participants, even without correction for multiple comparisons. Therefore, we combined the two data set into one YHV group for this study. All the participants provided informed consent, and the protocol was approved by the Research Ethics Committee of the Regroupement Neuroimagerie Québec.

rsfMRI Data Processing

All the data were pre-processed with the same procedure. We applied the NIAK pre-processing pipeline to the fMRI datasets (41). First, slice timing correction was performed with spline interpolation. After motion correction, slow time drift was removed from the blood oxygen level-dependent (BOLD) time series with a high-pass filter of 0.01 Hz. To avoid possible artificial correlation induced by low-pass filters (42), no low-pass filter was applied. To minimize artifacts due to excessive motion, all time frames showing a displacement > 0.5 mm were removed. A minimum of 40 un-scrubbed volumes per run was required for further analysis, and no scans were removed based on this criterion except the third run of one participant belonging to the PD-non-MCI group. The mean motion-corrected time-averaged functional volume was co-registered with the individual T1 scan (43), then transformed into the ICBM152 space using the acquired parameter at a 3 mm isotropic resolution. The following nuisance covariates were regressed out from fMRI time series: slow time drifts (basis of discrete cosines with a 0.01 Hz high-pass cut-off), average signals in conservative masks of the white matter and the lateral ventricles, and the first 3–10 principal components of the six rigid-body motion parameters and their squares (44, 45). The fMRI volumes were finally spatially smoothed with a 6 mm isotropic Gaussian blurring kernel.

Step 1. Connectivity Strength Between Clusters in OHV, PD-non-MCI, and PC-MCI

Bootstrap Analysis of Stable Clusters (BASC)

We applied the BASC algorithm to identify clusters that consistently exhibited similar spontaneous BOLD fluctuations in individual subjects and were spatially stable across subjects (46). We first applied a region-growing algorithm to reduce each fMRI dataset into a time × space array, with 957 regions (47). BASC replicates a hierarchical Ward clustering 1,000 times and computes the probability that a pair of regions fall in the same cluster, a measure called stability (46). The region × region stability matrix is fed into a clustering procedure to derive consensus clusters, which are composed of regions with a high average probability of being assigned to the same cluster across all replications. At the individual level, the clustering was applied to the similarity of regional time series, which was replicated using a circular block bootstrap. Consensus clustering was applied to the average individual stability matrix to identify group

TABLE 1 | Cognitive assessment.

Cognitive domain	Test	References
Attention	Digit Span	Wechsler, 1997
	Digit Symbol	Wechsler, 1997
Executive	Stroop	Golden and Freshwater, 1998
	Trial Making Test B, Time, and Error	Reitan and Wolfson, 1985
	Brixton	Burgess and Shallice, 1997
	Montreal d'Evaluation de la communication (MEC), Verbal fluency-orthographc criteria subtest	Joanette et al., 2004
Memory	Rey-Osterrieth Figure copy	Osterrieth, 1944
	Rey Auditory Verbal Learning Test (RAVLT)	Schmidt, 1996
	Logical Memory subtest of Wechsler Memory Scale (WMS-III)	Wechsler, 1999
Visuospatial	Hooper test	Hooper, 1958
	Rey-Osterrieth figure copy	Osterrieth, 1944
	Montreal Cognitive Assessment (MoCA), Clock drawing	Nasreddine et al., 2005
Language	MEC, semantic subtest	Joanette et al., 2004
	Boston Naming Test	Kaplan et al., 1983

References for cognitive tasks are shown in the ***Supplementary Information****.*

TABLE 2 | Demography of participants.

Group	OHV	PD-non-MCI	PD-MCI	
Number	21	20	15	
Age	70.0 ± 5.4 (62–78)	63.8 ± 7.4 (50–78)	69.4 ± 6.8 (61–85)	*,***
Sex(M:F)	5:16	10:10	10:5	*, **
Disease duration		6.7 ± 3.5	9.3 ± 5.2	
UPDRS (motor score)		26.7± 12.1 ($n = 17$)	29.9 ± 11.7 ($n = 12$)	
Education	15.5 ± 3.2	15.0 ± 2.2	14.8 ± 2.5	
MoCA	28.2 ± 1.5	28.5 ± 1.6	26.9 ± 2.0	**, ***
BDI-II	4.3 ± 4.2	7.7 ± 5.6	10.1 ± 4.9	*, **
L-DOPA equivalent dosage		496 ± 428	531 ± 394	

*t-test or χ^2-test. *$p < 0.05$ in HV vs. PD-non-MCI. **$p < 0.05$ in HV vs. PD-MCI. ***$p < 0.05$ in PD-non-MCI vs. PD-MCI.*

clusters. The group clustering was replicated via bootstrapping of subjects in the group. A consensus clustering was finally applied on the group stability matrix to generate group consensus clusters. The cluster procedure was carried out at a specific number of clusters (having a corresponding "resolution"). Using a "multiscale stepwise selection" (MSTEPS) method (48), we determined a subset of resolutions that provided an accurate summary of the group stability matrices generated over a fine grid of resolutions: K = [4, 10, 19, 35, 63, 118, 221, 393].

Derivation of Functional Connectomes

For each resolution K, and each pair of distinct clusters, the between-clusters connectivity was measured by the Fisher transform of the Pearson's correlation between the average time series of the clusters. The within-cluster connectivity was the Fisher transform of the average correlation between time series inside the cluster. An individual connectome was thus a K × K matrix.

Statistical Testing

To test for differences between, OHV vs. PD-non-MCI, OHV vs. PD-MCI, and PD-non-MCI vs. PD-MCI at a given resolution, a general linear model (GLM) for each connection between two clusters was applied. A GLM included an intercept, and the average frame displacement of the runs involved in this analysis (without including age as a covariate). In addition, a GLM including age as a covariate was also calculated to see the impact of age on the comparisons. The contrasts of interest (HV vs. PD-non-MCI, HV vs. PD-MCI, and PD-non-MCI vs. PD-MCI) was represented by a dummy covariate coding the difference in average connectivity between the two groups.

The false-discovery rate (FDR) across connections was controlled at qFDR $\leq$0.05 (49). We assessed the impact of that parameter by replicating the GLM analysis at the eight resolutions selected by MSTEPS. We implemented an omnibus test (family-wise error rate $\alpha \leq 0.05$) to assess the overall presence of significant differences between groups, pooling FDR results across all resolutions (18). If the omnibus test across resolutions was not significant, then no test would be deemed significant. Since this omnibus test was significant, we used the FDR threshold of $q \leq 0.05$ to explore single resolutions.

Step 2. Graph Theory Methodology

To investigate the between-network functional connectivity of the brain using a cluster-based method, a graph theory approach was applied (50). The same set of functional clusters ($n = 118$) as in step one was used. This set was selected because it included the maximal number of the clusters which showed significant differences between the PD-non-MCI and PD-MCI (see Results). The time series of the BOLD signal of each cluster, which was considered as a node in graph theory approach, were extracted for each participant. Then, the Pearson correlations were calculated between each pair of the 118 clusters, resulting in a symmetric 118 × 118 correlation matrix. We then applied a cost-threshold approach to the correlation matrix, as in our previous studies (33, 37). The cost is defined as the ratio between the actual number of connections and the maximum number of possible connections between every two clusters. As a function of cost, network features, such as global, local, cost efficiencies, were calculated. Global efficiency is an index of inverse path length, defined by an average minimum number of connections that link any two nodes of the network, and indicates the efficiency of information transfer among different brain regions (50). The cost efficiency is defined as "global efficiency—cost," and it is assumed that the brain operates optimally with the maximum cost efficiency, maximizing information transfer (24, 50). As a function of the cost between 0.5 and 50% with 0.5% step, cost efficiency was calculated to examine the economical cost, while maximizing cost efficiency. This process was identical to our previous study (33). We also confirmed the small-worldness with a parameter "omega," which is typically near 0 for networks with small-world properties (51). The average cost efficiency in each group was maximized which resulted in a range between 19.5 and 22%, depending on the group (YHV, 19.5%; OHV, 22.0%, PD-non-MCI, 20.0%; PD-MCI, 21.5%). Therefore, we used the cost (18–24%) with 0.5% step, where the omega was between −0.03 and 0.07 in all the groups, to generate whole brain networks with the 118 clusters. With each of the 13 costs, network features (degree, and between centrality, see below) were calculated and averaged individually, for further analysis. Graphs of the "cost efficiency" and omega, as the function of the cost are shown in **Figure S1**.

In graph theory analysis, degree is the number of connections attached to a given node in a designed binary graphed brain network, and betweenness centrality is the total number of all shortest paths linking to the given node (52). Hubs are nodes with high degree, or high centrality (19). For each cluster, in each participant, first, the degrees were calculated. We selected all the clusters which indicated more than mean + 1S.D. of all the clusters of all the subjects, at least in one group, considering them as hubs (53). Using these selected clusters, the betweenness centrality was also calculated. This was added based on the hypothesis that if the hub regions function effectively for the information transfer in the brain network, the nodes also have high betweenness centrality. In addition to the hub clusters, we examined clusters located in the basal ganglia (caudate, putamen, and globus pallidus) and hippocampus, because they are considered as important regions for integrating information from different brain modules (30, 54), and we have observed that they are the key regions of cognitive decline in PD patients (39, 55, 56). The total cluster number was 14 (**Figure 1**).

Group Difference of Degree and Betweenness Centrality

To examine the impact of pathology, age, and cognition separately, group difference (YHV vs. OHV, OHV vs. PD-non-MCI, PD-non-MCI vs. PD-MCI) of the degree and the betweenness centrality were investigated with student t-test in each hub-cluster. For the comparisons of OHV vs. PD-non-MCI and PD-non-MCI vs. PD-MCI, analyses including age as a covariate, were also performed applying a general linear model. Multiple comparisons with the selected clusters ($n = 14$) was applied and a significance threshold was determined at pFDR < 0.05. Predicted regions which have been linked to PD pathology and/or cognitive deficits in PD (e.g., caudate, globus pallidus, putamen, hippocampus, mPFC, posterior cingulate cortex, and precuneus) were also reported without multiple comparison correction using a threshold of $p < 0.05$.

Demographic Impact on Group Difference of Degree in Precuneus and Cingulate Cortex

Studies indicate that cognition in PD patients is associated not only with age, but also gender, depression, education, and

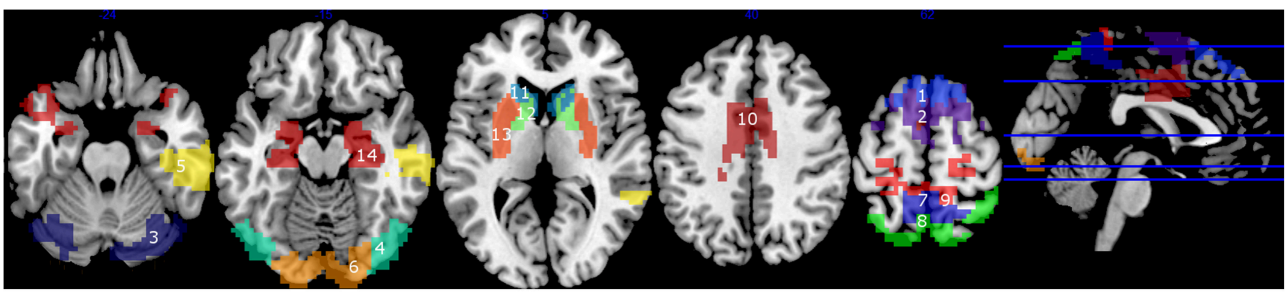

FIGURE 1 | Clusters with high degrees (> mean + 1 S.D.) (1–10), and the clusters in the basal ganglia and the hippocampus (11–14). 1, mPFC1; 2, mPFC2; 3, Cerebellum; 4, Middle Temporal; 5, right Temporal; 6, Occipital; 7, Precuneus1; 8, Precuneus2; 9, Precuneus+Primary Motor Area; 10, Cingulate Gyrus; 11, Caudate; 12, Globus pallidus; 13, Putamen; 14, Hippocampus.

severity of motor symptoms (7, 8). Accordingly, there also existed group difference between the PD-non-MCI and PD-MCI, in sex, and Beck's Depression Inventory II (BDI-II, as an index of depression), but not in education or UPDRS motor scores. It should be noted that UPDRS data were missing in six participants. We also performed the analyses described below on the 29 patients and found similar results as with the full 35 PD patients. Here, we only report the results with the full PD group.

Among the observations in the above section of "*Group difference of degree and betweenness centrality*," we were especially interested in the clusters (the precuneus and the cingulate cortex), which showed increased degrees in the PD-non-MCI compared to the OHV. To see the impacts of age, sex, and BDI-II, on the degrees in the clusters, we further performed group comparisons (OHV, PD-non-MCI, and PD-MCI), dividing each group into two subgroups according to age (younger vs. older), sex (male vs. female), and BDI-II (lower vs. higher), separately. Thresholds for dividing a group were set at 67.6 for the age, and 6.9 for the BDI-II. They were determined at the average of the whole groups (see **Table 4**). The average of the degree of the precuneus and the cingulate cortex (**Figure 1**, # 7, 8, 9 10) was calculated for each participant. Then the averaged degree was compared with two types of two-way ANOVA (group × subgroup), and two types of *t*-tests. One type of the ANOVA was with three groups (OHV, PD-non-MCI, and PD-MCI) × two subgroups of age, sex, and BDI, separately. The other type was with two groups (OHV and PD-non-MCI) × two subgroups of age, sex, and BDI-II, separately. Simple *t*-tests of OHV vs. PD-non-MCI, and PD-non-MCI vs. PD-MCI, were performed in each subgroup.

Significant threshold was set at $p < 0.05$.

Correlation Between Degree and Cognitive Function

We hypothesized that the regions with significant difference in the group comparisons above are associated with cognitive performance. Therefore, correlation analysis between the degree and/or betweenness centrality of the regions, with the mean Z-scores of the five cognitive domains (attention, executive, memory, visuospatial, and language; see **Table 1** for detail), was performed, in OHV and PD groups, separately. For the OHV, four regions (clusters # 1, 2, 12, 14, corresponding to the mPFC1 and 2, globus pallidus, and hippocampus) were selected based on group differences from the 14 clusters. For all PD patients (collapsing the PD-non-MCI and PD-MCI together), four regions (clusters # 7, 8, 9, 10, corresponding the three precuneus regions and the cingulate gyrus) were selected based on group differences from the 14 clusters. Multiple comparison with of all the correlations ($n = 4$) was applied at a significant threshold of pFDR < 0.05 in each group. Analyses with age covaried out was also performed for the PD patients, applying a general linear model.

RESULTS

Cognitive Assessment

Among the 35 PD participants, 15 were grouped in PD-MCI. Eleven showed single domain cognitive impairment (attention: 2, executive: 6, memory: 0, visuospatial: 3, and language: 1), and three showed impairment on multiple domains. Participant demographics are shown in **Table 2**. Group difference was observed in age, sex, MoCA and Beck's Depression Inventory II (BDI-II) (**Table 2**). A marginal group difference was observed in disease duration ($p = 0.089$). The mean Z-scores of each domain are shown in the **Figure S2**. Student *t*-tests indicated that all the Z-scores on these measures were lower in PD-MCI than HV ($p < 0.05$). The Z-scores in the PD-MCI were lower than PD-non-MCI in attention, executive language domains ($p < 0.05$), and marginally lower in memory domain ($p = 0.055$). Between the HV and the PD-non-MCI, significant difference was observed in the executive and language domains ($p < 0.05$).

Connectivity Analyses

Step 1. Connectivity Strength Between Clusters in OHV, PD-non-MCI, and PC-MCI

Across the resolutions, the omnibus tests indicated significant difference between the HV and PD-MCI groups (with age as a covariate), and between PD-non-MCI and the PD-MCI groups (without controlling for age), both indicating decreased connectivity in PD-MCI. Details are in **Table 3**. The results are stable across resolutions in PD-non-MCI vs. PD-MCI (without age as a covariate), showing a tendency of gradually decreasing percent of significantly different connectivities as the resolution increased. No difference was observed in OHV vs. PD-non-MCI comparisons (with age covariate). The detail results are shown in the SI. Briefly, when comparing PD-non-MCI with PD-MCI (without age covariate), with resolution 19, group connectivity differences was observed in most of the brain except the temporal area and the upper cerebellum (**Figure S3**, top). Discovery rate, indicating the rate of connections with significant effects for each cluster, were prominent in the medial part of the cortex corresponding to the motor area. With resolution 118, similar, but weaker group differences were observed (**Figure S3**, middle). Between the OHV vs. PD-MCI (with age covariate), with resolution 118, significant differences in the discovery rates were observed in the medial frontal motor cortex, the posterior cingulate cortex, right anterior prefrontal cortex, and occipital area (**Figure S3**, bottom).

Step 2. Graph Theory Analyses

Hub regions

The average of the degrees and the betweenness centrality of all the 118 clusters of all the participants were 24.6 ±11.6 and 132.9 ± 11.6, respectively. Ten clusters showed degrees greater than mean + 1S.D in at least one group (**Figures 1**, **2**, top). In the mPFC and the cerebellum (# 1, 2, 3) the higher (> mean + 1 S.D.) degrees were observed in YHV only. In four other medial structures covering the precuneus and cingulate gyrus (#7, 8, 9, 10) and in the occipital cortex (#6), the higher degrees were observed in PD-non-MCI, only. In the temporal and temporoparietal areas (#4,5), the higher degrees were observed in all the groups, except in PD-MCI for #5. Within these regions, higher betweenness centralities were observed in the mPFC and the cerebellum (#2, 3) in the YHV, and in the middle

TABLE 3 | Group differences in connectivity strength between clusters between groups.

Cluster number	4	10	19	35	63	118	221	393	*p*-value
WITHOUT AGE AS A COVARIATE									
HV vs. PD-non-MCI	0	0	0	0	0	0	0	0	1
HV vs. PD-MCI	0	0	0	0	0.001512	0.001149	0.001228	0.000699	0.0761
PD-non-MCI vs. PD-MCI	0.4375	0.26	0.085873	0.088980	0.011590	0.007182	0	0	0.0032
WITH AGE AS A COVARIATE									
HV vs. PD-non-MCI	0	0	0	0	0	0	0	0	1
HV vs. PD-MCI	0.125	0	0	0	0.005039	0.000862	0.001515	0.001463	0.0267
PD-non-MCI vs. PD-MCI	0	0	0.002770	0	0	0	0	0	0.0841

The numbers under each cluster number indicate the proportion of significantly different connectivity over all possible connections. The p-value is based on the omnibus test across all the resolutions.

temporal area (#4) and the precuneus (#7), in PD-non-MCI (**Figure 2**, bottom).

Group difference of degree and betweenness centrality

Results are summarized in **Figure 2**.

OHV vs. YHV. The YHV indicated higher degrees in the mPFC and the cerebellum (#2, 3) compared with the OHV (adjusted *p*-values 0.0018 and 0.017, respectively). A similar decrease in OHV was observed in the other cluster of the mPFC (#1) (uncorrected $p = 0.046$, adjusted $p = 0.13$). In the *a priori* predicted regions, higher degrees were observed in the globus pallidus (#12) and lower degrees in the hippocampus (#14) in OHV compared to YHV, though this did not survive correction for multiple comparisons (uncorrected *p*-values 0.019 and 0.020, respectively; adjusted *p*-values 0.070 and 0.070). Higher betweenness centralities were also observed in the mPFC and in the cerebellum (#1 and #3) in YHV compared with OHV (adjusted *p*-values 0.019 and 0.0004, respectively). In the cluster of the mPFC (#2), reduction was also observed in OHV compared to YHV (uncorrected $p = 0.0326$; adjusted $p = 0.114$). Decreased betweenness centrality in the hippocampus was also observed in the OHV compared with YHV (uncorrected $p = 0.018$; adjusted $p = 0.085$).

PD-non-MCI vs. OHV. Higher degrees were seen in PD-non-MCI compared to OHV in the precuneus and the cingulate cortex (#7, 10; adjusted *p*-values 0.020 and 0.020, respectively). Increases in PD-non-MCI participants were also seen in the clusters of the precuneus regions (#8, 9; *p*-value without multiple comparison = 0.018 and 0.023, respectively, and adjusted *p*-value = 0.063 and 0.053, respectively). When age was included as a covariate, group difference between OHV and PD-non-MCI was observed in the precuneus and the cingulate cortex (#7, 8, 10; adjusted *p*-values 0.047, 0.047, and 0.047, respectively). In the other cluster of the precuneus (#9), the same pattern was observed (*p*-value without multiple comparison with $p = 0.015$ and adjusted $p = 0.053$). No difference was observed in the betweenness centrality, with or without age-covaried out (adjusted $p > 0.3$).

PD-non-MCI vs. PD-MCI. Higher degrees were seen in PD-non-MCI in the precuneus (#9; adjusted $p = 0.046$). No significant difference of degrees was observed between the PD-non-MCI and PD-MCI in the other clusters of the presumes (#7, 8,10) (*p*-value without multiple comparison > 0.1). Higher betweenness centrality in the presumes (#9) was observed in the PD-non-MCI group ($p = 0.032$ without multiple comparison; adjusted $p = 0.20$). Controlling for age, the same pattern was observed in the presumes (#9) ($p = 0.044$; adjusted $p = 0.18$). No other difference was observed in the betweenness centrality, with or without including age as a covariate (*p*-value without multiple comparison >0.50).

Demographic impact on group difference of degree in precuneus and cingulate cortex

All the results are shown in the **Table 4**. In ANOVA, strong group effects, but neither subgroup effects nor interactions were observed, with subgroups of age, sex, and BDI-II. However, marginal interaction was observed between the two groups (OHV vs. PD-non-MCI) and the age (<67.6 vs. >67.6). In *t*-tests, in the younger participants (<67.6) and in the female patients, the averaged degree was strongly higher in PD-non-MCI compared with OHV. The mean of the averaged degree of the clusters in each subgroup is shown in **Figure 4**.

Correlation between degrees and cognitive function

In all PD patients, the degrees of the clusters of the presumes and the cingulate cortex (#7, 8, 9, 10) were positively correlated with the mean Z-score across all domains of the cognitive assessment (**Figure 3**). The correlation rates (*r*) were, 0.42, 0.42, 0.40, and 0.35, and the adjusted *p*-values were 0.027, 0.027, 0.27, and 0.042, respectively. When age was included as a covariate, significant correlations were observed in the clusters of the presumes (#7, 8, 9), but not in the cingulate cortex (#10) (uncorrected *p*-values 0.036, 0.017, 0.047, and 0.069, adjusted *p*-values 0.067, 0.67, 0.67, and 0.069, respectively). The result of correlation analysis for each cognitive domain is shown in the **Supplementary Information.** No relationship was observed in OHV between degrees and scores on cognitive assessments in any of the clusters that were significantly different from YHV [mPFC, globus pallidus, or hippocampus [#1, 2, 12, 14], uncorrected $p > 0.15$].

FIGURE 2 | Mean degrees (top) and the betweenness centralities (bottom) of each cluster, depending to the groups (YHV, OHV, PD-non-MCI, and PD-MCI). **the significant difference with correction for multiple comparisons, and *the significant difference without multiple comparison. The bar indicates the S.D.

DISCUSSION

Step 1

We investigated the connectivity differences among HV, PD-non-MCI and PD-MCI, applying BASC (36) and whole brain connectome with different resolutions (18). Our main observation was significant connectivity differences between PD-non-MCI and PD-MCI, without age covaried-out, across all the resolutions (**Table 3**). This result is in line with previous studies of PD patients with MCI (57–62). Here, the sensitivity was higher with lower resolution (<50), and lower but stable with higher resolution (>50). This is in agreement with studies

TABLE 4 | Group differences of averaged degrees in precuneus and cingulate cortex, between two subgroups of age, sex, and BDI.

		Age	Sex	BDI
Definition of subgroups	subgroup1	<67.6	Male	<6.9
	subgroup2	>67.6	Female	>6.9
NUMBER				
OHV	Subgroup1	8	5	17
	Subgroup2	13	16	4
PD-non-MCI	Subgroup1	12	10	9
	Subgroup2	8	10	11
PD-MCI	Subgroup1	7	10	4
	Subgroup2	8	5	11
TWO-WAY ANOVA (*p*-value)				
Group effect (OHV, PD-non-MCI, PD-MCI)		0.002	0.005	0.01
Subgroup effect (subgroup1, subgroup2)		0.705	0.261	0.344
Interuction (group × subgroup)		0.214	0.441	0.844
Group effect (OHV, PD-non-MCI)		<0.001	0.001	0.002
Subgroup effect (subgroup1, subgroup2)		0.943	0.829	0.259
Interuction (group × subgroup)		0.074	0.587	0.644
t-test (*p*-value)	Between groups			
OHV vs. PD-non-MCI	Subgroup1	0.001	0.083	0.015
	Subgroup2	0.119	0.002	0.055
PD-non-MCI vs. PD-MCI	Subgroup1	0.158	0.070	0.452
	Subgroup2	0.166	0.501	0.017

Numbers of subgroups, p-values of two-way ANOVA and t-test are shown.

in different patient groups using the same methodology (18, 63). The group difference was most prominent in connectivity with the medial cortex, including the primary motor cortex (**Figure S3**). Thus, considering the fact that the main symptom of the PD is motor dysfunction, the cognitive impairment might show pathophysiological overlap with motor dysfunction in PD patients, i.e., the connectivity impairment could potentially be attributed to the impairment in midbrain dopamine projections to the striatum. Interestingly, the difference between the OHV vs. PD-MCI was weaker, and only emerged when including age as a covariate (**Table 3**). In addition, in these comparisons the sensitivity was not higher with lower resolution (<50), which is atypical with this method (18, 63). Thus, we speculated that the reduction of the connectivity does not occur linearly as disease progresses. Instead, connectivity might be increased in some regions in PD-non-MCI patients likely reflecting a compensatory mechanism. In fact, increased and decreased overall connectivity has been reported in non-MCI and MCI PD patients compared to HV (57, 60).

Step 2

Applying graph theory on the same rs-fMRI data in the first step combined with rs-fMRI data from YHV, we investigated the age, pathological condition, and cognition effects separately, on the hub regions of the brain. The results indicated that (1) decreased hub function mainly in the mPFC in the OHV compared with the YHV, (2) increased hub function in the posterior medial structures (presumes and cingulate cortex) in the PD-non-MCI compared to PD-MCI, with and without age covariate out, and (3) positive correlation between the hub function in the medial structure and cognitive level in all PD patients.

Compatibility With Step 1

Based on the results of the first step, we hypothesized a possible increased connectivity in the PD-non-MCI patients. With a different approach here, we found that the degree of the medial structures (cingulate cortex and the precuneus) was increased in the PD-non-MCI group compared to the OHV, in agreement with our hypothesis. In step 1 analyses, when age was included as a covariate, no significant difference was observed for the group comparison between PD-non-MCI and PD-MCI. However, here we observed that the increased degrees of the medial structure survived when accounting for the effect of age. By also comparing OHV and YHV, we confirmed that the increase of the posterior medial structure was not associated with healthy aging, but rather occurred exclusively in the PD-non-MCI patients. The two approaches to the data broadly support each other.

Medial Prefrontal Cortex (mPFC)

We observed a high degree and betweenness centrality in the mPFC, corresponding to the pre-supplementary motor area (pre-SMA) and supplementary motor area (SMA), in the YHV. This is in agreement with previous studies of functional and anatomical connectivity, indicating these regions as hub connectors (25, 28, 64). The mPFC is considered to be an important region in learning associations between events and in linking adaptive responses (65). The higher degree and betweenness centrality in YHV could support this cognitive function. Both network

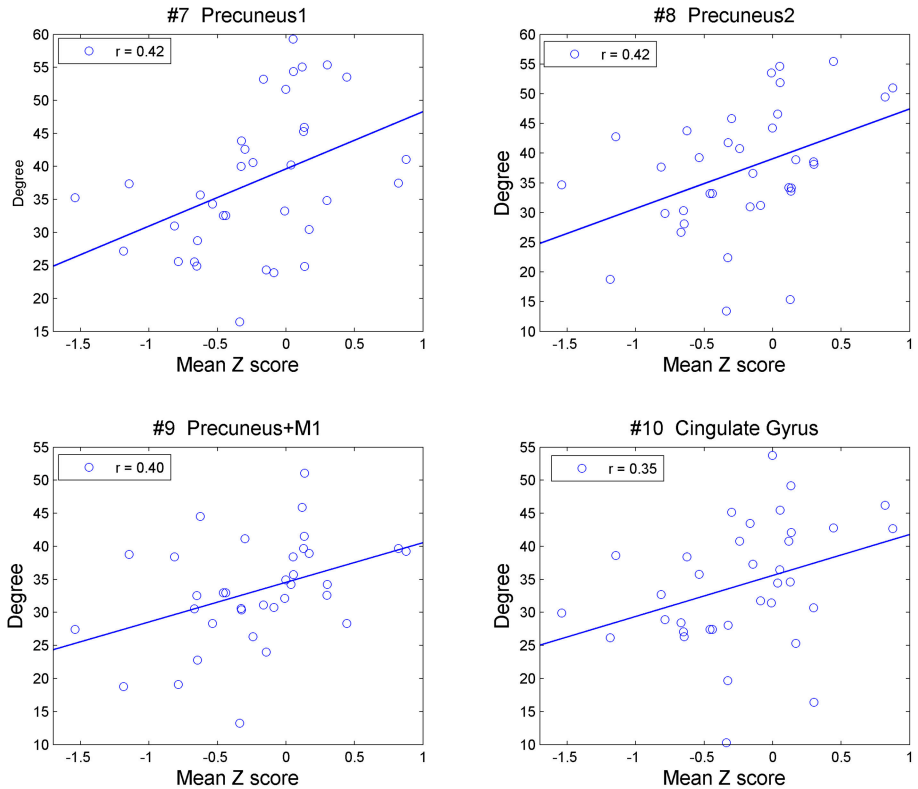

FIGURE 3 | Correlation between degrees of the precuneus (#7, 8, 9) and cingulate cortex (#10) with mean Z-values over all five cognitive domains in all the PD patients.

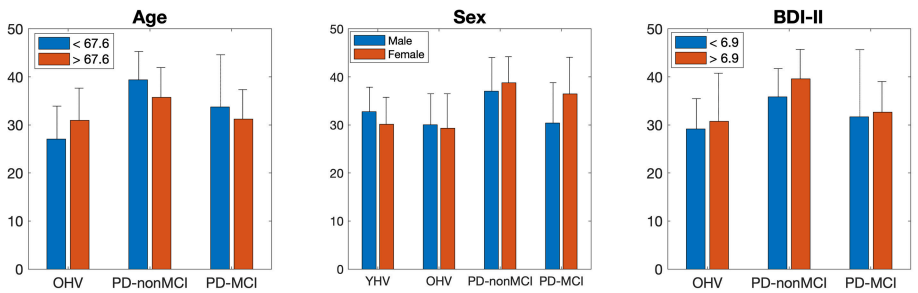

FIGURE 4 | Mean of the averaged degree of the precuneus and cingulate cortex, in each subgroup of age, sex, and BDI-II. The bar indicates the S.D.

indices were decreased in the OHV compared to the YHV in these regions. This is in agreement with previous studies that have found that reduced connectivity of these regions is associated with cognitive decline in aging (27, 28). However, in the present data, no significant correlation was observed between the degree or betweenness centrality of the mPFC and the average cognitive Z-scores in the OHV. The discrepancy might be due to methodological differences, such as using different imaging parameters and analyses, or by participants' demography. In particular, we carefully excluded participants with any MCI in this group, which restricted the range of cognitive scores and could have resulted in selection a sample of participants that are making optimal use of an existing neural network.

No significant difference was observed between the OHV and PD-non-MCI groups in these regions. Thus, loss of connectivity in these regions may be primarily attributed to age rather than pathology.

Posterior Medial Structures (Cingulate Cortex and Precuneus)

In the PD-non-MCI patients, degrees were significantly increased in the cingulate cortex and the precuneus relative to both OHV and PD-MCI, and this effect was not accounted for by age. Of note, additional direct comparison indicated that compared with YHV, the PD-non-MCI patients showed significantly increased degrees in the precuneus (#7, 9), and the cingulate cortex (#10)

(adjusted p-values 0.048, 0.023, and 0.054, respectively). Overall, this pattern suggests that PD-non-MCI patients recruit more the posterior medial structures and the functional regions they are associated with, but that this may be lost in PD-MCI patients. Moreover, the degree of these regions in all PD patients was positively correlated with the mean Z-score of the cognitive assessment (**Figure 3**). This is in agreement with our previous study, showing recruitment of the precuneus in PD patients during a set-shifting task (35). This supports the possibility that increased network activity in posterior medial structures might reflect compensatory mechanisms that protect against cognitive impairment in PD patients.

When each cognitive domain was considered, the degrees in the cingulate gyrus were correlated with the Z-scores of the attention domain, and the degrees in the precuneus were correlated with the Z-scores of the language domain. Moreover, the degrees in these clusters were marginally correlated with the Z-scores of the executive and memory domains (see **Supplementary Information**). Thus, the important function of the posterior medial structure in cognition could be a general function for cognition, i.e., hub function, plausibly to connect brain regions supporting specific cognitive functions, rather than being involved in specific cognitive function itself.

Aging, a Risk Factor for Cognitive Decline in PD Patients

As described above, we observed reduced hub function in the mPFC in OHV, but not in the PD-non-MCI. Instead, we observed increased hub function in the posterior medial structures in this latter group. The mPFC is a key region associated with cognitive decline observed in aging (27, 66). Thus, for PD patients, the mPFC could be an important hub region for good cognitive performance. However, the mPFC is one of the important output of the cortico-basal ganglia thalamocortical loops (29, 67), and the hub function for connecting the basal-ganglia and the motor area. This function seems to be impaired in PD patients (33). Moreover, pathological change in the mPFC were observed in PD patients (68), and decreased dopaminergic function in the mPFC is associated with dementia in PD patients (69). Thus, depending on its integrity, the mPFC may not be able to act as the main hub for cognition in PD patients. Interestingly, a front-cingulo-parietal module (including the frontal area, basal ganglia, and precuneus) acts as a connector in young people, but this module is divided into two modules (the fronto-striatal-thalamus and medial posterior) in older people (28). PD-non-MCI patients are likely to recruit only one part of the divided two modules.

In the PD-non-MCI patients, the degree in the posterior medial structure was increased compared to the OHV. However, the betweenness centrality was not significantly higher in PD-non-MCI compared with OHV, even before multiple comparison correction ($p > 0.15$). The betweenness centrality is the total number of all shortest paths linking to the given node (52). Thus, the recruited connectivity which could increase degrees, may not represent fully optimized information transfer in the brain.

Additionally, we investigated the impacts of age, sex, BDI-II, one by one, on the degrees in the posterior medial structure, by dividing each group into two subgroups. The results indicated main effect of the group (PD-non-MCI vs. PD-MCI), but not the effect of the subgroup, or interaction of the group × subgroup. However, in the younger (<67.6) and in the female participants, the averaged degree was strongly higher in PD-non-MCI compared with OHV (**Table 4**), and a marginal interaction was observed between the two groups (OHV vs. PD-non-MCI) and the age (<67.6 vs. >67.6). Studies indicate, in PD patients, risk factors of cognitive impairment are age, male gender, depression, education, and severity of motor symptoms (7, 8). Our results indicate that younger and female PD patients may be able to recruit the posterior medial structure as hub more efficiently, compared with the older and male PD patients, giving a positive impact of cognition. However, given the small number of the participants for each subgroup, further studies are required to confirm this finding.

Basal Ganglia and Hippocampus

We observed the basal ganglia and the hippocampus as non-hub regions, in agreement with previous studies (28).

In the basal ganglia (globus pallidus), the degree was increased in OHV, compared with YHV. In older people, some parts of the basal ganglia are likely to increase the importance of connector function in the brain (70, 71), supporting their motor and cognitive performance (71, 72). However, the basal ganglia are the main pathological target of the PD. Therefore, cognitive benefit possibly relating to increased degree in the basal ganglia would be limited to PD patients. Nevertheless, no difference was observed in the degrees between OHV vs. PD-non-MCI. The globus pallidus shows increased connectivity with the medial temporal region and the posterior medial structure in older people, compared to younger people, but has decreased connectivity with the somatomotor cortex (70). Thus, the observation may reflect the further increased connectivity with the posterior medial structure region in PD patients, rather than involvement in the traditional cortico-basal-ganglia-thalamocortical loops (29). More studies are required to confirm this observation.

In the hippocampus, degrees was decreased in OHV compared with YHV, in line with previous studies (73), and no difference was between OHV vs. PD-non-MCI. Although the hippocampal function in the PD patients plays an important role for supporting cognition (35, 39, 56), pathological change of dopaminergic system is also observed in the hippocampus in PD patients (68), associating with cognitive impairment in advanced stages of PD (55).

The increased and decreased degrees in the globus pallidus and the hippocampus between YHV vs. OHV were only observed without multiple comparisons (**Figure 2**). The impacts of the connectivity in these regions on cognition in PD patients while important, might be less crucial than connectivity in the medial structures.

CONCLUSION

Using rs-fMRI data with two different analyses, we investigated the effects of age, pathology, and cognitve impairment on brain

connectivity in PD patients. Cluster connectivity and graph theory analysis provided distinct but convergent information about these processes. The comparison of the connectivity strength indicated the reduction of the multiple connectivities in PD-MCI patients compared to PD-non-MCI. Results were not strongly influenced by cluster number and location, but differences were reduced when age was included as a covariate. Using a graph-theory approach, we observed (1) decreased hub function mainly in the mPFC in OHV compared with the YHV, (2) increased hub function in the posterior medial structure (precuneus and the cingulate cortex) in PD-non-MCI patients, and (3) positive correlation between the hub function in the medial structure and cognitive function in all PD patients. Because of our small sample size, our interpretations should be taken with caution. Nevertheless, based on our results together with those of previous studies, we propose that a combination of hub modifications affect cognition in PD including (1) age-related reduction of hub function in the mPFC, and (2) recruitment availability of the posterior medial structure possibly to compensate for damaged basal ganglia function in PD-non-MCI.

ETHICS STATEMENT

This study was carried out in accordance with the recommendations of the tri-council of Canada, Research Ethics Committee of the Regroupement Neuroimagerie Québec with written informed consent from all subjects. All subjects gave written informed consent in accordance with the Declarations of Helsinki. The protocol was approved by the Research Ethics Committee of the Regroupement Neuroimagerie Québec.

AUTHOR CONTRIBUTIONS

AN-S contributed to study design (second part), data acquisition, analyses, and writing. PB contributed to study design, methodological support, and analyses. AH, SJ, BM-C, and JL contributed to data acquisition A-LF and CD contributed to clinical feedback. KS and CB contributed to writing. OM contributed to study design, analyses, and writing.

FUNDING

This work was funded by an operating grant from the Canadian Institutes of Health Research (CIHR) (MOP-126017), the Canada Research Chair in non-motor deficits in Parkinson's disease and the Tourmaline Oil Chair in Parkinson's disease to Oury Monchi.

SUPPLEMENTARY MATERIAL

The Supplementary Material for this article can be found online at: https://www.frontiersin.org/articles/10.3389/fneur.2019.00267/full#supplementary-material

REFERENCES

1. Foltynie T, Brayne CE, Robbins TW, Barker RA. The cognitive ability of an incident cohort of Parkinson's patients in the UK. The CamPaIGN study. *Brain*. (2004) 127(Pt. 3):550–60. doi: 10.1093/brain/awh067
2. Aarsland D, Kurz MW. The epidemiology of dementia associated with Parkinson disease. *J Neurol Sci*. (2010) 289:18–22. doi: 10.1016/j.jns.2009.08.034
3. Williams-Gray CH, Foltynie T, Brayne CEG, Robbins TW, Barker RA. Evolution of cognitive dysfunction in an incident Parkinson's disease cohort. *Brain*. (2007) 130:1787–98. doi: 10.1093/brain/awm111
4. Litvan I, Goldman JG, Tröster AI, Schmand BA, Weintraub D, Petersen RC, et al. Diagnostic criteria for mild cognitive impairment in Parkinson's disease: movement Disorder Society Task Force guidelines. *Mov Disord*. (2012) 27:349–56. doi: 10.1002/mds.24893
5. Janvin CC, Larsen JP, Salmon DP, Galasko D, Hugdahl K, Aarsland D. Cognitive profiles of individual patients with Parkinson's disease and dementia: comparison with dementia with lewy bodies and Alzheimer's disease. *Mov Disord*. (2006) 21:337–42. doi: 10.1002/mds.20726
6. Litvan I, Aarsland D, Adler CH, Goldman JG, Kulisevsky J, Mollenhauer B, et al. MDS task force on mild cognitive impairment in Parkinson's disease: critical review of PD-MCI. *Mov Disord*. (2011) 26:1814–24. doi: 10.1002/mds.23823
7. Aarsland D, Bronnick K, Williams-Gray C, Weintraub D, Marder K, Kulisevsky J, et al. Mild cognitive impairment in Parkinson disease: a multicenter pooled analysis. *Neurology*. (2010) 75:1062–9. doi: 10.1212/WNL.0b013e3181f39d0e
8. Lin SJ, Baumeister TR, Garg S, McKeown MJ. Cognitive profiles and hub vulnerability in Parkinson's disease. *Front Neurol*. (2018) 9:482. doi: 10.3389/fneur.2018.00482
9. Prodoehl J, Burciu RG, Vaillancourt DE. Resting state functional magnetic resonance imaging in Parkinson's disease. *Curr Neurol Neurosci Rep*. (2014) 14:448. doi: 10.1007/s11910-014-0448-6
10. Tahmasian M, Bettray LM, van Eimeren T, Drzezga A, Timmermann L, Eickhoff CR, et al. A systematic review on the applications of resting-state fMRI in Parkinson's disease: does dopamine replacement therapy play a role? *Cortex*. (2015) 73:80–105. doi: 10.1016/j.cortex.2015.08.005
11. Tahmasian M, Eickhoff SB, Giehl K, Schwartz F, Herz DM, Drzezga A, et al. Resting-state functional reorganization in Parkinson's disease: an activation likelihood estimation meta-analysis. *Cortex*. (2017) 92:119–38. doi: 10.1016/j.cortex.2017.03.016
12. Helmich RC, Derikx LC, Bakker M, Scheeringa R, Bloem BR, Toni I. Spatial remapping of cortico-striatal connectivity in Parkinson's disease. *Cereb Cortex*. (2010) 20:1175–86. doi: 10.1093/cercor/bhp178
13. Luo CY, Guo XY, Song W, Chen Q, Cao B, Yang J, et al. Functional connectome assessed using graph theory in drug-naive Parkinson's disease. *J Neurol*. (2015) 262:1557–67. doi: 10.1007/s00415-015-7750-3
14. Sharman M, Valabregue R, Perlbarg V, Marrakchi-Kacem L, Vidailhet M, Benali H, et al. Parkinson's disease patients show reduced cortical-subcortical sensorimotor connectivity. *Mov Disord*. (2013) 28:447–54. doi: 10.1002/mds.25255
15. Hacker CD, Perlmutter JS, Criswell SR, Ances BM, Snyder AZ. Resting state functional connectivity of the striatum in Parkinson's disease. *Brain*. (2012) 135(Pt. 12):3699–711. doi: 10.1093/brain/aws281
16. Muller-Oehring EM, Sullivan EV, Pfefferbaum A, Huang NC, Poston KL, Bronte-Stewart HM, et al. Task-rest modulation of basal ganglia connectivity in mild to moderate Parkinson's disease. *Brain Imaging Behav*. (2015) 9:619–38. doi: 10.1007/s11682-014-9317-9

17. Yu R, Liu B, Wang L, Chen J, Liu X. Enhanced functional connectivity between putamen and supplementary motor area in Parkinson's disease patients. *PLoS ONE*. (2013) 8:e59717. doi: 10.1371/journal.pone.0059717
18. Bellec P, Benhajali Y, Carbonell F, Dansereau C, Albouy G, Pelland M, et al. Impact of the resolution of brain parcels on connectome-wide association studies in fMRI. *Neuroimage*. (2015) 123:212–28. doi: 10.1016/j.neuroimage.2015.07.071
19. Bullmore E, Sporns O. Complex brain networks: graph theoretical analysis of structural and functional systems. *Nat Rev Neurosci*. (2009) 10:186–98. doi: 10.1038/nrn2575
20. He Y, Evans A. Graph theoretical modeling of brain connectivity. *Curr Opin Neurol*. (2010) 23:341–50. doi: 10.1097/WCO.0b013e32833aa567
21. Biswal B, Yetkin FZ, Haughton VM, Hyde JS. Functional connectivity in the motor cortex of resting human brain using echo-planar MRI. *Magn Reson Med*. (1995) 34:537–41. doi: 10.1002/mrm.1910340409
22. Greicius MD, Krasnow B, Reiss AL, Menon V. Functional connectivity in the resting brain: a network analysis of the default mode hypothesis. *Proc Natl Acad Sci USA*. (2003) 100:253–8. doi: 10.1073/pnas.0135058100
23. Power JD, Cohen AL, Nelson SM, Wig GS, Barnes KA, Church JA, et al. Functional network organization of the human brain. *Neuron*. (2011) 72:665–78. doi: 10.1016/j.neuron.2011.09.006
24. Achard S, Bullmore E. Efficiency and cost of economical brain functional networks. *PLoS Comput Biol*. (2007) 3:e17. doi: 10.1371/journal.pcbi.0030017
25. Hagmann P, Cammoun L, Gigandet X, Meuli R, Honey CJ, Wedeen VJ, et al. Mapping the structural core of human cerebral cortex. *PLoS Biol*. (2008) 6:e159. doi: 10.1371/journal.pbio.0060159
26. Power JD, Schlaggar BL, Lessov-Schlaggar CN, Petersen SE. Evidence for hubs in human functional brain networks. *Neuron*. (2013) 79:798–813. doi: 10.1016/j.neuron.2013.07.035
27. Andrews-Hanna JR, Snyder AZ, Vincent JL, Lustig C, Head D, Raichle ME, et al. Disruption of large-scale brain systems in advanced aging. *Neuron*. (2007) 56:924–35. doi: 10.1016/j.neuron.2007.10.038
28. Meunier D, Achard S, Morcom A, Bullmore E. Age-related changes in modular organization of human brain functional networks. *Neuroimage*. (2009) 44:715–23. doi: 10.1016/j.neuroimage.2008.09.062
29. Alexander GE, DeLong MR, Strick PL. Parallel organization of functionally segregated circuits linking basal ganglia and cortex. *Annu Rev Neurosci*. (1986) 9:357–81. doi: 10.1146/annurev.ne.09.030186.002041
30. Bar-Gad I, Morris G, Bergman H. Information processing, dimensionality reduction and reinforcement learning in the basal ganglia. *Prog Neurobiol*. (2003) 71:439–73. doi: 10.1016/j.pneurobio.2003.12.001
31. Bogacz R, Gurney K. The basal ganglia and cortex implement optimal decision making between alternative actions. *Neural Comput*. (2007) 19:442–77. doi: 10.1162/neco.2007.19.2.442
32. Nagano-Saito A, Leyton M, Monchi O, Goldberg YK, He Y, Dagher A. Dopamine depletion impairs frontostriatal functional connectivity during a set-shifting task. *J Neurosci*. (2008) 28:3697–706. doi: 10.1523/JNEUROSCI.3921-07.2008
33. Nagano-Saito A, Martinu K, Monchi O. Function of basal ganglia in bridging cognitive and motor modules to perform an action. *Front Neurosci*. (2014) 8:187. doi: 10.3389/fnins.2014.00187
34. Marsden CD. Parkinson's disease. *Lancet*. (1990) 335:948–52. doi: 10.1016/0140-6736(90)91006-V
35. Nagano-Saito A, Al-Azzawi MS, Hanganu A, Degroot C, Mejia-Constain B, Bedetti C, et al. Patterns of longitudinal neural activity linked to different cognitive profiles in Parkinson's disease. *Front Aging Neurosci*. (2016) 8:275. doi: 10.3389/fnagi.2016.00275
36. Bellec P, Rosa-Neto P, Lyttelton OC, Benali H, Evans AC. Multi-level bootstrap analysis of stable clusters in resting-state fMRI. *Neuroimage*. (2010) 51:1126–39. doi: 10.1016/j.neuroimage.2010.02.082
37. Carbonell F, Nagano-Saito A, Leyton M, Cisek P, Benkelfat C, He Y, et al. Dopamine precursor depletion impairs structure and efficiency of resting state brain functional networks. *Neuropharmacology*. (2014) 84:90–100. doi: 10.1016/j.neuropharm.2013.12.021
38. Garrison KA, Scheinost D, Finn ES, Shen X, Constable RT. The (in)stability of functional brain network measures across thresholds. *Neuroimage*. (2015) 118:651–61. doi: 10.1016/j.neuroimage.2015.05.046
39. Nagano-Saito A, Habak C, Mejia-Constain B, Degroot C, Monetta L, Jubault T, et al. Effect of mild cognitive impairment on the patterns of neural activity in early Parkinson's disease. *Neurobiol Aging*. (2014) 35:223–31. doi: 10.1016/j.neurobiolaging.2013.06.025
40. Nagano-Saito A, Lissemore JI, Gravel P, Leyton M, Carbonell F, Benkelfat C. Posterior dopamine D2/3 receptors and brain network functional connectivity. *Synapse*. (2017) 71:1–13. doi: 10.1002/syn.21993
41. Bellec P, Lavoie-Courchesne S, Dickinson P, Lerch JP, Zijdenbos AP, Evans AC. The pipeline system for Octave and Matlab (PSOM): a lightweight scripting framework and execution engine for scientific workflows. *Front Neuroinform*. (2012) 6:7. doi: 10.3389/fninf.2012.00007
42. Davey CE, Grayden DB, Egan GF, Johnston LA. Filtering induces correlation in fMRI resting state data. *Neuroimage*. (2013) 64:728–40. doi: 10.1016/j.neuroimage.2012.08.022
43. Collins DL, Neelin P, Peters TM, Evans AC. Automatic 3D intersubject registration of MR volumetric data in standardized Talairach space. *J Comput Assist Tomogr*. (1994) 18:192–205. doi: 10.1097/00004728-199403000-00005
44. Giove F, Gili T, Iacovella V, Macaluso E, Maraviglia B. Images-based suppression of unwanted global signals in resting-state functional connectivity studies. *Magn Reson Imaging*. (2009) 27:1058–64. doi: 10.1016/j.mri.2009.06.004
45. Lund TE, Madsen KH, Sidaros K, Luo WL, Nichols TE. Non-white noise in fMRI: does modelling have an impact? *Neuroimage*. (2006) 29:54–66. doi: 10.1016/j.neuroimage.2005.07.005
46. Bellec P, Perlbarg V, Evans AC. Bootstrap generation and evaluation of an fMRI simulation database. *Magn Reson Imaging*. (2009) 27:1382–96. doi: 10.1016/j.mri.2009.05.034
47. Bellec P, Perlbarg V, Jbabdi S, Pelegrini-Issac M, Anton JL, Doyon J, et al. Identification of large-scale networks in the brain using fMRI. *Neuroimage*. (2006) 29:1231–43. doi: 10.1016/j.neuroimage.2005.08.044
48. Bellec P. Mining the hierarchy of resting-state brain networks: selection of representative clusters in a multiscale structure. *3rd International Workshop on Pattern Recognition in Neuroimaging*. (2013). p. 54–7. doi: 10.1109/PRNI.2013.23
49. Benjamini Y, Hochberg Y. Controlling the false discovery rate: a practical and powerful approach to multiple testing. *J R Stat Soc Ser B*. (1995) 57:289–300.
50. Achard S, Salvador R, Whitcher B, Suckling J, Bullmore E. A resilient, low-frequency, small-world human brain functional network with highly connected association cortical hubs. *J Neurosci*. (2006) 26:63–72. doi: 10.1523/JNEUROSCI.3874-05.2006
51. Telesford QK, Joyce KE, Hayasaka S, Burdette JH, Laurienti PJ. The ubiquity of small-world networks. *Brain Connect*. (2011) 1:367–75. doi: 10.1089/brain.2011.0038
52. Sporns O, Honey CJ, Kotter R. Identification and classification of hubs in brain networks. *PLoS ONE*. (2007) 2:e1049. doi: 10.1371/journal.pone.0001049
53. Liang X, He Y, Salmeron BJ, Gu H, Stein EA, Yang Y. Interactions between the salience and default-mode networks are disrupted in cocaine addiction. *J Neurosci*. (2015) 35:8081–90. doi: 10.1523/JNEUROSCI.3188-14.2015
54. Kassab R, Alexandre F. Integration of exteroceptive and interoceptive information within the hippocampus: a computational study. *Front Syst Neurosci*. (2015) 9:87. doi: 10.3389/fnsys.2015.00087
55. Nagano-Saito A, Kato T, Arahata Y, Washimi Y, Nakamura A, Abe Y, et al. Cognitive- and motor-related regions in Parkinson's disease: FDOPA and FDG PET studies. *Neuroimage*. (2004) 22:553–61. doi: 10.1016/j.neuroimage.2004.01.030
56. Nagano-Saito A, Washimi Y, Arahata Y, Kachi T, Lerch JP, Evans AC, et al. Cerebral atrophy and its relation to cognitive impairment in Parkinson disease. *Neurology*. (2005) 64:224–9. doi: 10.1212/01.WNL.0000149510.41793.50
57. Abos A, Baggio HC, Segura B, Garcia-Diaz AI, Compta Y, Marti MJ, et al. Discriminating cognitive status in Parkinson's disease through functional connectomics and machine learning. *Sci Rep*. (2017) 7:45347. doi: 10.1038/srep45347
58. Amboni M, Tessitore A, Esposito F, Santangelo G, Picillo M, Vitale C, et al. Resting-state functional connectivity associated with mild cognitive impairment in Parkinson's disease. *J Neurol*. (2015) 262:425–34. doi: 10.1007/s00415-014-7591-5

59. Baggio HC, Segura B, Sala-Llonch R, Marti MJ, Valldeoriola F, Compta Y, et al. Cognitive impairment and resting-state network connectivity in Parkinson's disease. *Hum Brain Mapp*. (2015) 36:199–212. doi: 10.1002/hbm.22622
60. Gorges M, Muller HP, Lule D, Consortium L, Pinkhardt EH, Ludolph AC, et al. To rise and to fall: functional connectivity in cognitively normal and cognitively impaired patients with Parkinson's disease. *Neurobiol Aging*. (2015) 36:1727–35. doi: 10.1016/j.neurobiolaging.2014.12.026
61. Lebedev AV, Westman E, Simmons A, Lebedeva A, Siepel FJ, Pereira JB, et al. Large-scale resting state network correlates of cognitive impairment in Parkinson's disease and related dopaminergic deficits. *Front Syst Neurosci*. (2014) 8:45. doi: 10.3389/fnsys.2014.00045
62. Lopes R, Delmaire C, Defebvre L, Moonen AJ, Duits AA, Hofman P, et al. Cognitive phenotypes in parkinson's disease differ in terms of brain-network organization and connectivity. *Hum Brain Mapp*. (2016) 38:1604–21. doi: 10.1002/hbm.23474
63. Tam A, Dansereau C, Badhwar A, Orban P, Belleville S, Chertkow H, et al. Common effects of amnestic mild cognitive impairment on resting-state connectivity across four independent studies. *Front Aging Neurosci*. (2015) 7:242. doi: 10.3389/fnagi.2015.00242
64. Tomasi D, Volkow ND. Association between functional connectivity hubs and brain networks. *Cereb Cortex*. (2011) 21:2003–13. doi: 10.1093/cercor/bhq268
65. Euston DR, Gruber AJ, McNaughton BL. The role of medial prefrontal cortex in memory and decision making. *Neuron*. (2012) 76:1057–70. doi: 10.1016/j.neuron.2012.12.002
66. Onoda K, Ishihara M, Yamaguchi S. Decreased functional connectivity by aging is associated with cognitive decline. *J Cogn Neurosci*. (2012) 24:2186–98. doi: 10.1162/jocn_a_00269
67. Draganski B, Kherif F, Kloppel S, Cook PA, Alexander DC, Parker GJ, et al. Evidence for segregated and integrative connectivity patterns in the human Basal Ganglia. *J Neurosci*. (2008) 28:7143–52. doi: 10.1523/JNEUROSCI.1486-08.2008
68. Braak H, Del Tredici K, Rub U, de Vos RA, Jansen Steur EN, Braak E. Staging of brain pathology related to sporadic Parkinson's disease. *Neurobiol Aging*. (2003) 24:197–211. doi: 10.1016/S0197-4580(02)00065-9
69. Ito K, Nagano-Saito A, Kato T, Arahata Y, Nakamura A, Kawasumi Y, et al. Striatal and extrastriatal dysfunction in Parkinson's disease with dementia: a 6-[18F]fluoro-L-dopa PET study. *Brain*. (2002) 125(Pt. 6):1358–65. doi: 10.1093/brain/awf134
70. Manza P, Zhang S, Hu S, Chao HH, Leung HC, Li CS. The effects of age on resting state functional connectivity of the basal ganglia from young to middle adulthood. *Neuroimage*. (2015) 107:311–22. doi: 10.1016/j.neuroimage.2014.12.016
71. Mathys C, Hoffstaedter F, Caspers J, Caspers S, Sudmeyer M, Grefkes C, et al. An age-related shift of resting-state functional connectivity of the subthalamic nucleus: a potential mechanism for compensating motor performance decline in older adults. *Front Aging Neurosci*. (2014) 6:178. doi: 10.3389/fnagi.2014.00178
72. Ystad M, Hodneland E, Adolfsdottir S, Haasz J, Lundervold AJ, Eichele T, et al. Cortico-striatal connectivity and cognition in normal aging: a combined DTI and resting state fMRI study. *Neuroimage*. (2011) 55:24–31. doi: 10.1016/j.neuroimage.2010.11.016
73. Ferreira LK, Busatto GF. Resting-state functional connectivity in normal brain aging. *Neurosci Biobehav Rev*. (2013) 37:384–400. doi: 10.1016/j.neubiorev.2013.01.017

Conflict of Interest Statement: The authors declare that the research was conducted in the absence of any commercial or financial relationships that could be construed as a potential conflict of interest.

frontiers in Neurology

ORIGINAL RESEARCH
published: 24 April 2019
doi: 10.3389/fneur.2019.00391

Beta Amyloid Deposition Is Not Associated With Cognitive Impairment in Parkinson's Disease

Tracy R. Melzer[1,2,3†], Megan R. Stark[1,2†], Ross J. Keenan[1,4], Daniel J. Myall[1], Michael R. MacAskill[1,2], Toni L. Pitcher[1,2,3], Leslie Livingston[1,2], Sophie Grenfell[1], Kyla-Louise Horne[1,2], Bob N. Young[1], Maddie J. Pascoe[1], Mustafa M. Almuqbel[1,2,4], Jian Wang[5], Steven H. Marsh[6], David H. Miller[1,2,7], John C. Dalrymple-Alford[1,2,3,8] and Tim J. Anderson[1,2,3,9]*

[1] New Zealand Brain Research Institute, Christchurch, New Zealand, [2] Department of Medicine, University of Otago, Christchurch, New Zealand, [3] Brain Research New Zealand Rangahau Roro Aotearoa Centre of Research Excellence, Christchurch, New Zealand, [4] Pacific Radiology Group, Christchurch, New Zealand, [5] Department of Neurology, Huashan Hospital, Fudan University, Shanghai, China, [6] Department of Physics and Astronomy, University of Canterbury, Christchurch, New Zealand, [7] Institute of Neurology, University College London, London, United Kingdom, [8] Department of Psychology, University of Canterbury, Christchurch, New Zealand, [9] Department of Neurology, Christchurch Hospital, Christchurch, New Zealand

The extent to which Alzheimer neuropathology, particularly the accumulation of misfolded beta-amyloid, contributes to cognitive decline and dementia in Parkinson's disease (PD) is unresolved. Here, we used Florbetaben PET imaging to test for any association between cerebral amyloid deposition and cognitive impairment in PD, in a sample enriched for cases with mild cognitive impairment. This cross-sectional study used Movement Disorders Society level II criteria to classify 115 participants with PD as having normal cognition (PDN, $n = 23$), mild cognitive impairment (PD-MCI, $n = 76$), or dementia (PDD, $n = 16$). We acquired 18F-Florbetaben (FBB) amyloid PET and structural MRI. Amyloid deposition was assessed between the three cognitive groups, and also across the whole sample using continuous measures of both global cognitive status and average performance in memory domain tests. Outcomes were cortical FBB uptake, expressed in centiloids and as standardized uptake value ratios (SUVR) using the Centiloid Project whole cerebellum region as a reference, and regional SUVR measurements. FBB binding was higher in PDD, but this difference did not survive adjustment for the older age of the PDD group. We established a suitable centiloid cut-off for amyloid positivity in Parkinson's disease (31.3), but there was no association of FBB binding with global cognitive or memory scores. The failure to find an association between PET amyloid deposition and cognitive impairment in a moderately large sample, particularly given that it was enriched with PD-MCI patients at risk of dementia, suggests that amyloid pathology is not the primary driver of cognitive impairment and dementia in most patients with PD.

Keywords: Parkinson's disease, amyloid PET, Florbetaben, dementia, centiloid, mild cognitive impairment

OPEN ACCESS

Edited by:
Salvatore Galati, Neurocenter of Southern Switzerland (NSI), Switzerland

Reviewed by:
Matthias Brendel, Ludwig Maximilian University of Munich, Germany
Paul Cumming, University of Bern, Switzerland

***Correspondence:**
Tim J. Anderson
tim.anderson@cdhb.health.nz

†These authors have contributed equally to this work and are co-first authors

Specialty section:
This article was submitted to Movement Disorders, a section of the journal Frontiers in Neurology

Received: *11 February 2019*
Accepted: *01 April 2019*
Published: *24 April 2019*

Citation:
Melzer TR, Stark MR, Keenan RJ, Myall DJ, MacAskill MR, Pitcher TL, Livingston L, Grenfell S, Horne K-L, Young BN, Pascoe MJ, Almuqbel MM, Wang J, Marsh SH, Miller DH, Dalrymple-Alford JC and Anderson TJ (2019) Beta Amyloid Deposition Is Not Associated With Cognitive Impairment in Parkinson's Disease. Front. Neurol. 10:391. doi: 10.3389/fneur.2019.00391

INTRODUCTION

Motor impairment is the cardinal feature of early Parkinson's disease (PD), but progressive cognitive impairment and dementia (PDD) eventually become major debilitating symptoms for patients (1). PDD arises in over 80% of patients (2), leading to substantial caregiver and financial burden, reduced quality of life, early institutionalization and premature death (3). Progression to PDD involves a complex, multisystem brain degeneration (1, 4). Alzheimer's disease (AD) neuropathology, including misfolded beta-amyloid (Aβ), may influence the emergence of PDD by acting synergistically with α-synucleinopathy (4–8). Neuropathological investigations of Aβ suggest an association with cognitive impairment and increased deposition in PDD, at least in a subset of patients (4, 5, 9–11). Similarly, increased concentrations of Aβ in cerebrospinal fluid have been associated with cognitive dysfunction and dementia in PD (12–16), although some studies have not found this relationship (17, 18). While both neuropathological and CSF markers suggest an association with cognitive decline, the cerebral deposition of amyloid is, however, not ubiquitous and the neuropathology underlying the development of PDD remains heterogeneous (19–21).

In vivo imaging of α-synuclein is currently not possible, but positron emission tomography (PET) imaging allows an *in vivo* test of an association between amyloid deposits and cognition in PD (22, 23). Amyloid PET imaging, however, has produced conflicting results in PD, especially with respect to cognitive decline. Gomperts and colleagues (22), found no difference in amyloid accumulation in the precuneus between a group of PD patients with mild cognitive impairment (PD-MCI) and cognitively normal patients at baseline, but the baseline presence of amyloid was weakly associated with cognitive decline an average of 2.5 years later, suggesting that amyloid may be a better marker of future rather than current cognitive status in PD. While Fiorenzato et al. (24), suggest a modest association with cognitive decline, other *in vivo* amyloid imaging studies suggest that amyloid deposition may occur in only a minority of PD patients, even in PDD (23, 25–31). However, these previous PET studies have used relatively small samples and the robustness of their findings may be compromised by low statistical power, lack of thorough cognitive characterization, or not accounting for age.

We therefore investigated the relationship between amyloid deposition and cognitive impairment in PD using [^{18}F] Florbetaben (FBB) PET imaging in a large, cognitively well-characterized group of PD participants that included cases with normal cognition (PDN), mild cognitive impairment (PD-MCI) and dementia (PDD). Patients meeting PD-MCI criteria are at a 7-fold higher risk of conversion to PDD over a 4-year period compared to patients who do not meet these criteria (32). Thus, the sample was enriched by recruiting a large proportion of PD-MCI patients; this is a group in whom intervention to prevent progression to dementia is particularly pertinent.

Since previous studies have suffered from inconsistent and variable standardization procedures, we used centiloid scaling in the present investigation. The centiloid scale facilitates direct comparison of amyloid deposition across different imaging centers, analysis methods, amyloid ligands (incorporating ^{11}C- and ^{18}F-based ligands), and diseases (33, 34). This is achieved by appling a linear scaling to amyloid PET data to an average value of zero in high-certainty amyloid-negative subjects, and to an average of 100 in typical AD subjects (33). In this first application of centiloid standardization in PD, we (1) investigated the relationship between amyloid deposition and cognitive impairment in a group of well-characterized PD participants representative of the broad cognitive spectrum, and (2) established the distribution of centiloid values across the cognitive spectrum in PD.

MATERIALS AND METHODS

As part of an ongoing longitudinal study, a convenience sample of 118 PD participants meeting the UK Parkinson's Disease Society's criteria for idiopathic PD (35) was recruited from volunteers at the Movement Disorders Clinic at the New Zealand Brain Research Institute, Christchurch, New Zealand. We invited people representative of the broad spectrum of cognitive status in PD to participate, i.e., from normal cognition to dementia, although we particularly encouraged participation from individuals with PD-MCI. Exclusion criteria included atypical Parkinsonian disorders; prior learning disability; previous history of other neurological conditions including moderate-severe head injury, stroke, vascular dementia; and major psychiatric or medical illness in the previous 6 months. Neuroradiological screening (RJK) excluded two participants with multifocal infarcts and one in whom part of the bolus injection extravasated into the soft tissue. Participants completed a neuropsychological battery, MRI scanning session, and [^{18}F] Florbetaben (FBB) PET imaging. All participants gave written informed consent, with additional consent from a significant other when appropriate. The study was approved by the regional Ethics Committee of the New Zealand Ministry of Health (No. URB/09/08/037).

Diagnostic Criteria and Assessment

Comprehensive neuropsychological assessment fulfilling the Movement Disorders Society (MDS) Task Force Level II criteria was used to diagnose PD-MCI (32, 36). Five cognitive domains were examined (executive function; attention, working memory and processing speed; learning and memory; visuospatial/visuoperceptual function; and language; see **Supplementary Table 1** for a list of the specific tests) (32). Within each cognitive domain, standardized scores from the constituent neuropsychological tests were averaged to provide individual cognitive domain scores; global cognitive performance for each participant was expressed as an aggregate z score obtained by averaging four domain scores (language domain excluded). PD-MCI cases had unimpaired functional activities of daily living, as verified by interview with a significant other, and scored 1.5 SD or more below normative data on at least two measures within at least one of the five cognitive domains (32). Dementia was defined using MDS criteria as significant cognitive impairments (2 SD below normative data) in at least two of five cognitive domains, plus evidence

of significant impairment in everyday functional activities, not attributed to motor impairments (37). Participants also completed the Montreal Cognitive assessment (MoCA). All assessments and scans were performed with no disruption to participants' usual medication regimen. PD participants were classified as either cognitively normal (PDN, $n = 23$), with mild cognitive impairment (PD-MCI; $n = 76$), or with dementia (PDD; $n = 16$). Assessors were blinded to amyloid status.

PET Acquisition

[^{18}F] Florbetaben (FBB) was manufactured in Melbourne, Australia, by Cyclotek Pty Ltd, and transported by air freight to Christchurch, New Zealand, with sufficient radioactivity for three participant doses, despite the passage of three half-lives in transit. After receiving an intravenous injection of 300 MBq ± 20% FBB, participants were scanned in "list mode" on a GE Discovery 690 PET/CT scanner, 90–110 min after injection. Images were reconstructed using an iterative time-of-flight plus SharpIR algorithm. Standardized uptake value (SUV), defined as the decay-corrected brain radioactivity concentration normalized for injected dose and body weight, was calculated at each voxel. A low dose CT scan was acquired immediately prior to PET scanning for attenuation correction. Voxel size in the reconstructed 20 min PET image was $1.2 \times 1.2 \times 3.2$ mm^3.

MRI Acquisition

MR images were acquired on a 3T General Electric HDxt scanner (GE Healthcare, Waukesha, USA) with an eight-channel head coil. A volumetric T1-weighted (inversion-prepared spoiled gradient recalled echo (SPGR), TE/TR = 2.8/6.6 ms, TI = 400 ms, flip angle = 15 deg, acquisition matrix = 256 × 256 × 170, FOV = 250 mm, slice thickness = 1 mm) was acquired to facilitate spatial normalization of FBB PET images. Additional T2-weighted and T2-weighted fluid-attenuated inversion recovery (FLAIR) images were acquired to enable a clinical read.

Classification of FBB Images

Visual classification of FBB scans as positive or negative is accurate and reliable for detection of cases with histology-defined plaques (38). A neuroradiologist (RJK, with both in-person and e-training), blinded to cognitive status, rated each scan as amyloid-positive or -negative. That judgment was based on the assessment of FBB uptake in gray vs. white matter in the lateral temporal, frontal, posterior cingulate/precuneus, and parietal lobes (in accordance with the NeuraCeq™ guidelines: https://www.accessdata.fda.gov/drugsatfda_docs/label/2014/204677s000lbl.pdf).

An additional approach using standardized uptake value ratios (SUVR) or centiloids (see below) was also used to categorize FBB scans. An ROC analysis [using the R package "pROC" (39)] was used to identify the optimum centiloid cut-off to separate positive and negative scans.

Image Processing

MRI

CAT12 (r934, http://www.neuro.uni-jena.de/cat/), a toolbox of SPM12 (v6685, http://www.fil.ion.ucl.ac.uk/spm/), running in Matlab 9.0.0 (R2016a), was used to process T1-weighted structural images. Images were bias corrected, spatially normalized via DARTEL (using the MNI-registered template provided within CAT12), modulated to compensate for the effect of spatial normalization, and classified into gray matter (GM), white matter (WM), and cerebrospinal fluid (CSF), all within the same generative model (40).

PET Data

FBB PET images were coregistered to each person's T1-weighted image and warped into MNI space using the MRI-derived deformation fields. We then created a standardized uptake value ratio (SUVR) image in each individual by scaling to the mean radioactivity in the Centiloid project whole cerebellum reference region of interest. Mean cortical SUVR was extracted from the standard centiloid cortical region. Lastly, SUVR images were smoothed using an 8 mm isotropic Gaussian kernel for whole-brain analysis.

Centiloid Calibration

We performed a level 3 centiloid calibration (**Supplementary Material**) to verify agreement between the standard centiloid processing method (which utilized SPM8) and our processing method (which utilized CAT12 normalization) (33, 34). All calibration parameters were within expected values, validating our processing methods (slope = 0.998, intercept = −0.187, and $R^2 = 0.995$). Cortical centiloid values were calculated in all PD participants using the FBB-to-centiloid conversion equation (centiloid units = $153.4 \times \text{SUVR}_{\text{FBB}} - 154.9$) (34).

Regions of Interest (ROIs)

While our principal analysis focused on cortical Aβ deposition, a number of both pathological and imaging studies suggest a potential relationship between Aβ accumulation in the striatum, thalamus, and globus pallidus and cognitive decline (10, 24, 41–43). We therefore specifically investigated *a priori* ROIs, including the caudate, putamen, thalamus, globus pallidus, and precuneus. The precuneus was included as a representative cortical region that exhibits very high amyloid load in AD (44). As standard centiloid regions do not exist for these structures, we calculated average SUVR within these regions defined by the Harvard-Oxford cortical and subcortical atlases in MNI152 space (45–48).

Statistical Analysis

Bayesian models were fitted using the "brms" (v2.2.0) package (49) in R (v3.4.4). In each model, four chains with 2,000 iterations each were used to generate the posterior sample. Model comparison using LOOIC (leave-one-out information criterion) was performed when models included correlated predictors or predictive performance was being evaluated (50). A lower LOOIC score, by at least twice the standard error of the estimated difference, indicated a model with a better fit, and consequently whether a specific predictor significantly improved model fit. Baseline demographic and neuropsychological group differences were analyzed using linear models (in brms). Analysis code and data are available at https://osf.io/5fqb9/.

Region of Interest (ROI) Analysis

We investigated the relationship between FBB uptake and cognition in PD using Bayesian regression models including age and sex.

(1) We first tested for evidence of varying cortical amyloid deposition (centiloid) across the cognitive subgroups (PDN, PD-MCI, PDD).
(2) We aimed to predict a continuous measure of global cognitive ability (aggregate cognitive z score) as a function of age, sex, and cortical FBB binding (centiloid). We evaluated the importance of predictors by model comparison, using LOOIC. That is, we compared a model predicting global cognitive ability with and without cortical FBB binding in order to determine whether cortical FBB binding improved prediction of global cognitive ability. This same procedure was repeated for the memory domain score.
(3) Lastly, regional SUVR from the *a priori* ROIs was modeled as a function of age, age-by-ROI, sex, and global cognitive ability-by-ROI interaction, in order to investigate the relationship between FBB uptake and cognition in the different ROIs.

Whole-Brain Voxel-Wise Analysis (SUVR)

We used a standard, frequentist ANCOVA model (with age and sex as covariates) to assess the spatial distribution of amyloid deposition across cognitive subgroups (we specifically investigated the contrasts: PDD > PD-MCI, PDD > PDN, and PD-MCI > PDN). In addition, we ran three multiple linear regression models to investigate the association between voxel-wise FBB SUVR and continuous measures of (1) global cognitive ability (cognitive z score), (2) memory domain score, and (3) age. Age and sex were included as covariates in the global cognitive ability and memory domain models; only sex was included in the age model. Voxel-wise comparisons were performed using a gray matter mask and a permutation-based inference tool for non-parametric thresholding ["randomise" (51) in FSLv5.0.9]. For each contrast, the null distribution was generated from 5,000 permutations and the alpha level set at $p < 0.05$, corrected for multiple comparisons [family-wise error correction using threshold-free cluster-enhancement (TFCE)].

RESULTS

Table 1 summarizes the demographic and clinical information for PD participants. Twenty-one of 115 (18%) had positive FBB scans on visual assessment. We identified a centiloid cut-off of 31.3 (equivalent SUVR = 1.21), which yielded sensitivity (to visually assessed positive scans) = 100%, specificity = 92.6%, and AUC [95% confidence interval] = 0.98 [0.97, 1.0]. We also identified a significant association between centiloid and age ($r = 0.011$ [0.005, 0.017] SUVR/year, or 9.3% per decade).

TABLE 1 | Demographic, cognitive, and clinical metrics.

	PDN	PD-MCI	PDD	Linear model
n	23	76	16	–
Female, No. [%]	8 (35)	18 (24)	3 (19)	–
Age, years	70 (6)	72 (6)	77 (6)	PDD > PDN & PD-MCI
Education, years	12 (2)	13 (3)	12 (2)	∼
PD symptom duration, years	7.4 (5)	7.3 (4)	8.5 (5)	∼
MoCA	26 (2)	23 (3)	16 (5)	PDN > PD-MCI > PDD
Cognitive Z score	0.28 (0.48)	−0.81 (0.53)	−1.89(0.57)[a]	PDN > PD-MCI > PDD
Memory domain score	0.52 (0.86)	−0.82 (0.85)	−1.82(0.67)[a]	PDN > PD-MCI > PDD
Dose, MBq	294 (20)	300 (16)	290 (27)	∼
Aβ positive, No. [%][b]	4 [17]	11 [14]	6 [38]	–
Mean cortical $SUVR_{NS}$	1.11 (0.13)	1.12 (0.18)	1.28 (0.30)	PDD > PDN & PD-MCI
Mean cortical CL	16 (19)	18 (27)	42 (44)	PDD > PDN & PD-MCI

Values are mean (standard deviation) unless specified; [a]Cognitive z scores and memory domain scores for seven PDD participants were imputed from restricted neuropsychological data due to their inability to complete the full cognitive assessment. [b]Visual assessment of amyloid positive/negative reported. ∼, no evidence of a difference; –, no statistical test applicable or was not performed. Pairwise group estimates were considered different if 95% uncertainty intervals did not overlap. MBq, megabecquerel; MoCA, Montreal Cognitive Assessment; Aβ, Amyloid beta; $SUVR_{NS}$, Standardized uptake value ratio with "non-standard" processing (see ***Supplementary Material****), CL, centiloid.*

Regional Amyloid Distribution in PD

With a simple model that only considered the discrete cognitive groups, we found evidence of increased cortical amyloid accumulation in PDD relative to PDN and PD-MCI (**Figure 1**; **Table 1**). However, adding age as a covariate to the model and using LOOIC to compare models, showed that age, rather than cognitive group, was predictive of increased cortical amyloid accumulation (**Figure 2B**; **Supplementary Material**). When attempting to predict cognition from cortical amyloid deposition, the addition of FBB uptake (centiloid) to a model resulted in marginally worse out-of-sample prediction of global cognitive score [LOOIC (standard error) = 1.8 (0.8), **Figure 2A**] and memory score [0.7 (2.1), data not shown] than simpler models, which only included age and an intercept. This indicates FBB uptake has little, if any, relationship with cognitive impairment in our PD sample. In *a priori* ROIs, including age and sex, we saw no evidence of association between FBB uptake (SUVR) and either global cognitive or memory score (**Figure 3**).

Whole-Brain Voxel-Wise Amyloid Distribution in PD

We identified no evidence of a difference in amyloid deposition across PD cognitive groups (TFCE-corrected, $p < 0.05$). Furthermore, we identified no evidence of association between SUVR and either global cognitive

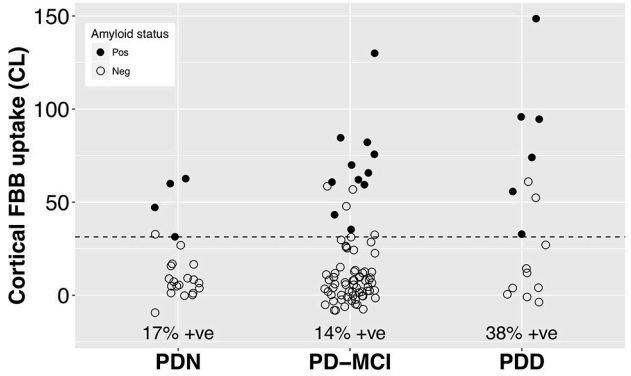

FIGURE 1 | Cortical FBB uptake by cognitive group. We found evidence of increased cortical amyloid accumulation in PDD relative to PDN and PD-MCI, however this was explained by the older age of the PDD group (**Table 1**). The dashed line at CL = 31.3 indicates the ROC-defined optimal centiloid cut-off in this sample, with sensitivity to clinically positive cases = 100%, specificity = 92.6%, AUC [95% confidence interval] = 0.98 [0.97, 1.0]. FBB, Florbetaben; PDN, Parkinson's with normal cognition; PD-MCI, Parkinson's with mild cognitive impairment; PDD, Parkinson's with dementia; CL, centiloid.

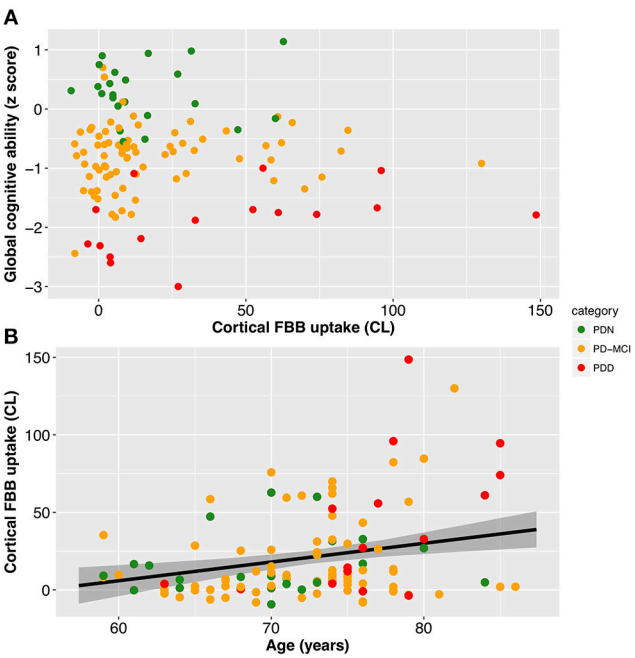

FIGURE 2 | Associations between cortical amyloid deposition and global cognitive ability and age. **(A)** Scatter plot showing no evidence of a significant association between global cognitive ability (Cognitive z score) and cortical amyloid (CL; **Table 1**). **(B)** Scatter plot of cortical amyloid (CL) vs. age (years). FBB uptake was associated with age (slope = 1.5 CL/year, 95% uncertainty interval [0.6, 2.3], equivalent to SUVR of 0.011/year [0.005, 0.017]). Black line depicts estimate from the Bayesian model fit and the shaded area indicates the 95% credible interval. Color represents cognitive status: green—Parkinson's with normal cognition (PDN), orange—Parkinson's with mild cognitive impairment (PD-MCI), red—Parkinson's with dementia (PDD). CL, centiloid.

ability or memory domain scores. There was, however, a widespread positive association between SUVR and age over the cortex (**Figure 4**).

DISCUSSION

Using FBB PET imaging in 115 PD patients across the cognitive spectrum, we observed significantly higher cortical amyloid accumulation in our PDD group relative to other cognitive subgroups, but model comparison indicated this was due to the older age of the PDD group.

Visual assessment revealed amyloid positive proportions of 17, 14, and 38% in PDN, PD-MCI, and PDD groups, respectively. The prevalence of amyloid positivity reported in the literature is variable, ranging from 0 to 53% in PDN (26, 27, 30, 31, 52), 0–47% in PD-MCI (23, 26, 27, 30, 31, 52), and an estimated point prevalence of 34% in PDD (23). Nevertheless, these proportions of amyloid positivity across the cognitive spectrum in PD are substantially lower than levels seen in Alzheimer's dementia (88%) (53) or amnestic MCI (69%) (54), and are closer to levels seen in elderly controls (11.6% at age 60, 23.8% at 70, and 34.5% at 80 years) (53). The association we observed between amyloid deposition and age (r = 0.011 [0.005, 0.017] SUVR/year, or 9.3% per decade) is similar to that reported in the healthy elderly population (^{11}C-PiB uptake increased at 0.016 SUVR/year, ∼10% per decade) (54), indicating that a PD-specific influence on amyloid accumulation is unlikely. Although global SUVR measures obtained from PiB and FBB PET in the same subjects have excellent linear correlation, the above rates are not directly comparable as different reference regions were used to define SUVR (for example, we used the whole cerebellum while Villemagne et al. (54), used the cerebellar cortex). Nevertheless, amyloid load in our PD sample appears to be consistent with levels seen in the general elderly population, as well as previous PD studies (2, 23, 31), and any increases in our PDD group can be explained by their older age. Not accounting for age may help explain the recent report of association between amyloid deposition and global cognition in a subset of the Parkinson's Progression Marker Initiative (24).

Ideally we would have used a predefined centiloid threshold derived from a large population study to define amyloid positivity in our PD sample. However, to the best of our knowledge, this is not currently possible. SUVR cut-off values are well established, but recent work demonstrates that specific thresholds are, as expected, highly dependent on the reference regions and processing methodology (7, 55). Therefore, a threshold derived using a particular method should not necessarily be applied to a different processing methodology, even after centiloid standardization (55). Many potential thresholds are available: a phase III FBB study identified a histopathologically-confirmed amyloid positivity cut-off of SUVR = 1.478 (56); Jack et al. (57), report a Pittsburgh Compound B-derived cut-off of SUVR = 1.42 and CL = 19; Bullich et al. (58), reported FBB thresholds using cerebellar cortex (SUVR = 1.43) and non-centiloid whole cerebellum (SUVR = 0.96) as reference regions. However, it would be inappropriate to apply these cut points to our current dataset as image processing and reference regions differed from the standard centiloid SUVR method. Su et al. (55), presented a centiloid cut-off using standard reference regions (CL = 6.8) based on an ROC analysis to classify young, amyloid negative

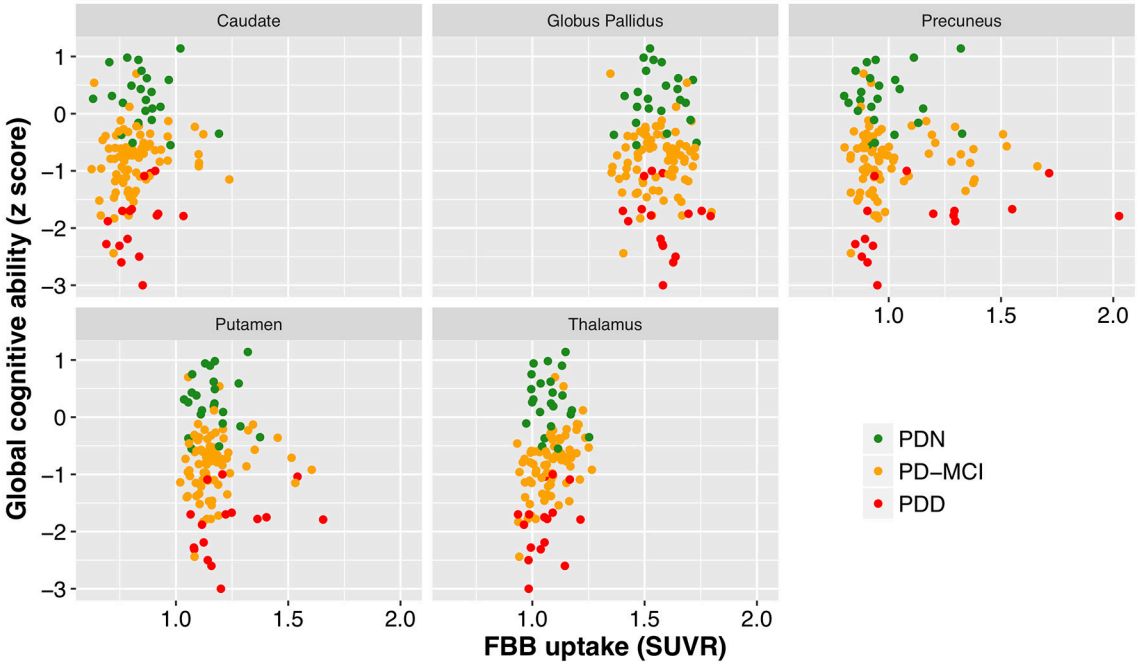

FIGURE 3 | Cognitive performance as a function of mean standardized uptake volume ratios (Florbetaben) within a number of brain regions. While different regions exhibited different levels of amyloid deposition, there was a clear lack of relationship between cognitive performance (cognitive z score) and SUVR within all of the regions examined. FBB, Florbetaben; SUVR, standardized uptake volume ratio. Color represents cognitive status: green—Parkinson's with normal cognition (PDN), orange—Parkinson's with mild cognitive impairment (PD-MCI), red—Parkinson's with dementia (PDD).

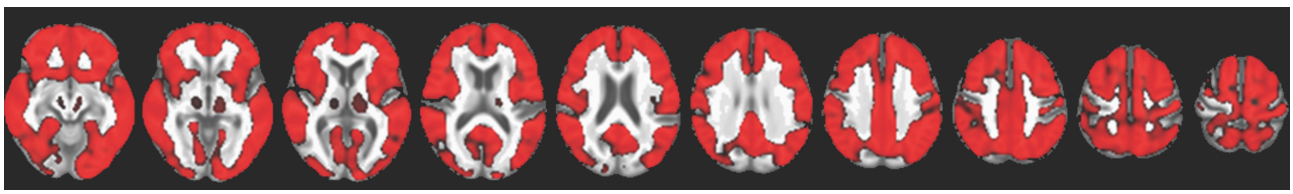

FIGURE 4 | Red indicates voxels with a significant positive association between FBB uptake and age (TFCE-corrected $p < 0.05$), overlaid on a study-specific structural image. This association was evident throughout the cortex and in the thalamus but not in the striatum.

participants from AD patients in the GAAIN dataset. This surprisingly low threshold may be driven by differences in non-specific binding and tracer delivery differences between young and old participants. In any case, standardized centiloid analyses of large cohorts are needed to establish appropriate centiloid thresholds, which will lead to greater applicability of the centiloid scale.

In this study, we used a well-validated visual assessment to clinically rate scans as being amyloid positive or negative (38). As there is not an accepted threshold based on standardized centiloid reference regions, we defined an amyloid positivity centiloid cut-off threshold in our sample. Our cut-off (CL = 31.3, SUVR = 1.21) corresponds well to the estimated value proposed by Rowe and colleagues (34) in the context of AD (CL = 25–30), however our estimated threshold may be biased by the low number of Aβ positive patients.

Our results suggest a lower prevalence of amyloid-positive PDD individuals than in dementia with Lewy bodies (DLB); neither of these two conditions exhibit the proportions of amyloid-positive cases reported in Alzheimer's dementia (23, 30, 59, 60). While some have reported an association between cognitive ability and cortical SUVR in DLB (28), the largest study (including the most thoroughly profiled group of DLB to date) did not find an association between amyloid deposition and clinical profile, despite showing increased amyloid accumulation vs. controls (59). We confirm here a similar lack of association in PD between amyloid deposition and cognitive impairment, with age explaining the increased FBB-uptake observed in our PDD group.

Most of our PD patients were within the normal centiloid range (comparted to control data from the Global Alzheimer's Association Information Network used for level 3 centiloid standardization: http://www.gaain.org/centiloid-project), with few showing AD-like levels of cortical amyloid. Hence Aβ pathology is unlikely to be a dominant causal factor in the majority of individuals with PD or PDD.

PET measures of amyloid do not suggest plaques as a primary pathology for dementia in PD, but amyloid may play a part in conjunction with other pathologies, such as alpha-synuclein and hyper-phosphorylated tau. It is expected that tau deposition will correlate more directly with current cognitive ability, due to its association with accelerating neuronal injury. Initial tau PET imaging in PD and DLB demonstrates a spectrum of deposition, with reports of both association (30, 52) and lack of association (26, 61) with cognitive impairments in PD. Thus, consideration of amyloid, tau, and alpha-synuclein deposition in the same individuals may ultimately provide a more complete description of how pathological processes potentially interact to affect cognition in PD. A potential scenario for prediction of future outcomes will most likely synthesize an array of biomarkers representative of these and other pathologies (21, 62).

Our results suggest that amyloid deposition is neither necessary nor sufficient to explain cognitive decline and dementia in PD. The current study cannot address the role that amyloid accumulation plays in AD, but it does raise the question as to the fundamental relationship between amyloid plaques and dementia. While the amyloid cascade hypothesis remains the leading candidate to explain the pathophysiology of AD, it not universally accepted (63, 64). Amyloid beta may be a downstream result, and not necessarily the cause, of AD (65).

Limitations of this study include the absence of a healthy control group. Analyses were restricted to the effects of varying levels of cognitive impairment within PD. All comparisons to healthy controls were based on comparable reports from the literature. However, the primary aim of this work was to investigate the relationship between amyloid deposition and cognitive impairment *within* a group of well-characterized PD participants. Even when following level II criteria for PD-MCI, considerable variability exists across those diagnosed as PD-MCI; some exhibit single domain and others multi-domain impairment (32). It is possible that different subtypes may exhibit greater or lesser underlying Aβ. Nonetheless, Aβ was not associated with global cognitive ability or memory function. We do not know the APOE genotype of our participants, which has been shown to correlate with amyloid deposition (31, 54). We also did not have histopathological confirmation of amyloid plaque accumulation, although recent work demonstrates tight agreement between visual assessment of amyloid PET and histopathological evidence in AD (58). Lastly, recent work suggests that partial volume correction can improve the ability of FBB PET to discriminate between AD patients and healthy controls (66). We did not perform this step because partial volume correction methods are still highly variable across centers, with no consensus on optimal methods, and have not been incorporated into centiloid standardization procedures yet (33).

In this cross-sectional investigation of a large, cognitively well-characterized PD group, we found increased cortical amyloid accumulation in PDD, but this was explained by the older age of the PDD group. We found no associations between amyloid load and continuous measures of cognitive performance. This suggests that Aβ accumulation is not the primary cause of cognitive impairments in PD. Low levels of amyloid may, however, still interact synergistically with other PD pathological processes, thereby accelerating other pathways to dementia.

DATA AVAILABILITY

Analysis code and data are available on the Open Science Framework at https://osf.io/5fqb9/.

ETHICS STATEMENT

All participants gave written consent, with additional consent from a significant other when appropriate. The study was approved by the regional Ethics Committee of the New Zealand Ministry of Health (No. URB/09/08/037).

AUTHOR CONTRIBUTIONS

TM, DJM, MM, TP, DHM, JD-A, and TA conceptualized and designed the study. TM, MS, and DJM drafted the manuscript, performed the image processing, and statistical analyses. TM, MM, DHM, RK, DJM, LL, JD-A, and TA obtained funding for the study. RK, LL, DJM, MM, TP, and SM provided administrative, technical, and material support. All authors contributed to acquisition, analysis, or interpretation of data. All authors contributed to manuscript revision, read, and approved the submitted version.

FUNDING

Research reported in this publication was supported by the Health Research Council of New Zealand (14/440), a Sir Charles Hercus Early Career Development Fellowship from the Health Research Council of New Zealand (17/039), a Neurological Foundation of New Zealand Philip Wrightson Posdoctoral Fellowship (1327-WF), the Canterbury Medical Research Foundation (15/08), the New Zealand Brain Research Institute, and a University of Otago Research Grant.

ACKNOWLEDGMENTS

We thank all of the participants for their willingness to take part in this study.

SUPPLEMENTARY MATERIAL

The Supplementary Material for this article can be found online at: https://www.frontiersin.org/articles/10.3389/fneur.2019.00391/full#supplementary-material

REFERENCES

1. Aarsland D, Creese B, Politis M, Chaudhuri KR, Ffytche DH, Weintraub D, et al. Cognitive decline in Parkinson disease. *Nat Rev Neurol*. (2017) 13:217–31. doi: 10.1038/nrneurol.2017.27
2. Hely MA, Reid WG, Adena MA, Halliday GM, Morris JG. The Sydney multicenter study of Parkinson's disease: the inevitability of dementia at 20 years. *Mov Disord*. (2008) 23:837–44. doi: 10.1002/mds.21956
3. Jones AJ, Kuijer RG, Livingston L, Myall D, Horne K, MacAskill M, et al. Caregiver burden is increased in Parkinson's disease with mild cognitive impairment (PD-MCI). *Transl Neurodegener*. (2017) 6:17. doi: 10.1186/s40035-017-0085-5
4. Irwin DJ, Lee VMY, Trojanowski JQ. Parkinson's disease dementia: convergence of [alpha]-synuclein, tau and amyloid-[beta] pathologies. *Nat Rev Neurosci*. (2013) 14:626–36. doi: 10.1038/nrn3549
5. Compta Y, Parkkinen L, O'Sullivan SS, Vandrovcova J, Holton JL, Collins C, et al. Lewy- and Alzheimer-type pathologies in Parkinson's disease dementia: which is more important? *Brain*. (2011) 134:1493–505. doi: 10.1093/brain/awr031
6. Kotzbauer PT, Cairns NJ, Campbell MC, et al. Pathologic accumulation of α-synuclein and aβ in parkinson disease patients with dementia. *Arch Neurol*. (2012) 69:1326–31. doi: 10.1001/archneurol.2012.1608
7. Lashley T, Holton JL, Gray E, Kirkham K, O'Sullivan SS, Hilbig A, et al. Cortical alpha-synuclein load is associated with amyloid-beta plaque burden in a subset of Parkinson's disease patients. *Acta Neuropathol*. (2008) 115:417–25. doi: 10.1007/s00401-007-0336-0
8. Irwin DJ, Xie SX, Coughlin D, Nevler N, Akhtar RS, McMillan CT, et al. CSF tau and beta-amyloid predict cerebral synucleinopathy in autopsied Lewy body disorders. *Neurology*. (2018) 90:e1038–46. doi: 10.1212/WNL.0000000000005166
9. Compta Y, Parkkinen L, Kempster P, Selikhova M, Lashley T, Holton JL, et al. The significance of alpha-synuclein, amyloid-beta and tau pathologies in Parkinson's disease progression and related dementia. *Neurodegener Dis*. (2014) 13:154–6. doi: 10.1159/000354670
10. Shah N, Frey KA, Muller ML, Petrou M, Kotagal V, Koeppe RA, et al. Striatal and cortical beta-amyloidopathy and cognition in Parkinson's disease. *Mov Disord*. (2016) 31:111–7. doi: 10.1002/mds.26369
11. Sabbagh MN, Adler CH, Lahti TJ, Connor DJ, Vedders L, Peterson LK, et al. Parkinson disease with dementia: comparing patients with and without Alzheimer pathology. *Alzheimer Dis Assoc Disord*. (2009) 23:295–7. doi: 10.1097/WAD.0b013e31819c5ef4
12. Buongiorno M, Compta Y, Marti MJ. Amyloid-beta and tau biomarkers in Parkinson's disease-dementia. *J Neurol Sci*. (2011) 310:25–30. doi: 10.1016/j.jns.2011.06.046
13. Compta Y, Ibarretxe-Bilbao N, Pereira JB, Junque C, Bargallo N, Tolosa E, et al. Grey matter volume correlates of cerebrospinal markers of Alzheimer-pathology in Parkinson's disease and related dementia. *Parkinsonism Relat Disord*. (2012) 18:941–7. doi: 10.1016/j.parkreldis.2012.04.028
14. Siderowf A, Xie SX, Hurtig H, Weintraub D, Duda J, Chen-Plotkin A, et al. CSF amyloid {beta} 1-42 predicts cognitive decline in Parkinson disease. *Neurology*. (2010) 75:1055-61. doi: 10.1212/WNL.0b013e3181f39a78
15. McMillan CT, Wolk DA. Presence of cerebral amyloid modulates phenotype and pattern of neurodegeneration in early Parkinson's disease. *J Neurol Neurosurg Psychiatry*. (2016) 87:1112–22. doi: 10.1136/jnnp-2015-312690
16. Goldman JG, Andrews H, Amara A, Naito A, Alcalay RN, Shaw LM, et al. Cerebrospinal fluid, plasma, and saliva in the BioFIND study: relationships among biomarkers and Parkinson's disease features. *Mov Disord*. (2018) 33:282–8. doi: 10.1002/mds.27232
17. Dolatshahi M, Pourmirbabaei S, Kamalian A, Ashraf-Ganjouei A, Yaseri M, Aarabi MH. Longitudinal alterations of alpha-synuclein, amyloid beta, total, and phosphorylated tau in cerebrospinal fluid and correlations between their changes in Parkinson's disease. *Front Neurol*. (2018) 9:560. doi: 10.3389/fneur.2018.00560
18. Kang JH. Cerebrospinal fluid amyloid beta1-42, tau, and alpha-synuclein predict the heterogeneous progression of cognitive dysfunction in Parkinson's disease. *J Mov Disord*. (2016) 9:89–96. doi: 10.14802/jmd.16017
19. Adler CH, Caviness JN, Sabbagh MN, Shill HA, Connor DJ, Sue L, et al. Heterogeneous neuropathological findings in Parkinson's disease with mild cognitive impairment. *Acta Neuropathol*. (2010) 120:827–8. doi: 10.1007/s00401-010-0744-4
20. Jellinger K. Heterogenous mechanisms of mild cognitive impairment in Parkinson's disease. *J Neural Transm*. (2012) 119:381–2. doi: 10.1007/s00702-011-0716-4
21. Compta Y, Pereira JB, Rios J, Ibarretxe-Bilbao N, Junque C, Bargallo N, et al. Combined dementia-risk biomarkers in Parkinson's disease: a prospective longitudinal study. *Parkinsonism Relat Disord*. (2013) 19:717–24. doi: 10.1016/j.parkreldis.2013.03.009
22. Gomperts SN, Locascio JJ, Rentz D, Santarlasci A, Marquie M, Johnson KA, et al. Amyloid is linked to cognitive decline in patients with Parkinson disease without dementia. *Neurology*. (2013) 80:85–91. doi: 10.1212/WNL.0b013e31827b1a07
23. Petrou M, Dwamena BA, Foerster BR, MacEachern MP, Bohnen NI, Muller ML, et al. Amyloid deposition in Parkinson's disease and cognitive impairment: a systematic review. *Mov Disord*. (2015) 30:925–35. doi: 10.1002/mds.26191
24. Fiorenzato E, Biundo R, Cecchin D, Frigo AC, Kim J, Weis L, et al. Brain amyloid contribution to cognitive dysfunction in early-stage Parkinson's disease: the PPMI dataset. *J Alzheimers Dis*. (2018) 66:229–37. doi: 10.3233/JAD-180390
25. Petrou M, Bohnen NI, Muller ML, Koeppe RA, Albin RL, Frey KA. Abeta-amyloid deposition in patients with Parkinson disease at risk for development of dementia. *Neurology*. (2012) 79:1161–7. doi: 10.1212/WNL.0b013e3182698d4a
26. Winer JR, Maass A, Pressman P, et al. Associations between tau, β-amyloid, and cognition in parkinson disease. *JAMA Neurology*. (2018) 75:227–35. doi: 10.1001/jamaneurol.2017.3713
27. Mashima K, Ito D, Kameyama M, Osada T, Tabuchi H, Nihei Y, et al. Extremely low prevalence of amyloid positron emission tomography positivity in Parkinson's disease without dementia. *Eur Neurol*. (2017) 77:231–7. doi: 10.1159/000464322
28. Gomperts SN, Locascio JJ, Marquie M, Santarlasci AL, Rentz DM, Maye J, et al. Brain amyloid and cognition in Lewy body diseases. *Mov Disord*. (2012) 27:965–73. doi: 10.1002/mds.25048
29. Edison P, Ahmed I, Fan Z, Hinz R, Gelosa G, Ray Chaudhuri K, et al. Microglia, amyloid, and glucose metabolism in Parkinson's disease with and without dementia. *Neuropsychopharmacology*. (2013) 38:938–49. doi: 10.1038/npp.2012.255
30. Lee SH, Cho H, Choi JY, Lee JH, Ryu YH, Lee MS, et al. Distinct patterns of amyloid-dependent tau accumulation in Lewy body diseases. *Mov Disord*. (2018) 33:262–72. doi: 10.1002/mds.27252
31. Akhtar RS, Xie SX, Chen YJ, Rick J, Gross RG, Nasrallah IM, et al. Regional brain amyloid-β accumulation associates with domain-specific cognitive performance in Parkinson disease without dementia. *PLoS ONE*. (2017) 12:e0177924. doi: 10.1371/journal.pone.0177924
32. Wood K-L, Myall DJ, Livingston L, Melzer TR, Pitcher TL, MacAskill MR, et al. Different PD-MCI criteria and risk of dementia in Parkinson's disease: 4-year longitudinal study. *NPJ Parkinson's Disease*. (2016) 2:15027. doi: 10.1038/npjparkd.2015.27
33. Klunk WE, Koeppe RA, Price JC, Benzinger TL, Devous MD, Sr., Jagust WJ, et al. The centiloid project: standardizing quantitative amyloid plaque estimation by PET. *Alzheimers Dement*. (2015) 11:1–15. doi: 10.1016/j.jalz.2014.07.003
34. Rowe CC, Doré V, Jones G, Baxendale D, Mulligan RS, Bullich S, et al. 18F-Florbetaben PET beta-amyloid binding expressed in centiloids. *Eur J Nucl Med Mol Imaging*. (2017) 44:2053–9. doi: 10.1007/s00259-017-3749-6
35. Hughes AJ, Daniel SE, Kilford L, Lees AJ. Accuracy of clinical diagnosis of idiopathic Parkinson's disease: a clinico-pathological study of 100 cases. *J Neurol Neurosurg Psychiatry*. (1992) 55:181–4. doi: 10.1136/jnnp.55.3.181
36. Litvan I, Goldman JG, Tröster AI, Schmand BA, Weintraub D, Petersen RC, et al. Diagnostic criteria for mild cognitive impairment in Parkinson's disease: Movement Disorder Society Task Force guidelines. *Mov Disord*. (2012) 27:349–56. doi: 10.1002/mds.24893
37. Emre M, Aarsland D, Brown RG, Burn DJ, Duyckaerts C, Mizuno Y, et al. Clinical diagnostic criteria for dementia associated with Parkinson's disease. *Mov Disord*. (2007) 22:1689–707. doi: 10.1002/mds.21507

38. Seibyl J, Catafau AM, Barthel H, Ishii K, Rowe CC, Leverenz JB, et al. Impact of training method on the robustness of the visual assessment of 18F-florbetaben PET scans: results from a phase-3 study. *J Nucl Med*. (2016) 57:900–6. doi: 10.2967/jnumed.115.161927
39. Robin X, Turck N, Hainard A, Tiberti N, Lisacek F, Sanchez J-C, et al. pROC: an open-source package for R and S+ to analyze and compare ROC curves. *BMC Bioinformatics*. (2011) 12:77. doi: 10.1186/1471-2105-12-77
40. Ashburner J, Friston KJ. Unified segmentation. *Neuroimage*. (2005) 26:839–51. doi: 10.1016/j.neuroimage.2005.02.018
41. Dugger BN, Serrano GE, Sue LI, Walker DG, Adler CH, Shill HA, et al. Presence of striatal amyloid plaques in Parkinson's disease dementia predicts concomitant Alzheimer's disease: usefulness for amyloid imaging. *J Parkinsons Dis*. (2012) 2:57–65. doi: 10.3233/jpd-2012-11073
42. Kalaitzakis ME, Graeber MB, Gentleman SM, Pearce RK. Striatal beta-amyloid deposition in Parkinson disease with dementia. *J Neuropathol Exp Neurol*. (2008) 67:155–61. doi: 10.1097/NEN.0b013e31816362aa
43. Chen Y, Nasrallah I, Akhtar R, Rick J, Chen-Plotkin A, Trojanowski J, et al. Comparing patterns of brain amyloid deposition in Parkinson's disease to Alzheimer's disease and cognitively normal controls using [^{18}F] florbetapir PET imaging. *J Nucl Med*. (2017) 58:416.
44. Becker GA, Ichise M, Barthel H, Luthardt J, Patt M, Seese A, et al. PET quantification of 18F-florbetaben binding to β-amyloid deposits in human brains. *J Nucl Med*. (2013) 54:723–31. doi: 10.2967/jnumed.112.107185
45. Makris N, Goldstein JM, Kennedy D, Hodge SM, Caviness VS, Faraone SV, et al. Decreased volume of left and total anterior insular lobule in schizophrenia. *Schizophr Res*. (2006) 83:155–71. doi: 10.1016/j.schres.2005.11.020
46. Frazier JA, Chiu S, Breeze JL, Makris N, Lange N, Kennedy DN, et al. Structural brain magnetic resonance imaging of limbic and thalamic volumes in pediatric bipolar disorder. *Am J Psychiatry*. (2005) 162:1256–65. doi: 10.1176/appi.ajp.162.7.1256
47. Desikan RS, Segonne F, Fischl B, Quinn BT, Dickerson BC, Blacker D, et al. An automated labeling system for subdividing the human cerebral cortex on MRI scans into gyral based regions of interest. *Neuroimage*. (2006) 31:968–80. doi: 10.1016/j.neuroimage.2006.01.021
48. Goldstein JM, Seidman LJ, Makris N, Ahern T, O'Brien LM, Caviness VS Jr., et al. Hypothalamic abnormalities in schizophrenia: sex effects and genetic vulnerability. *Biol Psychiatry*. (2007) 61:935–45. doi: 10.1016/j.biopsych.2006.06.027
49. Buerkner P. brms: an R package for Bayesian multilevel models using Stan. *J Stat Softw*. (2017) 80:1–28. doi: 10.18637/jss.v080.i01
50. Vehtari A, Gelman A, Gabry J. Practical Bayesian model evaluation using leave-one-out cross-validation and WAIC. *J Stat Comput*. (2017) 27:1413–32. doi: 10.1007/s11222-016-9696-4
51. Winkler AM, Ridgway GR, Webster MA, Smith SM, Nichols TE. Permutation inference for the general linear model. *Neuroimage*. (2014) 92:381–97. doi: 10.1016/j.neuroimage.2014.01.060
52. Gomperts SN, Locascio JJ, Makaretz SJ, Schultz A, Caso C, Vasdev N, et al. Tau positron emission tomographic imaging in the lewy body diseases. *JAMA Neurol*. (2016) 73:1334–441. doi: 10.1001/jamaneurol.2016.3338
53. Ossenkoppele R, Jansen WJ, Rabinovici GD, Knol DL, van der Flier WM, van Berckel BN, et al. Prevalence of amyloid pet positivity in dementia syndromes: a meta-analysis. *JAMA*. (2015) 313:1939–50. doi: 10.1001/jama.2015.4669
54. Villemagne VL, Pike KE, Chételat G, Ellis KA, Mulligan RS, Bourgeat P, et al. Longitudinal assessment of Aβ and cognition in aging and Alzheimer disease. *Ann Neurol*. (2011) 69:181–92. doi: 10.1002/ana.22248
55. Su Y, Flores S, Hornbeck RC, Speidel B, Vlassenko AG, Gordon BA, et al. Utilizing the centiloid scale in cross-sectional and longitudinal PiB PET studies. *Neuroimage*. (2018) 19:406–16. doi: 10.1016/j.nicl.2018.04.022
56. Sabri O, Sabbagh MN, Seibyl J, Barthel H, Akatsu H, Ouchi Y, et al. Florbetaben PET imaging to detect amyloid beta plaques in Alzheimer's disease: phase 3 study. *Alzheimers Dement*. (2015) 11:964–74. doi: 10.1016/j.jalz.2015.02.004
57. Jack CR, Wiste HJ, Weigand SD, Therneau TM, Lowe VJ, Knopman DS, et al. Defining imaging biomarker cut points for brain aging and Alzheimer's disease. *Alzheimers Dement*. (2017) 13:205–16. doi: 10.1016/j.jalz.2016.08.005
58. Bullich S, Seibyl J, Catafau AM, Jovalekic A, Koglin N, Barthel H, et al. Optimized classification of (18)F-florbetaben PET scans as positive and negative using an SUVR quantitative approach and comparison to visual assessment. *Neuroimage*. (2017) 15:325–32. doi: 10.1016/j.nicl.2017.04.025
59. Donaghy PC, Firbank MJ, Thomas AJ, Lloyd J, Petrides G, Barnett N, et al. Clinical and imaging correlates of amyloid deposition in dementia with Lewy bodies. *Mov Disord*. (2018) 33:1130–8. doi: 10.1002/mds.27403
60. Gomperts SN, Rentz DM, Moran E, Becker JA, Locascio JJ, Klunk WE, et al. Imaging amyloid deposition in Lewy body diseases. *Neurology*. (2008) 71:903–10. doi: 10.1212/01.wnl.0000326146.60732.d6
61. Hansen AK, Damholdt MF, Fedorova TD, Knudsen K, Parbo P, Ismail R, et al. *In vivo* cortical tau in Parkinson's disease using 18F-AV-1451 positron emission tomography. *Mov Disord*. (2017) 32:922–7. doi: 10.1002/mds.26961
62. Lanskey JH, McColgan P, Schrag AE, Morris HR, Acosta-Cabronero J, Rees G, et al. Can neuroimaging predict dementia in Parkinson's disease? *Brain*. (2018) 141:2545–60. doi: 10.1093/brain/awy211
63. Herrup K. The case for rejecting the amyloid cascade hypothesis. *Nat Neurosci*. (2015) 18:794. doi: 10.1038/nn.4017
64. Harrison JR, Owen MJ. Alzheimer's disease: the amyloid hypothesis on trial. *Br J Psychiatry*. (2016) 208:1–3. doi: 10.1192/bjp.bp.115.167569
65. Drachman DA. The amyloid hypothesis, time to move on: amyloid is the downstream result, not cause, of Alzheimer's disease. *Alzheimers Dement*. (2014) 10:372–80. doi: 10.1016/j.jalz.2013.11.003
66. Rullmann M, Dukart J, Hoffmann K-T, Luthardt J, Tiepolt S, Patt M, et al. Partial-volume effect correction improves quantitative analysis of 18F-florbetaben β-amyloid PET scans. *J Nucl Med*. (2016) 57:198–203. doi: 10.2967/jnumed.115.161893

Conflict of Interest Statement: DHM has received honoraria through payments to UCL Institute of Neurology for Advisory Committee and/or Consultancy advice from Novartis and Mitsubishi Pharma Europe, and grants through payments to UCL Institute of Neurology from Biogen Idec and Novartis.

The remaining authors declare that the research was conducted in the absence of any commercial or financial relationships that could be construed as a potential conflict of interest.

frontiers in Neurology

ORIGINAL RESEARCH
published: 28 January 2021
doi: 10.3389/fneur.2020.594213

Resting-State Cerebello-Cortical Dysfunction in Parkinson's Disease

William C. Palmer[1], Brenna A. Cholerton[2], Cyrus P. Zabetian[3,4], Thomas J. Montine[2], Thomas J. Grabowski[1,4] and Swati Rane[1]*

[1] Department of Radiology, University of Washington Medical Center, Seattle, WA, United States, [2] Department of Pathology, Stanford University School of Medicine, Stanford, CA, United States, [3] Geriatric Research Education and Clinical Center, Veterans Affairs Puget Sound Health Care System, Seattle, WA, United States, [4] Department of Neurology, University of Washington School of Medicine, Seattle, WA, United States

Purpose: Recently, the cerebellum's role in Parkinson's disease (PD) has been highlighted. Therefore, this study sought to test the hypothesis that functional connectivity (FC) between cerebellar and cortical nodes of the resting-state networks differentiates PD patients from controls by scanning participants at rest using functional magnetic resonance imaging (fMRI) and investigating connectivity of the cerebellar nodes of the resting-state networks.

Materials and Methods: Sixty-two PD participants off medication for at least 12 h and 33 normal controls (NCs) were scanned at rest using blood oxygenation level-dependent fMRI scans. Motor and cognitive functions were assessed with the Movement Disorder Society's Revision of the Unified Parkinson's Disease Rating Scale III and Montreal Cognitive Assessment, respectively. Connectivity was investigated with cerebellar seeds defined by Buckner's 7-network atlas.

Results: PD participants had significant differences in FC when compared to NC participants. Most notably, PD patients had higher FC between cerebellar nodes of the somatomotor network (SMN) and the corresponding cortical nodes. Cognitive functioning was differentially associated with connectivity of the cerebellar SMN and dorsal attention network. Further, cerebellar connectivity of frontoparietal and default mode networks correlated with the severity of motor function.

Conclusion: Our study demonstrates altered cerebello-cortical FC in PD, as well as an association of this FC with PD-related motor and cognitive disruptions, thus providing additional evidence for the cerebellum's role in PD.

Keywords: Parkinson's disease, cerebellum, BOLD fMRI, resting-state connectivity, resting-state networks

OPEN ACCESS

Edited by:
Peter Sörös,
University of Oldenburg, Germany

Reviewed by:
David M. Cole,
University of Zurich, Switzerland
Abraham Z. Snyder,
Washington University in St. Louis, United States

****Correspondence:***
William C. Palmer
wcp23@uw.edu

Specialty section:
This article was submitted to Applied Neuroimaging, a section of the journal Frontiers in Neurology

Received: *20 August 2020*
Accepted: *11 December 2020*
Published: *28 January 2021*

Citation:
Palmer WC, Cholerton BA, Zabetian CP, Montine TJ, Grabowski TJ and Rane S (2021) Resting-State Cerebello-Cortical Dysfunction in Parkinson's Disease. Front. Neurol. 11:594213. doi: 10.3389/fneur.2020.594213

INTRODUCTION

Parkinson's disease (PD), a common progressive neurodegenerative disorder, is characterized primarily by motor symptoms but also has cognitive symptoms. PD traditionally has three pathological hallmarks (1). The first is the progressive loss of dopaminergic neurons in the substantia nigra. Second, the result of nigral neuronal death is a marked depletion of dopamine in the striatum, which has been the principal target for treatment. Third, PD is indicated by the presence of Lewy bodies, composed of α-synuclein aggregates, in the nigra and other subcortical and cortical regions. Neuroimaging studies have played a critical role in our understanding of how

these trademark pathologies influence neuronal function in humans (2). However, most studies have focused on the cortex, even though the cerebellum has also been implicated in the disease state of PD (3).

Studies that have investigated the cerebellum demonstrate that PD patients have cerebellar atrophy (4, 5) and hyperactivity (6, 7). Resting-state functional connectivity (FC) studies have also uncovered abnormalities in the cerebellum. Initial studies have examined the cerebellum's primary output, the dentate nucleus, or motor regions of the cerebellum, such as lobules V and VI (8, 9). These studies suggest atypical connectivity in PD patients within the various cerebellar regions, as well as between the cerebellum and the cortex (prefrontal, parietal, and temporal) and subcortical areas of the motor system. However, the cerebellum has been demonstrated to be involved in tasks beyond motor functioning, such as cognitive and affective processes, and non-motor symptoms are observed in PD patients (1, 10). Cerebellar involvement in cognitive functioning is supported by supramodal zones, particularly crus I and II, that are functionally connected to association areas, such as prefrontal and posterior-parietal cortex (11, 12).

Recent studies have explored the FC of larger portions of the cerebellum. In a network investigation utilizing whole cerebellar parcellations defined by anatomical boundaries, PD patients showed increased positive connectivity between somatomotor regions of the cerebellum and somatomotor cortical areas compared to controls (13). Furthermore, abnormal subcortical connectivity was discovered within the cerebellum and between the cerebellum and reward system (nucleus accumbens and orbitofrontal regions). Weaker correlations between the striatum and somatomotor cerebellar regions have also been discovered previously in PD patients compared to controls (14). Impaired visuospatial performance was associated with decreased positive intracerebellar connectivity, decreased magnitude of negative cerebellar to visual network FC, and a switch from negative cerebellar to reward FC in controls to positive in PD (13). Other studies investigated cerebellar regions that combine multiple anatomical territories. Analyses using clustering methods have uncovered unusual FC within identified cerebellar networks and between these networks and cortical areas including occipital, parietal, and frontal cortices in PD patients (15, 16). In a seed-based analysis, O'Callaghan et al. (17) explored a sensorimotor subregion that included lobules V, VI, VII, and VIII and a cognitive subregion that consisted of Crus I and II. This study probed the cerebellum's FC to large-scale cortical resting-state networks (RSNs) and cerebellar atrophy. PD patients had decreased FC between the cognitive cerebellum and somatomotor network (SMN). Cerebellar atrophy was correlated with changes in FC between the cerebellum and SMN, default mode network (DMN), dorsal attention (DAN), and frontoparietal network (FPN). Finally, the Movement Disorder Society's Revision of the Unified Parkinson's Disease Rating Scale III (MDS-UPDRS III) score was negatively correlated with cerebellar atrophy and FC between both motor and cognitive cerebellum and the SMN. These correlations between cerebellar FC and PD test scores are evidence that the cerebellum is implicated in the neurophysiology of PD and may thus have potential as a therapeutic target.

We sought to perform a network-based seed analysis of the cerebellum's FC to the cerebral cortex. Parcellations of the cerebellum were determined by Buckner's 7-network cerebellar atlas, which defines cerebellar nodes of the dominant cerebral RSNs (12). These seeds were not segregated by lobule, but rather by their proper cortical RSNs. Lobular boundaries have been found to be inconsistent with functional subdivisions in the cerebellum (18). Instead of seeding the cortical RSNs, we used the Buckner cerebellar atlas to seed the cerebellum for FC. To validate the cerebellar seeds, we confirmed the RSNs generated by these seeds. We hypothesized that such analysis would continue to show differential FC between PD patients and controls especially in motor areas of cortex. We also investigated whether performance on non-motor tests was correlated with cerebello-cortical FC.

MATERIALS AND METHODS

Participants

This study included 95 participants, who were recruited from the Pacific Udall Center between 2016 and 2019. All participants underwent a full neuropsychological battery [including the Montreal Cognitive Assessment (MoCA)], a neurological examination, and the MDS-UPDRS III. Data from these assessments were reviewed at a diagnostic consensus conference, attended by at least two movement disorders neurologists and a neuropsychologist, to determine the diagnostic category [PD or normal control (NC)] and cognitive status [normal, mild cognitive impairment (MCI), dementia]. PD with dementia required classification of parkinsonism prior to dementia by at least 1 year to exclude patients with dementia with Lewy bodies. Other exclusion criteria included individuals who had pathogenic mutations other than apolipoprotein E (APOE) and glucocerebrosidase (GBA) [e.g., leucine-rich repeat kinase 2 (LRRK2), α-synuclein (SNCA), Parkinson's Disease gene (PARK)2, phosphatase and tensin homolog-induce dkinase 1 (PINK1), and PARK7] and individuals who had contraindications to MRI (e.g., pacemaker or claustrophobia) or were non-ambulatory. Complete descriptions of this process and diagnostic criteria have been detailed previously (19–21). Sixty-two participants were determined to meet UK Parkinson's Disease Society Brain Bank clinical diagnostic criteria for PD, and 33 participants were classified as NC without PD symptoms. Prior to the scan, PD patients had not taken their dopamine replacement therapy for at least 12 h. During the scan, participants were directed to keep their eyes open and fixate

Abbreviations: cSMN, cerebellar components of the somatomotor network; CSF, cerebrospinal fluid; DMN, default mode network; DAN, dorsal attention network; TE, echo time; FWE, family-wise error; FPN, frontoparietal network; FC, functional connectivity; fMRI, functional magnetic resonance imaging; GM, gray matter; TI, inversion time; MCI, mild cognitive impairment; MoCA, Montreal Cognitive Assessment; MDS-UPDRS III, Movement Disorder Society's Revision of the Unified Parkinson's Disease Rating Scale III; NC, normal control; PD, Parkinson's disease; ROI, region of interest; RSN, resting-state network; TR, repetition time; PCA, principal component analysis; SMN, somatomotor network; SMA, supplementary motor area; WM, white matter.

on a cross without thinking of anything in particular. MDS-UPDRS III was administered on the same day as the scan without dopamine replacement therapy for PD patients. Within 6 months of imaging, MoCA scores were also collected for each participant. MDS-UPDRS III and MoCA scores were used as measures of motor dysfunction and cognitive performance, respectively (22, 23). Higher scores on MDS-UPDRS III indicate more severe motor symptoms, while higher scores on the MoCA imply better cognitive performance.

Imaging

All scans were acquired on a Philips 3T Achieva scanner with a 32-channel head coil using Sensitivity Encoding Reception. Anatomical T1 weighted scans were 3D MPRAGE sagittal acquisition. Spatial resolution was $1 \times 1 \times 1$ mm^3, repetition time (TR)/echo time (TE) was 10.17/4.71 ms, and inversion time (TI) was 900 ms. The blood oxygen level-dependent (BOLD) functional MRI (fMRI) acquisition was a whole-brain 2D-echo planar imaging acquisition. Resolution was $3.5 \times 3.5 \times 3.5$ mm^3, matrix size was 64×64 mm^2, and TR/TE was 2,500/45.5 ms. Each fMRI run acquired 240 time points of data.

Analysis

Preprocessing was completed using FSL (v5.0), AFNI (v17.3), and SPM12 (24–26).

Anatomical Image Processing

The anatomical T1 images were segmented into gray matter (GM), white matter (WM), and cerebrospinal fluid (CSF) after brain extraction. Average GM probability was calculated from the segmented GM probability partial volume estimate.

Seed-Based fMRI Connectivity Analysis

First, fMRI data were motion corrected. Participants with motion >1 fMRI voxel were excluded from the study. Next, baseline drift was removed with a 0.01-Hz high pass filter in FSL. To remove extreme motion, despiking was conducted in AFNI. The remaining preprocessing and analysis were conducted in Conn (v18). Functional data were co-registered to corresponding T1-weighted anatomical images in 2-mm Montreal Neurological Institute (MNI) space and normalized to the standard space. The anatomical CompCor algorithm was used to remove physiological noise using masks of WM and CSF (27). Briefly, the masks are thresholded to ensure that mask voxels contain at least 99% WM or 99% CSF. The CompCor routine in Conn then extracts the time courses from the WM and CSF voxels in the mask, constructs the covariance matrix, and performs principal component analysis (PCA). The most significant components from the PCA are extracted and used as estimates of physiological noise. These components were then used as confounds and regressed from the BOLD time series. Lastly, smoothing was performed with an 8-mm full-width half-maximum kernel. Based on our voxel size, a kernel of 8 mm is appropriate to reduce bias, ensure homoscedasticity, and improve signal-to-noise ratio for group-level analysis (28, 29). We do not expect the voxel or smoothing kernel size to negatively impact our results, as our seeds (∼24–75 cc) are much larger than both the voxel size (∼0.043 cc) and smoothing kernel (0.512 cc). Quality assurance involved manual inspection of data after each preprocessing step. For a flowchart of software and commands used for each step, see **Supplementary Figure 1**.

A seed-to-voxel whole-brain analysis was performed using the cerebellar parcellations defined by Buckner's 7-network atlas (12). The networks included the SMN, FPN, DMN, DAN, ventral attention, visual, and limbic networks. For this study, the visual and limbic networks were excluded because our interests were in investigating motor and cognitive functioning. Additionally, the SMN, FPN, DMN, and DAN have mainly been implicated in PD (30). The cerebellar networks are larger than the traditional spherical regions of interest (ROIs). Our seeds are network seeds with multiple distinct ROIs on the cerebellum, such as bilateral ROIs (**Figure 1**). The averaged time series of all the ROIs within the network seeds was obtained for seed-to-voxel connectivity analysis. Connectivity was measured as the correlation between the average time series of all voxels within a cerebellar network ROI and the time series of each voxel

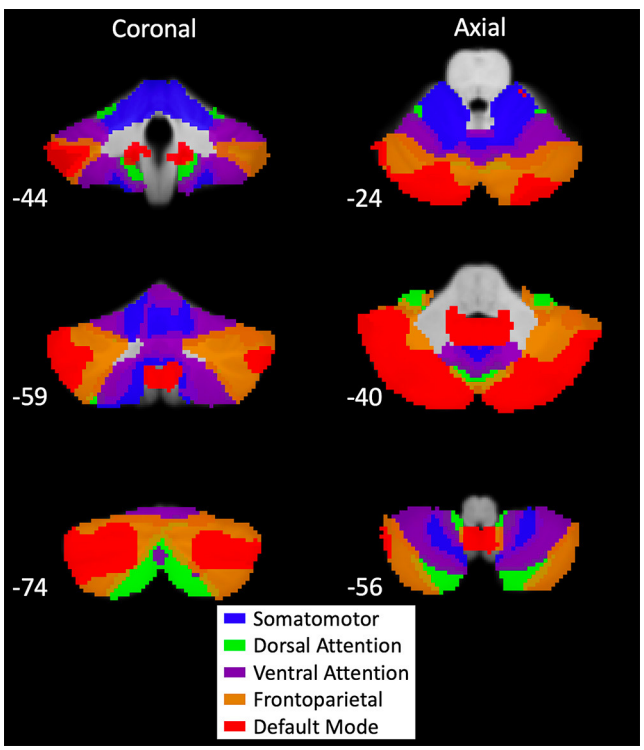

FIGURE 1 | Buckner's 7-network cerebellar atlas seeds. Map of cerebellar seeds produced by functional connectivity of large-scale resting-state networks to the cerebellum (12). Montreal Neurological Institute (MNI) coordinates are provided in the bottom left of each section. Networks included in our analysis were the somatomotor (blue), dorsal attention (green), ventral attention (purple), frontoparietal (orange), and default mode (red). Visual and limbic networks were excluded from analysis because only motor and cognitive functions were examined. These network seeds have multiple distinct regions of interest (ROIs) on the cerebellum. Average time series for seed-based analysis were generated using all ROIs within a network.

in the brain. While Buckner's atlas only considered positive correlations, both positive and negative correlations were used in this study. Statistical tests consisted of differences between groups, main effects of MDS-UPDRS III and MoCA scores, and interaction between MoCA score and group condition. Generalized linear models were adjusted for age, gender, average motion, and average GM probability. For all comparisons, we applied a two-sided voxel-wise thresholding at $p = 0.005$ and a cluster-size family-wise error (FWE) correction for multiple comparisons at $p = 0.05$.

Buckner's cerebellar atlas was derived from cortical RSNs. In this study, we seeded the cerebellar nodes of the RSNs to identify connectivity in cortical regions. Therefore, we first investigated the average connectivity of each cerebellar node to demonstrate it would reproduce the corresponding RSN (**Supplementary Figure 2**). Additionally, some previous studies chose lateralized ROIs in the cerebellum, and evidence of distinct functions of the left and right cerebellum exists (10). Hence, we split the SMN cerebellar seed by hemispheres and seeded both to investigate if our results are robust across hemispheres or have lateralized differences.

RESULTS

Clinical and Demographic Data

Fifty-seven PD participants (male = 40; female = 17) and 30 NC participants (male = 19; female = 11) were included in the final analysis. During quality assurance steps, eight participants were removed due to excessive motion or poor registration. Final analysis included six PD patients with dementia and 23 with MCI. On the other hand, no NC participants had dementia, but nine had MCI. While PD participants were 67.2 ± 8.1 (mean ± standard deviation) years old, NC participants were 70.7 ± 8.8 years old; the difference was not significant ($p = 0.07$). Among PD patients, the average MDS-UPDRS III score was 31.1 ± 12.1. Both PD (26.5 ± 2.6) and NC (26.6 ± 2.6) participants scored similarly on the MoCA, and the difference was not significant ($p = 0.87$). However, the difference in GM probability between PD (69.6 ± 1.3%) and NC (70.1 ± 1.3%) participants was significant ($p = 0.05$). This was expected because atrophy is well documented in PD (4, 5). In order to ensure that the FC differences exist despite the GM atrophy, the GM probabilities were included as a nuisance regressor in all subsequent analyses.

To assess for potential differences between PD and NC participants in movement during the scans, we compared motion between groups. Since participants with excess motion (>voxel size) were eliminated, the average motion (along X, Y, and Z axes) was 0.23 ± 0.34 mm in PD patients and 0.17 ± 0.13 mm in NC participants. This difference between groups was not statistically significant ($p = 0.26$). Still, the average motion estimates were included as a nuisance regressor to minimize the association of FC with motion. A summary of all demographic and clinical data is located in **Table 1**. For clarity of all FC analyses, cortical RSNs are denoted with abbreviations as above (e.g., SMN), while cerebellar components are denoted with a prefix "c" (e.g., cSMN).

Group Differences Between Parkinson's Disease Patients and Controls

Group differences were identified in FC of cSMN and cDAN to cortex. Compared to NC participants, PD patients had higher FC between the cSMN and the bilateral precentral gyrus, postcentral gyrus, and SMA ($p = 0.01$, depicted by yellow cluster in **Figure 2A**). PD patients had lower FC between the cSMN and the occipital lobe, specifically, bilateral intracalcarine cortex, occipital pole, lingual gyrus, right supracalcarine cortex, left occipital fusiform cortex, and temporal occipital fusiform cortex ($p = 0.0004$, purple cluster in **Figure 2A**), compared to controls. Furthermore, PD patients had lower FC between the cSMN and the lobule VI, crus I, and lobule VIII on only the left side ($p = 0.0004$, purple cluster in **Figure 2B**). PD participants also had higher right lateralized FC between the cDAN and the right post-central gyrus, pre-central gyrus, and superior parietal lobule ($p = 0.004$, yellow cluster in **Figure 2C**) compared to NC participants.

Similar differences were found when seeding the left and right hemispheres of the cSMN. For the left cSMN, there was higher FC to bilateral pre-central gyrus, SMA, and right post-central gyrus ($p = 0.01$, yellow cluster in **Supplementary Figure 3B**) but lower FC to occipital lobe ($p = 0.005$, purple cluster in **Supplementary Figure 3B**). On the other hand, FC for the right cSMN did not survive FWE correction at 0.05 but was evident at 0.07. With FWE correction at 0.07, right cSMN also had higher FC to bilateral precentral gyrus, postcentral gyrus, and SMA but lower FC to occipital lobe (**Supplementary Figure 3C**). These results support that our findings for the cSMN are robust and there are no major lateralized differences between the FC of the left and right cSMN.

TABLE 1 | Table of demographic and clinical data.

Condition	Male	Female	Age	Dementia	MCI	No CI	MDS-UPDRS III	MoCA	Motion (mm)	GM Prob* (%)
PD	40	17	67.2 ± 8.1	6	23	28	31.1 ± 12.1	26.5 ± 2.6	0.23 ± 0.34	69.6 ± 1.3
NC	19	11	70.7 ± 8.8	0	9	21	–	26.6 ± 2.6	0.17 ± 0.13	70.1 ± 1.3

*Data are stratified by condition (Parkinson's disease participants, PD; normal control, NC). Clinical data include cognitive diagnosis, which has three levels: dementia, mild cognitive impairment (MCI), and no cognitive impairment (No CI). The last two columns display average motion and gray matter probability in the two groups. Individual values were used as nuisance regressors in our analysis. All means are given with standard deviation (mean ± standard deviation). Other values are counts of participants belonging to that group. An asterisk indicates statistically significant differences (*p = 0.05). MoCA, Montreal Cognitive Assessment; MDS-UPDRS III, Movement Disorder Society's Revision of the Unified Parkinson's Disease Rating Scale III.*

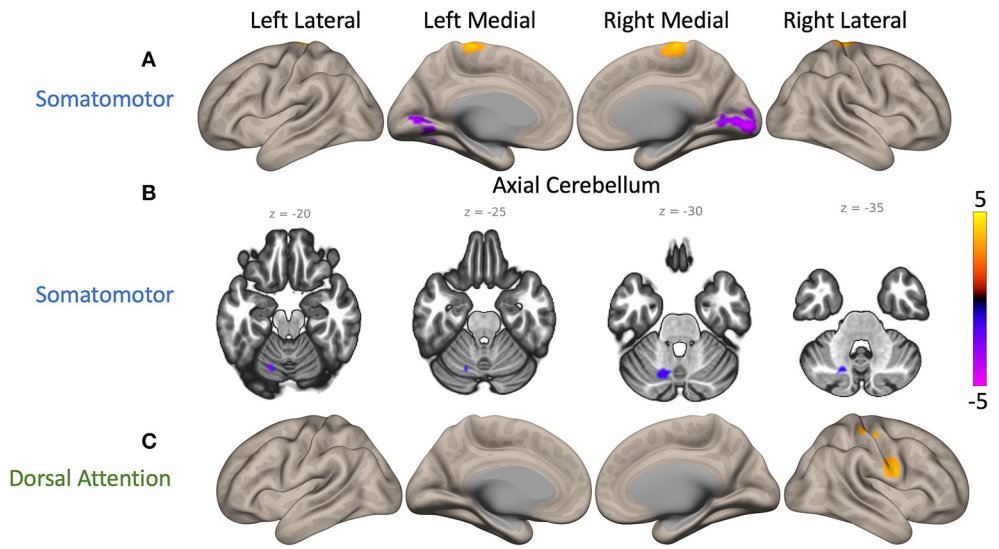

FIGURE 2 | Maps of cerebellar functional connectivity (FC) differences between Parkinson's disease (PD) patients and normal controls (NCs). Significant differences were found when seeding the cerebellar nodes of the somatomotor network (cSMN) and dorsal attention network (cDAN). The color bar represents *z*-scores, with yellow displaying where PD patient FC values were greater than NC participant values. **(A)** Two cerebral clusters were observed when seeding the cSMN. Compared to NC participants, PD patients showed greater FC between the cSMN and the precentral gyrus ($p = 0.01$, yellow) and lower FC between the cSMN and the right intracalcarine cortex ($p = 0.0004$, purple). **(B)** Another cluster located within lobule VI, crus I, and lobule VIII on the left side had lower FC with the cSMN in PD participants compared to controls ($p = 0.0004$, purple). **(C)** PD participants also had greater FC between the cDAN and the right postcentral gyrus than controls ($p = 0.004$, yellow). An average cortical connectivity map for all subjects can be found in **Supplementary Figure 2**.

In summary, compared to NC participants, PD patients had higher FC between the cSMN and the frontal regions of the cortex but lower FC from the cSMN to the posterior regions of the cortex. Furthermore, they had higher FC between the cDAN and the cortical somatomotor areas.

Main Effects of Movement Disorder Society's Revision of the Unified Parkinson's Disease Rating Scale III and Montreal Cognitive Assessment Scores

Significant effects of MDS-UPDRS III score were discovered on the FC of cFPN and cDMN. Higher MDS-UPDRS III scores (i.e., higher motor dysfunction) were associated with lower FC between the cFPN and the left superior frontal gyrus and precentral gyrus ($p = 0.04$, purple cluster in **Figure 3A**). A similar correlation was also present between MDS-UPDRS III scores and FC of the cDMN to the right precentral gyrus and middle frontal gyrus ($p = 0.03$, purple cluster in **Figure 3B**). No significant effects of MoCA score on cerebellar resting-state node FC were uncovered.

Interaction Between Montreal Cognitive Assessment Scores and Group

In both PD and NC participants, higher MoCA scores (i.e., better cognitive functioning) were associated with lower FC of cSMN to bilateral precentral gyrus, postcentral gyrus, SMA, and right superior parietal lobule (yellow cluster in **Figure 4A**). However, the correlation value in PD patients was significantly lower than that in NC participants ($p = 0.0004$). Higher MoCA score were also associated with higher FC between the cDAN and the right postcentral gyrus and precentral gyrus in both PD and NC participants (yellow cluster in **Figure 4B**). This correlation in PD patients was greater compared to NC participants ($p = 0.02$).

DISCUSSION

This study identified PD-related differences in the FC of cerebellar nodes of RSNs to cortex. As might be expected in a movement disorder, all tests identified clusters that included one or both paracentral lobules. FC levels were correlated with scores on both MDS-UPDRS III and MoCA, providing support for the cerebellum's role in PD.

All clusters identified in our analysis fit with previously discovered regions of dysfunction in PD both with and without cognitive impairment. Paracentral lobules, SMA, frontal gyrus, superior parietal, and occipital lobules have all been identified as areas with abnormal metabolism, connectivity, and/or neurotransmission (2). While occipital dysfunction is not observed consistently, alterations in cholinergic activity that are hypothesized to drive memory deficits are present in the occipital lobe in early PD (31, 32). This is consistent with our finding that there is decreased FC to occipital lobule in our early stage (duration = 7.7 ± 4.2 years) PD cohort. Decreased connectivity between the cerebellum and occipital lobe in PD patients compared to controls has been described previously and associated with visuospatial performance (13, 16). Furthermore, abnormal intracerebellar FC is a common finding

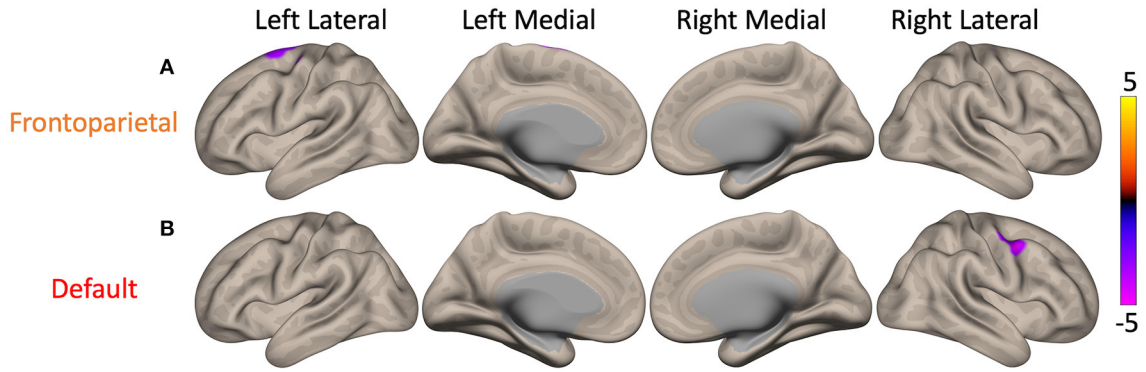

FIGURE 3 | Maps of the main effect of MDS-UPDRS III, Movement Disorder Society's Revision of the Unified Parkinson's Disease Rating Scale III (MDS-UPDRS III) scores on cerebellar functional connectivity (FC). There were significant main effects when seeding the cerebellar nodes of the frontoparietal (cFPN) and default mode network (cDMN). The color bar represents z-scores, with yellow showing where higher MDS-UPDRS III score (i.e., greater motor dysfunction) was associated with higher FC. **(A)** In Parkinson's disease patients, higher MDS-UPDRS III scores were associated with lower FC between the cFPN and the left superior frontal gyrus ($p = 0.04$, purple). **(B)** Higher MDS-UPDRS III scores were also correlated with lower FC between the cDMN and the right precentral gyrus ($p = 0.03$, purple).

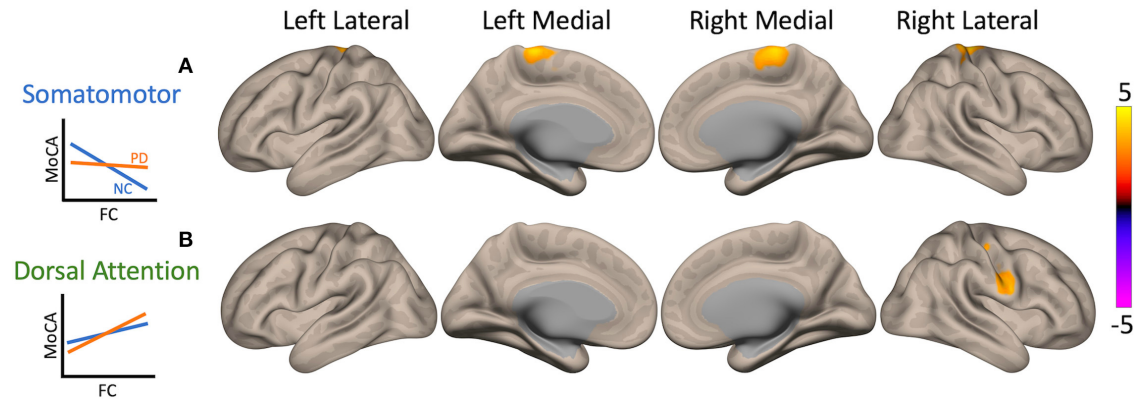

FIGURE 4 | Maps of interaction of Montreal Cognitive Assessment (MoCA) scores and patient condition on cerebellar functional connectivity (FC). Two clusters showed significant interactions when seeding the cerebellar nodes of the somatomotor network (cSMN) and dorsal attention network (cDAN). The color bar represents z-score, with yellow showing where Parkinson's disease (PD) patient correlation values were greater than normal control (NC) participant values. Interaction plots are presented on the left of the brain maps. The y-axis is MoCA score, and the x-axis is FC. PD patients are plotted in orange and NCs in blue. **(A)** In both PD and NC participants, higher MoCA scores (i.e., better cognitive functioning) were associated with lower FC between the cSMN and primarily right precentral gyrus, but PD patients had a weaker correlation compared to controls ($p = 0.0004$, yellow). **(B)** Higher MoCA scores were also associated with higher FC between cDAN and right postcentral gyrus and precentral gyrus; however, PD patients showed greater correlation compared to NC participants ($p = 0.02$, yellow).

in the literature; however, mixed results indicating that this connectivity is both increased and decreased warrant further investigation (8, 13, 15).

In addition, we found that FC between cSMN and somatomotor areas was significantly higher in PD participants compared to that in controls, as described previously (13, 33). FC between these areas was differentially associated with MoCA scores between groups. These differences can be attributed to PD symptoms because both PD and NC groups included participants with cognitive impairment and trends were still present after removal of patients with dementia. Relationships between MoCA score and motor functioning have been reported prior. One study found that motor severity scores significantly predicted worse MoCA scores (34). Additionally, a PD-related pattern of abnormal metabolism, associated with severity of cognitive symptoms, has been identified in patients without MCI or dementia and includes cortical motor areas and parts of the cerebellum (35, 36). On the other hand, we did not detect a significant effect of MDS-UPDRS III scores on FC between these areas. While some studies have reported significant associations between MDS-UPDRS III score and somatomotor cortical FC, others have not discovered this relationship, warranting further investigation of the correlation (13, 15, 17, 37).

The two cerebellar RSN nodes implicated with investigation of the main effect of MDS-UPDRS III score were cFPN and cDMN, both of which showed altered connectivity to somatomotor cortical areas. Similar relationships have been reported before (12, 17). In terms of function, FPN mediates the

transition between two contrasting states: a resting state driven by DMN and top-down attention state coordinated by DAN (38). Consistent with these known relationships, lower MDS-UPDRS III scores (i.e., better motor functioning) were associated with higher connectivity between these three networks when seeding the cFPN and cDMN.

The increased connectivity between the cerebellum and somatomotor cortical areas could be explained by the cerebellum's role in error detection and correction for both motor and cognitive functioning (39, 40). The constant error detection and correction occurring in patients with PD would result in strengthened connectivity between the cerebellum and cortex. Some studies have found evidence of a compensatory influence of the cerebellum in PD (17, 41, 42). However, further research is required to solidify the cerebellum's compensatory role (43).

While our findings are congruent with prior research, our ROIs were segregated by their proper RSN rather than traditional cerebellar anatomical structures (12). Since investigation of PD connectivity with a functionally defined cerebellar atlas is novel, future studies should conduct investigations with similar atlases to confirm our results. We chose to use Buckner's 7-network atlas because parcellations were determined by connectivity to large-scale RSNs (12). These networks inherently span multiple functional domains (motor and cognitive) and allowed the investigation of RSNs of interest. Other functionally defined cerebellar atlases should be investigated as well (18, 44, 45).

CONCLUSION

This study presents a novel investigation of dysfunction in cerebellar FC to cortex in patients with PD. Analyses conducted with the cerebellum parcellated by cortical RSNs showed FC differences between PD and NC participants. These FC differences were associated with MDS-UPDRS III and MoCA scores for motor and cognitive functioning. Overall, the study provides further evidence for the cerebellum's role in PD.

DATA AVAILABILITY STATEMENT

The datasets presented in this article are not readily available because data sharing would not comply with institutional review board approval. Requests to access the datasets should be directed to William C. Palmer, wcp23@uw.edu.

ETHICS STATEMENT

The studies involving human participants were reviewed and approved by Institutional Review Board of the University of Washington. The patients/participants provided their written informed consent to participate in this study.

AUTHOR CONTRIBUTIONS

SR conceptualized the study. BC and CZ identified the participants and assigned the diagnoses. TM and TG provided the data. WP executed the data analysis with oversight from SR and TG. WP also developed the manuscript. BC, CZ, TG, and SR reviewed and critiqued the manuscript. All authors contributed to the article and approved the submitted version.

FUNDING

This work was funded by grants from the National Institutes of Health (K01 AG055669 and 2P50 NS062684). The funding source did not provide scientific input for the study.

ACKNOWLEDGMENTS

This material is the result of work supported in part by resources and the use of facilities at the Veterans Affairs Puget Sound Health Care System.

SUPPLEMENTARY MATERIAL

The Supplementary Material for this article can be found online at: https://www.frontiersin.org/articles/10.3389/fneur.2020.594213/full#supplementary-material

REFERENCES

1. Davie CA. A review of Parkinson's disease. *Br Med Bull.* (2008) 86:109–27. doi: 10.1093/bmb/ldn013
2. Niethammer M, Feigin A, Eidelberg D. Functional neuroimaging in Parkinson's disease. *Cold Spring Harb Perspect Med.* (2012) 2:a009274. doi: 10.1101/cshperspect.a009274
3. Wu T, Hallett M. The cerebellum in Parkinson's disease. *Brain.* (2013) 136:696–709. doi: 10.1093/brain/aws360
4. Camicioli R, Gee M, Bouchard TP, Fisher NJ, Hanstock CC, Emery DJ, et al. Voxel-based morphometry reveals extra-nigral atrophy patterns associated with dopamine refractory cognitive and motor impairment in parkinsonism. *Parkinsonism Relat Disord.* (2009) 15:187–95. doi: 10.1016/j.parkreldis.2008.05.002
5. Borghammer P, Østergaard K, Cumming P, Gjedde A, Rodell A, Hall N, et al. A deformation-based morphometry study of patients with early-stage Parkinson's disease. *Eur J Neurol.* (2010) 17:314–20. doi: 10.1111/j.1468-1331.2009.02807.x
6. Rascol O, Sabatini U, Fabre N, Brefel C, Loubinoux I, Celsis P, et al. The ipsilateral cerebellar hemisphere is overactive during hand movements in akinetic parkinsonian patients. *Brain.* (1997) 120:103–10. doi: 10.1093/brain/120.1.103
7. Yu H, Sternad D, Corcos DM, Vaillancourt DE. Role of hyperactive cerebellum and motor cortex in Parkinson's disease. *Neuroimage.* (2007) 35:222–33. doi: 10.1016/j.neuroimage.2006.11.047
8. Liu H, Kale Edmiston E, Fan G, Xu K, Zhao B, Shang X, et al. Altered resting-state functional connectivity of the dentate nucleus in Parkinson's disease. *Psychiatry Res Neuroimaging.* (2013) 211:64–71. doi: 10.1016/j.pscychresns.2012.10.007
9. Dirkx MF, den Ouden HEM, Aarts E, Timmer MHM, Bloem BR, Toni I, et al. Dopamine controls Parkinson's tremor by inhibiting the cerebellar thalamus. *Brain.* (2017) 140:721–34. doi: 10.1093/brain/aww331

10. Stoodley CJ, Schmahmann JD. Functional topography in the human cerebellum: a meta-analysis of neuroimaging studies. *Neuroimage.* (2009) 44:489–501. doi: 10.1016/j.neuroimage.2008.08.039
11. O'Reilly JX, Beckmann CF, Tomassini V, Ramnani N, Johansen-Berg H. Distinct and overlapping functional zones in the cerebellum defined by resting state functional connectivity. *Cereb Cortex.* (2010) 20:953–65. doi: 10.1093/cercor/bhp157
12. Buckner RL, Krienen FM, Castellanos A, Diaz JC, Yeo BTT. The organization of the human cerebellum estimated by intrinsic functional connectivity. *J Neurophysiol.* (2011) 106:2322–45. doi: 10.1152/jn.00339.2011
13. Gratton C, Koller JM, Shannon W, Greene DJ, Maiti B, Snyder AZ, et al. Emergent functional network effects in Parkinson disease. *Cereb Cortex.* (2019) 29:2509–23. doi: 10.1093/cercor/bhy121
14. Hacker CD, Perlmutter JS, Criswell SR, Ances BM, Snyder AZ. Resting state functional connectivity of the striatum in Parkinson's disease. *Brain.* (2012) 135:3699–711. doi: 10.1093/brain/aws281
15. Onu M, Badea L, Roceanu A, Tivarus M, Bajenaru O. Increased connectivity between sensorimotor and attentional areas in Parkinson's disease. *Neuroradiology.* (2015) 57:957–68. doi: 10.1007/s00234-015-1556-y
16. Guimarães RP, Arci Santos MC, Dagher A, Campos LS, Azevedo P, Piovesana LG, et al. Pattern of reduced functional connectivity and structural abnormalities in Parkinson's disease: an exploratory study. *Front Neurol.* (2017) 7:243. doi: 10.3389/fneur.2016.00243
17. O'Callaghan C, Hornberger M, Balsters JH, Halliday GM, Lewis SJG, Shine JM. Cerebellar atrophy in Parkinson's disease and its implication for network connectivity. *Brain.* (2016) 139:845–55. doi: 10.1093/brain/awv399
18. King M, Hernandez-Castillo CR, Poldrack RA, Ivry RB, Diedrichsen J. Functional boundaries in the human cerebellum revealed by a multi-domain task battery. *Nat Neurosci.* (2019) 22:1371–8. doi: 10.1038/s41593-019-0436-x
19. Litvan I, Goldman JG, Tröster AI, Schmand BA, Weintraub D, Petersen RC, et al. Diagnostic criteria for mild cognitive impairment in Parkinson's disease: movement disorder society task force guidelines. *Mov Disord.* (2012) 27:349–56. doi: 10.1002/mds.24893
20. Cholerton BA, Zabetian CP, Quinn JF, Chung KA, Peterson A, Espay AJ, et al. Pacific Northwest Udall Center of Excellence clinical consortium: study design and baseline cohort characteristics. *J Park Dis.* (2013) 3:205–14. doi: 10.3233/JPD-130189
21. Cholerton BA, Zabetian CP, Wan JY, Montine TJ, Quinn JF, Mata IF, et al. Evaluation of mild cognitive impairment subtypes in Parkinson's disease. *Mov Disord.* (2014) 29:756–64. doi: 10.1002/mds.25875
22. Goetz CG, Fahn S, Martinez-Martin P, Poewe W, Sampaio C, Stebbins GT, et al. Movement disorder society-sponsored revision of the Unified Parkinson's Disease Rating Scale (MDS-UPDRS): process, format, and clinimetric testing plan. *Mov Disord.* (2007) 22:41–7. doi: 10.1002/mds.21198
23. Julayanont P, Nasreddine ZS. Montreal cognitive assessment (MoCA): concept and clinical review. In: Larner AJ, editor. *Cognitive Screening Instruments: A Practical Approach.* Cham: Springer International Publishing (2017). p. 139–95. doi: 10.1007/978-3-319-44775-9_7
24. Cox RW. AFNI: software for analysis and visualization of functional magnetic resonance neuroimages. *Comput Biomed Res Int J.* (1996) 29:162–73. doi: 10.1006/cbmr.1996.0014
25. Penny WD, Friston KJ, Ashburner JT, Kiebel SJ, Nichols TE. *Statistical Parametric Mapping: The Analysis of Functional Brain Images*. London; Burlington, MA; San Diego, CA: Elsevier (2007).
26. Jenkinson M, Beckmann CF, Behrens TEJ, Woolrich MW, Smith SM. FSL. *Neuroimage.* (2012) 62:782–90. doi: 10.1016/j.neuroimage.2011.09.015
27. Behzadi Y, Restom K, Liau J, Liu TT. A component based noise correction method (CompCor) for BOLD and perfusion based fMRI. *Neuroimage.* (2007) 37:90–101. doi: 10.1016/j.neuroimage.2007.04.042
28. Friston, K. J., Josephs, O., Zarahn, E., Holmes, A. P., Rouquette, S., and Poline, J.-B. (2000). To smooth or not to smooth? Bias and efficiency in fMRI time-series analysis. *Neuroimage.* 12, 196–208. doi: 10.1006/nimg.2000.0609
29. Mikl M, Mareček R, Hluštík P, Pavlicová M, Drastich A, Chlebus P, et al. Effects of spatial smoothing on fMRI group inferences. *Magn Reson Imaging.* (2008) 26:490–503. doi: 10.1016/j.mri.2007.08.006
30. Baggio HC, Segura B, Junque C. Resting-state functional brain networks in Parkinson's disease. *CNS Neurosci Ther.* (2015) 21:793–801. doi: 10.1111/cns.12417
31. Bohnen NI, Kanel P, Müller MLTM. Molecular imaging of the cholinergic system in Parkinson's disease. *Int Rev Neurobiol.* (2018) 141:211–50. doi: 10.1016/bs.irn.2018.07.027
32. Shimada H, Hirano S, Shinotoh H, Aotsuka A, Sato K, Tanaka N, et al. Mapping of brain acetylcholinesterase alterations in Lewy body disease by PET. *Neurology.* (2009) 73:273–8. doi: 10.1212/WNL.0b013e3181ab2b58
33. Wu T, Wang L, Hallett M, Chen Y, Li K, Chan P. Effective connectivity of brain networks during self-initiated movement in Parkinson's disease. *Neuroimage.* (2011) 55:204–15. doi: 10.1016/j.neuroimage.2010.11.074
34. Hu MTM, Szewczyk-Królikowski K, Tomlinson P, Nithi K, Rolinski M, Murray C, et al. Predictors of cognitive impairment in an early stage Parkinson's disease cohort. *Mov Disord.* (2014) 29:351–9. doi: 10.1002/mds.25748
35. Huang C, Mattis P, Tang C, Perrine K, Carbon M, Eidelberg D. Metabolic brain networks associated with cognitive function in Parkinson's disease. *Neuroimage.* (2007) 34:714–23. doi: 10.1016/j.neuroimage.2006.09.003
36. Huang C, Tang C, Feigin A, Lesser M, Ma Y, Pourfar M, et al. Changes in network activity with the progression of Parkinson's disease. *Brain.* (2007) 130:1834–46. doi: 10.1093/brain/awm086
37. Wu T, Wang L, Chen Y, Zhao C, Li K, Chan P. Changes of functional connectivity of the motor network in the resting state in Parkinson's disease. *Neurosci Lett.* (2009) 460:6–10. doi: 10.1016/j.neulet.2009.05.046
38. Spreng RN, Sepulcre J, Turner GR, Stevens WD, Schacter DL. Intrinsic architecture underlying the relations among the default, dorsal attention, and frontoparietal control networks of the human brain. *J Cogn Neurosci.* (2013) 25:74–86. doi: 10.1162/jocn_a_00281
39. Manto M, Bower JM, Conforto AB, Delgado-García JM, da Guarda SNF, Gerwig M, et al. Consensus paper: roles of the cerebellum in motor control—the diversity of ideas on cerebellar involvement in movement. *Cerebellum.* (2012) 11:457–87. doi: 10.1007/s12311-011-0331-9
40. Buckner RL. The cerebellum and cognitive function: 25 years of insight from anatomy and neuroimaging. *Neuron.* (2013) 80:807–15. doi: 10.1016/j.neuron.2013.10.044
41. Simioni AC, Dagher A, Fellows LK. Compensatory striatal–cerebellar connectivity in mild–moderate Parkinson's disease. *Neuroimage Clin.* (2016) 10:54–62. doi: 10.1016/j.nicl.2015.11.005
42. Xu S, He X-W, Zhao R, Chen W, Qin Z, Zhang J, et al. Cerebellar functional abnormalities in early stage drug-naïve and medicated Parkinson's disease. *J Neurol.* (2019) 266:1578–87. doi: 10.1007/s00415-019-09294-0
43. Martinu K, Monchi O. Cortico-basal ganglia and cortico-cerebellar circuits in Parkinson's disease: pathophysiology or compensation? *Behav Neurosci.* (2013) 127:222–36. doi: 10.1037/a0031226
44. Habas C, Kamdar N, Nguyen D, Prater K, Beckmann CF, Menon V, et al. Distinct cerebellar contributions to intrinsic connectivity networks. *J Neurosci.* (2009) 29:8586–94. doi: 10.1523/JNEUROSCI.1868-09.2009
45. Ji JL, Spronk M, Kulkarni K, Repovš G, Anticevic A, Cole MW. Mapping the human brain's cortical-subcortical functional network organization. *Neuroimage.* (2019) 185:35–57. doi: 10.1016/j.neuroimage.2018.10.006

Conflict of Interest: The authors declare that the research was conducted in the absence of any commercial or financial relationships that could be construed as a potential conflict of interest.

frontiers in Neurology

ORIGINAL RESEARCH
published: 04 May 2021
doi: 10.3389/fneur.2021.656041

Neuropsychiatric Symptoms in Parkinson's Disease After Subthalamic Nucleus Deep Brain Stimulation

Weibing Liu[1], *Tatsuya Yamamoto*[1,2*], *Yoshitaka Yamanaka*[1], *Masato Asahina*[3†], *Tomoyuki Uchiyama*[1,4], *Shigeki Hirano*[1], *Keisuke Shimizu*[1], *Yoshinori Higuchi*[5] *and Satoshi Kuwabara*[1]

[1] *Department of Neurology, Graduate School of Medicine, Chiba University, Chiba, Japan,* [2] *Division of Occupational Therapy, Department of Rehabilitation, Chiba Prefectural University of Health Sciences, Chiba, Japan,* [3] *Neurology Clinic, Tsudanuma, Japan,* [4] *Department of Neurology, International University of Health and Welfare, Ichikawa, Japan,* [5] *Department of Neurological Surgery, Graduate School of Medicine, Chiba University, Chiba, Japan*

OPEN ACCESS

Edited by:
Salvatore Galati, Neurocenter of Southern Switzerland, Switzerland

Reviewed by:
Abhishek Lenka, MedStar Georgetown University Hospital, United States
Chien Tai Hong, Taipei Medical University, Taiwan

***Correspondence:**
Tatsuya Yamamoto
tatsuya-yamamoto@mbc.nifty.com

†Present address:
Masato Asahina, Department of Neurology, Kanazawa Medical University, Kanazawa, Japan

Specialty section:
This article was submitted to Movement Disorders, a section of the journal Frontiers in Neurology

Received: *20 January 2021*
Accepted: *17 March 2021*
Published: *04 May 2021*

Citation:
Liu W, Yamamoto T, Yamanaka Y, Asahina M, Uchiyama T, Hirano S, Shimizu K, Higuchi Y and Kuwabara S (2021) Neuropsychiatric Symptoms in Parkinson's Disease After Subthalamic Nucleus Deep Brain Stimulation. Front. Neurol. 12:656041. doi: 10.3389/fneur.2021.656041

Background: Indications for subthalamic nucleus deep brain stimulation (STN-DBS) surgery are determined basically by preoperative motor function; however, postoperative quality of life (QOL) is not necessarily associated with improvements in motor symptoms, suggesting that neuropsychiatric symptoms might be related to QOL after surgery in patients with Parkinson's disease.

Objectives: We aimed to examine temporal changes in neuropsychiatric symptoms and their associations with QOL after STN-DBS.

Materials and Methods: We prospectively enrolled a total of 61 patients with Parkinson's disease (mean age = 65.3 ± 0.9 years, mean disease duration = 11.9 ± 0.4 years). Motor function, cognitive function, and neuropsychiatric symptoms were evaluated before and after DBS surgery. Postoperative evaluation was performed at 3 months, 1 year, and 3 years after surgery.

Results: Of the 61 participants, 54 completed postoperative clinical evaluation after 3 months, 47 after 1 year, and 23 after 3 years. Frontal lobe functions, depression, and verbal fluency significantly worsened 3 years after STN-DBS. Non-motor symptoms such as impulsivity and the Unified PD Rating Scale (UPDRS) part I score were associated with QOL after STN-DBS.

Conclusions: Frontal lobe functions, depression, and verbal fluency significantly worsened 3 years after STN-DBS. The UPDRS part I score and higher impulsivity might be associated with QOL after STN-DBS.

Keywords: Parkinson's disease, deep brain stimulation, quality of life, neuropsychiatric symptoms, UPDRS

INTRODUCTION

Parkinson's disease (PD) is a chronic, disabling neurodegenerative disease (1). Recent several studies reported in detail on the importance of non-motor dysfunctions such as cognitive, neuropsychiatric, and autonomic disorders (2–4).

Deep brain stimulation (DBS) is widely used to treat PD patients with motor complications such as wearing off and disabling dyskinesia, for which standard pharmacological treatment is ineffective (2). Ability to perform activities of daily living (ADLs) and quality of life (QOL) are also known to improve after DBS surgery (5–7).

However, our previous study showed that improvements in QOL after DBS surgery are minor compared with improvements in motor symptoms. We have also reported that QOL, as evaluated with the 39-item Parkinson's disease questionnaire (PDQ-39), is not necessarily correlated with motor function after DBS surgery, suggesting that non-motor symptoms might affect QOL after DBS surgery (8).

Some studies have shown that cognitive functions and neuropsychiatric symptoms worsen after DBS surgery in PD patients (9–11). Other studies have demonstrated that postoperative apathy can negate QOL improvement after subthalamic nucleus (STN)-DBS surgery (12). Changes in the depression and anxiety score after DBS surgery are also predictive of QOL after STN-DBS in PD patients (13). The results of these studies suggest that evaluation of the cognitive function and neuropsychiatric symptoms might be helpful in examining QOL after DBS surgery.

This study aimed to assess temporal changes in the cognitive function and neuropsychiatric symptoms (besides motor dysfunctions) after STN-DBS and to examine the relationship between cognitive and neuropsychiatric symptoms and QOL before and after STN-DBS.

MATERIALS AND METHODS

Participants

Between December 2009 and April 2019, we prospectively enrolled 61 PD patients who underwent bilateral STN-DBS at Chiba University Hospital. PD diagnosis was based on the clinical diagnostic criteria of the United Kingdom PD Society Brain Bank (14). All lead (Medtronic, Minneapolis, MN, USA) were implanted bilaterally into the STN in one session under local anesthesia. All participants reported medication-resistant fluctuations and complications in motor function. Before enrollment in the study, participants had been treated with antiparkinson medications and were taking levodopa/carbidopa, dopamine agonists, selegiline, istradefylline, zonisamide, and entacapone. No participants took anticholinergics immediately before or during the study, and motor functions in the "on" and "off" phases while on medications were evaluated with the Unified PD Rating Scale (UPDRS) parts I, II, III, and IV before and after STN-DBS. All postoperative assessments were performed under bilateral ON stimulation. Health-related QOL was assessed with the PDQ-39 Summary Index (SI) before and after STN-DBS, and cognitive functions were evaluated with the Mini Mental State Examination (MMSE), the Frontal Assessment Battery (FAB), and the Japanese version of the Montreal Cognitive Assessment (MoCA-J). The levodopa equivalent dose (LED) of the antiparkinson medications was calculated according to a description elsewhere (15).

In the neuropsychiatric evaluations, we used the verbal fluency test (VFT) to examine verbal fluency by counting the number of words such as animal and the words beginning with a specified word such as "fu," "a," and "ni" in Japanese (16). Furthermore, the Barratt Impulsiveness Scale 11 (BIS11) is used to assess the personality/behavioral construct of impulsiveness by a questionnaire composed of 30 items. The "attentional," "motor," and "non-planning" impulsiveness can be examined with the BIS11 (17). The Behavioral Inhibition System/Behavioral Activation System (BIS/BAS) scales evaluate impulsivity based on the theory that it can be understood as a joint function of the behavioral approach system (BAS) and the behavioral inhibition system (BIS) by a questionnaire composed of 20 items (18). The Japanese version of the Epworth Sleepiness Scale (JESS) and the rapid eye movement (REM) sleep behavior disorder screening questionnaire (RBD-Q) were used to assess for the presence of sleep disorder. A score of RBD-Q higher than 5 indicates the presence of RBD (19). The Self-Rating Depression Scale (SDS) and an apathy scale were used to evaluate depression and apathy, respectively.

Postoperative evaluations were performed at 3 months, 1 year, and 3 years after STN-DBS.

Statistical Analysis

All data are expressed as the mean ± standard errors of the mean, and all statistical analyses were performed using SPSS version 23.0 (IBM, Armonk, USA). Analysis of variance (ANOVA) with *post-hoc* analysis (Dunnet's test in this study) were used for comparisons between the baseline (preoperative) scores and the postoperative PDQ-39 Summary Index (SI), UPDRS sub-score, and cognitive functions (MMSE, FAB, and MoCA-J scores) at each follow-up point. ANOVA with *post-hoc* analysis were also used for comparisons between the baseline scores and postoperative neuropsychiatric symptoms (VFT, BIS11, BIS/BAS, JESS, SDS, apathy, and RBD-Q scores) at each follow-up point. Spearman's rank correlation coefficients were calculated to evaluate the relationship between the changes in LED (baseline and postoperative values) and the changes in the score of SDS. Multivariable linear regression analysis was used to determine which cognitive functions, neuropsychiatric symptoms besides the UPDRS sub-score, and LED influenced the QOL (PDQ-39 SI) at baseline and each follow-up point after surgery. Statistical significance was set at $p < 0.05$.

Ethical Considerations

The Chiba University Hospital Institutional Review Board approved this study. All 61 participants provided written informed consent, obtained during the "on" phase. The ethical standards committee at Chiba University gave approval to implement this study. All participants consented to the use of their examination scores for analysis.

RESULTS

A total of 61 patients with PD were enrolled in this study (mean age = 65.3 ± 0.9 years, mean disease duration = 11.9 ± 0.4 years). Of the 61 participants, 54 completed the postoperative clinical evaluation after 3 months, 47 after 1 year, and 23 after 3 years. The stimulation parameters were as follows: intensity, 2.7–3.2 V; pulse width, 60 μs; frequency, 130 Hz.

The mean LED decreased significantly from baseline dosage at each follow-up point after surgery ($p < 0.01$). The mean UPDRS parts II and III scores during the off phase (**Figures 1A,B**) and UPDRS part IV decreased significantly ($p < 0.01$) at each follow-up point after surgery compared to the baseline scores. The mean UPDRS part II scores during the on phase did not significantly change 3 months and 1 year after surgery and significantly increased 3 years after surgery (**Figure 1A**). The mean UPDRS part III scores during the on phase significantly decreased at 3 months and at 1 year after surgery, but the difference was not significant 3 years after surgery (**Figure 1B**). FAB scores decreased significantly 3 years after surgery ($p = 0.016$; **Figure 1C**). The cognitive functions as evaluated by the MMSE and MoCA-J did not change significantly from baseline at each follow-up point after surgery. The depression (SDS) score significantly worsened 3 years after surgery ($p = 0.021$). The VFT score in the animal portion was significantly worse 3 years after surgery than before surgery ($p < 0.01$; **Figure 1C**). The mean PDQ-39 SI significantly decreased from baseline to 1 year after surgery ($p = 0.015$; **Figure 1D**). An RBD questionnaire score higher than 5 indicates the presence of RBD (19), and because the mean score for the RBD questionnaire was around 4 before and after STN-DBS, the PD patients in this study tended to have RBD-related symptoms. All numerical data on the clinical scales used in this study are represented in **Table 1**.

Correlation Between the Changes in LED and the Changes in the Score of SDS

The correlation coefficients between the changes in LED and the changes in SDS at each follow-up point were 0.136 ($p = 0.596$; baseline, 3 months after DBS), −0.051 ($p = 0.828$; baseline, 1 year after DBS), and 0.066 ($p = 0.847$; baseline, 3 years after DBS).

Multivariable Linear Regression Analysis

At baseline, a higher UPDRS part III score during the off phase (standardized $\beta = 0.373$, $p = 0.046$), a higher part IV score (standardized $\beta = 0.335$, $p = 0.018$), and a higher BIS11 score (standardized $\beta = 0.576$, $p = 0.022$) were significantly associated with higher PDQ-39 SI. At 3 months after DBS, a higher UPDRS part I score (standardized $\beta = 0.594$, $p = 0.022$) and a higher BIS/BAS score (standardized $\beta = 0.822$, $p = 0.005$) were significantly associated with higher PDQ-39 SI. At 1 year after DBS, although no parameters were associated with PDQ-39 SI, a higher BIS11 score (standardized $\beta = 0.590$, $p = 0.064$) tended to be associated with higher PDQ-39 SI. At 3 years after DBS, a higher UPDRS part I score (standardized $\beta = 0.686$, $p = 0.014$) was associated with higher PDQ-39 SI.

The cognitive functions as evaluated by the MMSE, FAB, and MoCA did not significantly contribute to pre- and postoperative QOL (**Table 2**).

DISCUSSION

Although motor complications dramatically improved after DBS surgery, many PD patients are not necessarily satisfied with their QOL (8), suggesting that QOL after the surgery may be affected instead by non-motor parameters such as cognitive function and neuropsychiatric symptoms. Thus, we aimed to assess the temporal changes in cognitive function and neuropsychiatric symptoms and to determine which cognitive functions and neuropsychiatric symptoms were related to QOL after DBS surgery.

The present results revealed that the scores of UPDRS parts II and III during the off phase and the UPDRS part IV score decreased significantly from baseline after STN-DBS, which are compatible with the well-known clinical effect of STN-DBS on motor dysfunctions (1). The present study also revealed that frontal lobe function, depression, and verbal fluency significantly worsened 3 years after STN-DBS. Furthermore, preoperative QOL was significantly associated with the severity of preoperative motor symptoms (UPDRS part III during the off phase), motor complication (UPDRS part IV), and impulsivity (BIS 11), suggesting that worse motor complications and impulsivity led to worse QOL preoperatively. Postoperative QOL 3 months after surgery was significantly associated with non-motor symptoms (UPDRS part I) and impulsivity as evaluated by BIS/BAS, suggesting that worse non-motor symptoms and impulsivity led to worse QOL 3 months after surgery. Although no clinical parameters were significantly associated with postoperative QOL 1 year after surgery, postoperative QOL at 3 years was significantly associated with non-motor symptoms (UPDRS part I) and impulsivity as evaluated by BIS11, suggesting that worse non-motor symptoms and impulsivity led to worse QOL postoperatively 3 months after surgery.

In terms of a decline in frontal lobe function 3 years after STN-DBS, our previous report also revealed that the FAB score tended to decrease 3 years after STN-DBS, without statistical significance (8). Because this study included a larger number of PD patients compared to our previous study (8), the decline in frontal lobe function 3 years after STN-DBS compared to baseline probably became significant in this study. Although it is difficult to identify whether the decline in FAB score 3 years after STN-DBS was attributable to the effect of surgery or natural disease progression, our previous report revealed that PD patients who underwent STN-DBS showed a decrease of cerebral blood flow in the prefrontal and cingulate cortex 4.3 ± 1.1 months (range = 2.9–6.6 months) after STN-DBS (10). Hence, frontal lobe functions should be carefully examined for more than 3 years after STN-DBS.

This study also showed that depression worsened 3 years after STN-DBS. Although a reduction in LED might partially contribute to the worsening of depression, dopamine withdrawal syndrome usually occurs less than 1 year after STN-DBS (20).

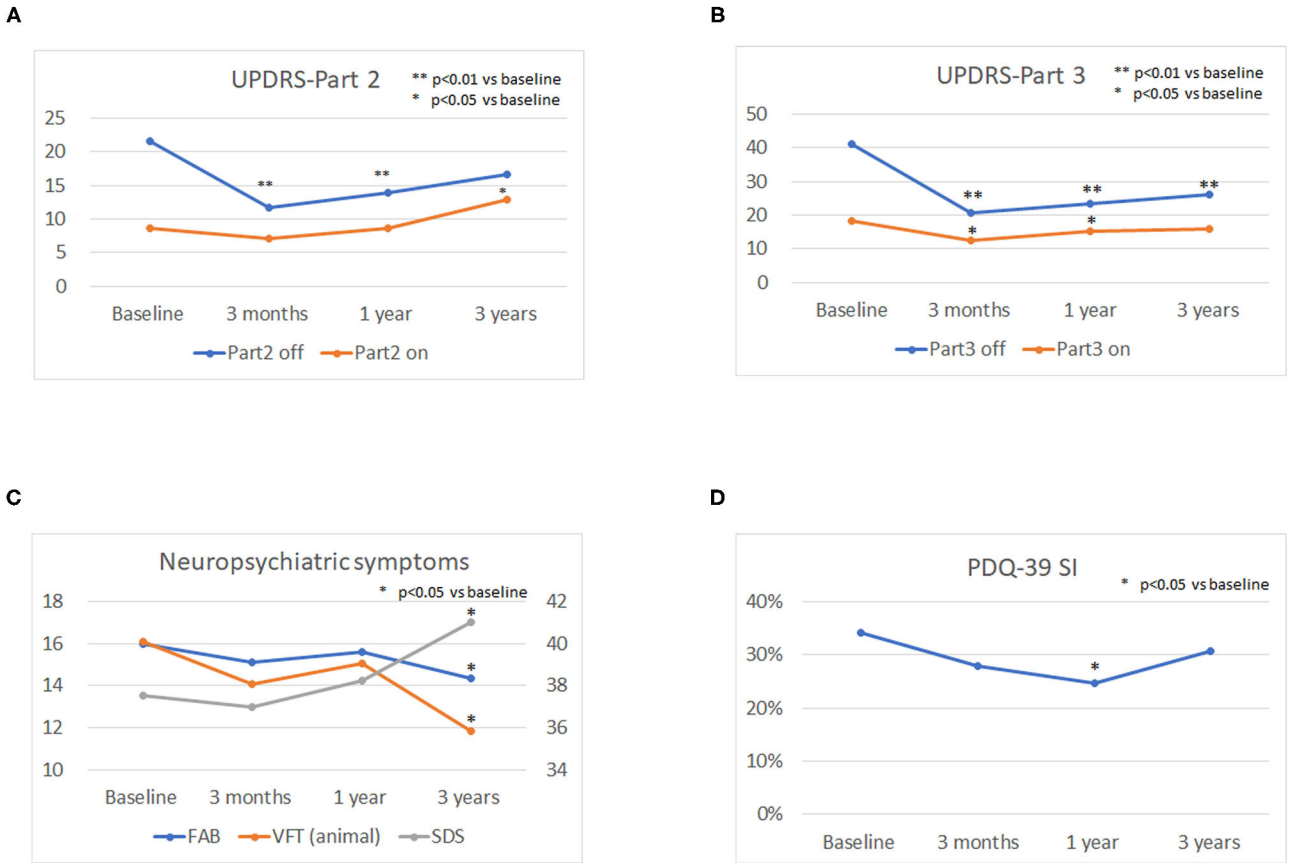

FIGURE 1 | Longitudinal changes in the Unified Parkinson's Disease Rating Scale (UPDRS) parts II and III scores, neuropsychiatric symptoms, and quality of life (QOL). The mean UPDRS parts II and III scores during the off phase **(A,B)** and the UPDRS part IV score decreased significantly ($P < 0.01$) at each follow-up point after surgery compared to the baseline scores. The mean UPDRS part II scores during the on phase did not significantly change 3 months and 1 year after surgery and significantly increased 3 years after surgery **(A)**. The mean UPDRS part III score during the on phase significantly decreased 3 months and 1 year after surgery, and the difference was not significant until 3 years after surgery **(B)**. The depression (SDS) score significantly worsened 3 years after surgery ($P = 0.021$). The verbal fluency test (VFT) score in the animal portion was significantly worse 3 years after surgery than before surgery ($p < 0.01$) **(C)**. The mean PDQ-39 SI significantly decreased from baseline to 1 year after surgery ($p = 0.015$) **(D)**.

Furthermore, the relationships between the changes in LED and the changes in the depression scale did not show significant correlations in this study. We do not know the exact reason why the depression score worsened significantly only at 3 years after STN-DBS, nor whether the worsening of depression scores is attributed to the effect of STN-DBS or is a natural disease progression.

Verbal fluency is well-known to worsen after STN-DBS (21). Although we do not know why the worsening of verbal fluency was significant only at 3 years after STN-DBS, chronic changes in the microlesion effect of the electrode trajectory might contribute to verbal fluency (22).

In terms of the associations between QOL and motor, cognitive, and neuropsychiatric symptoms, deteriorated motor symptoms during the off phase and severe motor complications were significantly associated with worse QOL preoperatively, which was reasonable because the indication for STN-DBS is the presence of motor complications accompanied by a severely deteriorated ADL during the off phase. The higher impulsivity was also associated with worse QOL preoperatively. Although we do not know the exact reason why a higher impulsivity leads to worse QOL preoperatively, a possible explanation might be that patients with higher impulsivity were more strongly dissatisfied with preoperative mobility and ADL (23).

On the contrary, postoperative QOL was associated with non-motor symptoms, as evaluated by UPDRS part I, rather than motor symptoms or ADL. The significant positive associations between the UPDRS part I score and the PDQ-39 SI were found 3 months and 3 years after STN-DBS. Because UPDRS part I includes questions on cognitive functions, hallucination, depression, and motivation, we might say that non-motor symptoms partially contribute to QOL after STN-DBS in PD patients. Although there are few studies examining the associations between the UPDRS part I score and PDQ-39 SI before and after STN-DBS, numerous studies have reported on the effect of STN-DBS on cognitive and neuropsychiatric

TABLE 1 | Temporal changes in levodopa equivalent dose, motor functions, cognitive functions, neuropsychiatric functions, and quality of life.

		Baseline ($n = 61$)	3 months ($n = 54$)	1 year ($n = 47$)	3 years ($n = 23$)
LED (mg)		1,127.90 ± 39.78	719.12 ± 44.79**	670.53 ± 43.11**	839.34 ± 72.93**
UPDRS	Part I	1.68 ± 0.29	1.22 ± 0.27	1.00 ± 0.19	2.55 ± 0.39
	Part II on	8.95 ± 0.95	7.22 ± 0.94	8.58 ± 0.99	13.05 ± 1.67*
	Part II off	22.83 ± 1.13	11.63 ± 1.73**	13.48 ± 2.06**	17.23 ± 1.87
	Part III on	19.71 ± 1.22	12.62 ± 1.20*	14.81 ± 1.40*	16.23 ± 1.79
	Part III off	42.66 ± 1.86	20.71 ± 2.26**	22.68 ± 2.80**	26.95 ± 2.95**
	Part IV	8.15 ± 0.38	3.45 ± 0.28**	3.14 ± 0.26**	4.10 ± 0.27**
QOL	PDQ-39 SI (%)	34.00 ± 2.64	28.71 ± 2.29 (−18.15% decrease from baseline)	23.45 ± 2.45* (−27.54% decrease from baseline)	31.68 ± 3.44 (−10.07% decrease from baseline)
Cognitive and neuropsychiatric functions	MMSE	28.63 ± 0.23	28.33 ± 0.34	28.78 ± 0.25	27.95 ± 0.61
	FAB	16.40 ± 0.24	15.09 ± 0.49	15.50 ± 0.39	14.37 ± 0.67*
	MoCA-J	26.05 ± 0.44	26.0 ± 0.61	25.65 ± 0.53	24.65 ± 0.85
	VFT (Katakana)	24.11 ± 1.97	24.47 ± 1.93	21.94 ± 2.77	21.53 ± 2.01
	VFT (animal)	16.36 ± 1.15	13.70 ± 1.11	15.08 ± 1.04	12.11 ± 1.63**
	BIS11	53.50 ± 3.34	48.53 ± 2.07	53.07 ± 2.64	56.44 ± 1.85
	BIS/BAS	47.78 ± 2.07	46.27 ± 1.95	49.71 ± 1.96	49.29 ± 2.85
	JESS	7.21 ± 1.24	7.47 ± 1.54	9.88 ± 1.60	8.18 ± 1.36
	SDS	34.74 ± 1.13	35.40 ± 1.43	37.69 ± 1.63	41.24 ± 1.45*
	Apathy	4.42 ± 0.93	7.80 ± 1.46	5.88 ± 1.16	6.29 ± 1.14
	RBDQ	4.11 ± 0.69	3.87 ± 0.49	4.19 ± 0.52	3.94 ± 0.53

Apathy, apathy scale; BIS11, Barratt impulsiveness scale 11; BIS/BAS, behavioral inhibition system/behavioral activation system; FAB, Frontal Assessment Battery; JESS, Japanese version of the Epworth Sleepiness Scale; LED, levodopa equivalent dose; MMSE, Mini Mental State Examination; MoCA-J, Japanese version of Montreal Cognitive Assessment; PDQ-39, 39-item Parkinson's disease questionnaire; QOL, quality of life; RBDSQ, REM sleep behavior disorder screening questionnaire; SDS, Self-Rating Depression Scale; SI, Summary Index; UPDRS, Unified Parkinson's Disease Rating Scale; VFT, verbal fluency test.
***$p < 0.01$ vs. preoperative values; *$p < 0.05$ vs. preoperative values.*

TABLE 2 | Standardized beta values of the factors determining quality of life at each follow-up point.

Quality of life at each follow-up point	Factors determining quality of life at each follow-up point	Standardized β	p
PDQ-39 SI before DBS surgery	BIS11 (impulsivity)	0.576	0.022
	UPDRS part III during the off phase	0.373	0.046
	UPDRS part IV	0.335	0.018
PDQ-39 SI 3 months after DBS surgery	UPDRS part I	0.594	0.022
	BIS/BAS	0.822	0.005
PDQ-39 SI 1 year after DBS surgery	None		
PDQ-39 SI 3 years after DBS surgery	UPDRS part I	0.686	0.014

PDQ-39 SI, 39-item Parkinson's disease questionnaire summary index; DBS, deep brain stimulation; BIS11, Barratt Impulsiveness Scale 11; UPDRS, Unified PD Rating Scale; BIS/BAS, behavioral inhibition system/behavioral activation system.

symptoms in PD patients (24–27). However, the effect of STN-DBS on cognitive functions and neuropsychiatric symptoms may differ, and a detailed interpretation of the positive associations between the UPDRS part I score and PDQ-39 SI is difficult. It is interesting that impulsivity, as evaluated by BIS/BAS, was significantly associated with postoperative QOL 3 months after surgery, whereas BIS11 was significantly associated with postoperative QOL 3 years after surgery. BIS11 classified impulsivity into "attentional," "motor," and "non-planning" impulsiveness (16), whereas BIS/BAS evaluate impulsivity based on the theory that it can be understood as a joint function of the behavioral approach system (BAS) and the behavioral inhibition system (BIS) (17). Despite the marked reductions in LED after surgery, impulsivity was significantly associated with postoperative QOL. Mosley et al. reported that greater connectivity of the stimulation site with the frontostriatal

network was related to greater postoperative impulsiveness and disinhibition (28). Although we do not know the exact reason why BIS/BAS was associated with postoperative QOL 3 months after surgery, whereas BIS11 was associated with postoperative QOL 3 years after surgery, a higher impulsivity might contribute to postoperative QOL, and impulsivity should be carefully examined after surgery.

Several limitations of this study should be considered. One major limitation is that not all patients completed the follow-up evaluations. Some patients at each follow-up point are now under investigation. Therefore, the smaller number of patients at each follow-up point compared to baseline does not indicate a high prevalence of the dropout rate in this study. Another limitation was that, although the postoperative score of UPDRS part I was associated with QOL, the cognitive functions (MMSE, FAB, and MoCA-J) and neuropsychiatric symptoms, except for impulsivity, were not associated with postoperative QOL at each follow-up point. One possible explanation for this discrepancy might be that the MMSE, FAB, SDS, and the apathy scale are not specific scales for PD patients, whereas UPDRS part I is specific for PD patients. However, these points should be further examined with a larger number of PD patients. It should also be addressed that the present study lacks a control group, which means that the postoperative changes in the cognitive and neuropsychiatric symptoms and their association with QOL may not solely result from STN-DBS, but the degeneration itself also has a contribution. However, it might be practically very difficult to compare advance-stage PD patients undergoing DBS surgery with PD patients who receive only the best medical treatment. Advance-stage PD patients who do not undergo DBS surgery usually have cognitive impairments and severe neuropsychiatric symptoms or less severe motor complications in which DBS surgery is not indicated. Because DBS is a clinically established surgery for PD patients suffering from motor complications, randomization of PD patients into a DBS group and a best medication group is currently difficult. Furthermore, the selection of a stimulation target might also result in selection bias. In our hospital, STN-DBS are basically administered to PD patients who were suffering from a wearing-off phenomenon rather than dyskinesia and *vice versa* for globus pallidus pars interna (GPi)-DBS. Since non-motor symptoms might be more prevalent and severe in PD patients receiving GPi-DBS compared to those receiving STN-DBS, selection of the stimulation target might lead to selection bias.

Nevertheless, the present results might be important because temporal changes in the cognitive and neuropsychiatric symptoms and their association with QOL were provided in this study. Since many of the previous studies usually examined non-motor symptoms at only one point, our results might be helpful for clinical practice.

CONCLUSION

Frontal lobe functions, depression, and verbal fluency significantly worsened 3 years after STN-DBS. The UPDRS part I score and a higher impulsivity might be associated with QOL after STN-DBS.

DATA AVAILABILITY STATEMENT

The original contributions presented in the study are included in the article/supplementary material, further inquiries can be directed to the corresponding author/s.

ETHICS STATEMENT

The studies involving human participants were reviewed and approved by Chiba University Hospital Institutional Review Board. The patients/participants provided their written informed consent to participate in this study.

AUTHOR CONTRIBUTIONS

All authors listed have made a substantial, direct and intellectual contribution to the work, and approved it for publication.

REFERENCES

1. Olanow CW, Stern MB, Sethi K. The scientific and clinical basis of the treatment of Parkinson disease. *Neurology*. (2009) 72:S1–136. doi: 10.1212/WNL.0b013e3181a1d44c
2. Massano J, Garrett C. Deep brain stimulation and cognitive decline in Parkinson's disease: a clinical review. *Front Neurol*. (2012) 3:66. doi: 10.3389/fneur.2012.00066
3. Chaudhuri KR, Schapira AHV. Non-motor symptoms of Parkinson's disease: dopaminergic pathophysiology and treatment. *Lancet Neurol*. (2009) 8:464–74. doi: 10.1016/S1474-4422(09)70068-7
4. Gallagher DA, Lees AJ, Schrag A. What are the most important nonmotor symptoms in patients with Parkinson's disease and are we missing them? *Mov Disord*. (2010) 25:2493–500. doi: 10.1002/mds.23394
5. Deuschl G, Schade-Brittinger C, Krack P, Volkmann J, Schäfer H, Bötzel K, et al. A randomized trial of deep-brain stimulation for Parkinson's disease. *N Engl J Med*. (2006) 355:896–908. doi: 10.1056/NEJMoa060281
6. Follett KA, Weaver FM, Stern M, Hur K, Harris CL, Luo P, et al. Pallidal versus subthalamic deep-brain stimulation for Parkinson's disease. *N Engl J Med*. (2010) 362:2077–91. doi: 10.1056/NEJMoa0907083
7. Weaver FM, Follett K, Stern M, Hur K, Harris C, Marks WJ, et al. Bilateral deep brain stimulation vs best medical therapy for patients with advanced Parkinson disease: a randomized controlled trial. *JAMA*. (2009) 301:63–73. doi: 10.1001/jama.2008.929
8. Yamamoto T, Uchiyama T, Higuchi Y, Asahina M, Hirano S, Yamanaka Y, et al. Long term follow-up on quality of life and its relationship to motor and cognitive functions in Parkinson's disease after deep brain stimulation. *J Neurol Sci*. (2017) 379:18–21. doi: 10.1016/j.jns.2017.05.037
9. Witt K, Daniels C, Reiff J, Krack P, Volkmann J, Pinsker MO, et al. Neuropsychological and psychiatric changes after deep brain stimulation for Parkinson's disease: a randomised, multicentre study. *Lancet Neurol*. (2008) 7:605–614. doi: 10.1016/S1474-4422(08)70114-5
10. Furukawa S, Hirano S, Yamamoto T, Asahina M, Uchiyama T, Yamanaka Y, et al. Decline in drawing ability and cerebral perfusion in Parkinson's disease patients after subthalamic nucleus

deep brain stimulation surgery. *Parkinsonism Relat Disord*. (2020) 70:60–6. doi: 10.1016/j.parkreldis.2019.12.002
11. Yakufujiang M, Higuchi Y, Aoyagi K, Yamamoto T, Sakurai T, Abe M, et al. Predicting neurocognitive change after bilateral deep brain stimulation of subthalamic nucleus for Parkinson's disease. *World Neurosurg*. (2021) 147:e428–36. doi: 10.1016/j.wneu.2020.12.081
12. Martinez-Fernandez R, Pelissier P, Quesada JL, Klinger H, Lhommée E, Schmitt E, et al. Postoperative apathy can neutralise benefits in quality of life after subthalamic stimulation for Parkinson's disease. *J Neurol Neurosurg Psychiatry*. (2016) 87:311–8. doi: 10.1136/jnnp-2014-310189
13. Daniels C, Krack P, Volkmann J, Raethjen J, Pinsker MO, Kloss M, et al. Is improvement in the quality of life after subthalamic nucleus stimulation in Parkinson's disease predictable? *Mov Disord*. (2011) 14:2516–21. doi: 10.1002/mds.23907
14. Gibb WR, Lees AJ. The relevance of the Lewy body to the pathogenesis of idiopathic Parkinson's disease. *J Neurol Neurosurg Psychiatry*. (1988) 51:745–52. doi: 10.1136/jnnp.51.6.745
15. Tomlinson CL, Stowe R, Patel S, Rick C, Gray R, Clarke CE. Systematic review of levodopa dose equivalency reporting in Parkinson's disease. *Mov Disord*. (2010) 25:2649–53. doi: 10.1002/mds.23429
16. Piatt AL, Fields JA, Paolo AM, Koller WC, Tröster AI. Lexical, semantic, and action verbal fluency in Parkinson's disease with and without dementia. *J Clin Exp Neuropsychol*. (1999) 21:435–43. doi: 10.1076/jcen.21.4.435.885
17. Patton JH, Stanford MS, Barratt ES. Factor structure of the Barratt impulsiveness scale. *J Clin Psychol*. (1995) 51:768–74. doi: 10.1002/1097-4679(199511)51:6<768::aid-jclp2270510607>3.0.co;2-1
18. Braddock KH, Dillard JP, Voigt DC, Stephenson MT, Sopory P, Anderson JW. Impulsivity partially mediates the relationship between BIS/BAS and risky health behaviors. *J Pers*. (2011) 79:793–810. doi: 10.1111/j.1467-6494.2011.00699.x
19. Miyamoto T, Miyamoto M, Iwanami M, Kobayashi M, Nakamura M, Inoue Y, et al. The REM sleep behavior disorder screening questionnaire: validation study of a Japanese version. *Sleep Med*. (2009) 10:1151–4. doi: 10.1016/j.sleep.2009.05.007
20. Thobois S, Ardouin C, Lhommée E, Klinger H, Lagrange C, Xie J, et al. Non-motor dopamine withdrawal syndrome after surgery for Parkinson's disease: predictors and underlying mesolimbic denervation. *Brain*. (2010) 133(Pt 4):1111–27. doi: 10.1093/brain/awq032
21. Aldridge D, Theodoros D, Angwin A, Vogel AP. Speech outcomes in Parkinson's disease after subthalamic nucleus deep brain stimulation: a systematic review. *Parkinsonism Relat Disord*. (2016) 33:3–11. doi: 10.1016/j.parkreldis.2016.09.022
22. Costentin G, Derrey S, Gérardin E, Cruypeninck Y, Pressat-Laffouilhere T, Anouar Y, et al. White matter tracts lesions and decline of verbal fluency after deep brain stimulation in Parkinson's disease. *Hum Brain Mapp*. (2019) 40:2561–70. doi: 10.1002/hbm.24544
23. Ryu DW, Kim JS, Yoo SW, Oh YS, Lee KS. The impact of impulsivity on quality of life in early drug-naïve Parkinson's disease patients. *J Mov Disord*. (2019) 12:172–6. doi: 10.14802/jmd.19004
24. Kurtis MM, Rajah T, Delgado LF, Dafsari HS. The effect of deep brain stimulation on the non-motor symptoms of Parkinson's disease: a critical review of the current evidence. *NPJ Parkinsons Dis*. (2017). 3:16024. doi: 10.1038/npjparkd.2016.24
25. Dulski J, Schinwelski M, Konkel A, Grabowski K, Libionka W, Waz P, et al. The impact of subthalamic deep brain stimulation on sleep and other non-motor symptoms in Parkinson's disease. *Parkinsonism Relat Disord*. (2019) 64:138–44. doi: 10.1016/j.parkreldis.2019.04.001
26. Dafsari HS, Ray-Chaudhuri K, Ashkan K, Sachse L, Mahlstedt P, Silverdale M, et al. Beneficial effect of 24-month bilateral subthalamic stimulation on quality of sleep in Parkinson's disease. *J Neurol*. (2020). 267:1830–41. doi: 10.1007/s00415-020-09743-1
27. Bargiotas P, Debove I, Bargiotas I, Lachenmayer ML, Ntafouli M, Vayatis N, et al. Effects of bilateral stimulation of the subthalamic nucleus in Parkinson's disease with and without REM sleep behaviour disorder. *J Neurol Neurosurg Psychiatry*. (2019). 90:1310–6. doi: 10.1136/jnnp-2019-320858
28. Mosley PE, Paliwal S, Robinson K, Coyne T, Silburn P, Tittgemeyer M, et al. The structural connectivity of subthalamic deep brain stimulation correlates with impulsivity in Parkinson's disease. *Brain*. (2020). 143:2235–54. doi: 10.1093/brain/awaa148

Conflict of Interest: The authors declare that the research was conducted in the absence of any commercial or financial relationships that could be construed as a potential conflict of interest.

frontiers in Neurology

ORIGINAL RESEARCH
published: 14 May 2021
doi: 10.3389/fneur.2021.619631

Motor Symptom Lateralization Influences Cortico-Striatal Functional Connectivity in Parkinson's Disease

Wen Su[1,2,3†], Kai Li[2,3†], Chun-Mei Li[3,4], Xin-Xin Ma[2,3], Hong Zhao[2,3], Min Chen[3,4], Shu-Hua Li[2,3], Rui Wang[3,4], Bao-Hui Lou[3,4], Hai-Bo Chen[2,3] and Chuan-Zhu Yan[1*]*

[1] Department of Neurology, Research Institute of Neuromuscular and Neurodegenerative Disease, Qilu Hospital of Shandong University, Jinan, China, [2] Department of Neurology, National Center of Gerontology, Beijing Hospital, Beijing, China, [3] Institute of Geriatric Medicine, Chinese Academy of Medical Sciences, Beijing, China, [4] Department of Radiology, National Center of Gerontology, Beijing Hospital, Beijing, China

OPEN ACCESS

Edited by:
Frederic Sampedro, Sant Pau Institute for Biomedical Research, Spain

Reviewed by:
Ignacio Aracil Bolaños, Institut de Recerca de l'Hospital de la Santa Creu i Sant Pau, Spain
Rachel Spooner, University of Nebraska Medical Center, United States

***Correspondence:**
Hai-Bo Chen
chenhb_bjh@hotmail.com;
chenhbneuro@263.net
Chuan-Zhu Yan
chuanzhuyan@163.com

[†] These authors have contributed equally to this work

Specialty section:
This article was submitted to Movement Disorders, a section of the journal Frontiers in Neurology

Received: 20 October 2020
Accepted: 08 April 2021
Published: 14 May 2021

Citation:
Su W, Li K, Li C-M, Ma X-X, Zhao H, Chen M, Li S-H, Wang R, Lou B-H, Chen H-B and Yan C-Z (2021) Motor Symptom Lateralization Influences Cortico-Striatal Functional Connectivity in Parkinson's Disease. Front. Neurol. 12:619631. doi: 10.3389/fneur.2021.619631

Objective: The striatum is unevenly impaired bilaterally in Parkinson's disease (PD). Because the striatum plays a key role in cortico-striatal circuits, we assume that lateralization affects cortico-striatal functional connectivity in PD. The present study sought to evaluate the effect of lateralization on various cortico-striatal circuits through resting-state functional magnetic resonance imaging (fMRI).

Methods: Thirty left-onset Parkinson's disease (LPD) patients, 27 right-onset Parkinson's disease (RPD) patients, and 32 normal controls with satisfactory data were recruited. Their demographic, clinical, and neuropsychological information was collected. Resting-state fMRI was performed, and functional connectivity changes of seven subdivisions of the striatum were explored in the two PD groups. In addition, the associations between altered functional connectivity and various clinical and neuropsychological characteristics were analyzed by Pearson's or Spearman's correlation.

Results: Directly comparing the LPD and RPD patients demonstrated that the LPD patients had lower FC between the left dorsal rostral putamen and the left orbitofrontal cortex than the RPD patients. In addition, the LPD patients showed aberrant functional connectivity involving several striatal subdivisions in the right hemisphere. The right dorsal caudate, ventral rostral putamen, and superior ventral striatum had decreased functional connectivity with the cerebellum and parietal and occipital lobes relative to the normal control group. The comparison between RPD patients and the controls did not obtain significant difference in functional connectivity. The functional connectivity between the left dorsal rostral putamen and the left orbitofrontal cortex was associated with contralateral motor symptom severity in PD patients.

Conclusions: Our findings provide new insights into the distinct characteristics of cortico-striatal circuits in LPD and RPD patients. Lateralization of motor symptoms is associated with lateralized striatal functional connectivity.

Keywords: Parkinson's disease, functional connectivity, asymmetry, resting-state functional magnetic resonance imaging, striatum

INTRODUCTION

Parkinson's disease (PD) is a neurodegenerative disorder commonly seen in the elderly, which manifests as classical motor symptoms such as bradykinesia, rigidity, and resting tremor, together with multiple non-motor symptoms (1). Dopamine deficiency in the striatum is a pathophysiological hallmark in PD and underlies motor and several neuropsychiatric symptoms. The striatum modulates motor activity, cognition, and behavior through multiple cortico-striatal circuits, which involve several striatal subregions (2, 3).

Lateralization is characteristic in PD. Motor symptoms usually present initially in one side of the body, and this asymmetry persists long after both sides show motor dysfunction (4, 5). Lateralization is unique and a clue for differential diagnosis from other neurological disorders presenting as parkinsonism (6). Uneven bilateral deficiency of dopamine in the striatum can explain this motor asymmetry (7–9), but this lateralization affects different cortico-striatal circuits simultaneously and is also related to various non-motor symptoms.

The interaction between cerebral hemisphere dominance and asymmetric brain impairment leads to different neuropsychological profiles in left-onset (LPD) PD and right-onset (RPD) patients. Studies evaluating cognitive function, anxiety, psychosis, and apathy symptoms showed a series of differences between LPD and RPD patients (10–13). Lateralization not only affects clinical profile in PD but also modulates therapeutic responses. In a study by Hanna-Pladdy et al. LPD and RPD patients had different responses to levodopa in attention and even paradoxical responses in verbal memory function (14). Due to different severities of dopamine deficiency in the more affected hemisphere and less affected hemisphere, levodopa may have an ameliorating or overdosing effect to different cortico-striatal circuits (14). Therefore, a better understanding of the effect of lateralization on various cortico-striatal circuits can shed light on a more precise treatment in PD.

Functional magnetic resonance imaging (fMRI) is increasingly used to assess cerebral activity based on the blood oxygen level-dependent (BOLD) effect, which can reflect cerebral blood flow and energy use (15). fMRI can be conducted when the subject is performing a specific task (task-based fMRI) or when the subject lies relaxed [resting-state fMRI (rs-fMRI)] (15). Due to its convenience, rs-fMRI is increasingly used in neurological research. Functional connectivity (FC) is defined as the temporal dependency between different brain regions and is an important approach to analyze rs-fMRI data (15). FC is an ideal technique to explore the impaired cortico-striatal circuits in PD.

There have been several studies showing altered FC between striatum and various brain regions in PD patients, but the seeds used in previous studies varied, and the influence of laterality has rarely been investigated. Some researchers used the nuclei of basal ganglia, such as putamen and caudate as the seeds (16–22); some divided putamen and caudate to the anterior and posterior parts as the seeds (23–29). Others chose representative seeds of the subregions of the striatum (30–35). Most of the studies merged LPD and RPD patients as a single group and compared fMRI data of PD patients with the controls (16, 17, 19, 20, 22, 23, 25, 28, 29, 31, 33–35); some studies only focused on the more severely involved striatum or combined bilateral striatal seeds (27, 30). These approaches cannot discern whether the changed FC was mainly contributed by the LPD or RPD patients or a common impairment shared by LPD and RPD patients.

In the last century, anatomical labeling techniques have demonstrated the existence of parallel cortico-striatal circuits, which are related to motor, cognitive, and limbic functions. In addition, these circuits display rostrocaudal and dorsoventral patterns (36–38). With the advent of functional imaging, studies on the striatum using rs-fMRI have been rapidly increasing. Postuma and Dagher conducted a meta-analysis of positron emission tomography (PET) and fMRI studies. They have revealed that functional imaging can disclose different parallel cortico-striatal circuits and suggested the boundaries between dorsal and ventral caudate and putamen, as well as the boundary between rostral and caudal putamen (39). Furthermore, Di Martino et al. carried out an rs-fMRI study. They integrated the results of the study by Postuma and Dagher and anatomical characteristics of the striatum subregions and defined six seeds in each side of the brain for the rs-fMRI study (3). The seeds chosen by Di Martino et al. can reflect the divergence of these striatal subdivisions and their corresponding FC profiles; these definitions performed well in the following studies (30–35). To date, how lateralization affects different cortico-striatal circuits remains unclear. The present study aimed to utilize rs-fMRI to comprehensively explore the changes of FC of distinct striatal subregions in LPD and RPD patients, in order to reveal the influence of asymmetry on cortico-striatal circuits in PD. The definitions of the seeds are consistent with the studies by Di Martino et al. (3) and Bell et al. (35).

MATERIALS AND METHODS

Participants

Between 2012 and 2014, we enrolled 63 PD patients and 33 age- and sex-matched control subjects without history of neurological or psychiatric disorders. All the participants were right handed and recruited from Beijing Hospital. A movement disorder specialist (W.S. or H.B.C) made the diagnosis based on the UK PD Society Brain Bank diagnostic criteria (6).

We collected demographic and clinical data, including medical history, and physical and neurological examinations from all the subjects. The side of disease onset was identified through retrospective medical records review and patients' reports and supported by neurological examination. The sum of the Unified Parkinson's Disease Rating Scale (UPDRS) part III (including tremor, rigidity, and bradykinesia-related items) score of the right and left limbs was calculated as right and left motor subscores; then we calculated the laterality index by subtracting the left motor subscore from the right motor subscore. Usually, RPD patients had a positive laterality index, and LPD patients had a negative laterality index (40). Patients whose side of onset could not be confirmed concordantly or with bilateral onset were not included. PD patients with dementia,

severe head tremor, deep-brain stimulation, substance abuse, head trauma, or other neurological or psychiatric diseases were also excluded.

The MRI scans and clinical and neuropsychological evaluations were performed in a practically defined "off" state, in which the patients had stopped all the antiparkinson agents for ∼12 h (overnight). The Hoehn–Yahr staging, UPDRS, Mini-Mental State Examination (MMSE), Hamilton Depression Rating Scale (HAMD), Hamilton Anxiety Rating Scale (HAMA), and Non-Motor Symptoms Questionnaire (NMSQ) were used to measure motor and non-motor symptoms. MMSE was employed to assess cognitive function of the control subjects.

The study was approved by the Ethics Committee of Beijing Hospital, and we conducted the study in keeping with the Declaration of Helsinki. All the subjects signed informed consent prior to participation.

TABLE 1 | The co-ordinates of the regions of interest.

Regions of interest	MNI coordinates		
	X	Y	Z
VSi	± 9	9	−8
VSs	± 10	15	0
DC	± 13	15	9
DCP	± 28	1	3
DRP	± 25	8	6
VRP	± 20	12	−3
PCP	± 26	−4	8

VSi, ventral striatum inferior; VSs, ventral striatum superior; DC, dorsal caudate; DCP, dorsal caudal putamen; DRP, dorsal rostral putamen; VRP, ventral rostral putamen; PCP, post-commissural putamen.

Image Acquisition

An Achieva 3.0T MRI scanner (Philips Medical Systems, Best, Netherlands) was used for data acquisition. Foam pads were utilized to reduce head motion, and headphones were employed to decrease the scanning noise. The participants were required to lie still with eyes closed, relaxed, and stay awake. A high-resolution T1-weighted anatomical image was acquired using the following parameters: repetition time (TR) = 7.4 ms, echo time (TE) = 3.0 ms, flip angle (FA) = 8°, field of view (FOV) = 240 × 240 mm, matrix size = 256 × 256, voxel dimensions = 0.94 × 0.94 × 1.20 mm, slice thickness = 1.2 mm, and slices = 140. For the rs-fMRI scan, echo-planar imaging (EPI) was performed with the following parameters: TR = 3,000 ms, TE = 35 ms, FA = 90°, FOV = 240 × 240 mm, matrix size = 64 × 64, voxel dimensions = 3.75 × 3.75 × 4.00 mm, slice thickness = 4 mm, slices = 33, and time points = 210 (41).

rs-fMRI Data Preprocessing

Images were preprocessed using RESTPlus version 1.2 (42), which was based on SPM 12 (http://www.fil.ion.ucl.ac.uk/spm). The preprocessing steps included removing the first 10 volumes to allow for magnetization stabilization, slice-timing to correct for interleaved acquisition, realignment for 3D motion correction, spatial normalization to the Montreal Neurological Institute (MNI) standard space using the co-registered T1 images (43), resampling to 3 × 3 × 3 mm^3, smoothing with a Gaussian kernel (full-width at half-maximum = 6 mm), time course detrending, nuisance covariate regression [Friston-24 parameters (44) and cerebrospinal fluid and white matter signals], and bandpass filtering ($0.01 < f < 0.1$ Hz). We excluded the subjects whose head movement exceeded 2 mm of displacement or 2° of rotation.

FC Analysis

FC maps were obtained using RESTPlus version 1.2, using a seed voxel correlation approach. Because of the dorsoventral and rostrocaudal differences in striatal function and dopamine loss in PD, we chose seeds distributing various locations of the striatum. Di Martino et al. have defined six seeds, including ventral striatum inferior (VSi), ventral striatum superior (VSs), dorsal caudate (DC), dorsal caudal putamen (DCP), dorsal rostral putamen (DRP), and ventral rostral putamen (VRP) (3). We defined six seeds of each hemisphere consistent with Di Martino et al. Since postcommissural putamen (PCP) is especially susceptible in PD and is closely related to motor symptoms (38, 45, 46), we selected a seed of PCP in accordance with Bell et al. (35). The coordinates of the seeds are shown in **Table 1**, and the positions of the seeds are illustrated in **Figure 1**. The mean time series of each seed were extracted; then voxel-wise FC analyses were conducted by calculating the temporal correlation between the time series of each seed and those of each voxel within the whole brain. Correlation coefficients were further transformed to z-values via Fisher's z-transformation.

Statistical Analysis

We used SPSS (version 23.0, IBM Corp, Armonk, NY) to analyze demographic and clinical information, as well as extracted FC values. The continuous variables are shown as mean ± standard deviation. Data normality was detected by the Kolmogorov–Smirnov test. One-way ANOVA, Kruskal–Wallis test, *t*-test, or Mann–Whitney *U*-test was employed for between-group comparisons on continuous data when applicable. Fisher's exact test or a chi-square test was used for analyses of categorical variables. $P < 0.05$ was considered statistically significant.

FC analyses were performed using DPABI version 4.2 (47). Analysis of covariance (ANCOVA) was employed to analyze between-group (LPD, RPD, and control groups) differences in FC of the 14 seeds, with age and gray matter density as covariates. The gray matter mask in DPABI version 4.2 was used in the analyses. *Post hoc* pairwise analyses were performed using the least significant difference (LSD) method. Multiple comparisons were corrected according to the Gaussian random field (GRF) theory (voxel level $P < 0.001$; cluster level $P < 0.05$; two-tailed) (48, 49). Cohen's ^{2} was used to evaluate the effect sizes, which was given by DPABI. Pearson's correlation or Spearman's rank correlation was used to investigate the association between the average FC values of significant clusters and clinical and neuropsychological data.

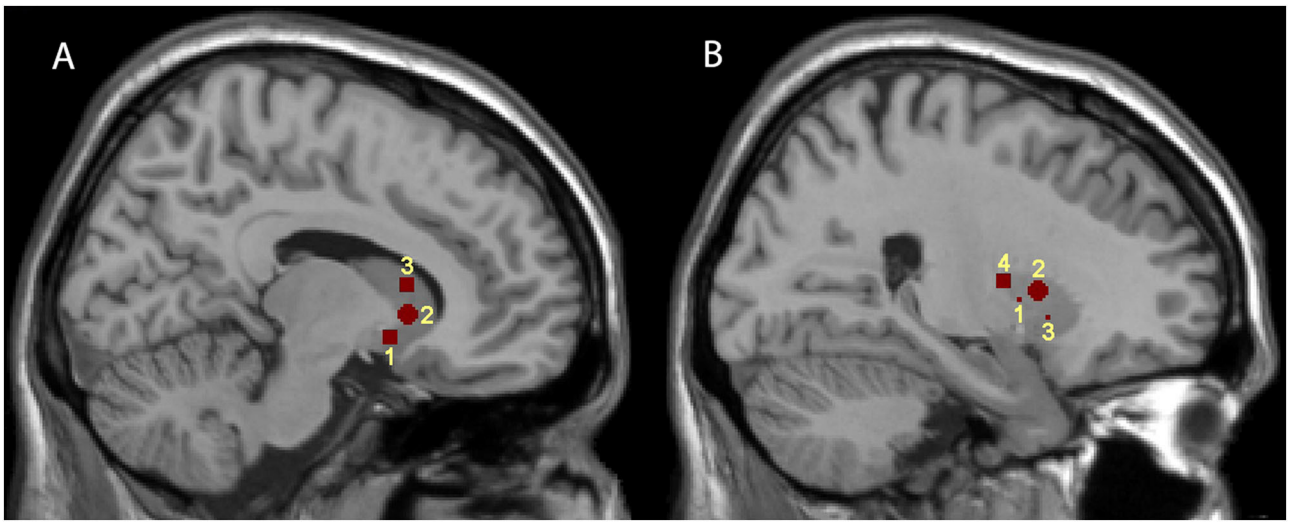

FIGURE 1 | Representations of the seven striatal seed regions. **(A,B)** are sagittal brain views at $x = 9$ and 24, respectively. **(A)** illustrates the positions of the three caudate subdivisions; 1, 2, and 3 represent VSi, VSs, and DC, respectively. **(B)** illustrates the positions of the four putamen subdivisions; 1, 2, 3, and 4 represent DCP, DRP, VRP, and PCP, respectively.

TABLE 2 | Demographic and clinical information of PD patients and controls.

	LPD	RPD	Controls	*P*-value
Number of subjects	30	27	32	
Age	62.63 ± 8.88	65.85 ± 6.982	62.41 ± 7.07	0.056
Gender (male/female)	14/16	14/13	16/16	0.924
Disease duration	6.80 ± 3.62	6.15 ± 3.59		0.499
Hoehn–Yahr staging	2.13 ± 0.71	2.28 ± 0.67		0.416
UPDRS	49.90 ± 18.82	48.85 ± 12.83		0.809
Laterality index	−5.52 ± 3.57	5.74 ± 3.40		<0.001
MMSE	28.50 ± 1.50	27.56 ± 2.28	27.78 ± 2.25	0.203
HAMD	9.07 ± 5.27	9.56 ± 5.09		0.724
HAMA	9.93 ± 5.04	10.52 ± 6.03		0.691
NMSQ	11.07 ± 5.77	11.56 ± 4.86		0.732

HAMA, Hamilton Anxiety Rating Scale; HAMD, Hamilton Depression Rating Scale; LPD, left-onset Parkinson's disease; MMSE, Mini-Mental State Examination; RPD, right-onset Parkinson's disease; NMSQ, Non-Motor Symptoms Questionnaire; UPDRS, Unified Parkinson's Disease Rating Scale.

RESULTS

Demographic and Clinical Characteristics

Finally, 57 PD patients and 32 controls were enrolled in the analysis, and seven subjects were excluded due to the following reasons: five PD patients and one control participant because of excessive head motion and one PD patient due to unsatisfactory image quality. Thirty PD patients were in the LPD group, and 27 PD patients were in the RPD group.

Table 2 illustrates the demographic and clinical information. The laterality index differed significantly between the two PD groups. Age, sex, and MMSE scores were comparable between the three groups. The LPD and RPD patients had similar mean disease duration, UPDRS score, Hoehn–Yahr staging, HAMD, HAMA, and NMSQ scores.

Group Differences in FC

ANCOVA and the followed *post hoc* pairwise analyses disclosed significant differences in FC between the two PD groups, as well as between the LPD patients and the controls.

In the comparison between the LPD patients and the RPD patients, only one seed showed significant difference in FC between the two groups. The LPD patients had lower FC between the left DRP and the left orbitofrontal cortex than the RPD patients (**Figure 2** and **Table 3**).

Compared with the controls, LPD patients showed altered FC in three seeds: the right DC, the right VRP, and the right VSs, all in the right side. The aberrant FCs in LPD patients were as follows: (1) decreased FC between the right DC and the cerebellum posterior lobe, the left occipital lobe, the left inferior parietal lobe, and the left superior parietal lobe compared with

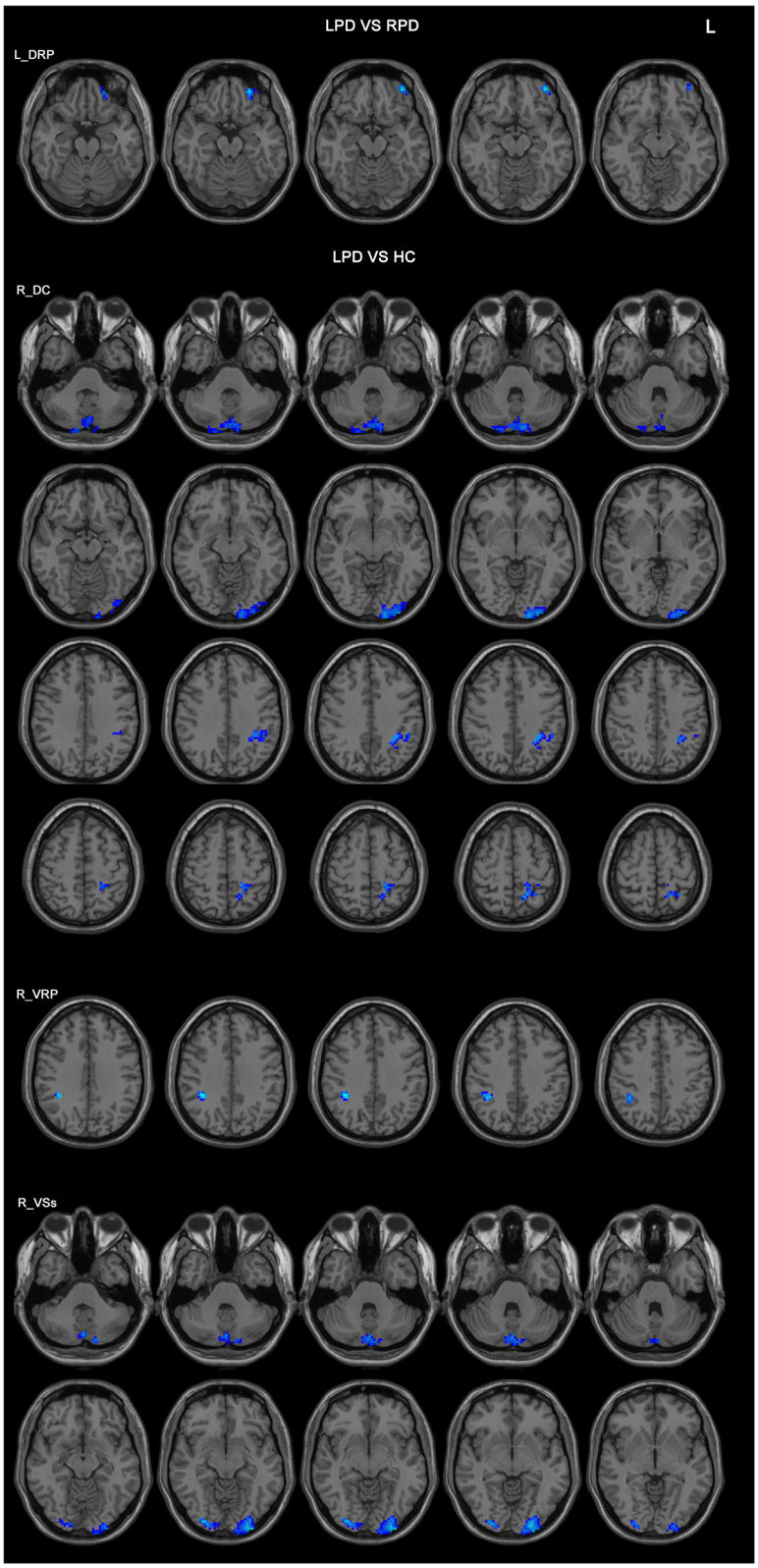

FIGURE 2 | Differences in the FC patterns between LPD and RPD patients and controls. The seed regions are indicated in the left side of the figure. LPD patients had lower FC between the left DRP and the left orbitofrontal cortex compared with RPD patients. LPD patients had lower FCs between the right DC, VRP, VSs, and various brain areas compared with controls. HC, healthy controls; DC, dorsal caudate; DRP, dorsal rostral putamen; L, left side of the brain; LPD, left-onset Parkinson's disease; RPD, right-onset Parkinson's disease; VRP, ventral rostral putamen; VSs, ventral striatum superior.

TABLE 3 | Differences in FC among PD patients and controls.

Seed regions	Connected area	Peak MNI coordinates			Number of voxels	*T*-value	Effect size (Cohen's f^2)
		X	Y	Z			
LPD < RPD							
Left DRP	Left orbitofrontal cortex	−36	51	−15	42	−4.22	0.23
LPD < HC							
Right DC	Cerebellum posterior lobe	18	−90	−45	231	−4.34	0.21
	Left occipital lobe	−15	−102	−6	186	−4.26	0.23
	Left inferior parietal lobe	−30	−45	39	76	−4.28	0.22
	Left superior parietal lobe	−15	−54	60	65	−4.18	0.24
Right VRP	Right parietal lobe	36	−42	36	50	−4.53	0.26
Right VSs	Cerebellum posterior lobe	0	−75	−39	110	−3.96	0.20
	Left occipital lobe	−30	−99	−9	129	−4.14	0.22
	Right occipital lobe	30	−90	−9	60	−4.08	0.22

HC, healthy controls; DC, dorsal caudate; DRP, dorsal rostral putamen; LPD, left-onset Parkinson's disease; MNI, Montreal Neurological Institute; RPD, right-onset Parkinson's disease; VRP, ventral rostral putamen; VSs, ventral striatum superior.

the controls (**Figure 2** and **Table 3**); (2) decreased FC between the right VRP and the right parietal lobe (**Figure 2** and **Table 3**); (3) decreased FC between the right VSs and the cerebellum posterior lobe, the left occipital lobe, and the right occipital lobe (**Figure 2** and **Table 3**).

Correlation Analysis

Pearson's correlation or Spearman's rank correlation was used to investigate the relationship between the left DRP–orbitofrontal cortex FC and Hoehn–Yahr staging, contralateral motor subscore of UPDRS part III, laterality index, MMSE, HAMD, HAMA, and NMSQ scores.

FC between the left DRP and the left orbitofrontal cortex was significantly associated with the right motor subscore of UPDRS part III and laterality index in PD patients ($r = 0.387$ and 0.418; $p = 0.003$ and 0.001, respectively) (**Figure 3**).

DISCUSSION

To the best of our knowledge, this is the first study systematically exploring FC related to striatal subregions in LPD and RPD patients separately. We demonstrated that FC between the left DRP and the left orbitofrontal cortex was different between LPD and RPD patients, and LPD patients had a series of differences in FC between various brain regions and the right DC, the right VRP, and the right VSs compared with the controls. The changed FC between the left dorsal rostral putamen and the left orbitofrontal cortex was associated with contralateral motor symptom severity and laterality index.

In healthy subjects, the activity of DRP is predominantly associated with sensorimotor areas (3), but in PD, the specificity of its connectivity is reduced and the FC of DRP extends to the ventromedial prefrontal cortex (3, 31). Our results showed that LPD and RPD patients differed in the FC between left DRP and left orbitofrontal cortex. In addition, the FC between left DRP and left orbitofrontal cortex was significantly associated with the severity of contralateral motor symptoms; the higher the FC, the more severe the contralateral motor symptoms. These results confirm the role of DRP in regulating movement and indicate that the altered left DRP–orbitofrontal cortex FC might be a pathological change in PD. The significant association between left DRP–orbitofrontal cortex FC and laterality index affirms our hypothesis that motor asymmetry can influence cortico-striatal circuits.

It is noteworthy that several aberrant FCs were identified only in LPD patients compared with the controls, and these abnormal FCs all involved the striatal seeds of the more severely impaired hemisphere. This finding corroborates our hypothesis that uneven impairment of the bilateral nigrostriatal function leads to lateralized FC changes in PD. On the other hand, the comparison between RPD patients and the controls obtained no significant difference. These two comparisons indicate that LPD patients might have more severe FC impairments than RPD patients, especially in the right hemisphere. Some clinical observations demonstrated that LPD and RPD patients might have different disease severities and risks of future motor complications and that RPD might be a slightly more benign subtype than LPD (50, 51). A study by Lee et al. compared gray matter volume across controls and LPD and RPD patients. They found several abnormalities of gray matter volume also in the right hemisphere in LPD patients, but they did not identify any significant difference between the two PD groups or between the controls and the RPD patients (52). Two additional MRI studies using structural and functional imaging techniques also showed more impairments in LPD patients than in RPD patients (41, 53). Our findings are consistent with the above studies; LPD patients may have more severe neurodegeneration or less compensation than RPD patients. Maybe a larger sample can better discriminate impaired FC in RPD patients. Additionally, we need to be aware that some controversy exists regarding which type is more susceptible; a study by Baumann et al. showed that RPD patients had a more rapid decline (54). Nevertheless, more clinical and imaging research is needed to clarify the role of laterality in PD.

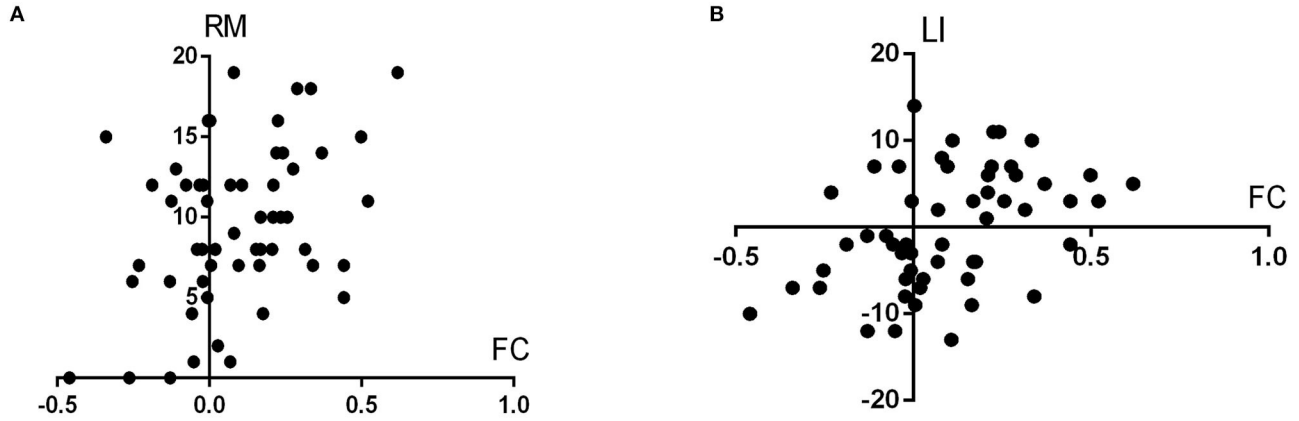

FIGURE 3 | (A,B) illustrate the scatterplots showing the associations between the left DRP–orbitofrontal cortex FC and the UPDRS part III score of the right side (RM in the figure, represents right motor score) and laterality index (LI), respectively.

On the whole, only one different FC was identified between the two PD groups; however, there were much more significant differences in the comparison between LPD patients and the controls. This phenomenon is not uncommon. Some previous studies using structural imaging and fMRI techniques failed to identify significant differences in the direct comparison between LPD and RPD patients, although these two groups showed different patterns of abnormalities compared with the controls (41, 52, 53, 55). In the present study, both PD groups had an average disease duration of more than 6 years and an average Hoehn–Yahr stage higher than 2. At the time of examination, most of the PD patients had bilateral striatal impairments. Although the laterality index showed that there was still obvious asymmetry in the PD patients, the impairments and compensation mechanism are complicated in this stage. The effects of asymmetry might be minor and difficult to detect sufficiently with a relatively small sample size and stringent multiple comparison corrections. Additionally, conflicting results exist on the persistence of laterality in PD; some researches showed a decreased degree of asymmetry with disease progression (5, 56). The laterality of FC might also decrease with disease progression. Maybe future studies recruiting PD patients in an earlier stage can better demonstrate the influence of lateralization on striatal FC.

There has been a variety of abnormal FCs reported in PD, from the early to late stages, but our comparison between RPD patients and the controls attained no significant findings. We need to take the methodological details into consideration. First of all, most of the previous studies combined LPD and RPD patients into a single group. This approach could increase the sensitivity of discovering impaired cortico-striatal FC in PD, particularly those impairments shared by LPD and RPD patients. Dividing the two subgroups according to the side of onset decreases the sample size of each group; this might partially contribute to our negative results in the comparison between RPD patients and the controls. Second, previously, a large number of the FC studies on PD used less strict multiple comparison corrections. To some extent, this might account for the large number of positive findings. This issue was raised by a widely concerned article published by Eklund et al. (57), in which several popular multiple comparison correction approaches had an unsatisfactory performance. For instance, the AlphaSim correction was popular (16, 17, 22, 25, 31, 58) and was not recommended by recent methodological studies (49, 57). Based on these methodological studies, we corrected for multiple comparisons based on GRF theory, with stringent thresholds (voxel level $P < 0.001$; cluster level $P < 0.05$; two-tailed). The stringent thresholds and small sample size may limit the sensitivity to disclose aberrant cortico-striatal FC in RPD patients. Future studies with a larger sample size and strict control for multiple comparisons may better reveal FC impairments in RPD patients. Finally, as we have mentioned, RPD patients may have a better neural reserve and/or greater neural plasticity than LPD patients. The impairment of FC of RPD patients may be milder than that of LPD patients and need a larger sample size to be detected.

Some limitations should be noted. First, the number of participants in this study is relatively small, and only right-handed PD patients were enrolled. Future studies recruiting more subjects and including left-handed PD patients can provide new insights on the topic of lateralization in PD. Second, the enrolled patients underwent chronic dopaminergic drugs, and the medications might interfere with the rs-fMRI results. To control the pharmacological effects, we evaluated the PD patients during the off period. Although the influence of these medications cannot be completely eliminated, this is a commonly used approach and helps compare with similar studies from other researchers. Furthermore, similar alterations of rs-fMRI results in *de novo* PD patients, and off-medication patients have been reported (59). Therefore, the influence of dopaminergic drugs should not be a major concern, and future studies using drug-naïve PD patients can better address this issue. Third, the cognitive function was evaluated with MMSE, which was not fully recommended by the Movement Disorder Society (MDS) task force (60). MMSE has limited coverage of executive function.

This is a limitation of the present study. The study was designed in 2011 and conducted between 2012 and 2014. In a review article published in 2007 (61), MMSE was proposed as a level 1 testing for the diagnosis of PD dementia. Therefore, MMSE was used as a screening instrument for cognitive dysfunction in the study. In future studies, we will use the Montreal Cognitive Assessment (MoCA) instead of MMSE. In addition, apathy is an important non-motor symptom in PD, but we did not assess apathy in this study. This insufficiency prevents us from analyzing the relationship between changed FC and apathy.

In conclusion, we found different cortico-striatal FC profiles between LPD and RPD patients and between LPD patients and controls. Lateralization of motor symptoms is associated with lateralized striatal FC. These results emphasize the necessity of separate investigations of the characteristics of brain activities of LPD and RPD patients in future studies using functional imaging modalities.

DATA AVAILABILITY STATEMENT

The raw data supporting the conclusions of this article will be made available by the authors, without undue reservation.

ETHICS STATEMENT

The studies involving human participants were reviewed and approved by The Ethics Committee of Beijing Hospital. The patients/participants provided their written informed consent to participate in this study.

AUTHOR CONTRIBUTIONS

WS, H-BC, and C-ZY conceived and designed the experiments. KL analyzed the fMRI data. MC, C-ML, RW, and B-HL were responsible for the fMRI scans and helped fMRI data analyses. WS, H-BC, and S-HL recruited the subjects. X-XM, HZ, KL, and S-HL collected the demographic, clinical, and neuropsychological information of the subjects. KL and WS wrote the manuscript. All the authors have read, revised, and approved the final manuscript.

FUNDING

This study was funded by the National Key R&D Program of China (Grant No. 2017YFC1310200), the 121 Project of Beijing Hospital (Grant No. 121-2016009), and the 12th Five-Year Plan for National Science & Technology Supporting Program (Grant Nos. 2012BAI10B03 and 2012BAI10B04). This study was also supported by the project National Major Multidisciplinary Cooperative Diagnosis and Treatment Capacity Building Project from the National Health Commission of the People's Republic of China.

REFERENCES

1. Postuma RB, Berg D, Stern M, Poewe W, Olanow CW, Oertel W, et al. MDS clinical diagnostic criteria for Parkinson's disease. *Mov Disord.* (2015) 30:1591–601. doi: 10.1002/mds.26424
2. Tekin S, Cummings JL. Frontal-subcortical neuronal circuits and clinical neuropsychiatry: an update. *J Psychosom Res.* (2002) 53:647–54. doi: 10.1016/S0022-3999(02)00428-2
3. Di Martino A, Scheres A, Margulies DS, Kelly AM, Uddin LQ, Shehzad Z, et al. Functional connectivity of human striatum: a resting state FMRI study. *Cereb Cortex.* (2008) 18:2735–47. doi: 10.1093/cercor/bhn041
4. Hoehn MM, Yahr MD. Parkinsonism: onset, progression and mortality. *Neurology.* (1967) 17:427–42. doi: 10.1212/WNL.17.5.427
5. Miller-Patterson C, Buesa R, McLaughlin N, Jones R, Akbar U, Friedman JH. Motor asymmetry over time in Parkinson's disease. *J Neurol Sci.* (2018) 393:14–7. doi: 10.1016/j.jns.2018.08.001
6. Hughes AJ, Daniel SE, Kilford L, Lees AJ. Accuracy of clinical diagnosis of idiopathic Parkinson's disease: a clinico-pathological study of 100 cases. *J Neurol Neurosurg Psychiatry.* (1992) 55:181–4. doi: 10.1136/jnnp.55.3.181
7. Kempster PA, Gibb WR, Stern GM, Lees AJ. Asymmetry of substantia nigra neuronal loss in Parkinson's disease and its relevance to the mechanism of levodopa related motor fluctuations. *J Neurol Neurosurg Psychiatry.* (1989) 52:72–6. doi: 10.1136/jnnp.52.1.72
8. Leenders KL, Salmon EP, Tyrrell P, Perani D, Brooks DJ, Sager H, et al. The nigrostriatal dopaminergic system assessed *in vivo* by positron emission tomography in healthy volunteer subjects and patients with Parkinson's disease. *Arch Neurol.* (1990) 47:1290–8. doi: 10.1001/archneur.1990.00530120034007
9. Booth TC, Nathan M, Waldman AD, Quigley AM, Schapira AH, Buscombe J. The role of functional dopamine-transporter SPECT imaging in parkinsonian syndromes, part 2. *AJNR Am J Neuroradiol.* (2015) 36:236–44. doi: 10.3174/ajnr.A3971
10. Verreyt N, Nys GM, Santens P, Vingerhoets G. Cognitive differences between patients with left-sided and right-sided Parkinson's disease. A review. *Neuropsychol Rev.* (2011) 21:405–24. doi: 10.1007/s11065-011-9182-x
11. Modestino EJ, Amenechi C, Reinhofer A, O'Toole P. Side-of-onset of Parkinson's disease in relation to neuropsychological measures. *Brain Behav.* (2017) 7:e00590. doi: 10.1002/brb3.590
12. Riederer P, Jellinger KA, Kolber P, Hipp G, Sian-Hulsmann J, Kruger R. Lateralisation in Parkinson disease. *Cell Tissue Res.* (2018) 373:297–312. doi: 10.1007/s00441-018-2832-z
13. Cubo E, Martin PM, Martin-Gonzalez JA, Rodriguez-Blazquez C, Kulisevsky J, Members EG. Motor laterality asymmetry and non-motor symptoms in Parkinson's disease. *Mov Disord.* (2010) 25:70–5. doi: 10.1002/mds.22896
14. Hanna-Pladdy B, Pahwa R, Lyons KE. Paradoxical effect of dopamine medication on cognition in Parkinson's disease: relationship to side of motor onset. *J Int Neuropsychol Soc.* (2015) 21:259–70. doi: 10.1017/S1355617715000181
15. Azeez AK, Biswal BB. A review of resting-state analysis methods. *Neuroimaging Clin N Am.* (2017) 27:581–92. doi: 10.1016/j.nic.2017.06.001
16. Shen B, Pan Y, Jiang X, Wu Z, Zhu J, Dong J, et al. Altered putamen and cerebellum connectivity among different subtypes of Parkinson's disease. *CNS Neurosci Ther.* (2020) 26:207–14. doi: 10.1111/cns.13259
17. Wang X, Li J, Yuan Y, Wang M, Ding J, Zhang J, et al. Altered putamen functional connectivity is associated with anxiety disorder in Parkinson's disease. *Oncotarget.* (2017) 8:81377–86. doi: 10.18632/oncotarget.18996
18. Potvin-Desrochers A, Mitchell T, Gisiger T, Paquette C. Changes in resting-state functional connectivity related to freezing of gait in Parkinson's disease. *Neuroscience.* (2019) 418:311–7. doi: 10.1016/j.neuroscience.2019.08.042
19. Yu R, Liu B, Wang L, Chen J, Liu X. Enhanced functional connectivity between putamen and supplementary motor area in Parkinson's disease patients. *PLoS ONE.* (2013) 8:e59717. doi: 10.1371/journal.pone.0059717
20. Sharman M, Valabregue R, Perlbarg V, Marrakchi-Kacem L, Vidailhet M, Benali H, et al. Parkinson's disease patients show reduced

cortical-subcortical sensorimotor connectivity. *Mov Disord.* (2013) 28:447–54. doi: 10.1002/mds.25255
21. Herz DM, Haagensen BN, Nielsen SH, Madsen KH, Løkkegaard A, Siebner HR. Resting-state connectivity predicts levodopa-induced dyskinesias in Parkinson's disease. *Mov Disord.* (2016) 31:521–9. doi: 10.1002/mds.26540
22. Owens-Walton C, Jakabek D, Li X, Wilkes FA, Walterfang M, Velakoulis D, et al. Striatal changes in Parkinson disease: an investigation of morphology, functional connectivity and their relationship to clinical symptoms. *Psychiatry Res Neuroimaging.* (2018) 275:5–13. doi: 10.1016/j.pscychresns.2018.03.004
23. Hou Y, Luo C, Yang J, Song W, Ou R, Liu W, et al. A resting-state fMRI study on early-stage drug-naïve Parkinson's disease patients with drooling. *Neurosci Lett.* (2016) 634:119–25. doi: 10.1016/j.neulet.2016.10.007
24. Ham JH, Cha J, Lee JJ, Baek GM, Sunwoo MK, Hong JY, et al. Nigrostriatal dopamine-independent resting-state functional networks in Parkinson's disease. *Neuroimage.* (2015) 119:296–304. doi: 10.1016/j.neuroimage.2015.06.077
25. Hou Y, Yang J, Luo C, Ou R, Song W, Liu W, et al. Patterns of striatal functional connectivity differ in early and late onset Parkinson's disease. *J Neurol.* (2016) 263:1993–2003. doi: 10.1007/s00415-016-8211-3
26. Luo C, Song W, Chen Q, Zheng Z, Chen K, Cao B, et al. Reduced functional connectivity in early-stage drug-naive Parkinson's disease: a resting-state fMRI study. *Neurobiol Aging.* (2014) 35:431–41. doi: 10.1016/j.neurobiolaging.2013.08.018
27. Manza P, Zhang S, Li CS, Leung HC. Resting-state functional connectivity of the striatum in early-stage Parkinson's disease: cognitive decline and motor symptomatology. *Hum Brain Mapp.* (2016) 37:648–62. doi: 10.1002/hbm.23056
28. Hacker CD, Perlmutter JS, Criswell SR, Ances BM, Snyder AZ. Resting state functional connectivity of the striatum in Parkinson's disease. *Brain.* (2012) 135:3699–711. doi: 10.1093/brain/aws281
29. Helmich RC, Derikx LC, Bakker M, Scheeringa R, Bloem BR, Toni I. Spatial remapping of cortico-striatal connectivity in Parkinson's disease. *Cereb Cortex.* (2010) 20:1175–86. doi: 10.1093/cercor/bhp178
30. Kwak Y, Peltier S, Bohnen NI, Muller ML, Dayalu P, Seidler RD. Altered resting state cortico-striatal connectivity in mild to moderate stage Parkinson's disease. *Front Syst Neurosci.* (2010) 4:143. doi: 10.3389/fnsys.2010.00143
31. Yang W, Liu B, Huang B, Huang R, Wang L, Zhang Y, et al. Altered resting-state functional connectivity of the striatum in Parkinson's disease after levodopa administration. *PLoS ONE.* (2016) 11:e0161935. doi: 10.1371/journal.pone.0161935
32. Kelly C, de Zubicaray G, Di Martino A, Copland DA, Reiss PT, Klein DF, et al. L-dopa modulates functional connectivity in striatal cognitive and motor networks: a double-blind placebo-controlled study. *J Neurosci.* (2009) 29:7364–78. doi: 10.1523/JNEUROSCI.0810-09.2009
33. Simioni AC, Dagher A, Fellows LK. Compensatory striatal-cerebellar connectivity in mild-moderate Parkinson's disease. *Neuroimage Clin.* (2016) 10:54–62. doi: 10.1016/j.nicl.2015.11.005
34. Lin WC, Chen HL, Hsu TW, Hsu CC, Huang YC, Tsai NW, et al. Correlation between dopamine transporter degradation and striatocortical network alteration in Parkinson's disease. *Front Neurol.* (2017) 8:323. doi: 10.3389/fneur.2017.00323
35. Bell PT, Gilat M, O'Callaghan C, Copland DA, Frank MJ, Lewis SJ, et al. Dopaminergic basis for impairments in functional connectivity across subdivisions of the striatum in Parkinson's disease. *Hum Brain Mapp.* (2015) 36:1278–91. doi: 10.1002/hbm.22701
36. Selemon LD, Goldman-Rakic PS. Longitudinal topography and interdigitation of corticostriatal projections in the rhesus monkey. *J Neurosci.* (1985) 5:776–94. doi: 10.1523/JNEUROSCI.05-03-00776.1985
37. Alexander GE, DeLong MR, Strick PL. Parallel organization of functionally segregated circuits linking basal ganglia and cortex. *Annu Rev Neurosci.* (1986) 9:357–81. doi: 10.1146/annurev.ne.09.030186.002041
38. Nakano K, Kayahara T, Tsutsumi T, Ushiro H. Neural circuits and functional organization of the striatum. *J Neurol.* (2000) 247(Suppl. 5):V1–15. doi: 10.1007/PL00007778
39. Postuma RB, Dagher A. Basal ganglia functional connectivity based on a meta-analysis of 126 positron emission tomography and functional magnetic resonance imaging publications. *Cereb Cortex.* (2006) 16:1508–21. doi: 10.1093/cercor/bhj088
40. Heinrichs-Graham E, Santamaria PM, Gendelman HE, Wilson TW. The cortical signature of symptom laterality in Parkinson's disease. *Neuroimage Clin.* (2017) 14:433–40. doi: 10.1016/j.nicl.2017.02.010
41. Li K, Su W, Chen M, Li CM, Ma XX, Wang R, et al. Abnormal spontaneous brain activity in left-onset Parkinson disease: a resting-state functional MRI study. *Front Neurol.* (2020) 11:727. doi: 10.3389/fneur.2020.00727
42. Jia X-Z, Wang J, Sun H-Y, Zhang H, Liao W, Wang Z, et al. RESTplus: an improved toolkit for resting-state functional magnetic resonance imaging data processing. *Sci Bull.* (2019) 64:953–1030. doi: 10.1016/j.scib.2019.05.008
43. Ashburner J. A fast diffeomorphic image registration algorithm. *Neuroimage.* (2007) 38:95–113. doi: 10.1016/j.neuroimage.2007.07.007
44. Friston KJ, Williams S, Howard R, Frackowiak RS, Turner R. Movement-related effects in fMRI time-series. *Magn Reson Med.* (1996) 35:346–55. doi: 10.1002/mrm.1910350312
45. Bruck A, Aalto S, Nurmi E, Vahlberg T, Bergman J, Rinne JO. Striatal subregional 6-[18F]fluoro-L-dopa uptake in early Parkinson's disease: a two-year follow-up study. *Mov Disord.* (2006) 21:958–63. doi: 10.1002/mds.20855
46. Kish SJ, Shannak K, Hornykiewicz O. Uneven pattern of dopamine loss in the striatum of patients with idiopathic Parkinson's disease. Pathophysiologic and clinical implications. *N Engl J Med.* (1988) 318:876–80. doi: 10.1056/NEJM198804073181402
47. Yan CG, Wang XD, Zuo XN, Zang YF. DPABI: data processing & analysis for (resting-state) brain imaging. *Neuroinformatics.* (2016) 14:339–51. doi: 10.1007/s12021-016-9299-4
48. Nichols T, Hayasaka S. Controlling the familywise error rate in functional neuroimaging: a comparative review. *Stat Methods Med Res.* (2003) 12:419–46. doi: 10.1191/0962280203sm341ra
49. Chen X, Lu B, Yan CG. Reproducibility of R-fMRI metrics on the impact of different strategies for multiple comparison correction and sample sizes. *Hum Brain Mapp.* (2018) 39:300–18. doi: 10.1002/hbm.23843
50. Ham JH, Lee JJ, Kim JS, Lee PH, Sohn YH. Is dominant-side onset associated with a better motor compensation in Parkinson's disease? *Mov Disord.* (2015) 30:1921–5. doi: 10.1002/mds.26418
51. Chung SJ, Yoo HS, Lee HS, Lee PH, Sohn YH. Does the side onset of Parkinson's disease influence the time to develop levodopa-induced dyskinesia? *J Parkinsons Dis.* (2019) 9:241–7. doi: 10.3233/JPD-181512
52. Lee EY, Sen S, Eslinger PJ, Wagner D, Kong L, Lewis MM, et al. Side of motor onset is associated with hemisphere-specific memory decline and lateralized gray matter loss in Parkinson's disease. *Parkinsonism Relat Disord.* (2015) 21:465–70. doi: 10.1016/j.parkreldis.2015.02.008
53. Kim JS, Yang JJ, Lee JM, Youn J, Kim JM, Cho JW. Topographic pattern of cortical thinning with consideration of motor laterality in Parkinson disease. *Parkinsonism Relat Disord.* (2014) 20:1186–90. doi: 10.1016/j.parkreldis.2014.08.021
54. Baumann CR, Held U, Valko PO, Wienecke M, Waldvogel D. Body side and predominant motor features at the onset of Parkinson's disease are linked to motor and non-motor progression. *Mov Disord.* (2014) 29:207–13. doi: 10.1002/mds.25650
55. Pelizzari L, Di Tella S, Lagana MM, Bergsland N, Rossetto F, Nemni R, et al. White matter alterations in early Parkinson's disease: role of motor symptom lateralization. *Neurol Sci.* (2020) 41:357–64. doi: 10.1007/s10072-019-04084-y
56. Marinus J, van Hilten JJ. The significance of motor (a)symmetry in Parkinson's disease. *Mov Disord.* (2015) 30:379–85. doi: 10.1002/mds.26107
57. Eklund A, Nichols TE, Knutsson H. Cluster failure: why fMRI inferences for spatial extent have inflated false-positive rates. *Proc Natl Acad Sci USA.* (2016) 113:7900–5. doi: 10.1073/pnas.1602413113
58. Baik K, Cha J, Ham JH, Baek GM, Sunwoo MK, Hong JY, et al. Dopaminergic modulation of resting-state functional connectivity in *de novo* patients with Parkinson's disease. *Hum Brain Mapp.* (2014) 35:5431–41. doi: 10.1002/hbm.22561
59. Choe IH, Yeo S, Chung KC, Kim SH, Lim S. Decreased and increased cerebral regional homogeneity in early Parkinson's disease. *Brain Res.* (2013) 1527:230–7. doi: 10.1016/j.brainres.2013.06.027
60. Skorvanek M, Goldman JG, Jahanshahi M, Marras C, Rektorova I, Schmand B, et al. Global scales for cognitive screening in Parkinson's disease: critique and recommendations. *Mov Disord.* (2018) 33:208–18. doi: 10.1002/mds.27233
61. Dubois B, Burn D, Goetz C, Aarsland D, Brown RG, Broe GA, et al. Diagnostic procedures for Parkinson's disease dementia:

recommendations from the movement disorder society task force. *Mov Disord*. (2007) 22:2314–24. doi: 10.1002/mds.21844

Conflict of Interest: The authors declare that the research was conducted in the absence of any commercial or financial relationships that could be construed as a potential conflict of interest.

frontiers in Neurology

ORIGINAL RESEARCH
published: 07 July 2021
doi: 10.3389/fneur.2021.679984

Association Between Amygdala Volume and Trajectories of Neuropsychiatric Symptoms in Alzheimer's Disease and Dementia With Lewy Bodies

Alberto Jaramillo-Jimenez[1,2,3,4,5,6*], *Lasse M. Giil*[7,8], *Diego A. Tovar-Rios*[1,9,10], *Miguel Germán Borda*[1,2,11], *Daniel Ferreira*[12,13], *Kolbjørn Brønnick*[1,2], *Ketil Oppedal*[1,14,15] *and Dag Aarsland*[1,16]

[1] Centre for Age-Related Medicine (SESAM), Stavanger University Hospital, Stavanger, Norway, [2] Faculty of Health Sciences, University of Stavanger, Stavanger, Norway, [3] Grupo de Neurociencias de Antioquia, School of Medicine, Universidad de Antioquia, Medellín, Colombia, [4] Grupo Neuropsicología y Conducta, School of Medicine, Universidad de Antioquia, Medellín, Colombia, [5] Semillero de Investigación SINAPSIS, School of Medicine, Universidad de Antioquia, Medellín, Colombia, [6] Semillero de Investigación NeuroCo, School of Medicine and Engenieering, Universidad de Antioquia, Medellín, Colombia, [7] Department of Clinical Science, University of Bergen, Bergen, Norway, [8] Department of Internal Medicine, Haraldsplass Deaconess Hospital, Bergen, Norway, [9] Universidad Del Valle, Grupo de Investigación en Estadística Aplicada - INFERIR, Faculty of Engineering, Santiago De Cali, Valle Del Cauca, Colombia, [10] Universidad Del Valle, Prevención y Control de la Enfermedad Crónica - PRECEC, Faculty of Health, Santiago De Cali, Valle Del Cauca, Colombia, [11] Semillero de Neurociencias y Envejecimiento, Medical School, Ageing Institute, Pontificia Universidad Javeriana, Bogota, Colombia, [12] Division of Clinical Geriatrics, Center for Alzheimer Research, Department of Neurobiology, Care Sciences and Society, Karolinska Institutet, Stockholm, Sweden, [13] Department of Radiology, Mayo Clinic, Rochester, MN, United States, [14] Stavanger Medical Imaging Laboratory, Department of Radiology, Stavanger University Hospital, Stavanger, Norway, [15] Department of Electrical Engineering and Computer Science, University of Stavanger, Stavanger, Norway, [16] Department of Old Age Psychiatry, Institute of Psychiatry, Psychology, and Neuroscience, King's College London, London, United Kingdom

OPEN ACCESS

Edited by:
Frederic Sampedro, Sant Pau Institute for Biomedical Research, Spain

Reviewed by:
Chien Tai Hong, Taipei Medical University, Taiwan
Juan Marín-Lahoz, Hospital Universitario Miguel Servet, Spain

***Correspondence:**
Alberto Jaramillo-Jimenez
alberto.jaramilloj@udea.edu.co

Specialty section:
This article was submitted to Movement Disorders, a section of the journal Frontiers in Neurology

Received: 12 March 2021
Accepted: 27 May 2021
Published: 07 July 2021

Citation:
Jaramillo-Jimenez A, Giil LM, Tovar-Rios DA, Borda MG, Ferreira D, Brønnick K, Oppedal K and Aarsland D (2021) Association Between Amygdala Volume and Trajectories of Neuropsychiatric Symptoms in Alzheimer's Disease and Dementia With Lewy Bodies. Front. Neurol. 12:679984. doi: 10.3389/fneur.2021.679984

Introduction: The amygdala is implicated in psychiatric illness. Even as the amygdala undergoes significant atrophy in mild dementia, amygdala volume is underexplored as a risk factor for neuropsychiatric symptoms (NPS).

Objective : To analyze the association between baseline amygdala volume and the longitudinal trajectories of NPS and cognitive decline in Alzheimer's disease (AD) and dementia with Lewy bodies (DLB) over 5 years.

Methods: Eighty-nine patients with mild dementia were included (AD = 55; DLB = 34). Amygdala volume was segmented from structural magnetic resonance images (sMRI) using a semi-automatic method (Freesurfer 6.0) and normalized by intracranial volumes. The intracranial volume-normalized amygdala was used as a predictor of the Neuropsychiatric Inventory (NPI) total score, ordinal NPI item scores (0 = absence of symptoms, 1–3 = mild symptoms, ≥4 = clinically relevant symptoms), and Mini-Mental State Examination (MMSE) as measured annually over 5 years using gamma, ordinal, and linear mixed-effects models, respectively. The models were adjusted for demographic variables, diagnosis, center of sMRI acquisition, and cognitive performance. Multiple testing-corrected p-values (q-values) are reported.

Results: Larger intracranial volume-normalized amygdala was associated with less agitation/aggression (odds ratio (OR) = 0.62 [0.43, 0.90], $p = 0.011$, $q = 0.038$) and less MMSE decline per year (fixed effect = 0.70, [0.29, 1.03], $p = 0.001$, $q = 0.010$) but more depression (OR = 1.49 [1.09, 2.04], $p = 0.013$, $q = 0.040$).

Conclusions: Greater amygdala volume in mild dementia is associated with lower odds of developing agitation/aggression, but higher odds of developing depression symptoms during the 5-year study period.

Keywords: magnetic resonance imaging, amygdala, neuropsychiatric symptoms, Alzheimer's disease, dementia with lewy bodies

INTRODUCTION

Among structural imaging markers for neurodegenerative dementias, the hippocampal volume has been extensively investigated in Alzheimer's disease (AD) and dementia with Lewy bodies (DLB) (1, 2). Clinical correlates of hippocampal atrophy include disease progression and decline in various cognitive functions, for instance, episodic memory impairment in AD (3, 4). However, much less is known about medial temporal lobe structures of the limbic system such as the amygdala, localized in the anterior portion of the medial temporal lobe (5, 6).

Multicenter studies using structural magnetic resonance imaging (sMRI) have reported that the extent of the atrophy in the amygdala seems to be comparable to hippocampal atrophy in patients with mild AD (7). Nevertheless, the amygdala volume has received less attention than hippocampal volume, even as amygdala volume also predicts AD progression (8), and is associated with cognitive performance (9). Importantly, the amygdala is an essential structure for emotion regulation and is part of the salience neural network (9). Of note, several systematic reviews and meta-analyses have linked amygdala structure and function with psychiatric disorders such as major depressive disorder, depression with comorbid anxiety, schizophrenia, and bipolar disorder (10–13). However, the role of the amygdala as a potential marker of neuropsychiatric symptoms (NPS) during the course of dementia remains elusive.

A few cross-sectional studies have suggested associations between the amygdala volume and NPS in AD, including aberrant motor behavior (7), irritability, aggression/agitation (14), anxiety (15), and apathy (16). In spite of it, less is known about these relationships in the early stage of dementia. Furthermore, as NPS fluctuate considerably (17, 18), it is essential to evaluate these associations in longitudinal studies. Especially in DLB, this association has not been studied as far as we know. Understanding such association is important to elucidate the role of early patterns of volume reduction that could be relevant markers of the risk of NPS in clinical practice, which could help to implement specific interventions in at-risk patients.

Based on previous reports in AD showing that amygdala lesions are involved in NPS (9, 19), and considering our preliminary findings that NPS are common and fluctuate during the course of AD and DLB (17, 18), here we aimed to analyze the association between amygdala volumes and the longitudinal development of NPS in AD and DLB.

MATERIALS AND METHODS

Study Design and Setting

This is a secondary analysis of the "The Dementia Study of Western Norway" (DemVest) cohort (20). The latter included patients with mild dementia due to different etiologies recruited between 2005 and 2007 across all the dementia clinics in Hordaland and Rogaland counties in Norway. All patients had annual follow-up until death. Exclusion criteria consisted of absence of dementia, moderate or severe dementia, delirium, personal history of bipolar or psychotic disorder, terminal illness, or recently diagnosed major somatic disease. Details of the design, recruitment, and assessments are stated elsewhere (20). The study was approved by the regional ethics committee and the Norwegian authorities. All patients signed informed consent before enrollment in the study.

In the current analysis, we did not include patients with other causes of dementia recruited in the DemVest cohort ($n = 26$) since segmentation of sMRI was only available for AD and DLB patients; more details about imaging availability can be found elsewhere (21).

Sample

Only subjects with an available baseline high-resolution sMRI were included. Thus, we included a total sample of 89 subjects with mild dementia who had a clinical diagnosis of AD ($n = 55$) or DLB ($n = 34$). Data from the first 5 years (i.e., Baseline + 5 annual follow-ups) of the DemVest study were used in the current study.

Clinical Assessment

Four clinical specialists independently applied diagnostic criteria. Dementia diagnosis was mainly established using the DSM-IV criteria (22). When non-amnesic features were present, diagnosis of dementia was made through consensus based on the DLB operationalized diagnostic criteria (23). Subjects were further classified as AD (according to the National Institute of Neurological and Communicative Disorders, Stroke-Alzheimer's Disease and Related Disorders Association) (24) or DLB (according to the International consensus criteria) (23). Patients with a Mini-Mental State Examination (MMSE) (25) score $\geq$20 or a Clinical Dementia Rating scale (CDR) (26) global score equal to 1 were considered to have a mild stage of dementia.

A subset ($AD = 36$; $DLB = 20$) had autopsy confirmation. High congruency between the clinical, imaging, and neuropathological diagnosis was achieved as previously reported (20, 27). Diagnosis was re-assessed regularly during the follow-up by four specialists in geriatric medicine and psychiatry.

The final diagnosis (used for analysis in the current study) was based on the last consensus diagnosis, considering clinical and imaging findings but giving priority to neuropathological diagnosis when available.

Annual structured medical evaluations, relevant information regarding past medical history and medical records were used to obtain complete and detailed medical background.

Global cognition was assessed using the MMSE score.

NPS Assessment

NPS were assessed annually over 5 years with the Neuropsychiatric Inventory (NPI) (28). The NPI was based on the carer report and includes 10 items (in its original version) for various NPS (i.e., Delusions, Hallucinations, Agitation/aggression, Dysphoria/depression, Anxiety, Euphoria/elation, Apathy/indifference, Disinhibition, Irritability/lability, and Aberrant motor behavior). Each symptom is rated in severity (ranging 0–3) and frequency of presentation (ranging 0–4). Thus, multiplying severity by frequency, a resulting item score (or domain score) can be obtained for each symptom (ranging 0–12).

For our analyses, item scores $\geq$ 4 were considered "clinically relevant symptoms," item scores between 1 and 3 were considered "mild symptoms," and item scores = 0 were considered "absence of symptoms" following previously reported methods (17, 18, 29–32). Thus, individual trajectories of NPS were estimated for each of the NPI domains, based on the item scores (and NPI total score) of each patient at each time point of the study (i.e., Baseline + 5 annual follow-ups).

Amygdala Volumes Segmentation

Baseline sMRI were acquired in three different research centers using 1.5-T scanners at the three involved research centers (Philips Intera in Stavanger and Haugesund, and General Electric Signa Excite in Bergen), with a voxel resolution of $1 \times 1 \times \approx$ 1.5 mm. Detailed sMRI protocols for each center were available elsewhere (21). The sMRI were acquired in coronal planes in the three research centers. Images with artifacts on visual inspection were excluded. The standardized processing pipeline from FreeSurfer 6.0 (http://surfer.nmr.mgh.harvard.edu/) was applied to multicenter sMRI data as follows: movement correction, non-brain tissues removal, automated calculation of Talairach transformation, intensity normalization, subcortical white and gray matter segmentation, cortex boundary tessellation, fully automatic topology correction, and surface deformation to determine CSF/gray matter and gray/white matter boundaries (33–35). For amygdala segmentation and volume calculation, the FreeSurfer 6.0 automated pipeline for subcortical structures segmentation was implemented. A detailed explanation of the FreeSurfer 6.0 subcortical segmentation methods can be found elsewhere (33). Visual inspection of the final Freesurfer amygdala segmentation was conducted by one researcher blinded to diagnosis for accuracy verification. The right and left amygdala volumes of each hemisphere were summed to obtain the total amygdala volume. To control for the effect of head size and gender differences, the intracranial volume-normalized amygdala was estimated as follows: [Total amygdala volume in mm^3/total intracranial volume in mm^3] * 100%, based on previously published evidence and recommendations on studying the amygdala volume in neurodegenerative diseases (36, 37).

Statistical Analysis

Baseline demographic (i.e., age, gender, and years of education) and sMRI variables were compared between the AD and DLB subgroups using independent samples *t*-test for continuous variables and Chi-square test for categorical variables. Diagnosis-related differences in the intracranial volume-normalized amygdala were adjusted using ANCOVA followed by *post-hoc* pairwise Tukey test given the possible confounder effect of covariates such as gender, age, and center of sMRI acquisition. Non-parametric subgroup differences in clinical variables (i.e., MMSE, and NPI total) were examined using the Mann–Whitney *U*-test.

To assess the trajectories of NPS, each NPI item score (i.e., frequency $\times$ severity) was collapsed into an ordinal variable with three levels that indicate the "absence of symptoms" (NPI item score = 0), "mild symptoms" (NPI item score = 1–3), or "clinically relevant symptoms" (NPI item score $\geq$ 4). Frequency plots for clinically relevant symptoms were created overall and by diagnosis subgroup.

As repeated observations of individuals are not independent (i.e., correlated), and each patient had a subject-specific trajectory of NPS over time (varying not only in the baseline NPS), mixed-effects models were used to estimate the mean of per-person means over 5 years. Mixed-effects models consider the mean population response for ordinal NPI domains over time (fixed effect), as well as the error in that trajectory associated with differences in patient characteristics (random effect). Detailed revision of the application of mixed models in medicine can be found elsewhere (38).

After the exploratory analysis of our dataset, the center of sMRI acquisition was observed as a possible source of variability in demographic and volumetric variables across individuals (**supplementary Figures 1**, **2** and **supplementary tables 1**, **2**). Therefore, subsequent analyses (i.e., mixed-effects models) included this factor as covariate. Time in the study was also included as a covariate, and the random effects of time were also considered.

For statistical purposes, the intracranial volume-normalized amygdala values were rescaled, multiplying them by 1,000 to avoid the boundary value problem in the subsequent models' estimations.

First, to analyze the associations between amygdala volumes and global NPS in the total sample, we conducted generalized mixed-effects models. In these models, the intracranial volume-normalized amygdala was used as the independent variable and the absolute NPI total score at each time point of the study was used as the dependent variable (added a constant of one to obtain a strictly positive distribution). These generalized mixed-effects models were based on gamma distribution with random intercepts and slopes in an unstructured variance–covariance matrix. Time in study, center of sMRI acquisition, gender,

TABLE 1 | Baseline characteristics of the AD and DLB subgroups.

	Total sample ($N = 89$)	AD($N = 55$)	DLB ($N = 34$)	p-value	Adjusted p-value [b]
Age	75.4 (7.17)	74.9 (7.28)	76.3 (7.01)	0.383	-
Gender				**<0.001**	**-**
Women (%)	53 (59.55)	41 (74.55)	12 (35.29)	-	-
Men (%)	36 (40.45)	14 (25.45)	22 (64.71)	-	-
Years of education	9.5 (2.79)	9.5 (2.55)	9.4 (3.02)	0.864	-
MMSE [a]	24 (2.62)	24 (3)	24 (5)	0.966	-
NPI total [a]	12 (17)	8 (16.5)	16.5 (16)	**0.006**	-
Amygdala (% ICV)	0.154 (0.042)	0.152 (0.045)	0.158 (0.039)	0.487	0.569

AD, Alzheimer's disease; DLB, Dementia with Lewy bodies; SD, Standard deviation; IQR, Interquartile range; MMSE, Mini-Mental State Examination; NPI, Neuropsychiatric inventory; ICV, Total intracranial volume.

Values are presented as mean (SD), and frequency (%) for gender.

$p < 0.05$ are printed in bold.

[a] *Values are presented as median (IQR), Mann–Whitney U.*

[b] *ANCOVA (df = 6), controlling for age, gender, and center of sMRI acquisition with post-hoc Tukey pairwise test by diagnosis.*

diagnosis, and MMSE total score were included as covariates in a fully adjusted model.

Second, we conducted separate ordinal mixed-effects models using intracranial volume-normalized amygdala as the independent variable and each of the ordinal NPI items (i.e., delusions, hallucinations, agitation/aggression, depression, anxiety, apathy, disinhibition, irritability, and aberrant motor behavior) at each time point of the study as the outcome variable. Euphoria was not included in analyses due to its low frequency and thus lack of power in this study to detect any relevant finding. We again used random intercepts and slopes in an unstructured variance–covariance matrix. All these models were conducted as unadjusted, partly adjusted, and fully adjusted models as follows: The unadjusted models included time and center of sMRI acquisition as covariates. The partly adjusted models also included age, gender, and diagnosis as covariates. The fully adjusted models included the same above covariates as well as longitudinal MMSE scores (i.e., the absolute score of MMSE at each time point of the study). All models included any significant interactions.

Considering potential confounder effects of MMSE on the NPI total and the NPI items estimations, we also examined the associations between intracranial volume-normalized amygdala (independent variable) and the absolute score of MMSE at each study time point (dependent variable) using linear mixed-effects models. Again, we included random intercepts and slopes in an unstructured variance–covariance matrix. This unadjusted model included time and center of sMRI as covariates, and an adjusted model included also age, gender, and diagnosis.

Time interactions with intracranial volume-normalized amygdala were also evaluated in the NPI total score and the MMSE models based on the Akaike Information Criterion (AIC) and the Bayesian Information Criterion (BIC). Significant time * diagnosis, time * MMSE, and time * NPI total score interactions were considered for analysis.

Effect sizes are reported as fixed effects (FE, for NPI total score and MMSE) and odds ratios (OR, for each of the NPI items).

The resulting p-values of the predictors in all the above mixed-effects models were corrected for multiple testing using the false discovery rate (FDR) (39). Given the dependence of these p-values, we used a tail-area-based FDR (40). The statistical significance level was defined as alpha = 0.05 for all analyses. FDR-adjusted p-values (q-values) are reported.

Missing data during follow-up, mostly due to death, were assumed to be missing at random, supported by previous publications showing that age, gender, diagnosis, and cognitive decline all predict mortality in this cohort (41).

Additional exploratory analyses for ordinal NPI items, NPI total, and MMSE were conducted stratified by diagnosis. Given the small sample size of each subgroup, these models only included time and center as covariates. Also, considering the exploratory nature of analyses, the resulting p-values were not corrected for multiple testing.

Statistical analyses were performed using Stata © version 15.1. RStudio © version 1.1.456 was used for the FDR correction (fdrtool package) and illustrations (ggplot2, seaborn) (40–43).

The current study is reported following the Strengthening the Reporting of Observational Studies in Epidemiology (STROBE) statement (44).

RESULTS

Participants

A total of 89 patients with mild dementia were included ($AD = 55$; $DLB = 34$). Demographic and clinical baseline characteristics, as well as the intracranial volume-normalized amygdala, are presented in **Table 1**. At baseline, age and MMSE were comparable in AD and DLB subgroups. There were significant group differences in gender ($p < 0.001$), where the DLB subgroup had a higher number of men compared to AD. In the DLB subgroup, the baseline NPI total score was higher ($p = 0.006$), but MMSE at baseline was comparable between AD and DLB patients ($p = 0.966$). **Figure 1** shows the number of individuals at each time point of the study including dropouts due to death and loss to follow-up. The dropout rate at the latest

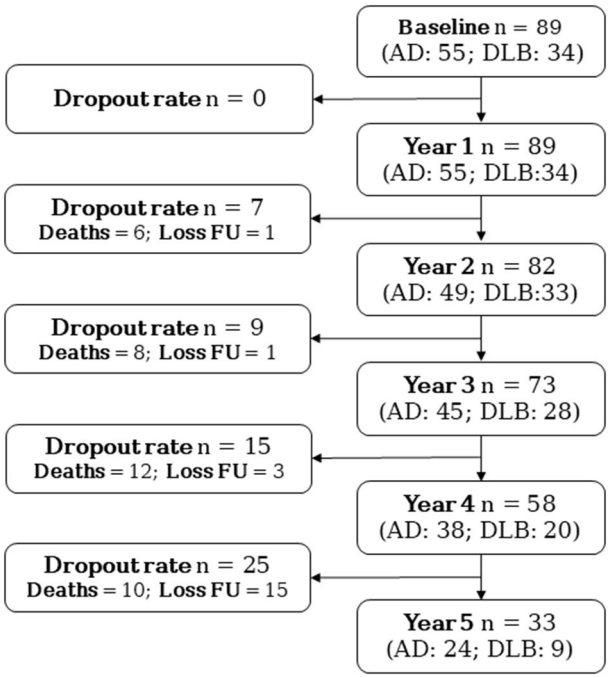

FIGURE 1 | Flowchart of patients at each time point of the study including dropouts. AD, Alzheimer's disease; DLB, Dementia with Lewy bodies; Loss FU, Loss to follow-up.

follow-up examination was 62.9% ($n = 56$), especially due to death, which represents the 64.3% ($n = 36$) among the causes of dropout.

Amygdala Volume at Baseline

Figure 2 illustrates the values of the intracranial volume-normalized amygdala in the total sample and by diagnosis subgroup. Intracranial volume-normalized amygdala was comparable between the AD and the DLB subgroups ($t = -0.699$, $p = 0.487$). Similar results were obtained when including age, gender, and center of sMRI acquisition as covariates (ANCOVA – $P_{\text{Tukey}} = 0.569$) (**Table 1**).

Significant group differences were observed for the center of sMRI acquisition (t-test, $p < 0.001$) but these differences disappeared (ANCOVA, $p = 0.205$) after controlling for age, gender, diagnosis proportion in each center, as well as age * gender, center * diagnosis, and center * age interactions (**supplementary Figure 1** and **supplementary table 1**). Descriptive statistics of the intracranial volume-normalized amygdala by gender are presented in **supplementary Figure 2** and **supplementary table 2**.

NPS Over Time

Detailed graphical abstract of the frequency of clinically relevant symptoms is presented in **Figure 3**, as well as **supplementary table 3**. **Figure 3** depicts the frequency (in percent of symptomatic) of individuals with clinically relevant NPS (i.e., a domain score ≥ 4) at each time point of the study. Overall, the most frequent symptom in the total sample was apathy.

At baseline, the more frequent clinically relevant symptoms were apathy (30.3%), followed by depression (19.1%) and irritability (18%), whereas euphoria (0%), agitation (5.6%), and disinhibition (7.9%) were the less frequent clinically relevant symptoms. Similarly, at the first annual follow-up, apathy (39.3%), depression (21.4%), and irritability (19.1%) were the more frequent clinically relevant symptoms, while euphoria (3.4%), agitation (11.2%), and disinhibition (4.5%) were the less frequently presented. At the second annual follow-up, apathy was consistently the most presented symptom (47.6%), followed by aberrant motor behavior (32.9%), and depression (25.6%), while clinically relevant euphoria (0%), hallucinations (12.2%), and agitation (13.4%) were the less presented symptoms. In line with this, the higher frequency of presentation at the third annual follow-up was accounted by clinically relevant apathy (53.4%), aberrant motor behavior (32.9%), and depression (26%), but clinically relevant euphoria (4.1%), disinhibition (11%), and delusions (13.7%) were the less frequently presented symptoms. At the fourth annual follow-up, the increasing trend of presenting clinically relevant apathy (48.3%) and aberrant motor behavior (31%) was slightly reduced, but the frequency of clinically relevant depression augmented (27.6%). Besides, clinically relevant euphoria (5.7%), disinhibition (12.1%), and delusions (15.5%) were the less presented symptoms. Finally, at the end of follow-up, clinically relevant apathy (48.3%), irritability (33.3%), and aberrant motor behavior (27.3%) were the more frequent symptoms whereas euphoria (6.1%), delusions (18.2%), and depression (18.2%) were symptoms with the lower frequency of presentation (**Figure 3A** and **supplementary table 3**).

In both AD and DLB subgroups, the most frequent symptom during the follow-up was apathy. In DLB patients, the frequency of hallucinations was greater when compared to AD, while aberrant motor behavior was more common in the AD subgroup (**Figure 3B**, **C** and **supplementary table 3**).

These results were consistent with previously published analyses of the total DemVest cohort (17, 18).

Association Between Amygdala Baseline Volume and Trajectories of Global NPS

In an unadjusted model with time and center as predictors, the intracranial volume-normalized amygdala had a significant association with the NPI total score (fixed effect—FE—of −0.14, 95% confidence interval [−0.25, −0.02], $p = 0.014$, $q = 0.041$). **Table 2A** summarizes the results of the partly adjusted (Model 1) and fully adjusted model (Model 2) for predicting trajectories of the NPI total score in the total sample.

A partly adjusted model showed that the intracranial volume-normalized amygdala had a significant effect over the NPI total score (FE = −0.14 [−0.25, −0.04], $p = 0.049$), but this effect was no longer significant after multiple testing correction ($q = 0.091$). A fully adjusted model did not show significant findings, but a significant effect of MMSE was observed as reported in **Table 2A**, Model 2.

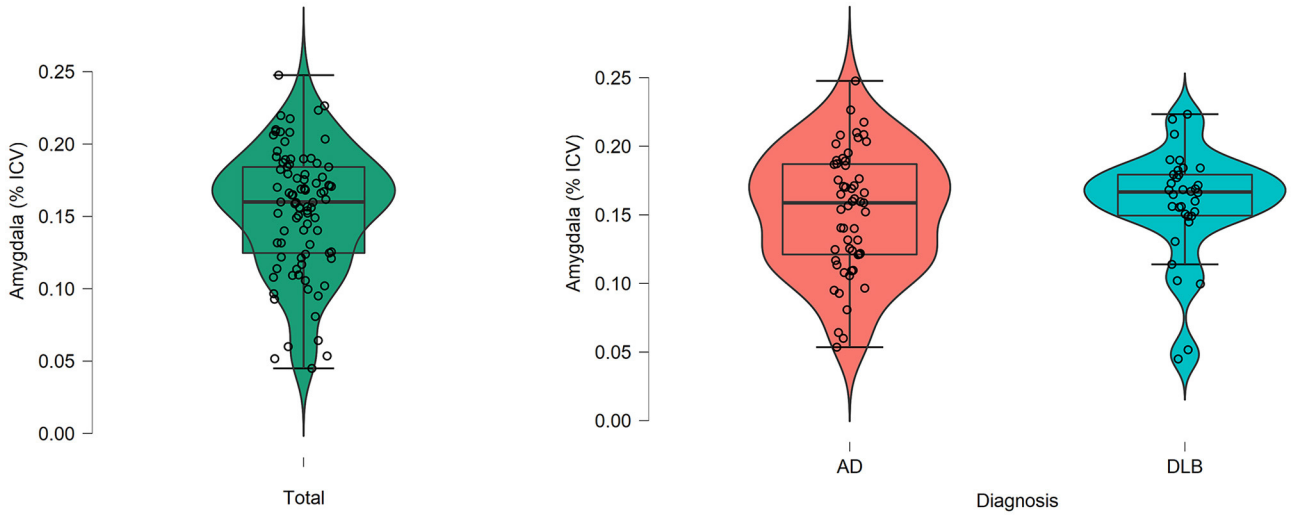

FIGURE 2 | Amygdala volumes after normalization for total intracranial volume in the total sample as well as the AD and DLB groups. Intracranial volume-normalized amygdala (i.e., [Total amygdala volume in mm^3/total intracranial volume in mm^3] * 100%). AD, Alzheimer's disease; DLB, Dementia with Lewy bodies; ICV, Total intracranial volume in mm^3.

Association Between Amygdala Baseline Volume and Trajectories of Various NPS

Figure 4 summarizes the results of the unadjusted, partly adjusted, and fully adjusted models for predicting trajectories of NPS in the total sample. The odds ratio (OR) refers to the risk of being in a one-level higher group on the ordinal NPI domains (i.e., presenting mild symptoms or developing clinically relevant symptoms).

The unadjusted model showed that patients with higher intracranial volume-normalized amygdala had a reduced odds for presenting mild symptoms of agitation/aggression or developing clinically relevant agitation/aggression over 5 years (OR = 0.55, 95% confidence interval [0.32, 0.84], $p = 0.006$, $q = 0.030$). Similar results were obtained for agitation/aggression in the partly adjusted model (OR = 0.54 [0.36, 0.80], $p = 0.002$, $q = 0.018$), as well as in the fully adjusted model (OR = 0.62 [0.43, 0.90], $p = 0.011$, $q = 0.038$).

Besides, those patients with greater intracranial volume-normalized amygdala had an increased odds for presenting mild symptoms of depression or developing clinically relevant depression as observed in the fully adjusted model (OR = 1.49 [1.09, 2.04], $p = 0.013$, $q = 0.040$). Consistent results were observed in the unadjusted (OR = 1.41 [1.04, 1.90], $p = 0.026$, $q = 0.061$) and partly adjusted models for depression (OR = 1.37 [1.03, 1.80], $p = 0.034$, $q = 0.070$) with a trend to significance in the multiple testing-corrected q-values.

In addition, the partly adjusted models showed lower odds for presenting mild symptoms of apathy or developing clinically relevant apathy trajectories in those patients with higher amygdala volumes (OR = 0.67 [0.46, 0.97], $p = 0.033$). However, these results were not significant following correction for multiple testing ($q = 0.069$).

No other NPI domains were significantly predicted by the intracranial volume-normalized amygdala in the main analysis.

Association Between Amygdala Baseline Volume and Trajectories of Global Cognition

The unadjusted model showed the interaction of intracranial volume-normalized amygdala and time interaction (FE = 0.70 [0.24, 1.16], $p = 0.003$, $q = 0.020$, see **Table 2B**, Model 3). After adjusting for age, gender, diagnosis, and their significant time interactions, the intracranial volume-normalized amygdala showed a significant FE of 0.66 [0.29, 1.03], $p = 0.001$, $q = 0.010$, **Table 2B**, Model 4.

In the total sample, **Figure 5A** shows the predicted MMSE score over 5 years according to the intracranial volume-normalized amygdala. Patients with higher intracranial volume-normalized amygdala had lesser MMSE decline per year after adjusting for the time in study, center of sMRI acquisition, age, gender, and diagnosis. Consistently, **Figure 5B** depicts the predicted MMSE score over 5 years according to the intracranial volume-normalized amygdala in both AD and DLB subgroups. In the DLB subgroup, the predicted MMSE score over 5 years according to the intracranial volume-normalized amygdala was lower compared to the AD subgroup.

Exploratory Analyses by Diagnosis Subgroup

Supplementary Table 4 summarizes the results of the additional exploratory analyses conducted separately in the DLB and AD subgroups. The intracranial volume-normalized amygdala showed a statistically significant

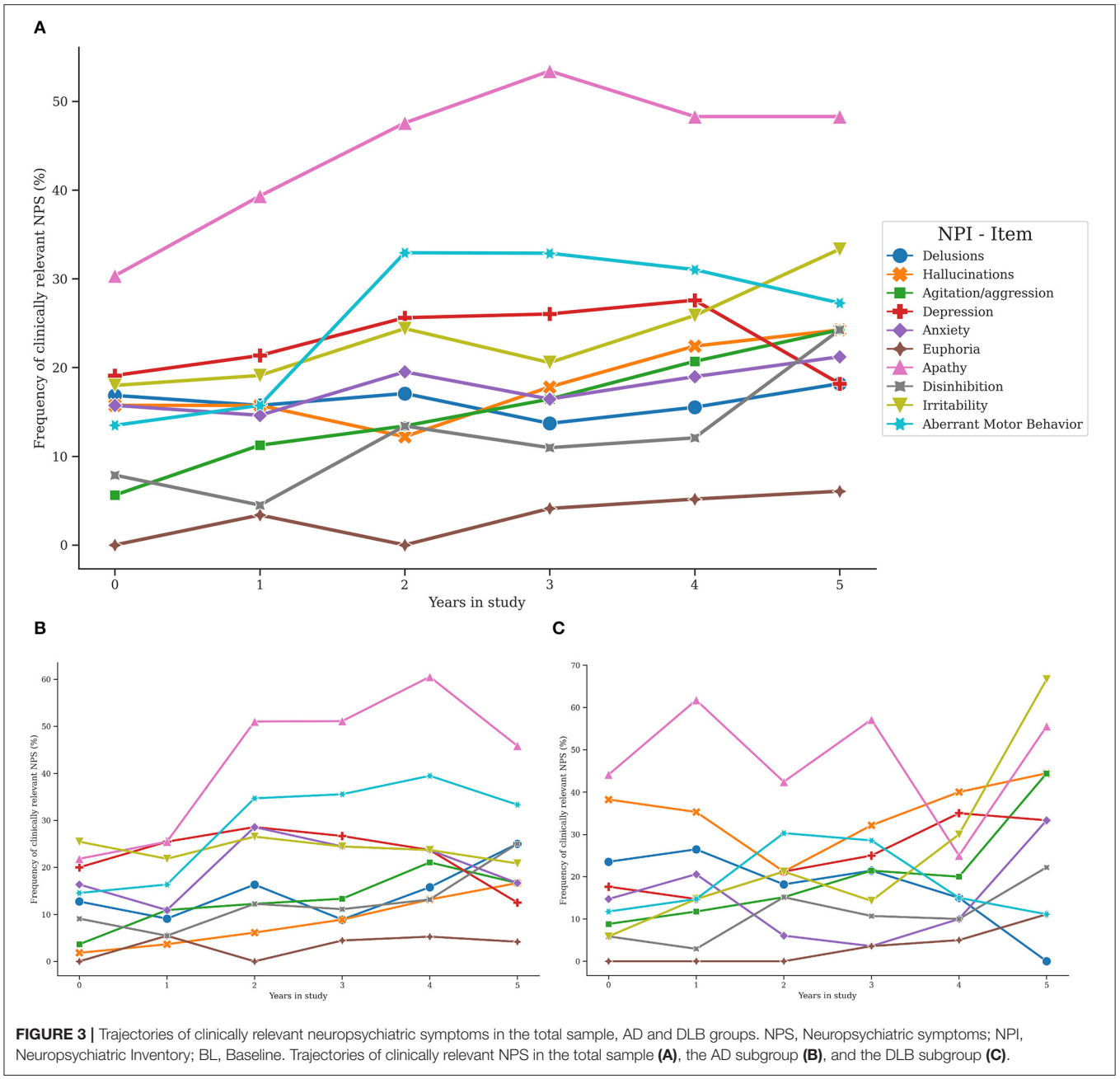

FIGURE 3 | Trajectories of clinically relevant neuropsychiatric symptoms in the total sample, AD and DLB groups. NPS, Neuropsychiatric symptoms; NPI, Neuropsychiatric Inventory; BL, Baseline. Trajectories of clinically relevant NPS in the total sample **(A)**, the AD subgroup **(B)**, and the DLB subgroup **(C)**.

effect predicting the MMSE * time interaction (representing points decline per year per unit of amygdala volume) in AD (FE = 0.53 [0.13, 0.93], p = 0.010), and stronger in DLB (FE = 1.19 [0.31, 2.07], p = 0.008). The NPI total was only significantly predicted in the DLB subgroup ($FE = -0.13$ [−0.25, −0.02], $p = 0.027$).

The lower odds of presenting mild symptoms of agitation or developing clinically relevant agitation with higher amygdala volumes were similar in AD (OR = 0.57 [0.36, 0.90], p = 0.015) and DLB (OR = 0.47 [0.18, 1.22], p = 0.120) but not significant in DLB, likely due to the small sample size. Similar findings were observed in both AD (OR = 1.45 [1.02, 2.06], p = 0.041) and DLB groups (OR = 1.38 [0.83, 2.29], p = 0.211) for the higher odds of presenting mild symptoms of depression or developing clinically relevant depression.

Interestingly, the DLB subgroup showed a reduced odds of presenting mild symptoms of hallucinations or developing clinically relevant hallucinations in those individuals with a higher intracranial volume-normalized amygdala (OR = 0.49 [0.31, 0.78], p = 0.002), which was not observed in AD (OR = 0.94 [0.49, 1.78], p = 0.845). Intracranial volume-normalized amygdala was not a significant predictor for other NPS.

TABLE 2A | Amygdala volume and the Neuropsychiatric Inventory total score over 5 years.

	Model 1[a]				Model 2[a]			
	FE	**95% CI**	***p*-value**	***q*-value**	**FE**	**95% CI**	***p*-value**	***q*-value**
Time	0.14	0.08, 0.19	**< 0.001**		0.07	0.02, 0.13	**0.010**	
Center[b]								
1	−0.22	−0.56, 0.13	0.223		−0.15	−0.49, 0.19	0.380	
2	−0.47	−0.82, −0.12	**0.008**		−0.44	−0.80, −0.08	**0.017**	
Age	0.03	0.01, 0.04	**0.002**		0.02	0.01, 0.04	**0.006**	
Gender (female)	−0.22	−0.47, 0.03	0.082		−0.21	−0.44, 0.02	0.088	
DLB	0.19	−0.04, 0.42	0.102		0.18	−0.03, 0.39		
MMSE					−0.03	−0.04, −0.02	**<0.001**	
Amygdala (%ICV)	−0.14	−0.25,−0.04	**0.049**	0.091	−0.10	−0.22, 0.01	0.072	0.118

TABLE 2B | Amygdala volume and MMSE over 5 years.

	Model 3[c]				Model 4[c]			
	FE	**95% CI**	***p*-value**	***q*-value**	**FE**	**95% CI**	***p*-value**	***q*-value**
Time (T)	−3.01	−3.41, −2.59	**<0.001**		−2.64	−3.08, −2.20	**<0.001**	
Center[b]								
1	0.25	−2.40, 2.90	0.852		1.20	−1.49, 3.91	0.381	
2	−0.32	−2.77, 2.13	0.797		0.16	−2.22, 2.55	0.894	
Age					−0.16	−0.23, −0.09	**<0.001**	
Age × T					0.07	0.01, 0.14	**0.025**	
Gender (female)					0.66	−0.69, −2.01	0.336	
Diagnosis (DLB)					0.74	−0.65, 2.13	0.295	
Diagnosis (DLB) × T					−1.07	−1.99, −1.16	**0.022***	
Amygdala (% ICV)	0.06	−0.95, 1.07	0.906	NA	0.16	−0.81, 1.12	0.747	NA
Amygdala (% ICV) × T	0.70	0.24, 1.16	**0.003**	**0.020**	0.66	0.29, 1.03	**0.001**	**0.010**

DLB, Dementia with Lewy bodies; FE, Fixed effect; CI, Confidence interval; MMSE, Mini-mental State Examination; NPI, Neuropsychiatric inventory; ICV, Total intracranial volume; T, Time.

[a]Generalized mixed-effects model with the absolute NPI total score (added a constant of one to provide strictly positive distribution) at each time point of the study as the dependent variable, and intracranial volume-normalized amygdala as independent variable, based on gamma distribution and log-link with random intercepts and slopes in an unstructured variance–covariance matrix with covariates as listed. In a model with time and center as predictors (not in Table), Amygdala (% ICV) had an FE of −0.14 [−0.25, −0.02], p = 0.014, q = 0.041.

[b]Twenty-three participants from reference center (Bergen), 11 in center coded as 1 (Haugesund), 55 in center coded as 2 (Stavanger).

[c]Linear mixed-effects model with the absolute MMSE score at each time point of the study as the outcome variable, intracranial volume-normalized amygdala as independent variable, random intercepts, and slopes in an unstructured variance–covariance matrix and covariates as listed.

Time interactions with intracranial volume-normalized amygdala were also evaluated in the NPI total score and the MMSE models based on the Akaike Information Criterion (AIC) and the Bayesian Information Criterion (BIC). Any significant interaction was included in the above models.

p-values and q < 0.05 are printed in bold. Multiple testing corrected p-values (q-values) are listed only for Amygdala (% ICV) (Models 1 and 2), or its interaction with time (Models 3 and 4).

DISCUSSION

This study analyzed the associations between amygdala volume and NPS in AD and DLB, over 5 years of follow-up. We have found that amygdala volumes were comparable between AD and DLB patients at the mild stage of dementia. Greater baseline amygdala volume in patients with mild dementia was associated with lower odds for developing agitation/aggression symptoms. Besides, higher odds for developing symptoms of depression were associated with greater baseline amygdala volume.

The reduction of amygdala volume has been widely studied in AD, but few cross-sectional studies have compared amygdala volume in AD and DLB (45–47), reporting conflicting results (48) that might be attributed to differences in study designs and methods of analysis. In line with our findings, a preliminary study with a matched-sample design combined manual and automatic segmentation and did not find group differences in the amygdala volumes of AD and DLB patients (47). By contrast, two studies found larger amygdala volumes in DLB (45–47), but the lack of adjustment for gender could have influenced their results.

Amygdala atrophy has been demonstrated in moderate and severe AD, but it is also prominent in the early stages of AD (7, 49). Functional and structural brain abnormalities may reflect the neuropathological features of dementia (i.e., Lewy bodies, tau, and amyloid-beta), and a relationship between the burden of Lewy bodies in the amygdala and reduced amygdala volume has

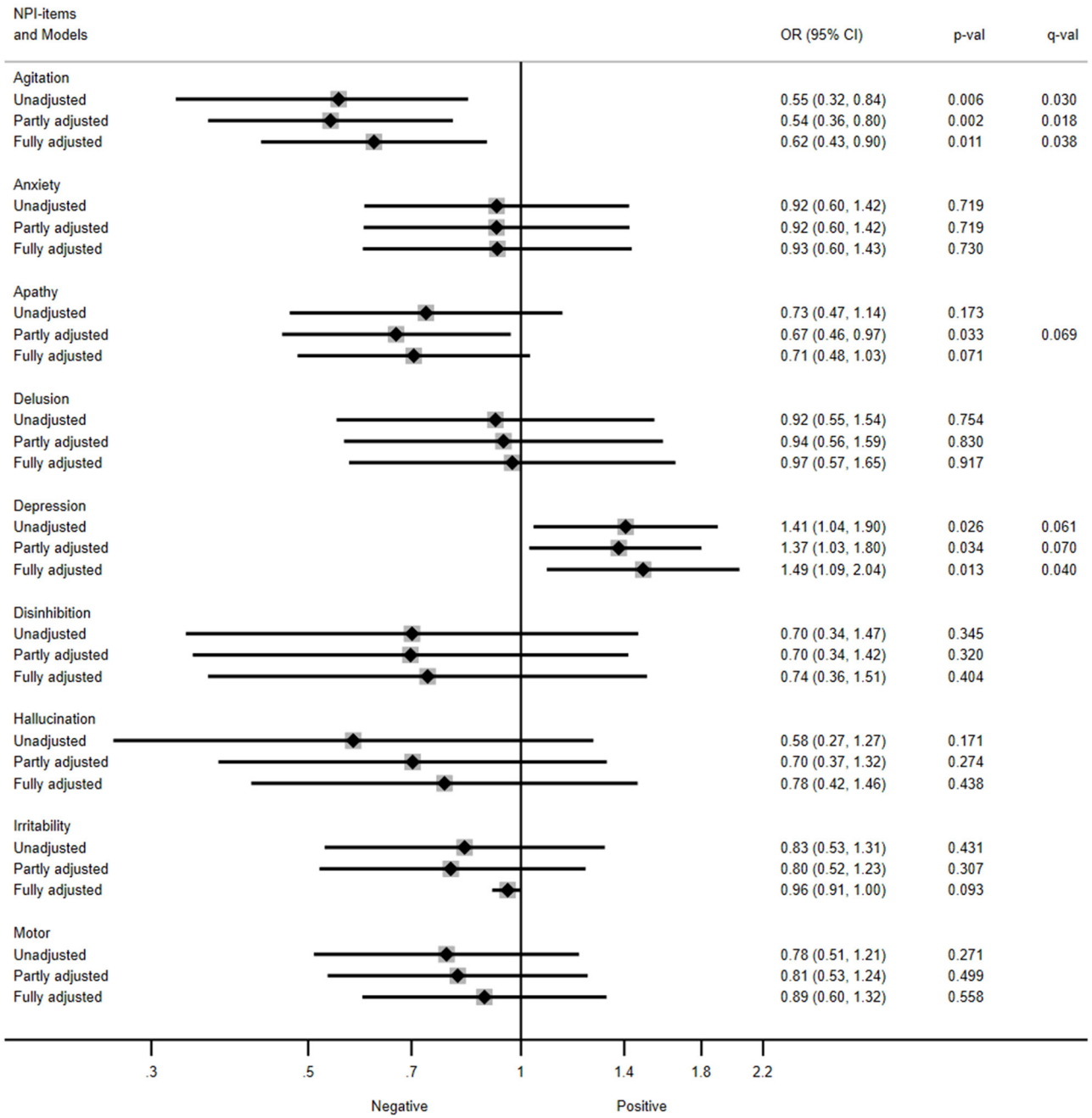

FIGURE 4 | Association between amygdala volume and trajectories of neuropsychiatric symptoms in the total sample. NPI, Neuropsychiatric inventory; OR, Odds ratios; CI, Confidence interval. Unadjusted model included amygdala and time as covariates; partly adjusted model also included age, gender, and diagnosis as covariates; fully adjusted model included MMSE score over 5 years as covariate. The OR (95% CI) refers to the risk of being in a one-level higher group on each of the ordinal NPI items (i.e., presenting mild symptoms, or developing a clinically relevant symptom). Multiple testing-corrected *p*-values (*q*-values) > 0.1 are listed.

been demonstrated in postmortem studies (48). Examining brain volumes in key regions can contribute to the understanding of the structural substrates of different NPS in dementia.

In AD, one longitudinal (2-year study) and several cross-sectional studies suggest close relationships between amygdala volume, cognitive performance, and presence of NPS (7, 9, 19, 49), including agitation/aggression (7, 9, 50). However, none of the available studies have investigated the amygdala volume as an early marker of long-term risk of NPS, and follow-up periods are relatively smaller compared to ours, which can affect the results considering the within-subject fluctuation of NPS over time (17).

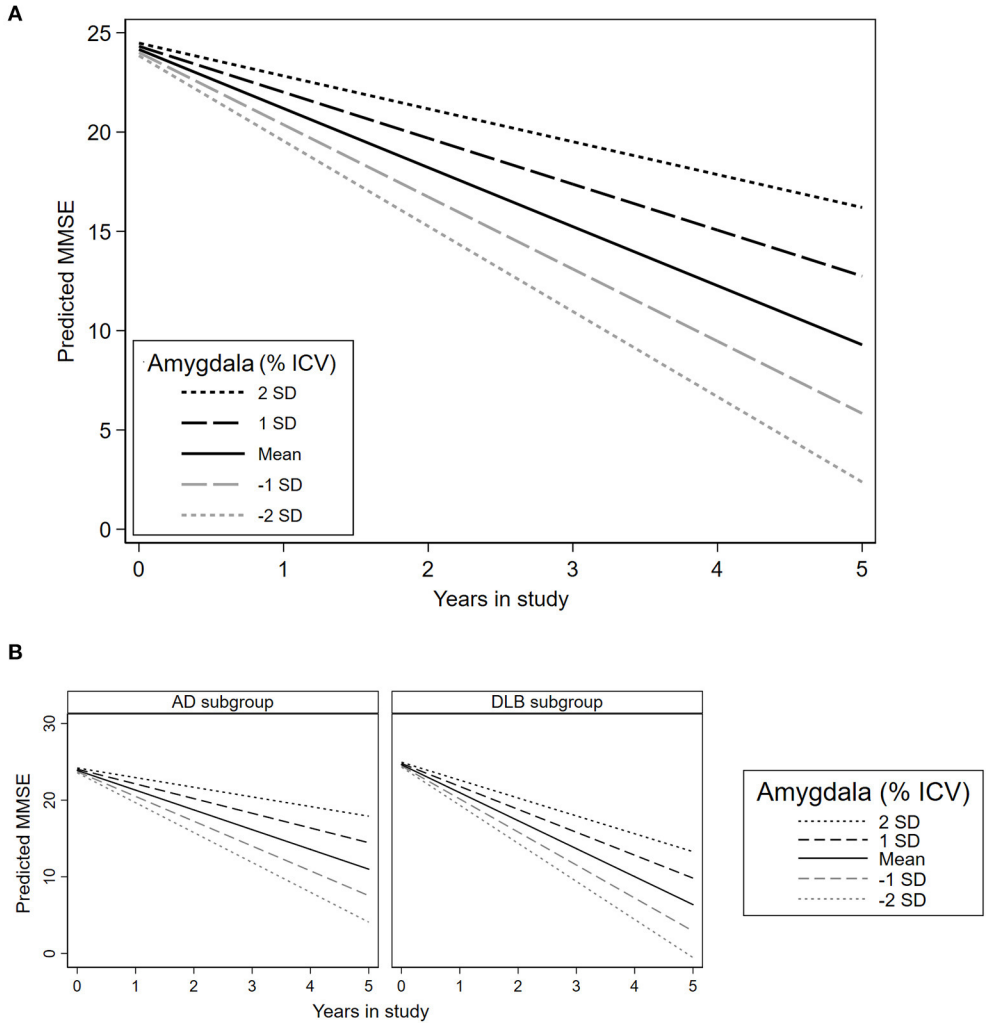

FIGURE 5 | Association between amygdala volume and trajectories of global cognition in the total sample and each diagnosis subgroup. MMSE, Mini-mental state examination; SD: Standard deviation. **(A)** Predictions in the total sample. **(B)** Predictions in the AD and DLB subgroups. This plot is based on the estimations presented in **Table 2B**, Model 4 (adjusted for time in study, age, gender, diagnosis, and center of sMRI acquisition).

We found that baseline amygdala volume had a significant inverse association with the trajectories of agitation/aggression in the total sample, as well as in the AD subgroup. This might reflect damage in circuits underlying behavioral and cognitive avoidance, which could explain clinical features present in agitated/aggressive patients such as overestimation and overreaction to threats, difficulties to modulate strong emotional responses, or increased vigilance and reactivity (9, 50). Aggression circuits involve the amygdala, as well as the insular, anterior cingulate, and orbitofrontal cortexes, which are also described in apathy (9, 19, 50). Thus, an imbalance between the default mode network and the salience network, characterized by increased connectivity in the latter, is hypothesized in those patients with agitation and apathy (9).

An association between baseline amygdala volume and the trajectories of depression was also observed in this study. Of note, this has not been previously reported in dementia patients with longitudinal data. Prior reports in young patients or patients with a first depressive episode linked depression to enlarged amygdala volume (51, 52). Nevertheless, conflicting results also reported an opposite direction for this relationship (53). Large meta-analyses concluded that a direct association between amygdala volume and major depression was particularly observed in depressed patients with comorbid anxiety (10), or those who were under antidepressive treatment (13). In AD, the presence of concomitant Lewy pathology in the amygdala increases the risk for major depression (54). Therefore, longitudinal designs will contribute to filling current knowledge gaps in specific imaging markers of depression in patients with cognitive decline, those with a history of early- and late-onset depression, and healthy older adults.

We adjusted the final models for cognitive decline under the assumption that cognitive deterioration could confound the amygdala volume/NPS association. However, it is equally if not more plausible that cognitive deterioration is an intermediate variable (55), in which case the partially adjusted models would be more appropriate. Therefore, we highlight the findings of the partly adjusted models in agitation/aggression, which are robust across all levels of adjustment and are supported by the available evidence. Also, interesting findings were observed in the partly adjusted models for the trajectories of apathy and depression with a trend to significance after correction for multiple testing.

Previously published cross-sectional evidence has linked apathy and the amygdala (16, 19, 56). In the behavioral variant of frontotemporal dementia, apathy has been considered the result of a disruption of emotional-affective mechanisms functionally linked to the ventromedial prefrontal cortex, the amygdala, and the ventral striatum (57). However, a recent review has pointed out that both emotional-affective and cognitive aspects may lead to impaired motivation and reduced self-generated goal-oriented behaviors that depend on the integrity of cortical and subcortical structures connecting the limbic system and the prefrontal cortex (56). Dopaminergic deficits in the mesolimbic system, especially in the basal amygdala, have also been suggested as a possible underlying mechanism for apathy (58).

Exploratory subgroup analyses showed consistent results in the AD subgroup for agitation and depression. In the DLB group, amygdala volume seems to be associated with the trajectories of hallucinations, but not with other NPS. Remarkably, visual hallucinations have been described as a strong predictor of Lewy pathology; thus, increased burden of Lewy bodies in the amygdala has been reported in DLB patients with visual hallucinations (59).

In conclusion, greater amygdala volume in mild dementia is associated with lower odds of developing agitation/aggression but higher odds of developing depression symptoms during the 5-year study period (particularly in AD). We encourage future works studying NPS in dementia to examine the external validity of our findings.

STRENGTHS AND LIMITATIONS

Assessing NPS through a standardized, valid, reliable, and widely available instrument contributes to the reproducibility and external validity of our findings. From the clinical standpoint, defining NPS as "clinically relevant" favors a consistent distinction between overlapping symptoms such as depression and apathy (17); it also facilitates the interpretation of the results. These cutoffs have been widely used in previously published studies (17, 18, 29–32) but have not been validated yet. Conversely, the NPI does not capture the whole spectrum of NPS of dementia and was based on the carer report.

We included patients with a sufficiently long follow-up, considering NPS present from the early to the severe stage of dementia. However, sMRI segmentation from other causes of dementia with remarkable NPS, such as frontotemporal dementia, was not available. In addition, the small sample size and rate of dropouts due to mortality, especially in the DLB group, could lead to underestimations of the trajectories of NPS. Besides, a potential recruitment bias may be present in our data due to the referrals of patients with complicated dementia or NPS from primary care units. However, psychiatric, geriatric, and neurology clinics, as well as GPs, were invited to refer every patient with suspected dementia to minimize this potential source of bias. Also, no control group was available for contrasting our results with normal aging, but clinically relevant NPS were not expected in normal aging (31).

On the other hand, preliminary reports have shown that the amygdala volumes based on the FreeSurfer pipeline have higher validity (i.e., strongly correlations to manual tracing) than other automatic segmentation tools (60, 61). Nevertheless, automatic methods for sMRI segmentation seem to overestimate amygdala volumes, but this does not necessarily imply a lack of validity with adequate visual quality control (61). Also, we are aware of various normalization methods for structural volumes that control for gender differences and head size. However, we conducted amygdala/ICV ratios as it has been demonstrated to control for gender differences in the amygdala volume and facilitate interpretation of the results (36, 37). Further studies with standardized and harmonized normalization protocols can address these limitations. Finally, longitudinal sMRI could be used to estimate atrophy rates and elucidate the potential effects of volume changes over time and the severity of NPS.

DATA AVAILABILITY STATEMENT

The datasets presented in this article are not readily available because we do not have ethical approval to freely share data to non-related groups. Requests to access the datasets should be directed to Dag Aarsland, daarsland@gmail.com.

ETHICS STATEMENT

The studies involving human participants were reviewed and approved by Stavanger University Hospital. The patients/participants provided their written informed consent to participate in this study.

AUTHOR CONTRIBUTIONS

AJ-J: conception of work, visualization, formal analysis, methodology, preparation of the initial draft, writing, reviewing, and approval. LG and DT-R: formal analysis, methodology, writing, reviewing, editing, and approval. MB: conception of work, writing, reviewing, and approval. DF, KB, KO, and DA: supervision, methodology, visualization, writing, reviewing, and approval. All authors contributed to the article and approved the submitted version.

FUNDING

This paper represents independent research supported by the Norwegian government, through hospital owner Helse Vest (Western Norway Regional Health Authority). Also, this work is funded by the National Institute for Health Research (NIHR) Biomedical Research Centre at South London and Maudsley NHS Foundation Trust, King's College London, and Center for Innovative Medicine (CIMED). The views expressed are those of the author(s) and not necessarily those of the NHS, the NIHR, or the Department of Health and Social Care.

ACKNOWLEDGMENTS

We want to thank all the participants, researchers, and technical staff who have made the DemVest study possible.

SUPPLEMENTARY MATERIAL

The Supplementary Material for this article can be found online at: https://www.frontiersin.org/articles/10.3389/fneur.2021.679984/full#supplementary-material

REFERENCES

1. Chow N, Aarsland D, Honarpisheh H, Beyer MK, Somme JH, Elashoff D, et al. Comparing hippocampal atrophy in Alzheimer's dementia and dementia with lewy bodies. *Dement Geriatr Cogn Disord.* (2012) 34:44–50. doi: 10.1159/000339727
2. Oppedal K, Ferreira D, Cavallin L, Lemstra AW, ten Kate M, Padovani A, et al. A signature pattern of cortical atrophy in dementia with lewy bodies: a study on 333 patients from the european dLB consortium. *Alzheimers Dement.* (2019) 15:400–9. doi: 10.1016/j.jalz.2018.09.011
3. Dawe RJ, Bennett DA, Schneider JA, Arfanakis K. Neuropathologic correlates of hippocampal atrophy in the elderly: a clinical, pathologic, postmortem mRI study. *PLoS ONE.* (2011) 6:e26286. doi: 10.1371/journal.pone.0026286
4. Peng GP, Feng Z, He FP, Chen ZQ, Liu XY, Liu P, et al. Correlation of hippocampal volume and cognitive performances in patients with either mild cognitive impairment or Alzheimer's disease. *CNS Neurosci Ther.* (2015) 21:15–22. doi: 10.1111/cns.12317
5. Oler JA. "Medial Temporal Lobe," in *Encyclopedia of Clinical Neuropsychology*, eds J. S. Kreutzer, J. DeLuca, B. Caplan (New York, NY: Springer New York), 1538–40.
6. Raslau FD, Mark IT, Klein AP, Ulmer JL, Mathews V, Mark LP. Memory part 2: the role of the medial temporal lobe. *Am J Neuroradiol.* (2015) 36:846. doi: 10.3174/ajnr.A4169
7. Poulin SP, Dautoff R, Morris JC, Barrett LF, Dickerson BC. Amygdala atrophy is prominent in early Alzheimer's disease and relates to symptom severity. *Psychiatry Res Neuroimaging.* (2011) 194:7–13. doi: 10.1016/j.pscychresns.2011.06.014
8. Rodríguez JJ, Noristani HN, Verkhratsky A. The serotonergic system in ageing and Alzheimer's disease. *Prog Neurobiol.* (2012) 99:15–41. doi: 10.1016/j.pneurobio.2012.06.010
9. Rosenberg PB, Nowrangi MA, Lyketsos CG. Neuropsychiatric symptoms in Alzheimer's disease: what might be associated brain circuits? *Mol Aspects Med.* (2015) 43–44:25–37. doi: 10.1016/j.mam.2015.05.005
10. Espinoza Oyarce DA, Shaw ME, Alateeq K, Cherbuin N. Volumetric brain differences in clinical depression in association with anxiety: a systematic review with meta-analysis. *J Psychiatry Neurosci.* (2020) 45:406–29. doi: 10.1503/jpn.190156
11. Ho NF, Chong PLH, Lee DR, Chew QH, Chen G, Sim K. The amygdala in schizophrenia and bipolar disorder: a Synthesis of structural mRI, diffusion tensor imaging, and resting-State functional connectivity findings. *Harv Rev Psychiatry.* (2019) 27:150–64. doi: 10.1097/HRP.0000000000000207
12. Anticevic A, Van Snellenberg JX, Cohen RE, Repovs G, Dowd EC, Barch DM. Amygdala recruitment in schizophrenia in response to aversive emotional material: a meta-analysis of neuroimaging studies. *Schizophr Bull.* (2012) 38:608–21. doi: 10.1093/schbul/sbq131
13. Hamilton JP, Siemer M, Gotlib IH. Amygdala volume in major depressive disorder: a meta-analysis of magnetic resonance imaging studies. *Mol Psychiatry.* (2008) 13:993–1000. doi: 10.1038/mp.2008.57
14. Wright CI, Dickerson BC, Feczko E, Negeira A, Williams D. A functional magnetic resonance imaging study of amygdala responses to human faces in aging and mild Alzheimer's disease. *Biol Psychiatry.* (2007) 62:1388–95. doi: 10.1016/j.biopsych.2006.11.013
15. Davidson RJ. Anxiety and affective style: role of prefrontal cortex and amygdala. *Biol Psychiatry.* (2002) 51:68–80. doi: 10.1016/S0006-3223(01)01328-2
16. Kile SJ, Ellis WG, Olichney JM, Farias S, Decarli C. Alzheimer abnormalities of the amygdala with klüver-Bucy syndrome symptoms: an amygdaloid variant of alzheimer disease. *Arch Neurol.* (2009) 66:125–29. doi: 10.1001/archneurol.2008.517
17. Vik-Mo AO, Giil LM, Ballard C, Aarsland D. Course of neuropsychiatric symptoms in dementia: 5-year longitudinal study. *Int J Geriatr Psychiatry.* (2018) 33:1361–9. doi: 10.1002/gps.4933
18. Vik-Mo AO, Giil LM, Borda MG, Ballard C, Aarsland D. The individual course of neuropsychiatric symptoms in people with Alzheimer's and lewy body dementia: 12-year longitudinal cohort study. *Br J Psychiatry.* (2020) 216:43–8. doi: 10.1192/bjp.2019.195
19. Tascone L dos S, Bottino CM de C. Neurobiologia dos sintomas neuropsiquiátricos na doença de Alzheimer: uma revisão crítica com foco na neuroimagem. *Dement e Neuropsychol.* (2013) 7:236–43. doi: 10.1590/S1980-57642013DN70300002
20. Aarsland D, Rongve A, Piepenstock Nore S, Skogseth R, Skulstad S, Ehrt U, et al. Frequency and case identification of dementia with lewy bodies using the revised consensus criteria. *Dement Geriatr Cogn Disord.* (2008) 26:445–52. doi: 10.1159/000165917
21. Borda MG, Jaramillo-Jimenez A, Tovar-Rios DA, Ferreira D, Garcia-Cifuentes E, Vik-Mo AO, et al. Hippocampal subfields and decline in activities of daily living in Alzheimer's disease and dementia with lewy bodies. *Neurodegener Dis Manag.* (2020) 10:357–67. doi: 10.2217/nmt-2020-0039
22. Diagnostic statistical manual of mental disorders: *DSM-IV*. 4th Edn. Washington, DC : American Psychiatric Association, (1994) Available online at: https://search.library.wisc.edu/catalog/999733358502121
23. McKeith IG, Dickson DW, Lowe J, Emre M, O'Brien JT, Feldman H, et al. Diagnosis and management of dementia with lewy bodies: third report of the dLB consortium. *Neurology.* (2005) 65:1863–72. doi: 10.1212/01.wnl.0000187889.17253.b1
24. McKhann G, Drachman D, Folstein M, Katzman R, Price D, Stadlan EM. Clinical diagnosis of Alzheimer's disease: report of the nINCDS-ADRDA work group? under the auspices of department of health and human services task force on Alzheimer's disease. *Neurology.* (1984) 34:939–44. doi: 10.1212/WNL.34.7.939
25. Folstein MF, Folstein SE, McHugh PR. "Mini-mental state". A practical method for grading the cognitive state of patients for the clinician. *J Psychiatr Res.* (1975) 12:189–98. doi: 10.1016/0022-3956(75)90026-6
26. Hughes CP, Berg L, Danziger WL, Coben LA, Martin RL. A new clinical scale for the staging of dementia. *Br J Psychiatry.* (1982) 140:566–572. doi: 10.1192/bjp.140.6.566
27. Skogseth R, Hortobágyi T, Soennesyn H, Chwiszczuk L, Ffytche D, Rongve A, et al. Accuracy of clinical diagnosis of dementia with lewy bodies versus neuropathology. *J Alzheimer's Dis.* (2017) 59:1139–52. doi: 10.3233/JAD-170274

28. Cummings JL, Mega M, Gray K, Rosenberg-Thompson S, Carusi DA, Gornbein J. The neuropsychiatric inventory: comprehensive assessment of psychopathology in dementia. *Neurology.* (1994) 44:2308–14. doi: 10.1212/WNL.44.12.2308
29. Zhang M, Wang H, Li T, Yu X. Prevalence of neuropsychiatric symptoms across the declining memory continuum: an observational study in a memory clinic setting. *Dement Geriatr Cogn Dis Extra.* (2012) 2:200–8. doi: 10.1159/000338410
30. Teipel SJ, Thyrian JR, Hertel J, Eichler T, Wucherer D, Michalowsky B, et al. Neuropsychiatric symptoms in people screened positive for dementia in primary care. *Int Psychogeriatrics.* (2015) 27:39–48. doi: 10.1017/S1041610214001987
31. Lyketsos CG, Lopez O, Jones B, Fitzpatrick AL, Breitner J, Dekosky S. Prevalence of neuropsychiatric symptoms in dementia and mild cognitive impairment: results from the cardiovascular health study. *J Am Med Assoc.* (2002) 288:1475–83. doi: 10.1001/jama.288.12.1475
32. Aalten P, Verhey FRJ, Boziki M, Bullock R, Byrne EJ, Camus V, et al. Neuropsychiatric syndromes in dementia: results from the european alzheimer disease consortium: part i. *Dement Geriatr Cogn Disord.* (2007) 24:457–63. doi: 10.1159/000110738
33. Fischl B, Salat DH, Busa E, Albert M, Dieterich M, Haselgrove C, et al. Whole brain segmentation: automated labeling of neuroanatomical structures in the human brain. *Neuron.* (2002) 33:341–55. doi: 10.1016/S0896-6273(02)00569-X
34. Fischl B, van der Kouwe A, Destrieux C, Halgren E, Ségonne F, Salat DH, et al. Automatically parcellating the human cerebral cortex. *Cereb Cortex.* (2004) 14:11–22. doi: 10.1093/cercor/bhg087
35. Jovicich J, Czanner S, Greve D, Haley E, van der Kouwe A, Gollub R, et al. Reliability in multi-site structural mRI studies: effects of gradient non-linearity correction on phantom and human data. *Neuroimage.* (2006) 30:436–43. doi: 10.1016/j.neuroimage.2005.09.046
36. Whitwell JL, Crum WR, Watt HC, Fox NC. Normalization of cerebral volumes by use of intracranial volume: implications for longitudinal quantitative mR imaging. *Am J Neuroradiol.* (2001) 22:1483.
37. Voevodskaya O. The effects of intracranial volume adjustment approaches on multiple regional mRI volumes in healthy aging and Alzheimer's disease. *Front Aging Neurosci.* (2014) 6:264. doi: 10.3389/fnagi.2014.00264
38. Brown H, Prescott R. *Applied Mixed Models in Medicine*, 3rd Edn. Chichester, England:Wiley Blackwell. (2015).
39. Storey JD. A direct approach to false discovery rates. *J R Stat Soc Ser B Stat Methodol.* (2002) 64:479–98. doi: 10.1111/1467-9868.00346
40. Strimmer K. fdrtool: a versatile r package for estimating local and tail area-based false discovery rates. *Bioinformatics.* (2008) 24:1461–2. doi: 10.1093/bioinformatics/btn209
41. Ibrahim JG, Molenberghs G. Missing data methods in longitudinal studies: a review. *Test.* (2009) 18:1–43. doi: 10.1007/s11749-009-0138-x
42. Wickham H. *ggplot2: Elegant Graphics for Data Analysis.* (2016) Available online at: https://ggplot2.tidyverse.org
43. Waskom M. Seaborn: statistical data visualization. *J. Open Source Soft.* 6(60):3021. https://doi.org/10.21105/joss.03021
44. Vandenbroucke JP, Von Elm E, Altman DG, Gøtzsche PC, Mulrow CD, Pocock SJ, et al. Strengthening the reporting of observational studies in epidemiology (STROBE): explanation and elaboration. *PLoS Med.* (2007) 4:1628–1654. doi: 10.1371/journal.pmed.0040297
45. Burton EJ, Karas G, Paling SM, Barber R, Williams ED, Ballard CG, et al. Patterns of cerebral atrophy in dementia with lewy bodies using voxel-Based morphometry. *Neuroimage.* (2002) 17:618–30. doi: 10.1006/nimg.2002.1197
46. Barber R, Ballard C, McKeith IG, Gholkar A, O'Brien JT. MRI volumetric study of dementia with lewy bodies: a comparison with aD and vascular dementia. *Neurology.* (2000) 54:1304–9. doi: 10.1212/WNL.54.6.1304
47. Hashimoto M, Kitagaki H, Imamura T, Hirono N, Shimomura T, Kazui H, et al. Medial temporal and whole-brain atrophy in dementia with lewy bodies: a volumetric mRI study. *Neurology.* (1998) 51:357–62. doi: 10.1212/WNL.51.2.357
48. Burton EJ, Mukaetova-Ladinska EB, Perry RH, Jaros E, Barber R, O'Brien JT. Neuropathological correlates of volumetric mRI in autopsy-confirmed lewy body dementia. *Neurobiol Aging.* (2012) 33:1228–36. doi: 10.1016/j.neurobiolaging.2010.12.015
49. Klein-Koerkamp Y, Heckemann R, Ramdeen K, Moreaud O, Keignart S, Krainik A, etal. Disease Neuroimaging Initiative for the. Amygdalar Atrophy in Early Alzheimer's Disease. *Curr Alzheimer Res.* (2014) 11:239–52. doi: 10.2174/1567205011666140131123653
50. Trzepacz PT, Yu P, Bhamidipati PK, Willis B, Forrester T, Tabas L, et al. Frontolimbic atrophy is associated with agitation and aggression in mild cognitive impairment and Alzheimer's disease. *Alzheimers Dement.* (2013) 9:S95–S104.e1. doi: 10.1016/j.jalz.2012.10.005
51. Frodl T, Meisenzahl EM, Zetzsche T, Born C, Jäger M, Groll C, et al. Larger amygdala volumes in first depressive episode as compared to recurrent major depression and healthy control subjects. *Biol Psychiatry.* (2003) 53:338–44. doi: 10.1016/S0006-3223(02)01474-9
52. Lange C, Irle E. Enlarged amygdala volume and reduced hippocampal volume in young women with major depression. *Psychol Med.* (2004) 34:1059–64. doi: 10.1017/S0033291703001806
53. Omura K, Constable RT, Canli T. Amygdala gray matter concentration is associated with extraversion and neuroticism. *Neuroreport.* (2005) 16:1905–8. doi: 10.1097/01.wnr.0000186596.64458.76
54. Lopez OL, Becker JT, Sweet RA, Martin-Sanchez FJ, Hamilton RL. Lewy bodies in the amygdala increase risk for major depression in subjects with alzheimer disease. *Neurology.* (2006) 67:660–5. doi: 10.1212/01.wnl.0000230161.28299.3c
55. Ananth C V, Schisterman EF. Confounding, causality and confusion: the role of intermediate variables in interpreting observational studies in obstetrics hHS public access. *Am J Obs Gynecol.* (2017) 217:167–75. doi: 10.1016/j.ajog.2017.04.016
56. Pagonabarraga J, Kulisevsky J, Strafella AP, Krack P. Apathy in Parkinson's disease: clinical features, neural substrates, diagnosis, and treatment. *Lancet Neurol.* (2015) 14:518–31. doi: 10.1016/S1474-4422(15)00019-8
57. Quaranta D, Marra C, Rossi C, Gainotti G, Masullo C. Different apathy profile in behavioral variant of frontotemporal dementia and Alzheimer's disease: a preliminary investigation. *Curr Gerontol Geriatr Res.* (2012) 2012:719250. doi: 10.1155/2012/719250
58. Le Heron C, Holroyd CB, Salamone J, Husain M. Brain mechanisms underlying apathy. *J Neurol Neurosurg Psychiatry.* (2019) 90:302–12. doi: 10.1136/jnnp-2018-318265
59. O'brien J, Taylor JP, Ballard C, Barker RA, Bradley C, Burns A, Collerton D, et al. Visual hallucinations in neurological and ophthalmological disease: pathophysiology and management. *J Neurol Neurosurg Psychiatry.* (2020) 91:512–19. doi: 10.1136/jnnp-2019-322702
60. Morey RA, Petty CM, Xu Y, Pannu Hayes J, Wagner HR, Lewis D V., et al. A comparison of automated segmentation and manual tracing for quantifying hippocampal and amygdala volumes. *Neuroimage.* (2009) 45:855–866. doi: 10.1016/j.neuroimage.2008.12.033
61. Schoemaker D, Buss C, Head K, Sandman CA, Davis EP, Chakravarty MM, et al. Hippocampus and amygdala volumes from magnetic resonance images in children: assessing accuracy of freeSurfer and fSL against manual segmentation. *Neuroimage.* (2016) 129:1–14. doi: 10.1016/j.neuroimage.2016.01.038

Conflict of Interest: The authors declare that the research was conducted in the absence of any commercial or financial relationships that could be construed as a potential conflict of interest.

frontiers in Neurology

ORIGINAL RESEARCH
published: 07 July 2021
doi: 10.3389/fneur.2021.678652

Mild Cognitive Impairment as an Early Landmark in Huntington's Disease

*Ying Zhang[1], Junyi Zhou[2], Carissa R. Gehl[3], Jeffrey D. Long[3,4], Hans Johnson[3,5], Vincent A. Magnotta[3,6], Daniel Sewell[4], Kathleen Shannon[7] and Jane S. Paulsen[7]**

[1] Department of Biostatistics, College of Public Health, University of Nebraska Medical Center, Omaha, NE, United States, [2] Department of Biostatistics, Indiana University Fairbanks School of Public Health, Indianapolis, IN, United States, [3] Department of Psychiatry, College of Medicine, University of Iowa, Iowa City, IA, United States, [4] Department of Biostatistics, College of Public Health, University of Iowa, Iowa City, IA, United States, [5] Department of Electrical and Computer Engineering, University of Iowa, Iowa City, IA, United States, [6] Department of Radiology, College of Medicine, University of Iowa, Iowa, City, IA, United States, [7] Department of Neurology, University of Wisconsin, Madison, WI, United States

OPEN ACCESS

Edited by:
Frederic Sampedro, Sant Pau Institute for Biomedical Research, Spain

Reviewed by:
Arushi Gahlot Saini, Post Graduate Institute of Medical Education and Research (PGIMER), India
Emilia J. Sitek, Medical University of Gdansk, Poland

***Correspondence:**
Jane S. Paulsen
paulsen@neurology.wisc.edu

Specialty section:
This article was submitted to Movement Disorders, a section of the journal Frontiers in Neurology

Received: *10 March 2021*
Accepted: *24 May 2021*
Published: *07 July 2021*

Citation:
Zhang Y, Zhou J, Gehl CR, Long JD, Johnson H, Magnotta VA, Sewell D, Shannon K and Paulsen JS (2021) Mild Cognitive Impairment as an Early Landmark in Huntington's Disease. Front. Neurol. 12:678652. doi: 10.3389/fneur.2021.678652

As one of the clinical triad in Huntington's disease (HD), cognitive impairment has not been widely accepted as a disease stage indicator in HD literature. This work aims to study cognitive impairment thoroughly for prodromal HD individuals with the data from a 12-year observational study to determine whether Mild Cognitive Impairment (MCI) in HD gene-mutation carriers is a defensible indicator of early disease. Prodromal HD gene-mutation carriers evaluated annually at one of 32 worldwide sites from September 2002 to April 2014 were evaluated for MCI in six cognitive domains. Linear mixed-effects models were used to determine age-, education-, and retest-adjusted cut-off values in cognitive assessment for MCI, and then the concurrent and predictive validity of MCI was assessed. Accelerated failure time (AFT) models were used to determine the timing of MCI (single-, two-, and multiple-domain), and dementia, which was defined as MCI plus functional loss. Seven hundred and sixty-eight prodromal HD participants had completed all six cognitive tasks, had MRI, and underwent longitudinal assessments. Over half (i.e., 54%) of the participants had MCI at study entry, and half of these had single-domain MCI. Compared to participants with intact cognitive performances, prodromal HD with MCI had higher genetic burden, worsened motor impairment, greater brain atrophy, and a higher likelihood of estimated HD onset. Prospective longitudinal study of those without MCI at baseline showed that 48% had MCI in subsequent visits and data visualization suggested that single-domain MCI, two-domain MCI, and dementia represent appropriate cognitive impairment staging for HD gene-mutation carriers. Findings suggest that MCI represents an early landmark of HD and may be a sensitive enrichment variable or endpoint for prodromal clinical trials of disease modifying therapeutics.

Keywords: prognosis, clinical trials, observational study, all cognitive disorders, dementia, mild cognitive impairment, Huntington's disease

INTRODUCTION

It is well-known that Huntington's disease (HD) manifests as a triad of clinical symptoms (motor, cognitive, psychiatric); however, its diagnosis continues to rely primarily on the presence of motor impairment (1). Along with a paradigm shift in other movement disorders to examine non-motor components, cognitive impairment prior to HD motor diagnosis is now widely reported (2–5). Moreover, nearly two decades of research in persons with the gene expansion for HD have documented measures of earlier disease, but none are yet accepted as endpoints for preventive clinical trials. Patients with diagnosed or manifest HD are currently undergoing Phases II and III clinical trials for gene silencing using antisense oligonucleotides (6). Phase I clinical trials targeting somatic expansion have been announced, UniQure is testing a adeno-associated virus (AAV5) vector carrying an artificial micro-RNA specifically tailored to silence the huntingtin gene and several investigators are focusing on the genome-editing technology CRISPR. This work motivates the need for additional endpoints for clinical trials in early HD.

Mild cognitive impairment (MCI) has been used to describe individuals who experience cognitive difficulties greater than expected for their age but who fall short of a diagnosis of dementia. It has generally been reported that individuals with MCI progress to dementia more rapidly than their cognitively intact peers (7–10). Despite the evidence for cognitive deterioration in HD, MCI has largely been unused as a descriptor in the HD literature. It is well-known that individuals with MCI progress to develop a wide range of diagnostic conditions (Alzheimer's disease, vascular dementia, dementia with Lewy bodies, etc.) suggesting its applicability to a wide range of neurodegenerative disease. Increasingly, MCI has been recognized as an important diagnostic consideration in other movement disorders, such as Parkinson's disease (11, 12). MCI has been commonly determined by the age- and education-adjusted cut-off values in neurocognitive tests that are 1.5 standard deviations below the mean of its control peers (7, 10). One prior study (5) looked at applying the MCI criteria in prodromal HD finding that nearly 40% of their sample of individuals with HD met criteria for MCI. A recent study (13) also investigated MCI in motor-manifest HD individuals and reported the rate of MCI as high as 90% in this cohort according to the criteria.

MCI has been utilized as a means to identify individuals at increased risk of developing neurodegenerative disease (i.e., Alzheimer's disease) to enroll in formal clinical trials (14). However, heterogeneity among those with the MCI diagnosis has presented a challenge to these clinical trials (15). As HD is caused by expansion of the trinucleotide cytosine-adenine-guanine (CAG) in the *HTT* gene (16), there is the ability to identify individuals who will develop HD prior to symptomatic presentation of the disease. Validation of earlier signs of the disease may be timely to facilitate preventive clinical trials prior to motor diagnosis.

Our analysis relies on PREDICT-HD, which is an observational study with a large cohort of individuals with the gene mutation for HD who were clinically determined to be free of motor diagnosis at study entry based on traditional motor criteria. There are two main goals of this study: the first is to classify the gene-expanded individuals as either having MCI or not based on the controls (not gene-expanded) and to examine the extent to which the classification is valid; the second goal is to estimate the timing of MCI and construct a model for the evolution of cognitive impairment over time, from cognitively-intact to MCI to dementia. The results will be informative for evaluating the extent to which MCI in HD gene-mutation carriers is a defensible indicator of early disease potentially appropriate as an endpoint in preventive trials.

MATERIALS AND METHODS

Study Design and Participants

The PREDICT-HD study was a 12-year prospective observational study at 32 sites in six countries (USA, Canada, Germany, Australia, Spain, and UK) from September, 2002 to April, 2014. The study recruited a total of 1,155 HD gene-expanded individuals and 317 controls (not gene-expanded) individuals who were mainly family members of the gene-expanded individuals. The gene-expanded individuals (CAG length >35) previously underwent independent genetic testing for the HD gene-expansions, and had diagnostic confidence level (DCL) ratings of the Unified Huntington's Disease Rating Scale (UHDRS) <4 at the study entry. Ancillary studies supported continuation of this research at a reduced number of sites ($n = 8$) through 2017. All individuals enrolled in PREDICT-HD had independently undergone predictive testing for HD and know their genetic finding. All study participants underwent annual evaluation.

Standard Protocol Approvals, Registrations, and Patient Consents

Ethical standards were reviewed at the primary grant institution and all participating sites. All participants signed a written informed consent allowing data sharing for future research. The multi-site research study is identified on ClinicalTrials.gov Identifier: NCT00051324, Neurobiological Predictors of Huntington's Disease (PREDICT-HD) and is shared in dbGaP.

Study Variables

Cognition

Since cognitive assessment was comprehensive in the PREDICT-HD study, we used previous findings to choose a smaller discrete set of cognitive tasks. Harrington et al. (17) conducted a factor analysis of 18 tests to identify latent factors that elucidated core cognitive constructs for prodromal HD. Findings showed six cognitive factors in prodromal HD including inhibition, working memory, motor planning, information integration, sensory processing, and learning memory (17). For each cognitive factor, we chose the one test outcome with the largest sample size to represent each cognitive domain: the Stroop Color Word Test (STROOP) (18) for inhibition, WAIS-III Letter Number Sequencing (LNS) (19) for working memory, paced tapping (PACE) (20) for motor planning, Symbol Digit Modalities Test (SDMT) (21) for information integration, smell identification test

(SMELL) (22) for sensory processing and the Hopkins Verbal Learning Test free recall (HVLT) (23) for learning with total observations of 7,492, 4,203, 2,547, 7,503, 4,556, and 2,505, respectively. The large variation in cognitive task frequencies is because the UHDRS cognitive assessments were administered every year whereas all other cognitive tasks were administered every other year to maximize the number of tasks piloted for sensitivity in this first-in-human multi-site prodromal HD study. Cognitive tasks were started and stopped during the 12-year study based on feasibility, psychometric principles (reliability, construct validity) participant burden, and effect size differences from controls at baseline and change over time. There were 768 prodromal HD individuals who had completed all selected cognitive measures, had MRI and longitudinal assessment. Comparison of these cognitive outcomes with other research showed that three (of four) were used in our previous MCI cross-sectional paper (5), four (of five) were used in our paper showing the best cognitive tasks for HD neuroanatomical associations using MRI (24), and all six cognitive outcomes were used in a study to examine the greatest changes over time in prodromal HD (4). These six cognitive tasks were selected for the current study to examine the clinical utility of a brief battery for clinical care and MCI diagnostics.

MRI acquisitions were collected using high resolution anatomical MR images at 32 collection sites (53 unique scanners) using General Electric, Phillips, and Siemens scanners with field strengths of 1.5 T (Tesla) or 3 T. T1 images at each site were obtained using three-dimensional (3D) T1-weighted inversion recovery turboflash (MP-RAGE) sequences. Each imaging data set was processed through data processing pipelines optimized for data harmonization across multiple sites (BAW-REF) (25). The fully automated processing includes automated landmark detection (BCD), bias field correction (BABC, BABC) (26, 27), and multi-atlas label fusion (MALF) (28).

Genetic burden was defined using the CAG repeat length by age product, or CAP (29) score, where the CAG repeat length is scaled and then multiplied by age at entry (Age_0) for each individual research participant, i.e., $CAP = Age_0 \times (CAG - 33.66)$. Thus, individuals with higher genetic burden/CAP scores are statistically nearer to motor diagnosis (29).

Severity of motor impairments was defined using the sum of the 31-item Total Motor Score (TMS) from the UHDRS (30, 31). The TMS is the sum of motor abnormalities observed during a standardized neurological examination and ranges from 0 to 124.

HD Diagnosis

A research diagnosis of HD was given by a certified motor rater trained by the Huntington Study Group (HSG) who scored each research participant on the UHDRS Diagnostic Confidence Level (DCL) (30). DCL ranges from 0 = having no motor abnormalities to 4 = >99% confident that motor abnormalities are definitive signs of HD, and DCL = 4 is the definition of motor diagnosis.

Total Functional Capacity (TFC) is a type of activities of daily living scale from the UHDRS. Specifically, the TFC is a clinician-rated measure of functional capacity based on a standardized interview with the participant and available family members of current independent functioning in these domains: finances, driving, living independently, bathing, feeding, and walking. The scale ranges from 1 to 13 and any loss in independence is considered abnormal for persons without disability.

Statistical Methods

The analysis consisted of three steps, the first being the classification of gene-expanded individuals as MCI performed at each visit, the second step was to use MCI status at baseline to predict the timing of HD onset, the third step was to demarcate stages in longitudinal cognitive decline. For the first step, a control-referenced (or norm-referenced) approach to MCI classification was used, which is in the same spirit as in the general approach often used in Alzheimer's (32), Parkinson's (33), and Huntington's disease (5, 13), but with a more advanced modeling technique to accommodate the longitudinally-collected neurocognitive test information. For each of the six cognitive variables, a linear mixed-effects model (LMEM) was fitted for the PREDICT-HD controls, adjusted for age, education years, and number of the same test that had been done prior, to obtain the age-, education-, practice effect-adjusted prognostic distribution of test values. The fitted control distribution of these test values was treated as the reference distribution for classifying gene-expanded individuals as MCI. At each visit, a gene-expanded individual was classified as MCI if their score was worse than or equal to 1.5 standard deviations below the mean of the control individuals adjusted for age, education level and practice effect. The age that the gene-expanded individual's test value crossed the adjusted cut-off the first time was defined as the age at detected MCI for that individual and for the domain represented by the cognitive variable. The detailed model derivation for the cut-off of MCI classification can be found in the Web Supporting Materials.

As a check on the validity of the classification, for each cognitive domain several baseline variables were compared between individuals with MCI and those who were cognitively intact. Comparisons of baseline variables were conducted using *t*-test for continuous variables and chi-square tests for categorical variables. At study entry, brain atrophies for prodromal HD participants in terms of percentage loss of brain volume were compared to the mean of control individuals. Several structures were considered, including caudate, putamen, globus pallidus, total gray matter, total white matter, and 95% confidence intervals were estimated. For all the comparisons, the significance level was set at 0.05.

The second step in the analysis was to formulate a prediction model for examining the ability of MCI status at baseline to predict the timing of the HD onset indicated by motor diagnosis, adjusting for covariates. All 1,155 gene-expanded individuals were used for the analysis. MCI status at study entry was coded into one of three impairment levels: 0-No; 1-Yes; 2-unknown, with the latter being due to missing observations. Flexible accelerated failure time (AFT) models with interval-censored (34) observations for HD onset were used, with adjustment variables being CAP and TMS at study entry. Interval-censoring was assumed because PREDICT-HD has annual visits and the exact time of HD onset cannot be exactly determined (e.g., conversion could happen mid-way between two visits).

Consistent with best practice, several parametric forms of the AFT were fitted, and the log-logistic AFT model (29) was found to be optimal based on Akaike's Information Criterion (AIC). The predicted median onset time of HD in years since study entry and its 95% confidence interval (CI) for any given CAP and TMS values were calculated based on the log-logistic AFT model.

The third and final step was to stage the cognitive impairment for each prodromal HD individual, based on the following taxonomy assumed to be ordered in time. Cognitively-intact: no evidence of MCI or other cognitive impairment; MCI-Single: MCI classification in only one cognitive domain; MCI-Duo: MCI classification in two cognitive domains; MCI-Multiple: MCI classification in three or more cognitive domains; dementia (DM): HD-specific dementia defined as MCI classification in any domain with at least a one-point loss on the TFC. For each interval-censored stage of cognitive impairment (left-censored if the stage was diagnosed at the first observation, interval-censored if the stage was determined in adjacent times during the follow-up, and right-censored if the stage was not able to classify at the last observation), we fitted a Weibull AFT model for the onset age using both CAG and CAG (2) as predictors because this AFT model was found to be optimal based on the AIC. We then calculated the CAG-specific median onset age and its 95% CI to ascertain the time gap between the median onset ages among the stages of cognitive impairment.

Data Availability Policy

All data, including raw and processed images, are provided in dbGaP PREDICT-HD Huntington's Disease Study: ninds-dac@mail.nih.gov.

RESULTS

In the PREDICT-HD study, the HD gene-expanded individuals had a mean age 39.9 years (SD 10.6; range 18.1–75.9), a mean education year 14.5 years (SD 2.6; range 8–20), 64.4% were women, and 97.1% were white. The control individuals were statistically a little older ($p < 0.0001$) than the HD gene-expanded individuals with a mean age 44.1 years (SD 12.1; range 19.2–83.7) and received comparable education with a mean education year 14.9 years (SD 2.4; range 9–20), though statistically different at level 0.05 ($p = 0.012$) due to large sample size. 64.8% and 98.9% of the control individuals were women and white, respectively, which were not statistically different from the gene-expanded individuals at level 0.05.

Table 1 shows the nature and frequency of the MCI classification at baseline. Among all 768 gene-mutation carriers who had complete cognitive assessment data, 411 (54%) showed MCI at baseline and 357 were cognitively intact (46%). 207 (27%) were classified with MCI in a single domain, 105 had MCI in two domains, and 99 had MCI in three or more domains.

Table 2 provides clinical and demographic data at study entry comparing gene-expanded individuals who were classified as MCI vs. those who were not (cognitively intact or pre-MCI). Individuals classified as MCI in any cognitive domain had significantly higher genetic burden (CAP) and worse motor impairment (TMS) at baseline. The most prevalent MCI was observed in information integration (31%), followed by learning (28%), and then motor planning (25%); the remaining MCIs were observed in <19% of the sample.

TABLE 1 | The frequency of MCI patterns at study entry (baseline).

MCI patterns	Frequency
Cognitively intact	357
MCI in single domain	
Inhibition	15
Working memory	18
Motor planning	63
Information integration	36
Sensory processing	35
Learning—memory	40
Subtotal	207
MCI in two domains	
Inhibition and motor planning	6
Inhibition and Information integration	7
Inhibition and sensory processing	1
Inhibition and verbal learning—memory	2
Working memory and motor planning	2
Working memory and information integration	6
Working memory and sensory processing	1
Working memory and learning—memory	6
Motor planning and information integration	21
Motor planning and sensory processing	14
Motor planning and learning—memory	11
Information integration and sensory processing	4
Information integration and learning—memory	16
Sensory processing and learning—memory	8
Subtotal	105
MCI in at least three domains	99
Total	768

MCI, Mild Cognitive Impairment.

Table 3 shows volumes and average percentage brain loss at baseline compared to the mean of control individuals (with 95% confidence intervals) for the six brain regions. Except for cerebral gray matter, MCI individuals showed significant brain atrophy in caudate, putamen, globus pallidus, and cerebral white matter at study entry relative to controls. Particularly in the regions of caudate, putamen and globus pallidus, the cognitively intact (pre-MCI) group showed 10% or more loss in brain volume on average in reference to the mean volume of controls. For individuals with any MCI diagnosis at study entry, brain atrophy was >20% loss, on average.

Supplementary Table A shows the results of the log-logistic AFT model for time to HD onset from baseline, using MCI classification, CAP, and TMS at baseline as predictors. The motor planning MCI ($p = 0.014$) had a statistically significant effect and

TABLE 2 | Summary statistics of clinical and demographic variables among MCI groups at study entry (baseline).

	Cognitively intact	MCI-inhibition	MCI-working memory	MCI-motor planning	MCI-information integration	MCI-sensory processing	MCI-learning—memory
N (% of total prodromal HD sample)	357 (47%)	130 (17%)	94 (12%)	195 (25%)	240 (31%)	145 (19%)	214 (28%)
Continuous variables							
Age							
Mean	40.3	38.7	41.3	40.8	38.6*	42.5*	40.3
SD	9.4	9.9	10.0	9.8	10.4	11.1	10.0
Range	[21.8, 72.9]	[20.3, 65.7]	[26.0, 65.6]	[18.1, 75.9]	[20.0, 67.9]	[18.1, 75.9]	[23.2, 75.0]
CAP							
Mean	316.4	379.9***	392.6**	390.9**	386.0**	391.0**	382.1***
SD	70.7	98.7	82.7	87.4	92.8	88.1	90.4
Range	[145.7, 505.5]	[168.1, 845.8]	[186.2, 652.0]	[168.1, 845.8]	[111.1, 845.8]	[119.0, 652.0]	[160.3, 845.8]
TMS							
Mean	3.3	10.1**	8.6**	7.6**	8.8**	7.9**	8.0***
SD	3.5	9.7	9.1	6.4	8.7	9.2	7.9
Range	[0, 18]	[0, 47]	[0, 44]	[0, 34]	[0, 47]	[0, 47]	[0, 44]
Categorical variable *n* (%)							
Sex							
Female	232 (65.0)	80 (61.5)	57 (60.5)	152 (78.5)**	139 (57.9)**	66 (45.5)**	100 (44.6)**
Male	125 (35.0)	50 (38.5)	37 (39.5)	43 (21.5)	101 (42.1)	79 (54.5)	113 (55.4)
Race							
White	347 (97.2)	126 (96.9)	94 (100)	192 (98.5)	236 (98.3)	139 (95.9)	207 (96.7)
Others	10 (2.8)	4 (3.1)	0 (0)	3 (1.5)	4 (1.7)	6 (4.1)	7 (3.3)

MCI, Mild Cognitive Impairment; CAP, CAG by Age Product; TMS, Total Motor Score from the Unified HD Rating Scale.
*** $p < 0.001$; ** $0.001 \leq p < 0.01$; * $0.01 \leq p < 0.05$.

contributed to prediction of HD onset above and beyond genetic burden (CAP) and motor abnormality (TMS).

For the prodromal HD individuals who were cognitively intact at baseline, 343 had follow-up observations for cognitive assessments. Among them, 48% were classified for having MCI during follow-up: 92 showed single domain MCI, 31 showed MCI in two domains and 40 had MCI in three or more cognitive domains (see **Supplementary Table B**).

Figure 1 shows the estimated median time to HD onset from baseline and its 95% confidence interval (CI) at selected values of CAP (the 25th percentile = 279.6; 50th percentile = 340.5; and 75th percentile = 394.2) and TMS (0; 1–3; >3) and TMS classification made by 0 (no motor impairment) and 3 (median value of motor impairment at study entry) by MCI group. The figure indicates that the median time tends to be shorter as TMS increases and MCI group increases in severity. For example, for those with CAP at the 75th percentile and TMS >3 at study entry, the median time to HD onset from baseline was estimated at 7.7 years (95% CI 6.2–9.2) for cognitively intact (pre-MCI), and 3.2 years (95% CI 2.3–4.0) for MCI in motor planning, information integration and others at the study entry. The non-overlapping of the 95% CIs indicates a statistically significant difference in median HD onset times between the two groups that only differ in MCI severity.

Figure 2 shows the staging results in the form of the estimated median age at onset for each stage of cognitive impairment (and its 95% CI). For brevity, we present results for CAG values between 40 and 44, based on the Weibull AFT model. Within any CAG stratum, the three MCI stages are quite separated. For example, for prodromal HD individuals with CAG values of 40, the median onset age was 51.1 years for MCI-Single (95% CI 48.9–53.2), 65.2 for MCI-Duo (95% CI 62.6–67.7), and 71.2 for MCI-Multiple (95% CI 68.3–4.1). There was much less separation for dementia (DM) and MCI-Multiple, with the CIs for each always overlapping.

DISCUSSION

Cognitive impairment has long been documented among individuals with prodromal HD (2, 4, 35, 36). Recently, a task force in the Movement Disorder Society has been formed to propose new classifications of HD that considered cognitive impairment in addition to motor disorder, and called for longitudinal ascertainment of cognitive disorder (37). As an early index event for cognitive impairment, MCI was originally defined and widely accepted in Alzheimer's disease (32), and extended to Parkinson's disease (33) and Huntington's disease (5, 13) though the concept of MCI has been controversial for Parkinson's and Huntington's diseases (38). Following the criteria of HD specific MCI (5, 13), we developed the sophisticated statistical models to identify age at MCI onset for various cognitive domains for HD gene-expanded individuals by leveraging PREDICT-HD 12-year

TABLE 3 | Summary of average percentage brain atrophy (and its 95% confidence interval) in the six selected brain regions for prodromal HD individuals with and without MCI.

MRI volumes	Control group mean	Cognitively intact	MCI inhibition	MCI working memory	MCI motor planning	MCI information integration	MCI sensory processing	MCI learning memory
Caudate	6590.5	−9.9 (−12.3, −7.6)	−20.6 (−24.7, −16.5)	−24.5 (−28.8, −20.3)	−25.4 (−28.3, −22.4)	−22.5 (−25.4, −19.6)	−21.2 (−24.9, −17.5)	−18.5 (−21.6, −15.5)
Putamen	8554.2	−11.2 (−13.4, −8.9)	−21.7 (−25.8, −17.6)	−24.5 (−28.5, −20.5)	−27.1 (−30.0, −24.2)	−23.2 (−26.1, −20.3)	−22.9 (−26.6, −19.2)	−18.6 (−21.7, −15.5)
Globus Pallidum	2765.3	−12.8 (−15.0, −10.5)	−22.2 (−26.6, −17.7)	−26.5 (−30.7, −22.2)	−29.0 (−32.0, −26.0)	−23.9 (−26.9, −20.9)	−23.2 (−27.0, −19.2)	−18.8 (−22.1, −15.5)
Cerebral Gray Matter	112116.6	0.3 (−1.4, 2.1)	−0.4 (−2.8, 2.0)	0.3 (−2.0, 2.7)	−1.1 (−3.0, 1.0)	0.6 (−1.4, 2.6)	2.6 (0.2, 5.0)	1.8 (−0.2, 3.9)
Cerebral White Matter	26074.3	−3.8 (−6.0, −1.5)	−4.5 (−7.6, −1.3)	−5.5 (−9.2, −1.4)	−8.4 (−10.7, −6.0)	−4.5 (−7.1, −1.8)	−2.8 (−5.9, 0.4)	−3.1 (−5.8, −0.4)

MRI, Magnetic Resonance Imaging; MCI, Mild Cognitive Impairment.
Values are mean differences in percentage relative to the control group (negative indicates less than control mean).

FIGURE 1 | Prediction of HD motor onset. The estimated median motor onset time from the baseline and its 95% confidence interval stratified by TMS (0, >0–3, and >3) for individuals with CAP at the 25th, 50th, and 75th percentiles.

follow-up data on neurocognitive assessments, which helped shed light on classification of early HD (37).

As a whole, our results provide biological and prognostic validity for MCI in prodromal HD. For our sample, MCI was prevalent at baseline, affecting more than half the sample. Furthermore, for those who did not have MCI at baseline, about half were classified as MCI over time. Longitudinal MCI trends suggest that gene-expanded individuals start with single-domain MCI, then develop multiple-domain MCI and eventually dementia.

The supporting evidence for the MCI classification at baseline is compelling. Compared with cognitively intact prodromal HD

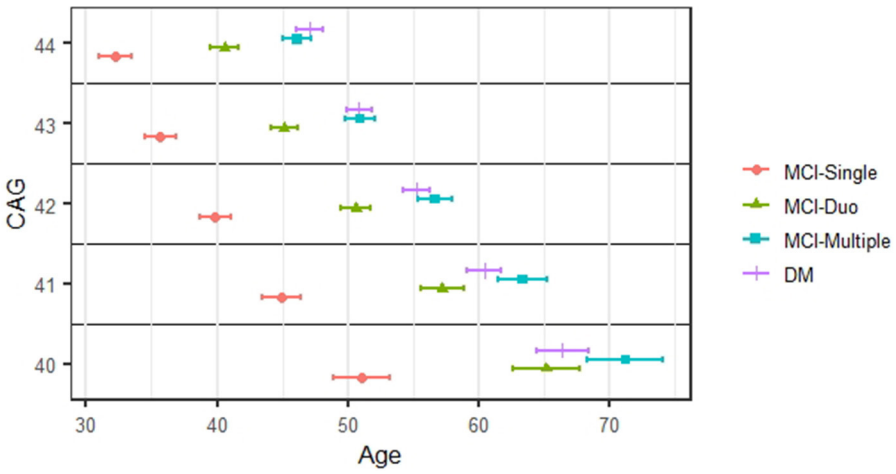

FIGURE 2 | Staging of cognitive impairment. The estimated median onset age and its 95% confidence interval for each stage of cognitive impairments.

individuals at study entry, brain atrophy was significantly worse among those who showed MCI in any of six domains. The results of brain atrophy reference to the control group shown in **Table 3** were conservative since the control cohort was a little older than the gene-expanded cohort in the PREDICT-HD study. The atrophy would be more significant should age be adjusted. Additionally, MCI was a clinically relevant prognostic marker for HD motor onset; prodromal HD individuals with MCI at study entry had earlier HD motor onset than those who were cognitively intact at study entry. Notably, for prodromal HD individuals who were classified as MCI in motor planning, brain atrophy in the basal ganglia was most severe. Prognostic validity for MCI in HD remained after adjusting for known predictors of HD onset (i.e., CAP and TMS), prodromal HD individuals with motor planning MCI at study entry had significantly elevated risk for earlier manifestation of HD motor onset when compared with their counterparts without motor planning MCI.

These findings have clinical and research implications for individuals at HD risk. First, our results support the viewpoint that MCI should be recognized as a clinically important early landmark event in the course of HD parallel to its importance in both Alzheimer's and Parkinson's diseases. Early clinical identification of MCI can facilitate future planning for individuals with HD and their families. Second, while MCI has largely been used as a means for identifying a population to enroll in clinical trials for Alzheimer's disease, the high prevalence of MCI among prodromal HD individuals and the significant biological and prognostic validity for HD diagnosis suggest that MCI has potential value as a study endpoint in clinical trials for disease modification. Finally, MCI may prove an enrichment strategy for the design of clinical trials. For example, utilizing the presence or absence of MCI within a cohort of individuals with prodromal HD could seek to reduce heterogeneity within a prodromal sample and further clarify the probable nearness to clinical onset of motor symptoms and thus formal diagnosis of HD.

Findings from this study document that 54% of the sample met criteria for MCI at study entrance, which is higher than previously published rates (5). This increase is not surprising given that the current study used all six cognition domains (vs. their use of 4 cognitive domains) identified in a large factor analysis of premanifest HD participants (17). The MCI literature emphasizes that breadth and depth of cognitive domains selected for MCI consideration can impact its detection. A research study combining the Framingham Heart Study (n = 915) with the Mayo Clinic Study of Aging (n = 1,969) suggested that though dementia incidence rates were similar across studies, heterogeneity was observed in hazard ratios and positive predictive values across cognitive domains (39). The authors concluded that the popularly-used cutoff score of−1.5 SD below the mean "represents a reasonable compromise for making the categorical diagnosis of MCI clinically meaningful (p. 1718)," though risk of future dementia is logically related to the distinct depth and breadth of cognitive assessments conducted and related depth and breadth of impairments found. The current study builds upon the earlier MCI HD study in that it provides additional documentation regarding the relationship between the classification of MCI in prodromal HD and other indicators of disease burden including basal ganglia atrophy and years to motor onset. Moreover, longitudinal assessment of MCI classification is offered. Altogether, this provides additional support for the validity of the use of MCI in prodromal HD.

Numerous clinical trials have implemented the use of MCI as a means of selecting individuals for clinical trials in Alzheimer's disease (14, 40–43). Unfortunately, to date, all have failed to show efficacy of any targeted interventions. Petersen and colleagues (15) speak eloquently regarding the probable impact of significant heterogeneity in the MCI samples contributing to these findings. In addition, they speak about the importance of consideration of endpoint measures noting that for some MCI samples with mild deficits, dementia may be too distant of an endpoint. Ultimately, they call for combined use of the

MCI diagnosis and other biomarkers to stratify and thus reduce heterogeneity in the sample.

In the consideration of clinical trials for individuals with prodromal HD, these difficulties encountered in the MCI clinical trials must be considered. The present findings are encouraging with regard to these possible prodromal HD clinical trials. First, the use of MCI as a selection tool may help to reduce heterogeneity within the prodromal sample. That is individuals with prodromal HD and MCI would reflect a group at high risk for development of the motor diagnosis of HD, particularly if used in conjunction with information regarding their CAG repeat length and age. Additionally, unlike the MCI clinical trials completed to date, the genetic nature of HD provides the opportunity to use MCI as a clinical endpoint for individuals with prodromal HD. Such a clinical trial may allow for clinical trials even earlier in the course of their disease, a goal for neurodegenerative disease clinical trials in general.

While this work constitutes a comprehensive study for MCI in prodromal HD individuals, it has limitations. Since individuals pursuing HD genetic testing, like those in this study, comprise a smaller proportion of individuals at-risk of HD (16) the PREDICT-HD sample may not represent the whole prodromal HD population. Because observations of neuropsychological tests in selected cognitive domains were not balanced in size at each study visit, replications are expected to reveal minor variations in proportions of each MCI domain, based on tasks and domains used. That is, some tests may detect fewer MCI observations in prodromal HD whereas other tasks may detect more. Further research is warranted to validate the most sensitive assessment strategy for the earliest detection and tracking of disease in HD. Though it might have been preferable to use the composite score for each of the factor score domains (17) for diagnoses of MCI, it is not possible due to the inconsistently administered cognitive assessments from PREDICT-HD and the subsequently reduced numbers of cognitive tasks being integrated into ongoing observational studies such as ENROLL. The definition of MCI in this paper did not consider any social cognition measures included in the *Diagnostic and Statistical Manual-Fifth Edition* (44) as they did not meet our sample size criteria for inclusion. Measures of social cognition in PREDICT-HD have been reported elsewhere (e.g., emotion recognition) and are likely to increase the frequencies of MCI in HD when included. It is also important to note that a high proportion of HD gene-mutation carriers display significant anosognosia through the course of HD (35), which may be highly correlated with cognitive impairment (13, 45). However, PREDICT-HD did not contain measures for subjective cognitive complaint and therefore did not allow for assessing the potential impact of anosognosia on MCI in HD. The HD community must await an appointed task force for consensus definition of HD-specific MCI for more widespread adoption in clinical and research practices.

Despite these limitations, this work provides a vivid description of cognitive change in prodromal HD and increased validation of the use of MCI in this sample. MCI occurs in over half of persons at genetic risk for HD, is associated with brain atrophy of the basal ganglia, and has prognostic validity for age at motor onset and dementia. Such information may help researchers and clinicians alike better understand and identify cognitive progression in Huntington disease.

DATA AVAILABILITY STATEMENT

Publicly available datasets were analyzed in this study. This data can be found at: National Center for Biotechnology Information (NCBI) dbGaP, https://www.ncbi.nlm.nih.gov/gap/, PREDICT-HD Huntington Disease Study (phs000222.v6.p2).

ETHICS STATEMENT

The studies involving human participants were reviewed and approved by Ethical standards were reviewed at the primary grant institution and all participating sites. All participants signed a written informed consent allowing data sharing for future research. The multi-site research study is identified on ClinicalTrials.gov Identifier: NCT00051324, Neurobiological Predictors of Huntington's Disease (PREDICT-HD). The patients/participants provided their written informed consent to participate in this study.

AUTHOR CONTRIBUTIONS

YZ and JP conceived and designed the study. YZ, JZ, and JP acquired, analyzed, or interpreted the data, and drafted the manuscript. CG, JL, HJ, VM, DS, and KS provided critical insights on intellectual content and important revision of the manuscript. YZ and JZ conducted statistical analysis. JP and YZ obtained funding to conduct this study. All authors contributed to the article and approved the submitted version.

FUNDING

This study was supported by the National Center for Advancing Translational Sciences, the National Institutes of Health (NIH; NS040068, NS105509, and NS103475), and the CHDI foundation.

ACKNOWLEDGMENTS

The authors thank the PREDICT-HD sites, the study participants, the National Research Roster for Huntington Disease Patients and Families, the Huntington's Disease Society of America, the Huntington Study Group, and the European Huntington's Disease Network.

SUPPLEMENTARY MATERIAL

The Supplementary Material for this article can be found online at: https://www.frontiersin.org/articles/10.3389/fneur.2021.678652/full#supplementary-material

REFERENCES

1. Paulsen JS, Langbehn DR, Stout JC, Aylward E, Ross CA, Nance M, et al. Detection of Huntington's disease decades before diagnosis: the Predict-HD study. *J Neurol Neurosurg Psychiatry.* (2008) 79:874–80. doi: 10.1136/jnnp.2007.128728
2. Paulsen JS. Cognitive impairment in Huntington disease: diagnosis and treatment. *Curr Neurol Neurosci Rep*. (2011) 11:474–83. doi: 10.1007/s11910-011-0215-x
3. Stout JC, Jones R, Labuschagne I, O'Regan AM, Say MJ, Dumas SM, et al. Evaluation of longitudinal 12 and 24 month cognitive outcomes in premanifest and early Huntington's disease. *J Neurol Neurosurg Psychiatry*. (2012) 83:687–94. doi: 10.1136/jnnp-2011-301940
4. Paulsen JS, Smith MM, Long JD, PREDICT-HD investigators and coordinators of the Huntington Study Group. Cognitive decline in prodromal Huntington Disease: implications for clinical trials. *J Neurol Neurosurg Psychiatry.* (2013) 84:1233–9. doi: 10.1136/jnnp-2013-305114
5. Duff K, Paulsen JS, Mills J, Beglinger DJ, Moser MM, Smith D, et al. Mild cognitive impairment in prediagnosed Huntington disease. *Neurology.* (2010) 75:500–7. doi: 10.1212/WNL.0b013e3181eccfa2
6. Tabrizi SJ, Leavit BR, Landwehrmeyer GB, Wild EJ, Chir MB, Saft C, et al. Targeting Huntingtin expression in patients with Huntington's disease. *N Engl J Med.* (2019) 380:2307–16. doi: 10.1056/NEJMoa1900907
7. Petersen RC, Smith GE, Waring SC, Ivnik RJ, Tangalos EG, Kokmen E. Mild cognitive impairment: clinical characterization and outcome. *Arch Neurol.* (1999) 56:303–8. doi: 10.1001/archneur.56.3.303
8. Winblad B, Palmer K, Kivipelto M, Jelic V, Fratiglioni L, Wahlund LO, et al. Mild cognitive impairment–beyond controversies, towards a consensus: report of the International Working Group on Mild Cognitive Impairment. *J Intern Med.* (2004) 256:240–6. doi: 10.1111/j.1365-2796.2004.01380.x
9. Petersen RC, Stevens JC, Ganguli M, Tangalos EG, Cummings JL, DeKosky ST. Practice parameter: early detection of dementia: mild cognitive impairment (an evidence-based review). report of the quality standards subcommittee of the American Academy of Neurology. *Neurology.* (2001) 56:1133–42. doi: 10.1212/WNL.56.9.1133
10. Petersen RC, Doody R, Kurz A, Morris JC, Rabins PV, Ritchie K, et al. Current concepts in mild cognitive impairment. *Arch Neurol.* (2001) 58:1985–92. doi: 10.1001/archneur.58.12.1985
11. Caviness JN, Driver-Dunckley E, Connor DJ, Sabbagh MN, Hentz JG, Noble B, et al. Defining mild cognitive impairment in Parkinson's disease. *Mov Disord.* (2007) 22:1272–7. doi: 10.1002/mds.21453
12. Wen M, Chan LL, Tan LCS, Tan EK. Mild cognitive impairment in Parkinson's disease: a distinct clinical entity? *Translat Neruodegen.* (2017) 6:24. doi: 10.1186/s40035-017-0094-4
13. Julayanont P, McFarland NR, Heilman KM. Mild cognitive impairment and dementia in motor manifest Huntington's disease: classification and prevalence. *J Neurol Sci.* (2020) 408:116523. doi: 10.1016/j.jns.2019.116523
14. Doody RS, Ferris SH, Salloway S, Sun Y, Goldman R, Watkins WE, et al. Donepezil treatment of patients with MCI: a 48-week randomized, placebo-controlled trial. *Neurology.* (2009) 72:1555–61. doi: 10.1212/01.wnl.0000344650.95823.03
15. Petersen RC, Thomas RG, Aisen PS, Mohs RC, Carrillo M, Albert MS. Alzheimer's Disease Neuroimaging Initiative (ADNI) and Foundation for NIH (FNIH) biomarkers consortium AD MCI placebo data analysis project team. randomized controlled trials in mild cognitive impairment: sources of variability. *Neurology.* (2017) 88:1751–8. doi: 10.1212/WNL.0000000000003907
16. Walker FO. Huntington's disease. *Semin Neurol.* (2007) 27:143–50. doi: 10.1055/s-2007-971176
17. Harrington DL, Smith MM, Zhang Y, Carlozzi NE, Paulsen JS, PREDICT-HD Investigators of the Huntington Study Group. Cognitive domains that predict time to diagnosis in prodromal Huntington disease. *J Neurol Neurosurg Psychiatry*. (2012) 83:612–9. doi: 10.1136/jnnp-2011-301732
18. Stroop JR. Studies of interference in serial verbal reactions. *J Exp Psychol.* (1935) 18:643–62. doi: 10.1037/h0054651
19. Scale WDWAI, Edition T. *The Psychological Corporation*. San Antonio, TX (1997).
20. Rowe KC, Paulsen JS, Langbehn DR, Duff K, Beglinger LJ, Wang C, et al. Self-paced timing detects and tracks change in prodromal Huntington disease. *Neuropsychology.* (2010) 24:435–42. doi: 10.1037/a0018905
21. Smith A. *Symbol Digit Modalities Test*. Los Angeles, CA: Western Psychological Services (1991).
22. Doty RL, Shaman P, Kimmelman CP, Dann MS. University of Pennsylvania smell identification test: a rapid quantitative olfactory function test for the clinic. *Laryngoscope.* (1984) 94:176–8. doi: 10.1288/00005537-198402000-00004
23. Brandt J, Benedict R. *Hopkins Verbal Learning Test-Revised (HVLT-R) Psychological Assessment Resources*. Lutz, FL: PAR (2001).
24. Harrington DL, Liu D, Smith MM, Mills JA, Long JD, Aylward EH, et al. Neuroanatomical correlates of cognitive functioning in prodromal Huntington disease. *Brain Behav.* (2014) 4:29–40. doi: 10.1002/brb3.185
25. Kim RE, Nopoulos P, Paulsen JS, Johnson H. Efficient and extensible workflow: reliable whole brain segmentation for large-scale, multi-center longitudinal human MRI analysis using high performance/throughput computing resources. In: *Workshop on Clinical Image-Based Procedures.* Munich: Springer (2015). p. 54–61. doi: 10.1007/978-3-319-31808-0_7
26. Kim EY, Johnson HJ. Robust multi-site MR data processing: iterative optimization of bias correction, tissue classification, and registration. *Front Neuroinform.* (2013) 7:29. doi: 10.3389/fninf.2013.00029
27. Ghayoor A, Paulsen JS, Kim RE, Johnson HJ. Tissue classification of large-scale multi-site MR data using fuzzy k-nearest neighbor method. In: *Medical Imaging 2016: Image Processing*. San Diego, CA: International Society for Optics Photonics: 97841V (2016). doi: 10.1117/12.2216625
28. Kim EY, Lourens S, Long JD, Paulsen JS, Johnson HJ. Preliminary analysis using multi-atlas labeling algorithms for tracing longitudinal change. *Front Neurosci.* (2015) 9:242. doi: 10.3389/fnins.2015.00242
29. Zhang Y, Long JD, Mills JA, Warner JH, Lu W, Paulsen JS, the PREDICT-HD Investigators and Coordinators of the Huntington Study Group. Indexing disease progression at study entry with individuals at-risk for Huntington disease. *Am J Med Genet B Neuropsychiatry Genet*. (2011) 156B:751–63. doi: 10.1002/ajmg.b.31232
30. Huntington Study Group. Unified Huntington's disease rating scale: reliability and consistency. *Mov Disord*. (1996) 11:136–42. doi: 10.1002/mds.870110204
31. Hogarth P, Kayson E, Kieburtz K, Marder K, Oakes D, Rosas D, et al. Interrater agreement in the assessment of motor manifestations of Huntington's disease. *Mov Disord.* (2005) 20:293–7. doi: 10.1002/mds.20332
32. Clark LR, Koscik RL, Nicholas CR, Okonkwo OC, Engelman CD, Bratzke LC, et al. Mild cognitive impairment in late middle age in the Wisconsin Registry for Alzheimer's Prevention Study: prevalence and characteristics using robust and standard neuropsychological normative data. *Arch Clin Neuropsychol.* (2016) 31:675–88. doi: 10.1093/arclin/acw024
33. Litvan I, Goldman JG, Tr?ster AI, Schmand BA, Weintraub D, Peterson RC, et al. Diagnostic criteria for mild cognitive impairment in Parkinson's disease: movement disorder society task force guidelines. *Mov Disord.* (2012) 27:349–56. doi: 10.1002/mds.24893
34. Chen D, Sun J, Peace KE. *Interval-Censored Time-to-Event Data: Methods and Application*. Boca Raton, FL: Chapman & Hall/CRC Biostatistics Series (2013).
35. Beglinger LJ, Nopoulos PC, Jorge RE, Langbehn DR, Mikos AE, Moser DJ, et al. White matter volume and cognitive dysfunction in early Huntington's disease. *Cogn Behav Neurol.* (2005) 18:102–7. doi: 10.1097/01.wnn.0000152205.79033.73
36. Paulsen JS, Conybeare RA. Cognitive changes in Huntington's disease. *Adv Neurol.* (2005) 96:209–25.
37. Ross CA, Reilmann R, Cardoso F. McCusker EA, Testa CM, Stout JC, et al. Movement disorder society task force viewpoint: Huntington's disease diagnostic categories. *Move Disord Clin Practice.* (2019) 6:541–546. doi: 10.1002/mdc3.12808
38. Sitek EJ. Mild cognitive impairment in Huntington's disease? *J Neurol Sci.* (2020) 413:116779. doi: 10.1016/j.jns.2020.116779
39. Knopman DS, Beiser A, Machulda MM, Fields J, Roberts RO, Pankratz VS, et al. Spectrum of cognition short of dementia: Framingham Heart Study and Mayo Clinic Study of Aging. *Neurology.* (2015) 85:1712–21. doi: 10.1212/WNL.0000000000002100

40. Petersen RC, Thomas RG, Grundman M, Bennett D, Doody R, Ferris S, et al. Vitamin E and donepezil for the treatment of mild cognitive impairment. *N Engl J Med*. (2005) 352:2379–88. doi: 10.1056/NEJMoa050151
41. Windblad B, Gauthier S, Scinto L, Feldman H, Wilcock GK, Mayorga TA, et al. Safety and efficacy of galantamine in subjects with mild cognitive impairment. *Neurology*. (2008) 70:2024–35. doi: 10.1212/01.wnl.0000303815.69777.26
42. Feldman HH, Ferris S, Windblad B, Sfikas N, Mancione L, He Y, et al. Effect of rivastigmine on delay to diagnosis of Alzheimer's disease from mild cognitive impairment: the InDDEx study. *Lancet Neurol*. (2007) 6:501–12. doi: 10.1016/S1474-4422(07)70109-6
43. Thal LJ, Ferris SH., Kirby L, Block GA, Lines CR, Yuen E, et al. A randomized, double-blind, study of rofecoxib in patients with mild cognitive impairment. *Neuropsychopharmacology*. (2005) 30:1204–15. doi: 10.1038/sj.npp.1300690
44. American Psychiatric Association. *Diagnostic and Statistical Manual of Mental Disorders, Fifth Edition*. Washington, DC: American Psychiatric Association (2013). doi: 10.1176/appi.books.9780890425596
45. Sitek EJ, Thompson JC, Craufurd DC, Snowden JS. Unawareness of deficits in Huntington's disease. *J Huntington's Dis*. (2014) 3:125–35. doi: 10.3233/JHD-140109

Conflict of Interest: The authors declare that the research was conducted in the absence of any commercial or financial relationships that could be construed as a potential conflict of interest.

frontiers in Neurology

SYSTEMATIC REVIEW
published: 05 November 2021
doi: 10.3389/fneur.2021.733570

Imaging Cognitive Impairment and Impulse Control Disorders in Parkinson's Disease

Antonio Martín-Bastida[1,2], *Manuel Delgado-Alvarado*[3], *Irene Navalpotro-Gómez*[4,5,6] *and María Cruz Rodríguez-Oroz*[1,2,7]*

[1] Department of Neurology, Clínica Universidad de Navarra, Pamplona, Spain, [2] CIMA, Center of Applied Medical Research, Universidad de Navarra, Neurosciences Program, Pamplona, Spain, [3] Neurology Service, Sierrallana Hospital-IDIVAL, University of Cantabria, Satander, Spain, [4] Cognitive Impairment and Movement Disorders Unit, Neurology Department, Hospital del Mar, Barcelona, Spain, [5] Clinical and Biological Research in Neurodegenerative Diseases, Integrative Pharmacology and Systems Neurosciences Research Group, Neurosciences Research Program, Hospital del Mar Research Institute (IMIM), Barcelona, Spain, [6] Barcelonabeta Brain Research Center, Pasqual Maragall Foundation, Barcelona, Spain, [7] IdiSNA, Instituto de Investigación Sanitaria de Navarra, Pamplona, Spain

OPEN ACCESS

Edited by:
Frederic Sampedro, Sant Pau Institute for Biomedical Research, Spain

Reviewed by:
Saul Martinez-Horta, Hospital de la Santa Creu i Sant Pau, Spain
Asuncion Avila, Hospital of Sant Joan Despí Moisès Broggi, Spain
Juan Marín-Lahoz, Hospital Universitario Miguel Servet, Spain

***Correspondence:**
María Cruz Rodríguez-Oroz
mcroroz@unav.es

Specialty section:
This article was submitted to Movement Disorders, a section of the journal Frontiers in Neurology

Received: 30 June 2021
Accepted: 28 September 2021
Published: 05 November 2021

Citation:
Martín-Bastida A, Delgado-Alvarado M, Navalpotro-Gómez I and Rodríguez-Oroz MC (2021) Imaging Cognitive Impairment and Impulse Control Disorders in Parkinson's Disease. Front. Neurol. 12:733570. doi: 10.3389/fneur.2021.733570

Dementia and mild forms of cognitive impairment as well as neuropsychiatric symptoms (i. e., impulse control disorders) are frequent and disabling non-motor symptoms of Parkinson's disease (PD). The identification of changes in neuroimaging studies for the early diagnosis and monitoring of the cognitive and neuropsychiatric symptoms associated with Parkinson's disease, as well as their pathophysiological understanding, are critical for the development of an optimal therapeutic approach. In the current literature review, we present an update on the latest structural and functional neuroimaging findings, including high magnetic field resonance and radionuclide imaging, assessing cognitive dysfunction and impulse control disorders in PD.

Keywords: impulse control disorders (ICD), Parkinson's disease dementia (PDD), mild cognitive impairment (MCI), magnetic resonance imaging (MRI), positron emission tomography (PET), single photon computed tomography (SPECT)

INTRODUCTION

Parkinson's disease (PD) is the second most common neurodegenerative disease in the world. Formerly considered to predominately be a movement disorder caused by the degeneration of dopaminergic neurons of the substantia nigra pars compacta (SNc) (1, 2). PD is now accepted to also present with non-motor features as part of the clinical manifestations. Among them, cognitive decline and neuropsychiatric alterations are highly debilitating and frequent.

In fact, the risk of developing dementia is about six times higher in PD patients than in age-and-gender matched populations (3). Importantly, within the first 10 years of PD progression, dementia appears in more than 50% of patients (4), reaching up to 80% in the long-term (3, 5). Furthermore, mild cognitive impairment is highly prevalent in PD (PD-MCI) (mean 26.7%; range 18.9–38.2%) (6–9) and is a risk factor for the development of dementia (PDD) (10). Longitudinal studies have revealed that the conversion to dementia occurs in roughly 25–50% (6, 11) of PD-MCI patients within 5 years.

The pathological basis of PDD is multifactorial, as demonstrated in post-mortem and clinical studies (12). For example, studies have reported dopaminergic neurodegeneration within the medial areas of the SNc, ventral tegmentum areas, and fronto-limbic areas (13), and neurotransmitter dysfunction in the cholinergic projections from the nucleus basalis of Meinert

as well as in the serotoninergic and noradrenergic efferent fibres from the raphe nucleus and locus coeruleus, which play an important role in cognitive dysfunction (14–16). Furthermore, alpha-synuclein deposition in the form of Lewy bodies and Lewy neuritis spreading to the amigdalar complex, hippocampus, fusiform gyrus and temporal cortex along with synergistic Alzheimer's disease (AD) pathology with beta-amyloid plaques and phosphorylated tau (neurofibrillary tangles) (17) are also critical in the pathogenesis of the cognitive decline.

Apart from cognitive impairment, psychiatric conditions are also common in PD, affecting the majority of patients during the course of the illness. The most frequent and problematic are affective disorders (depression and anxiety), psychosis (mainly visual hallucinations), apathy, and impulse control disorders (ICDs) (18). The most common ICDs experienced by PD patients include pathological gambling, binge eating, hypersexuality, and compulsive shopping, as well as other impulsive-compulsive behaviours (ICBs), such as punding, hobbyism or walkabout. To further complicate matters, approximately 14–17% of PD patients treated with dopaminergic replacement therapy, in particular with dopaminergic agonists (DA), may develop ICDs (19) although the cumulative incidence can be much higher (over 46%) (20) ICDs often result in devastating financial, legal, or psychosocial problems (19). Unfortunately the management of these behaviours, which typically involves reducing DA treatment, can be challenging and often carries the risk of motor worsening or the development of DA withdrawal syndrome (21).

The development of neuroimaging techniques, including high field structural and functional magnetic resonance (MRI) and nuclear imaging, using positron emission tomography (PET) and single photon emission computed tomography (SPECT), helps in the diagnosis and monitoring of the motor and cognitive impairments associated with PD. Furthermore, neuroimaging can be used to shed light on the underlying pathophysiological aspects of cognitive impairment and neuropsychiatric manifestations, which in turn are associated with high levels of patient disability and morbidity.

In the current review, and for the sake of brevity, we will focus on cognitive decline and ICDs in patients with PD. To this end, we conducted a literature review of existing functional and structural imaging studies in cognitive dysfunction and ICD in PD. We performed a thorough search of the PubMed database selecting for English language articles containing "Parkinson's disease dementia," "mild cognitive impairment," "impulse control disorders," "imaging," "PET," and "MRI" published up until the 15th of March, 2021. The abstracts were screened for relevance, and carefully read if they were suitable. This review highlights the imaging modalities that detect consistent brain changes associated with cognitive impairment and ICD in PD.

COGNITIVE IMPAIRMENT AND DEMENTIA

Magnetic Resonance Imaging

Grey Matter

Grey matter (GM) abnormalities have been the focus of numerous MRI studies in PD. Methodological approaches have substantially changed over the years. Analytical tools did only allow for regions of interest (ROIs) approach in early studies, which consisted of delineating certain brain areas, measuring their volume, and comparing them among different groups. This approach has been clearly overtaken by whole-brain approaches, which are able to disclose differences in GM volume without an *a priori* hypothesis. There are two main techniques, voxel-based morphometry (VBM) and surface-based analyses (SBA), both of them widely used in current studies. Whereas VBM measures GM volume, SBA is able to measure cortical thickness. As compared to VBM, cortical thickness is more sensitive to cortex changes, possibly because it is less dependent on cortical folding and the overall brain size (22). In the present review, we only include VBM and SBA studies (see **Table 1**).

Early whole-brain studies found higher levels of atrophy in PDD and PD-MCI patients compared to their cognitively normal counterparts (PD-NC) and control subjects [for review see (70, 71)], particularly in the parietal, occipital, mesial temporal, and frontal lobes, as well as in the hippocampus, amygdala, caudate, putamen, thalamus and substantia innominata. Furthermore, compared to PD-MCI patients, PDD patients exhibit GM reductions in the temporal and prefrontal areas (25), the amygdala (26), the anterior cingulate, the entorhinal and orbitofrontal cortices as well as in the parahippocampus, temporal pole, precuneus, and fusiform and lingual areas (28). A recent meta-analysis of voxel based morphometry (VBM) studies found that PD-MCI patients exhibited greater atrophy in the left anterior insula compared to PD-NC patients (35). However, PD-MCI is a heterogeneous clinical entity in which one or several cognitive domains may be affected. Therefore, the focus of the field over the last few years has been to elucidate what type of PD-MCI confers a higher risk of progression to dementia. Most studies in PD-MCI patients, who were prospectively followed and classified according to conversion (or not) to PDD, found that frontal atrophy was associated with conversion to dementia (36, 72, 73). In fact, PD-MCI patients who converted to dementia in <3 (36) or 4 years (37) had greater widespread atrophy and cortical thinning in the frontal, insular, and left middle temporal lobes at baseline than non-converters, with frontal lobe atrophy being the strongest predictor of progression to dementia (37). These findings were reinforced by a cross-sectional study showing that patients who developed PD-MCI within 2 years of diagnosis exhibited greater atrophy in the superior frontal gyrus than those with later cognitive decline (40). In addition, longitudinal studies in PD-NC patients who converted to PD-MCI patients over time showed greater GM atrophy in the frontal, parietal, and temporal areas (32), as well as in the insular cortex and caudate nucleus (29, 32, 39). Overall, the presence of frontal lobe atrophy seems to be a good predictor for cognitive decline in both PD-MCI to PDD and PD-NC to PD-MCI patients, which in turn is associated with lower cognitive scores on frontal/executive, language, and memory domains (7, 72–74).

Alzheimer's disease (AD)-related pathology is also present in cognitively impaired PD patients, specifically of the amnestic type (75). In fact, the presence of AD-related atrophy, such as hippocampal atrophy, has been described in PD patients with cognitive impairment. Previous studies have found increased hippocampal and entorhinal cortex atrophy in PDD patients

TABLE 1 | Magnetic resonance imaging studies of cognitive impairment or dementia in Parkinson's disease.

References	Population	Radioligand and technique	State	Main results/findings
Grey matter imaging				
Camicioli et al. (23)	PD-MCI PD-NC	VBM	Resting	↓ hippocampus (AD < PD-NC < PDD < HC) ↓ left hippocampus correlated with recognition memory and MMSE
Brück et al. (24)	PD-NC	VBM	Resting	↓ hippocampus and prefrontal (PD < HC) ↓ left hippocampus correlated with verbal memory ↓ prefrontal atrophy correlated with sustained attention tests
Song et al. (25)	PD-MCI PDD PD-NC	VBM	Resting	↓ bilateral temporal, left prefrontal, insular, right occipital (PDD < PD-MCI < HC) ↓ right parietal, middle frontal, insular, striatum (PDD < PD-MCI < PD-NC) ↓ PCC correlated with disease duration in PDD
Choi et al. (26)	PDD PD-MCI PD-NC	VBM	Resting	↓ substantia innominata (PDD > PD-MCI and PD-NC) ↓ substantia innominata correlates with MMSE, attention and object naming domains.
Beyer et al. (27)	PD-MCI PD-NC	VBM	Resting	↓ hippocampal volume (CA1, CA3 and subiculum area) (PD-MCI, PD-NC < HC) ↓ hippocampal volume correlated with CVLT-2 delayed free recall ↓ right hippocampal CA1 and subicular region correlated with CVLT-2 recognition score
Pagonabarraga et al. (28)	PDD PD-NC	SBA	Resting	↓ parietal, temporal, occipital areas (PDD < PD-MCI < PD-NC) ↓ temporal correlated with attentional and language deficits ↓ occipital correlated with attentional, memory and language deficits.
Lee et al. (29)	PDD PD-MCI PD-NC	VBM	Resting (Longitudinal)	↓ left prefrontal, left insular and CN (PDD converters < PD-MCI no converters) PDD converters associated with ↓ executive function, verbal memory, visual recognition memory
Filoteo et al. (30)	PD-NC	VBM	Resting	↓ medial temporal and frontostriatal areas correlated with memory deficits ↓ frontostriatal volumes correlated with executive function ↓ frontal and occipital volumes with visuospatial function
Kandiah et al. (31)	PD-NC	VBM	Resting (longitudinal)	↓ Hippocampal volume is a risk factor for PD-MCI and PDD
Wen et al. (32)	PD-NC	VBM	Resting (longitudinal)	↓ frontal areas in PDD converters ↓ frontal and parietal areas associated with global cognitive scrores
Foo et al. (33)	PD-NC PD-MCI	VBM	Resting (longitudinal)	↓ right hippocampus at baseline (PD-MCI < HC) ↓ baseline right CA1 correlated with attention ↓ CA 2-3 at follow-up correlated with episodic memory in PDD converters
Low et al. (34)	PD-NC	SBA	Resting (longitudinal)	↓ global hippocampal at baseline predicted PDD ↓subiculum and fimbria volume correlated with attention and executive functions
Zheng et al. (35)	PD-MCI PDD PD-NC	VBM	Resting (meta-analysis)	↓ left anterior insula in PD-MCI < PD-NC (predictor)
Gasca-Salas et al. (36)	PD-NC PD-MCI	SBA	Resting (meta-analysis)	↑ thinning in bilateral frontal, insular and left middle temporal areas (PD-MCI converters > PD-MCI non-converters > controls)
Chung et al. (37)	PD-MCI PDD PD-NC	SBA	Resting	↑ thinning from posterior cortical area to frontal cortex (PDD converters > PDD non-converters) ↑ thinning in right medial superior frontal and olfactory cortices distinguishes PDD converters from PDD non-converters.
Xu et al. (38)	PD-NC	VBM	Resting (longitudinal)	↓ bilateral hippocampal at baseline (PD-NC < HC) correlated with MMSE ↓ bilateral CA4, ML, GC-DG subfields, and left CA2/3 and right presubiculum subfields at follow-up (PD-MCI < PD-NC) correlated with MMSE and MOCA. .
Zhou et al. (39)	PD-MCI PDD	VBM	Resting (longitudinal)	↓right temporal at baseline and left temporal and frontal lobe at follow-up (PDD converters < non-converters)
Donzuso et al. (40)	PD-MCI PD-NC	VBM	Regional	↓ frontal gyrus, precuneus, angular gyrus, temporal lobe and cerebellum (PD-MCI < HC) ↓ frontal gyrus correlated with RCPM ↓ precuneus correlated with accuracy of Barrage ↓ Inferior frontal gyrus with Stroop test.
White matter imaging				
Kamagata et al. (41)	PDD PD-NC	DTI	Resting	↓ FA in prefrontal white matter and genu of corpus callosum (PDD < PD-NC) ↓ FA in prefrontal white matter and genu of corpus correlated with MMSE

(Continued)

TABLE 1 | Continued

References	Population	Radioligand and technique	State	Main results/findings
Hattori et al. (42)	PDD DLB PD-NC	DTI	Resting	↓ FA in bilateral in SLF; ILF, IFO, UNF, CIN, INC, CCA, CRA (DLB, PDD, PD-MCI < PD-NC and controls) ↓ FA in parietal WM areas with MMSE
Deng et al. (43)	PDD PD-MCI PD-NC	DTI	Resting	↓ FA left frontal and right temporal WM (PDD, PD-MCI < PD-NC) ↓ FA left AC and CC splenium correlated with disease duration
Meltzer et al. (44)	PDD PD-MCI PD-NC	DTI	Resting	↓ FA and ↑ MD in SLF, IFU, UNF and corpus callosum (PDD , PD-NC < HC) ↓ FA in anterior WM tracts correlated with executive function ↑ MD in anterior WM tracts correlated with global cognition deficits
Agosta et al. (45)	PD-MCI PD-NC	DTI	Resting	↓ FA in SFO, IFO UNF, genu and body of CC (PD-MCI < HC)
Auning et al. (46)	PD-MCI PD-NC AD	DTI	Resting	↓ FA in WM of temporal-parietal tracts (PD-MCI < HC). No differences PD-MCI vs AD. ↓ FA in WM prefrontal tracts with executive and visuospatial deficits.
Chen et al. (47)	PDD PD-NC	DTI	Resting	↓ FA left hippocampus (PDD < PD-HC) ↑ MD in SLF, SFO, UNF, genu of corpus callosum (PDD > PD-HC) ↓ FA in SLF, SFO and hippocampus correlated with MOCA
Bledsoe et al. (48)	PDD PD-NC	DTI	Resting	↑ MD and AD in anterior segments in CC (PDD > PD-NC) ↑ MD and AD in anterior CC associated with global and specific cognitive domains in PDD.
Chondrogiorgi et al. (49)	PDD PD-NC	DTI	Resting	↓ FA body corpus callosum, cingulum, corona radiate (PDD < PD-NC) ↓ FA and ↑ MD in limbic, prefrontal and CC tracts associated with PD-CRS
Beyer et al. (50)	PDD PD-NC	WMH	Resting	↑ WMH in deep WM and periventricular areas (PDD > PD-NC) WMH is associated with MMSE
Lee et al. (51)	PDD PD-NC AD	WMC	Resting	↑ WMH in PDD > PD-NC WMH correlated with UDPRS, MMSE and PD-CDR
Joki et al. (52)	PDD DLB PD-NC AD	WMC	Resting	↑ WMH in DLB and AD > PDD > PD-HC and HC
Huang et al. (53)	PD-MCI PD-NC	WM	Resting	WHM burden associated with PD-MCI ($p < 0.05$) besides the presence of CV risk factors Periventricular WMH burden associated with executive function and visuospatial function
Functional MRI				
Lewis et al. (54)	PD-NC PD-MCI	fMRI	Working memory task	↓activity of caudate nuclei during retrieval and manipulation. (PD-MCI < PD-NC) Underactivation of dorsolateral and ventrolateral prefrontal cortex and right putamen
Monchi et al. (55)	PD-MCI	fMRI	Card-sorting task	↓activity in tasks involving the caudate nucleus in DLPFC and VLPFC in PD ↑ activity in tasks that do not require the caudate nucleus in DLPFC and VLPFC, premotor, posterior prefrontal
Seibert et al. (56)	PDCN PDD	fMRI	Resting	No differences in FC of the DMN (PD-NC = PDD)
Baggio et al. (57)	PDCN PD-MCI	fMRI	Resting	↓ connectivity in long-range connections and increased local interconnectedness (PD-MCI < PD-NC)
Lebedev et al. (58)	PD	fMRI	Resting	Executive impairment associated with altered balance between cortical and subcortical processing at rest
Amboni et al. (59)	PD-MCI PD-CN	fMRI	Resting	↓ FC of bilateral prefrontal cortex within left F-P network (PD-MCI < PD-NC). Positive correlation between visuospatial function Z score and left prefrontal cortex ICA z score.
Baggio et al. (60)	PD-MCI PDCN	fMRI	Resting	↓ FC of the DAN with widespread, right sided, frontal/insular areas, thalami and left striatum (PD-MCI < HC) . ↓ FC less extensive, and regions of DAN itself and of the right FPN. (PD-MCI < PD-CN)
Gorges et al. (61)	PDCN PD-MCI	fMRI	Resting	↓ intrinsic FC within the DMN, the motor network, and the DAN (PD-MCI < HC) ↓ intrinsic FC preferentially in the DMN, but also in the motor, DAN, VAN, and basal ganglia-thalamic intrinsic functional networks (PD-MCI < PD-CN)

(Continued)

TABLE 1 | Continued

References	Population	Radioligand and technique	State	Main results/findings
Shin et al. (62)	PDCN PD-MCI (early/late)	fMRI	fResting	↓ FC in parahippocampal gyrus, DLPC temporal, and precuneus; ↑ FC in the inferior frontal, primary motor, and occipital areas (PD-MCI early vs PD-CN) ↓ in the medial frontal areas andcingulate cortex and ↑ FC in the parietal and occipital areas (PD-MCI (longer) vs PD-CN)
Chen et al. (63)	PDCN PD-MCI	fMRI	Resting	↓ in PCC-prefrontal cortex, left parieto-occipital juntion, and right temporal gyrus (PD-MCI < PD-CN) ↓ PCC- left inferior temporal gyrus, hippocampus, inferior parietal lobules and PCC/precuneus (PD-MCI <. HC)
Bezdicek et al. (64)	PD-CN PD-MCI	fMRI	Resting	↓ FC in bilateral superior parietal lobule and precuneus (PD-MCI < PDCN) ↓ interconnectedness of the lentiform nuclei and midcingulate cortex, precuneus, the superior parietal cortex and extended portions of the temporoparietal associative cortex bilaterally (PD-MCI < HC)
Diez-Cirada et al. (65)	PDCN PD-MCI HC	fMRI	Resting	No differences (PD-MCI vs. PDCN) ↓ internetwork FC between the somatomotor and cognitive control networks, somatomotor and visual networks, somatomotor and auditory networks, cognitive control and visual and subcortical and DMN (PD-MCI < HC).
Hou et al. (66)	PD-MCI PD-NC	fMRI	Resting	↓ activity betweem DMN and prefrontal cortex (PD-MCI < PD-CN)
Wolters et al. (67)	PDD PD-MCI PD-NC	fMRI	Resting (meta-analysis)	↓ activity in Dorsomedial prefrontal cortex (within the DMN) in PD-MCI
Fathy et al. (68)	PD-MCI PD-NC	fMRI	Resting	↓ FC of DMN and dorsal anterior insula associated with cognitive performance in PD. ↓ connectivity between dAI and ACC was associated with reduced CAMCOG scales
Pan et al. (69)	PD-MCI PD-NC	fMRI	Resting	↑ FC between dAI and superior parietal gyrus (PD-MCI vs PD-NC) correlated with memory and executive tests ↑ FC between dAI and cingulated gyrus (PD-MCI vs HC) correlated with attention/working memory, visuospatial function, and language

PD-NC, PD with normal cognition; PD-MCI, PD with cognitive impairment; PDD, PD with dementia; LBD, Lewy Body Dementia; AD, Alzheimer's disease; MMSE, Mini metal State Examination; MOCA, Montreal Cognitive Examination Test; RCPM, Raven Coloured Progressive VBM, Voxel-Based Morphometry; SBA, Surface-based approach; CVLT II, California Verbal Learning Test II; FA, fractional anisotropy; MD, mean diffusivity; AD, axial diffusivity; OCC, Occipital; SLF, Superior longitudinal fasciculus; IFL, Inferior longitudinal fasciculus; SFO, Superior frontooccipital fasciculus; IFO, Inferior frontooccipital fasciculus; UNF, Uncinate fasciculus; CIN, Cingulum; INC, Internal capsule; CCA, Corpus callosum; CRA, Corona radiata.; WMH, White matter connectivity; FC, functional connectivitiy; rs-fMRI, resting state functional magnetic resonance imaging; DMN, default mode network; DAN, dorsal attention network; VAN, ventral attention network,; DLPFC, dorsolateral prefrontal cortex; VLPDF, ventrolateral prefrontal cortex; CAMCOG, Cambridge Cognition Examination.

compared to non-demented patients (70, 71), which was associated with memory impairment (24, 27, 30). In addition, reduced hippocampal volume has been associated with the development of PD-MCI and PDD in longitudinal studies (29, 31, 76). Recent advances in analytical imaging procedures have allowed the analysis of hippocampal subfields volume, indicating that the atrophy of some regions might confer higher risk of dementia (33, 34, 38).

The association of certain gene variants and cognition and their influence on structural changes have been assessed in some studies. Among genes associated with PD, glucocerebrosidase (GBA) mutations confer the highest risk of dementia. PD patients with GBA mutations as compared to those without GBA mutations experienced a more rapid motor and cognitive decline together with a greater, earlier and faster cortical thinning in posterior parieto-occipital regions as well as frontal and orbito-frontal cortices as demonstrated in longitudinal study (77). The catechol O-methyltransferase (COMT) Val158Met polymorphism has also been associated with cognitive decline. It has been recently shown that PD patients harbouring the Val/Val genotype had widespread reduction in GM, including fronto-subcortical and parieto-temporal territories (78). Finally, microtubule-associated protein tau (MAPT) H1/H1 genotype is considered a risk factor for taupathies in addition to cognitive dysfunction in PD. In an interesting study from Sampedro et al. (79) cross-sectional and longitudinal GM reductions in parieto-temporal areas were found in PD patients with homozygous for MAPT H1 compared to PD patients not harbouring this genetic mutation.

In summary, GM atrophy occurs in the early stages of cognitive decline in PD, and steadily increases along with the progression of cognitive deficits, before broadly affecting the cortical and subcortical areas in the dementia stage. Therefore, atrophy in frontal areas and certain hippocampal subfields might lead to the development of dementia in PD and should be considered as a potential biomarker.

White Matter

Several studies have shown that fractional anisotropy (FA) is reduced and mean diffusivity (MD) is increased in the main

white matter (WM) tracts (the superior and inferior longitudinal, inferior fronto-occipital, cingulate and uncinated fasciculi, and the anterior limb of the internal capsule) of PDD patients compared to PD-NC patients or controls [for review see (70, 71)]. Similarly, PD-MCI patients exhibit less FA than PD-NC patients or controls in the inferior fronto-occipital and uncinate fasciculi corpus callosum as well as the corona radiate (42–45, 80). Interestingly, a previous longitudinal study observed higher widespread MD in patients with PD-MCI than in those with PD-NC at 18 months follow-up (81), which correlated with lower executive and attention cognitive scores. It has been suggested that WM alterations conveying a cortical-subcortical disconnection may precede GM changes in PD patients during the process of cognitive decline. Indeed, Hattori et al. found prominent WM changes in both PDD and PD-MCI patients, while concurrent GM changes were only observed in subjects with PDD (42).

The role of WM tracts in cognition is further supported by several studies reporting correlations between cognitive functions and WM abnormalities in PD-NC patients. In fact, global cognition has been shown to be correlated with low FA values in the superior and inferior longitudinal fasciculi, the inferior fronto-occipital fasciculus, the corpus callosum, the uncinated fasciculus, and the cingulum (41, 47, 82, 83). Furthermore, impairments in executive function have been consistently found to be associated with WM abnormalities in the frontal and parietal regions (46, 48, 49, 84).

Another, seemingly more imprecise, way of assessing WM integrity is detecting the presence of WM hyperintensities (WMHs), which has yielded heterogeneous results. For example, several longitudinal studies did not find any significant differences in WMHs between PD-MCI, PDD and PD-NC patients (51, 85, 86) or any association between WMHs and clinically relevant cognitive decline in studies (86). However, others studies have reported greater deep WMHs and periventricular WMHs in PDD patients compared to PD-NC patients (50–52) and in PD-MCI to PD-NC patients (68).

In summary, WM integrity is disrupted in the main tracts in PD-MCI and PDD patients. These changes might precede GM atrophy suggesting that abnormalities within key WM tracts may be the first structural changes resulting in functional asynchrony of interconnected brain regions devoted to cognitive function. The value of several WM related metrics, such as FA and MD, in the early diagnosis of cognitive decline deserve further attention.

Functional MRI

Functional connectivity (FC) studies assess regional activation of the brain or the level of dependency between two or several anatomic locations through functional MRI (fMRI) in resting state or with the execution of experimental paradigms. The default mode network (DMN) symmetrically involves the medial prefrontal cortex, precuneus, posterior cingulate gyrus, inferior parietal lobes, and lateral temporal cortices (87) and is activated during cognitively demanding tasks requiring higher-order conceptual representations (87). It is the most studied resting-state network in PD, showing enhanced activity during rest and decreased activity during experimental tasks.

Importantly, there is a clear direct association between DMN activity and cognition in PD. For example, a resting-state fMRI study (88) found that PD-NC patients displayed a positive correlation between the connectivity of their right medial temporal lobe and the DMN in the context of memory performance, as well as between the inferior parietal cortex and the DMN in visuospatial performance. A recent meta-analysis found that cognitive impairment in PD was associated with brain FC alterations, predominantly in the DMN (67). Studies in PD-MCI patients have also revealed functional hypoconnectivity of the DMN (61–63, 89, 90), which was positively associated with global cognitive function (63, 68, 91, 92). Interestingly, DMN connectivity with the occipital and posterior parietal cortical regions was found to be increased in PD-MCI patients (60), which in turn was correlated with visuospatial performance and occipital-parietal cortical thinning (57). Findings from other studies suggest that DMN connectivity abnormalities can be used to characterise PD patients, regardless of their cognitive status (66, 93), and that other resting-state networks, such as the fronto-parietal network (FPN), are more specifically linked to PD-MCI (59). Nevertheless, abnormalities in other resting-state networks, such as in the sensorimotor network (SMN) (65, 89), the ventral attention network (VAN) (94), the dorsal attention network (DAN) (64), and the salience network (SN) (69) have been found to be associated with PD-MCI, and with low cognitive performance in PD patients (54, 58, 95). However, differences in pre-processing and analysis methods as well as in the PD-MCI criteria may explain the heterogeneity of these results.

Importantly, fMRI task-based studies have shown that PD-NC patients demonstrate weaker recruitment of several areas, including the anterior cingulate cortex, caudate, putamen, and left precentral gyrus as well as the medial, dorsolateral and ventrolateral prefrontal cortices during working memory or executive function tasks (55, 96, 97). However, those changes are also found in PD-MCI patients, hence they may be associated with the presence of executive dysfunction (54).

Recognition memory is typically impaired in patients with dementia (98). fMRI while performing a verbal memory paradigm PD patients showed a weaker deactivation than controls in the inferior orbitofrontal and temporal cortices that correlated with verbal recognition memory (99).

In conclusion, an altered pattern of resting FC in the DMN seems to be associated with cognitive impairments in PD, which in turn is associated with posterior cortical cognitive deficits that eventually progress to dementia. Functional brain changes might precede structural abnormalities and thus, the value of fMRI in early diagnosis is a promising tool to be considered in further studies.

Nuclear Imaging

Brain Glucose Metabolism

Several [18F] fluoro-D-glucose ([18F]FDG) PET studies with PD-MCI patients show reduced frontal, temporoparietal, occipital and precuneal metabolism as well as the caudate nucleus compared to healthy controls, and in less degree to PD-NC (100–104), being regional hypometabolic changes more

marked in multi-domain PD-MCI patients than in single-domain (103). Furthermore, extensive areas of hypometabolism, mostly affecting the posterior cortical regions, including the parieto-occipital, associative parietal, and inferior temporal cortices (102) and to a lesser degree, the striatum and prefrontal cortex (101, 104, 105), have been observed in PDD patients when compared to controls, PD-NC and PD-MCI (see **Table 2**).

Several longitudinal studies have assessed the progression of regional metabolic changes in PD with cognitive dysfunction (100, 107, 108). The aforementioned studies showed severe bilateral hypometabolism in parieto-occipital areas, especially within the visual association cortex (Broadman area 18) and posterior cingulate cortices (100), as well as the fusiform gyrus (107), predicting cognitive decline after more than 2 years follow up, thus heralding the conversion from PD-NC and PD-MCI to PDD.

The role of regional hypometabolism in cognition is further supported by several studies reporting correlations between memory and visuospatial functions in the posterior temporal and parietal regions and also with attentional, executive, and language functions in the frontal regions in patients with PD-MCI and PDD (101, 144). Furthermore, in a prospective study (145) found that the association between reduced regional metabolism in temporoparietal and occipital areas and the presence of visual hallucinations in linked with the conversion from PD-NC to PDD.

Using voxel-based spatial covariance analysis of FDG imaging, previous studies described the presence of a *PD cognition-related pattern* (PDCP) (106) consisting of hypometabolism in the medial prefrontal, premotor, precuneus, and parietal association areas. This pattern increased over time along with cognitive decline (146), and was associated with dopaminergic denervation in the nucleus caudate (116), as well as with executive and memory performance in PD-MCI patients (106). The expression of PDCP has been considered as a potential imaging biomarker for cognitive dysfunction in PD, although its prognostic value is yet to be ascertained (147).

The relationship between cerebral metabolism and atrophy displays dissociable patterns along cognitive impairment in PD, with regional hypometabolism preceding spatially matching structural atrophy areas (105). Thus, in PD-MCI patients, areas with hypometabolism exceed atrophy in the angular gyrus, occipital, orbital, and frontal lobes, however in PPD patients; these hypometabolic areas are replaced by atrophy and widespread cortical and subcortical reductions in metabolism is observed surrounding the atrophy areas. This indicates that there is a specific gradient of severity in cortical changes as cognitive dysfunction progresses in PD, with atrophy lagging behind hypometabolism as the pathological stages continue.

In conclusion, changes in brain glucose metabolism are present at the early stages of cognitive impairment in PD with hypometabolism in posterior parieto-occipital areas in PD-MCI, which steadily extends to the frontal and subcortical areas in PDD. Hypometabolism in the posterior cortex may point to the development of dementia in PD, representing an earlier step to grey matter atrophy.

Dopamine

Several studies have suggested that cognitive dysfunction in PD is partially based on striatal dopaminergic degeneration, which leads to dysfunction of the frontostriatal pathways (109, 110, 114, 115). In fact, studies have found that PDD and in less degree PD-MCI patients have a greater striatal dopaminergic deficit than PD-NC patients, as assessed with either ^{123}I Ioflupane FP-CIT SPECT (110, 114) or ^{18}Flurodopa (F-Dopa) PET (109, 111).

In particular, higher dopaminergic denervation in the caudate nucleus has been found to be associated with dysfunction in working memory, attention, and verbal fluency (109, 112–114) in both PDD and PD-MCI patients. Importantly, the associative fronto-striatal circuitry (orbitofrontal and dorsolateral prefrontal cortices) is known to be modulated by caudate dopaminergic signalling in PD patients suffering from executive dysfunction (115). Dopamine transporter (DAT) binding in the caudate nucleus is associated with the expression of the *PD-related cognitive pattern* (PDCP) (116), highlighting the importance of nigral dopaminergic input in the caudate nucleus and its cognitive functioning in PD. According to previous studies, reduced DAT availability in the caudate nucleus may be used as a potential predictor of cognitive dysfunction in PD (148), but only when combined with other diagnostic biomarkers in a multiple regression analysis including CSF ($A\beta_{42}$ to t-tau ratio) and non-motor clinical scales (Montreal Cognitive Assessment (MoCA) and University of Pennsylvania Smell Identification Test (UPSIT) scores).

Dopaminergic depletion in extrastriatal areas derived from mesocortical and mesolimbic projections is also involved in the cognitive dysfunction associated with PD. For example, previous studies have found that frontal areas, including the anterior cingulate cortex (ACC) and middle frontal gyrus as well as the caudate nucleus, displaying reduced dopaminergic F-dopa-PET uptake in patients with PDD (109, 111, 112) when compared to PD-NC and controls. Moreover, the dopaminergic reduction in frontal areas shows inverse correlation with executive and attentional dysfunction in PDD (109).

Furthermore, the availability of post-synaptic dopaminergic D2 tracers such as ^{11}C Raclopride is found to be decreased along the mesolimbic and mesocortical areas in patients with PDD compared to PD-NC and controls (117). In contrast, reduced availability of D2 receptors is showed in bilateral insula, ACC and parahippocampal giry in patients with PD-MCI when compared to PD-NC (118), being in turn associated with executive and memory deficits.

The relationship between striatal dopaminergic degeneration and cortical degeneration is of special interest in PD. In a multimodal study, Sampedro et al. (149) showed that dopaminergic loss in caudate nucleus in early stage PD patients as measured with DAT is associated with reduced cortical thickness in both frontal, temporal and posterior cortices in cross-sectional and longitudinal cohorts, which in turn are associated with neuropsychological deficits. Previous results are important to remark as reduced caudate DAT uptake as well as cortical thickness in temporo-parieto-occipital areas in PD-NC patients could potentially predict the conversion to PD-MCI (70).

TABLE 2 | Radionuclide imaging studies of cognitive impairment or dementia in Parkinson's disease.

Studies	Population	Radioligand and technique	State	Main results/findings
Glucose metabolism				
Huang et al. (106)	PD-MCI PD-NC	PET FDG	Resting	↓ posterior cortical prefrontal and parietal (PD-MCI < PD-NC ↑metabolism in brainstem and cerebellum (PD-MCI > PD-NC) Expression of PDCP ($p > 0.05$)
Hosokai et al. (102)	PD-MCI PD-NC	PET FDG	Resting	↓ posterior cortical regions (temporo-parieto-occipital junction) (PD-MCI < PD-NC, HC)
Pappatá et al. (104)	PD-MCI PD-NC	PET FDG	Resting	↓ prefontal, parietal, associative cortices and striatum (PD-MCI < PD-NC, HC)
Bohnen et al. (100)	PDD PD-NC	PET FDG	Resting (Longitudinal)	↓ caudate, occipital PCC and associative visual cortex (BA 18) in PDD < PD-NC and HC) baseline. ↓ follow up at thalamus, PCC, occipital, parietal and frontal in (PDD < PD-NC).
García-García et al. (86)	PDD PD-MCI PD-NC	PET FDG	Resting	↓ frontal and parietal (PD-MCI < PD-NC); ↓ arietal, temporal and occipital (PDD < PD-MCI) Executive function correlated with parieto-temporo-occipital and frontal metabolism; memory correlated with temporo-parietal metabolism; visuospatial correlated with parieto-temporo-occipital metabolism; Language with frontal metabolism
González-Redondo et al. (105)	PDD PD-MCI PD-NC	PET FDG VBM	Resting	↓ metabolism > atrophy in angular gyrus, occipital, orbital and frontal lobes (PD-MCI > PDD) ↓ metabolism areas replaced by atrophy with widespread hypometabolism (PDD > PD-MCI)
Tard et al. (107)	PDD PD-NC	PET FDG	Resting (Longitudinal)	↓ follow up metabolism bilateral precuneus, left temporal and fusiform gyrus (PDD < PD-NC)
Baba et al. (108)	PDD PD-MCI PD-NC	PET FDG	Resting (Longitudinal)	↓ follow up metabolism bilateral parieto-occipital cortices (PDD < PD-MCI and PD-NC)
Dopaminergic imaging				
Rinne et al. (109)	PD-NC	PET [^{18}F]fluorodopa	Resting	Put, CN and Frontal cortex (PD < HC) ↓FDOPA in CN correlated with Stroop interference task ↓FDOPA in Frontal cortex correlated with digit span, verbal fluency and recall tests.
Walker et al. (110)	PD-NC DLB AD	SPECT [^{123}I]FP-CIT	Resting	Put, CN (PD, DLB < AD, HC)
Ito et al. (111)	PD-NC PDD	PET [^{18}F]fluorodopa	Resting	CN, VS and ACC (PDD < PD-NC, HC) ↓DaT in CN correlated with MMSE
Nagano-Saito et al. (112)	PD-NC	PET [^{18}F]fluorodopa PET FDG	Resting	RCPM score positively correlated with the FDOPA Ki in the left hippocampus and ACC
Van Beilen et al. (113)	PD-NC	PET [^{18}F]fluorodopa	Resting	↓FDOPA in CN correlated with executive, memory and language composite scores
Nobili et al. (114)	PD-NC ET	SPECT [^{123}I]FP-CIT	Resting	Caudate and right putamen (PD-NC < ET) ↓DaT in CN correlated with executive score deficits
Polito et al. (115)	PD-NC	SPECT [^{123}I]FP-CIT PET FDG	Resting	↓DaT in CN correlated with verbal fluency performance ↓DaT in CN modulates hypometabolism in ACC and DLPFC
Niethammer et al. (116)	PD-NC	SPECT [^{123}I]FP-CIT PET FDG	Resting	Correlation of DAT CN uptake and PDCP expression
Sawamoto et al. (117)	PD-NC	PET [^{11}C]-raclopride PET FDG	Resting	↓ RAC binding in ACC and MPFC in PD ↓ dopamine release in CN in PD in working memory task
Christopher et al. (118)	PD-MCI PD-NC	[^{11}C]FLB 457 PET [^{11}C]-DTBZ PET	Resting	↓ D2 binding in salience network PD-MCI < PD-NC ↓ D2 binding in PHG and insula correlated with memory performance ↓ D2 binding in ACC and insula correlated with executive function
Cholinergic imaging				
Bohnen et al. (119)	PDD PD-NC LBD	[^{11}C]-PMP AChE	Resting	↓Global cortical AChE of 12.9% in PD-NC, 19.8% in PDD < HC

(Continued)

TABLE 2 | Continued

Studies	Population	Radioligand and technique	State	Main results/findings
Hilker et al. (120)	PDD PD-NC	[^{11}C]-MP4A AChE	Resting	↓Global cortical AChE of 29.7% in PDD and 10.7% in PD-NC < HC) ↓AChE in left inferior parietal lobule, precentral gyrus, and right PCC (PDD < PD-NC)
Gilman et al. (121)	PD-NC	[^{11}C]-PMP AChE	Resting	↓Global cortical AChE of 15.3% (PD-NC < HC) Regional reductions mainly located in temporal, parietal,occipital cingulate cortices as well as amygdala and hippocampus.
Klein et al. (122)	PD-NC PDD LBD	[^{11}C]-MP4A AChE ^{18}F Fdopa ^{18}FDG PET	Resting	↓Global cortical AChE of 22.6% in PD-NC, 33.2% in PDD < HC Global cortical reductions from frontal to occipital areas PDD < PD-NC and HC
Kotagal et al. (123)	PD-NC PDD LBD	^{11}C]-PMP AChE	Resting	↓thalamic AChE of 12.8% in PD-NC, 19.8% < HC
Shimada et al. (124)	LBD AD	[^{11}C]-MP4A AChE	Resting	↓Global cortical AChE of 27.8% (LBD<AD) Regional reductions mainly located in temporal, parietal, occipital, cingulate cortices (in order of reduction)
Meyer et al. (125)	PD-NC PD-MCI	[^{18}F]-Fluoro-A-85380	Resting	↓Global cortical and subcortical α4β2*-nicotinic acetylcholine receptor PD-MCI <PD, Regional reductions in hippocampus, amygdala, cerebellum, thalamus, and putamen
Colloby et al. (126)	DLB AD	[123I]-5-IA-85380	Resting	↓Global cortical and subcortical nicotinic acetylcholine receptor in left frontal gyri and ACC DLB < AD ↓Global nicotinic acetylcholine receptor correlated with executive tasks.
Protein deposition				
A. Amyloid				
Edison et al. (127)	PDD LBD PD-NC	[^{11}C]PIB-PET	Resting	Amyloid positive were found in PDD (2/12) and DLB (11/13) when compared to PD-NC and healthys Regional amyloid deposition in associative, cingulate cortices and striatum
Jokinen et al. (128)	PDD PD-NC	[^{11}C]PIB-PET FDG PET	Resting	No differences in amyloid deposition
Gomperts et al. (129)	PD-MCI PD-NC	[^{11}C]PIB-PET	Resting	No differences in amyloid deposition in precuneus at baseline (PD-NC = PD-MCI) ↑PiB retention in precuneus at baseline predicted a greater risk of conversion to PDD.
Petrou et al. (130)	PDD PD-MCI LBD PD-NC	[^{11}C]PIB-PET	Resting (meta-analysis)	PiB-positive prevalence: - DLB group: 0.68 (95% CI, 0.55-0.82) - PDD group: 0.34 (95% CI, 0.13-0.56) - PD-MCI and PD-NC groups:0.05 (95% CI, −0.07-0.17)
Shah et al. (131)	PD-NC	[^{11}C]PIB-PET	Resting	↑cortical (37%) and striatal (16%)-amyloid deposition (PD > HC) Combined presence of striatal and cortical amyloid associated with lower cognitive z score
Ahktar et al. (132)	PD-MCI PD-NC	[^{18}F]-florbetapir	Resting	Amyloid-positive scans do not help for diagnosis of PD-MCI ↑ amyloid in PCC correlated with verbal memory performance ↑ amyloid in precuneus, frontal cortex and ACC correlated with naming perfomace
Fiorenzato et al. (133)	PD-NC	[^{18}F]florbetaben	Resting	Amyloid positive 10/48 (21%) in PD Regional amyloid deposition in cortical and subcortical areas associated with reduced MOCA and SDMT
Melzer et al. (134)	PD-MCI PDD PD-NC	[^{18}F]florbetaben	Resting	No differences in amyloid deposition (PD-NC = PD-MCI = PDD) Absence of clinical associations
Na et al. (135)	PDD	[^{18}F]florbetaben	Resting	Amyloid positive were found in PDD (4/23) ↑ amyloid correlated with executive function
Biundo et al. (136)	PDD PD-MCI LBD PD-NC	[^{18}F]flutemetamol	Resting	Amyloid positive was 50% in PD and 50 % in LBD at baseline ↑ amyloid associated with reduced MOCA, MMSE, executive and language scores At follow-up there amyloid was associated with dementia.

(Continued)

TABLE 2 | Continued

Studies	Population	Radioligand and technique	State	Main results/findings
B. Tau				
Gomperts et al. (137)	PDD LBD PD-NC	[^{18}F]T807 PET [^{11}C]PIB-PET	Resting	↑ cortical tau in inferior temporal gyrus and precuneus (PDD, LBD > PD-NC) ↑ cortical tau in inferior temporal gyrus correlated with MMSE and CDR
Kantarci et al. (138)	DLB AD	[^{18}F]T807 PET [^{11}C]PIB-PET	Resting	↑ cortical tau in medial temporal cortex (AD > DLB) ↑ cortical tau in posterior temporoparietal and occipital cortices (DLB > AD)
Buongiorno et al. (139)	PD-NC PDD	[^{18}F]-FDDNP	Resting (longitudinal)	↑ cortical tau in lateral temporal cortices in PD-NC with longitudinal progression to PDD
Neuroinflammation				
A. Microglial activation				
Edison et al. (140)	PDD PD-NC	[^{11}C](*R*)PK11195-PET [^{11}C]PIB-PET FDG-PET	Resting	↑ microglial activation in ACC, PCC, frontal, temporal, pariental cortices and striatum (PDD > PD-NC and HC)
Fan et al. (141)	PDD AD	[^{11}C](*R*)PK11195-PET FDG-PET	Resting	↑ microglial activation correlated with MMSE in AD and PDD
Femminela et al. (142)	PDD AD	[^{11}C](*R*)PK11195-PET FDG-PET	Resting	↑ microglial activation in hippocampal/parahippocampal areas were associated with cortical atrophy and metabolism in PDD and ADD.
B. Astroglial activation				
Wilson et al. (143)	PD-NC	[^{11}C]-BU99008 PET	Resting	↓ astroglial expression in posterior cortical and subcortical areas in PD with moderate-advanced stages Astroglial expression correlated with MOCA in moderate-advanced PD.

PD-NC: PD with normal cognition; PD-MCI: PD with cognitive impairment; PDD: PD with dementia; LBD: Lewy Body Dementia; AD: Alzheimer's disease; ET: essential tremor; PET: positron emission tomography; SPECT: single-photon emission computed tomography; PDCP: Parkinson's disease cognitive pattern; DAT: dopamine transporter; AAC: anterior cingulate cortex; PCC: posterior cingulate cortex, CN: caudate nucleus; Put; Putamen; VS: ventral striatum; DLPC: dorsolateral prefrontal cortex; MPFC: medial prefrontal cortex; PHG: parahyppocampal gyrus; MMSE: minimental test of Folstein; MOCA: Montreal cognitive assessment test; SMDT; symbol Digit Modalities Test; CDR: clinical dementia rating; RCPM; Raven's coloured progressive matrices.

In summary, dopaminergic depletion in the caudate nucleus, as well as in the extrastriatal mesocortical and mesolimbic areas, are associated with the progression of cognitive decline in PD. Furthermore, reduced caudate dopaminergic function may be a surrogate marker of cognitive decline in PD, but first and foremost, this deficit indicates the presence of executive dysfunction.

Acetylcholine Activity

Cholinergic transmission from the basal forebrain and brainstem (nucleus basalis of Meynert and pedunculo-pontine nucleus, respectively) has been found to be reduced in PD patients (150), suggesting that it plays a relevant role in cognitive dysfunction (150).

Several radioligands that bind the vesicular acetylcholine transporter, analogues of the acetylcholinesterase, and post-synaptic nicotinic and muscarinic receptors have been assessed using SPECT and PET techniques (151).

Patients with PDD and PD-MCI show a significant cortical reduction of cholinesterase activity in the temporal, occipital, parietal, frontal, and anterior cingulate cortices (119, 121, 123, 124), as well as in the amygdala and thalamus (121, 123), compared to PD-NC patients. Interestingly, loss of cortical cholinesterase activity may also occurs in early stages of the disease in *de novo* PD-NC patients showing significant (12%) losses in the medial occipital cortex (121) when compared to healthy controls. In addition, reduction of acetylcholinesterase activity in PDD patients is associated with poorer performance in global cognition (152) as well as working memory and attention deficits (151) but not with the severity of motor symptoms.

Furthermore, significant changes in post-synaptic Ach receptors have been found parallel cognitive dysfunction in PD patients (151). PD-MCI had reduced binding of nicotinic receptors in the thalamus, temporal and parietal cortices as well as hippocampus when compared to PD-NC and healthy controls, which in turn was associated with the severity of the cognitive deficit when measured with global cognitive scales (125). Importantly, post-synaptic cholinergic receptors may display compensatory increase, no change, or a decrease probably due to degeneration of non-cholinergic systems, such as noradrenergic and serotoninergic systems, to which these receptors are coupled (153) which has to be taken into account in the interpretation of the findings.

It is important to note that both dopaminergic and cholinergic dysfunction provide divergent contributions to cognitive dysfunction in PD according the "dual-syndrome" hypothesis (154). In fact, multi-radiotracer studies (120, 122) have showed cholinergic denervation and glucose hypometabolism is present in the neocortex from the frontal to the occipital areas in PDD patients, as well as minimal cholinergic denervation in PD-NC patients, compared to controls. On the other hand, dopaminergic denervation in the striatum, limbic, and associative cortices is

found in both PD-NC and PDD. The relationship between cortical cholinergic loss and striatal dopaminergic denervation in PDD suggests that cognitive decline in PD appears when the disease spreads from SNc neurons to the cortex, hence the presence of cholinergic dysfunction facilitates the appearance of cognitive decline in PD.

In conclusion, cholinergic imaging in PD patients suffering from cognitive impairments offers an interesting approach for understanding the pathophysiological aspects of PD, especially when used in combination with dopaminergic and glucose tracers.

Protein Deposition Imaging

β-Amyloid

The development of β-amyloid specific tracers using ^{11}C-Pittsburg compound B (PiB) and other radiotracers (^{18}F-Florbetaben and ^{18}F-Florbetapir) have provided a means for measuring *in vivo* amyloid pathology. To date, several studies have reported heterogeneous results in PDD and PD-MCI patients, taking into account "amyloid positivity" as AD-range of cortical amyloid deposition with PET imaging using PiB. Some studies observed the complete absence of amyloid (127, 128, 134) while others showed mild to moderate amyloid deposition (130, 131) in PDD and PD-MCI patients compared to controls.

Importantly, due to the small sample size of the studies, a meta-analysis (130) found substantial variability of PiB positive results in PD patients with cognitive impairment, with higher levels of binding in patients with Lewy body dementia than in patients with PDD and PD-MCI compared to controls.

Cross-sectional and longitudinal amyloid PET studies show significant associations between cortical amyloid load and global cognitive decline as well as executive dysfunction in PDD patients (133, 135) with respect to PD-NC and controls. However, other studies have observed an association between memory performance with amyloid load in PDD patients (132). One longitudinal PET study (129) found that baseline amyloid binding predicted the severity of cognitive dysfunction over time in PD-NC. Furthermore, a recent prospective amyloid PET study (136) reported that cortical amyloid deposition in PDD and Lewy body dementia is associated with global cognitive deficit as well as language and attention-executive dysfunction when compared to PD-MCI and PD-NC. Interestingly, Shah et al. showed that the combination of amyloid deposition in the striatum and cortex is associated with greater cognitive impairment than amyloid deposition only in the cortex (131).

In summary, although β-amyloid deposition as measured by PET is not always observed in the brain of PDD patients, its presence may predict the presence of cognitive decline and dementia over time.

Tau

The recent development of selective and high affinity radioligands capable of binding to tau, such as ^{18}F-AV-1451, has paved the way for the assessment of tau deposition in PD patients with cognitive impairment. A cross-sectional study by Gomperts et al. found that increased ^{11}F-AV-1451 binding was present in the precuneus and inferior temporal gyrus only in patients with PDD, which in turn was associated with an impairment in global cognitive scales (137).

To date, a few double tracer studies have examined the co-pathology between amyloid and tau in PD. The presence of tau deposition in the posterior cortical areas is in line with previous studies reporting global β-amyloid deposition in PDD patients, compared to those with PD-NC (138). In addition, a previous study found that tau binding was increased in patients with Aβ-positive scans compared to those with Aβ-negative scans, suggesting that tau and β-amyloid deposition display parallel patterns of deposition. Interestingly, in this study (155) tau deposition did not differ in PD-NC, PD-MCI patients, and normal controls.

A longitudinal PD study (139) using another radiotracer (^{18}F-FDDNP) that binds both amyloid and tau, reported increased baseline lateral temporal binding in PD-NC patients who eventually progressed to PDD, suggesting that the basal deposition of tau and amyloid is associated with poorer future cognitive function in PD.

Although, to date, only a few imaging studies have measured tau deposition in PD, their findings suggest that it is increased in PDD patients; whereas, they found tau deposition to be relatively absent in PD-MCI and PD-NC patients. In addition, cortical tau deposition is higher with concomitant β-amyloid deposits, indicating the feasibility of detecting *in vivo* co-pathology of protein deposition as demonstrated in post-mortem studies (17).

Neuroinflammation Imaging

Neuroinflammation has been reported to be associated with the loss of dopaminergic neurons in the SNc of PD patients (156). Microglial cells can structurally and functionally change when they are activated by the presence of diverse agents, such as oxidative stress, α-synuclein protein aggregation, and neurodegeneration (157). It is thought that activated microglia may display a dual role, both protective and deleterious, thus enhancing the chronic neuroinflammatory process (156). However, whether the progressive neurodegeneration is associated with increased activation of microgliosis remains unclear (158). Nevertheless, post-mortem studies have observed increased microglial activation in the limbic and cortical regions of PDD patients (159). Thus, *in vivo* measurements of microglial activation have begun to be pursued over the last few years.

Importantly, the expression of mitochondrial translocator protein (TSPO) is known to be associated with microglial activation. In fact, first generation TSPO tracers, such as ^{11}C-(R)PK11195, have revealed increased cortical binding in PDD patients predominating in the posterior cortical regions, which is associated with reduced cortical metabolism, as measured with 18F-FDG, and with low global clinical cognitive performance (140, 141). Microglial activation has also been shown to be correlated with cortical atrophy in the hippocampus and parahippocampus in PDD patients (142). Due to the non-specific binding of ^{11}C-(R) PK11195, new second-generation TSPO radioligands have been developed, including ^{11}C-DPA713 and ^{18}F-FEPPA. However, to date, there have been no studies using these second-generation TSPO ligands to assess cognitive decline in PD (160, 161).

Astrocytes are the most abundant glial cells in the brain. Similar to microglia, astrocytes change in function and number in the presence of oxidative stress, neurodegeneration, and other factors (162). However, little is known about the role of astrogliosis and the development of cognitive impairment in PD.

Imaging of glial fibrillary acidic protein (163), an astrocytic intermediate filament, with ^{11}C-BU990088 (143) revealed widespread binding in the brainstem and cortex in early PD-NC patients compared to controls. In the same study, patients with moderate-late stage PD were observed to have reduced astrocyte expression in the posterior cortical and subcortical areas. They also found that glial fibrillary acidic protein expression was positively associated with global cognitive scores, suggesting a neuroprotective and compensatory mechanism of astroglial activation.

Due to the small number of microglial imaging studies, as well as the lack of specificity of the radiotracers used, the possible role of microglial activation in the cognitive dysfunction associated with PD remains unknown. Similarly, the involvement of astroglial activation in PD is beginning to emerge (164). The recent development of new TSPO radioligands and astroglial tracers will allow researchers to study the role of glial cells in the cognitive decline associated with PD more effectively.

NEUROIMAGING OF IMPULSE CONTROL DISORDERS IN PATIENTS WITH PARKINSON'S DISEASE

Magnetic Resonance Imaging

Grey Matter

Whole brain studies using VBM and SBA have also been undertaken in PD patients suffering from abnormal impulsivity. There is some evidence pointing towards higher cortical thickness in PD patients with ICD (PD-ICD) in the ACC, rostral pole and OFC compared to PD patients without ICD (PD-nonICD) (165–167). However, other studies have shown reduced cortical thickness in PD-ICD patients in the inferior frontal gyrus and pars orbitalis (168, 169) or a lack of corticometric changes between PD patients with or without ICD (170, 171). In a prospective study (172) found a small area of increased atrophy the anterior limb of the left internal capsule adjacent to the left caudate nucleus in PD-ICD when compared to the PD-nonICD, with no other significant cortical changes. Interestingly, Tessitore et al. (167) described positive correlations between cortical thickness in the ACC and OFC and ICD severity scores (see **Table 3**).

In summary, morphometric studies have not yet reached conclusive results in PD-ICD patients although it might be that changes in grey matter volume are associated with lack of inhibition related to ICD behaviours in PD.

White Matter

Diffusion tensor imaging (DTI) tractography studies have reported widespread WM tract damage in PD-ICD. In particular, increased radial and axial diffusivity of the genu of corpus callosum, uncinate fasciculus, parahippocampal and pedunculopontine tracts in PD-ICD patients as compared to PD-nonICD and controls, regardless of depression and apathy severity (169, 173–175). However, a recent study found that although PD-ICD patients had increased FA in several WM tracts, the WM regions known to be involved in reward- related behaviours were preserved (173).

In summary, only few DTI studies are available in the literature, thus future diffusional imaging studies are needed in order to ascertain the role of WM integrity in ICD.

Functional MRI

Resting fMRI studies in PD-ICD patients have observed reduced or enhanced activation in regions known to support cognitive control and inhibition of inappropriate behaviours, such as the PFC, OFC, inferior frontal cortex and ACC (165, 178, 181, 203, 209). In fact, RS fMRI studies have reported both reduced (165, 171, 176) or increased (178, 180) cortico-striatal FC in areas of the limbic circuit as well as others brain-wide networks including the salience, executive, and default-mode networks (169, 170, 177, 181, 210). Interestingly, these studies support the idea that dopaminergic medication is able to alter limbic cortical signals to the VS, impairing the ability to change behavioural focus in response to a change in stimulus salience (177, 178, 186).

A recent studying using a dynamic functional network connectivity approach found dynamic functional engagement of local connectivity involving the limbic circuit, which led to the inefficient modulation of emotional processing and reward-related decision-making (179). It is worth mentioning that there have been very few studies assessing the topological characteristics of brain networks in these patients using graph theory analysis (171, 190). The studies above suggest that, in PD-ICD patients, connectivity is dysfunctional within and between dopaminergic neuronal circuitries involving disrupted communications between important subcortical and limbic-cognitive cortical regions. This implies that the neural mechanisms associated with ICDs in PD patients span molecular to system levels, which are complex and dynamic, and that they cannot already draw a clear and complete picture of ICDs in PD patients.

Previous fMRI studies using reward-related tasks in PD-ICD patients have reported discrepant results. While two studies pointed towards diminished activation in the right VS, OFC and ACC (182, 184), three other studies reported higher activation in the VS, anterior prefrontal cortex (PFC), ACC, and OFC (183, 185, 186). Interestingly, a recent study proposed a hypothesis for this cortico-subcortical interaction, suggesting that the right VS plays a critical role in modulating the functional dynamics of inhibitory-control in frontal regions when PD-ICD patients face penalties (187) pointing to the possibility that these non-unidirectional changes are mediated by various psychological and neural mechanisms.

Furthermore, previous studies have investigated the role of dopaminergic medications during the execution of an ICD-related task. For example, one study performed in PD-ICD patients with and without dopaminergic medication during a gambling task reported medication-independent and medication-related differences in neural activity, which may set a permissive stage for the emergence of ICD during dopamine replacement therapy in PD patients (188).

TABLE 3 | Magnetic resonance imaging and radionuclide imaging studies of cognitive impairment of impulsive control disorders in Parkinson's disease.

References	Population	Radioligand and technique	State	Main results/findings
Magnetic Resonance Imaging				
Grey Matter Studies				
Biundo et al. (168)	PD-ICD	Structural MRI	SBA	↑ cortical thinning in fronto-striatal circuitry and ↑ in the left amygdala (PD-ICD)
Pellicano et al. (166)	PD-ICD	Structural MRI	SBA	↑of cortical thickness in rostral ACC and frontal pole (PD-ICD)
Yoo et al. (173)	PD-punding	Structural MRI	VBM	Atrophy in dlPFC area spreading to OFC (PD-ICD punding)
Tessitore et al. (167)	PD-ICD	Structural MRI	VBM	No findings Thicker cortex in ACC and OFC correlated with ICD severity (PD-ICD)
Tessitore et al. (170)	PD-ICD	Structural MRI	VBM	No differences
Imperiale et al. (169)	PD-ICB	Structural MRI	SBA Tractography	Left precentral and superior frontal cortical thinning, and motor and extramotor white matter tract damage (PD-ICD)
Hammes et al. (165)	PD	Structural MRI	SBA	CT and severity of PD-ICD were positively correlated in the subgenual rostral ACC
White Matter Imaging				
Yoo et al. (73)	PD-ICD	Structural MRI	DTI	↑FA in corpus callosum, internal capsule, PCC and right thalamus (PD-ICD)
Canu et al. (174)	PD-ICD punding	Structural MRI	Tractography	Alteration in left pedunculopontine tract and splenium of the corpus callosum (PD-ICD punding)
Mojtahed Zadeh et al. (175)	PD-ICD No treatment	Structural MRI	Diffusion MRI connectometry	Disrupted connectivity in the network of connections between cerebellum, basal ganglia, cortex, and its spinal projections (PD-ICD)
Functional MRI				
a) Rs-fMRI and FC				
Carriere et al. (176)	PD-ICD	Structural MRI	FC	Functional disconnection between the left anterior Pur and left inferior temporal gyrus and the left ACC
Tessitore et al. (170)	PD-ICD	Rs-fMRI	FC Longitudinal	↓FC in DMN and central executive network and ↑FC in salience during follow-up (PD-ICD)
Tessitore et al. (177)	PD-ICD	Rs-fMRI	FC Transversal	↑FC in salience and DMN, which correlates with ICD severity (PD-ICD) ↓FC in frontal executive network (PD-ICD)
Ye et al. (171)	PD-ICD	Rs-fMRI	FC + AD administration	In somatosensory network: ↓FC between caudate and other cortical regions
Petersen et al. (178)	PD-ICD/ICB	Rs-fMRI	FC	↑FC between VS and ACC, OFC, insula, putamen, globus pallidum (PD-ICD)
Imperiale et al. (169)	PD-ICD	Rs-fMRI	FC	ICD severity and duration modulate FC between somatosensory, visual and cognitive networks (PD-ICD)
Hammes et al. (165)	PD	Rs-fMRI	FC	PD patients with more severe ICB had a ↓ FC between rostral ACC and the nucleus accumbens
Navalpotro-Gomez et al. (179)	PD-ICD	Rs-fMRI	DNFC	Dynamic functional engagement of local connectivity involving the limbic circuit and increased local efficiency in all the aforementioned areas (ICD+)
Koh et al. (180)	PD-high impulsivity (HI)	Rs-fMRI	FC	↑FC between the right frontoparietal network and medial visual network (PD-HI)
Mata-Marin et al. (181)	PD-HS	Rs-fMRI	FC	↑salience network activity with significant ↑ in the right IFG (HS+). Functional disconnection between associative and limbic striatum with precuneus and superior parietal lobe (HS+)

(Continued)

TABLE 3 | Continued

References	Population	Radioligand and technique	State	Main results/findings
a) fMRI during task or stimulus				
Rao et al. (182)	PD-ICD	Perfusion fMRI	Balloon Analogue Risk Task	↓BOLD activity in the right VS during risk taking and significantly ↓ resting CBF in the right VS (PD-ICD)
Frosini et al. (183)	PD-PG	fMRI with visual reward	Gambling-related visual cues/ neutral stimuli/rest periods	↑activation in bilateral ACC, medial and superior frontal gyri, precuneus, right inferior parietal lobule and VS (PD-ICD)
Voon et al. (184)	PD-ICD (PG or CB)	fMRI with task	Gambling task DA administration	↑more risky choices in the "Gain" relative to the "Loss" condition along with ↓ OFC and ACC activity (ICD+) ↑ sensitivity to risk along with ↓ VS activity (ICD+)
Politis et al. (185)	PD-HS	fMRI with visual reward	Visual sexual cues On/off	↑activation in regions within limbic, paralimbic, temporal, occipital, somatosensory and PFC cortices and correlated with increased sexual desire in VS, ACC and OFC (HS+) Off: ↓activation during stimuli
Petersen et al. (178)	PD-ICD/ICB	fMRI with pharmacologic stimuli and task	AD administration Reward learning	↑FC between amígdala and midbrain ↑FC between VS and ACC, not with punishment-avoidance learning
Girard et al. (186)	PD-HS	fMRI with visual stimuli	Delay-discounting of erotic rewards On/off	↑delayed visual stimuli in *on* PD-HS Association between VS, vmPFC and PCC
Paz-Alonso et al. (187)	PD-ICD	fMRI during task	Iowa Gambling Task	↑activation in subcortical and cortical regions typically associated with reward processing and inhibitory control (PD-ICD) Association between ICD severity and regional activations in the right insula and right IFG, mediated by FC with the right VS (PD-ICD)
Haagensen et al. (188)	PD-ICD	fMRI during task	Seuqential gambling task On/off	↓"continue-to-gamble" activity in right IFG and subthalamic nucleus (PD-ICD) Individual risk-attitude scaled positively with "continue-to-gamble" activity in right subthalamic nucleus and striatum (PD-ICD) Dopaminergic therapy ↓ FC between IFG and subthalamic nucleus during "continue-to-gamble" decisions and attenuated striatal responses towards accumulating reward
Radionuclide imaging				
Glucose metabolism				
Tahmasian et al. (189)	PD-ICD	PET FDG	Resting	Patients with ↑ impulsivity ↑ metabolism in OFC, ACC and right insula
Verger et al. (190)	PD-ICD	PET FDG	Resting	Right middle and inferior temporal gyri (ICD+ >ICD) ↑connectivity of these areas with OFC. ↓connectivity with right parahippocampus and with the left caudate (PD-ICD)
Marin-Lahoz et al. (191)	PD-ICD	PET FDG	Resting	↑metabolism in widespread areas comprising PFC, both amygdalae and default mode network hubs (PD-ICD > PD-nonICD-) ↓metabolism in right caudate (PD-ICD < HC)
Molecular studies focusing dopaminergic system				
a) Dopamine transporter (DaT) or F-Dopa				
Cilia et al. (192)	PD-PG	SPECT [^{123}I]FP-CIT	Resting	↓VS (PD-ICD < PD-nonICD)

(Continued)

TABLE 3 | Continued

References	Population		Radioligand and technique	State	Main results/findings
Joutsa et al. (193)	PD-ICD		PET [^{18}F]fluorodopa	Resting	↓Medial OFC (PD-ICD < PD-nonICD) No striatal differences
Voon et al. (194)	PD-ICD		SPECT [^{123}I]FP-CIT	Resting	↓VS (PD-ICD < PD-nonICD)
Lee et al. (29)	PD-ICD		PET [^{123}I]FP-CIT	Resting	Right vmPFC (PD-ICD < PD-nonICD) Tendency left accumbens nucleus (PD-ICD < PD-nonICD)
Vriend et al. (195)	PD-ICD		SPECT [^{123}I]FP-CIT	Resting (longitudinal) Retrospective PD naïve	↓VS (PD-ICD < PD-nonICD)
Smith et al. (196)	PD-ICD		SPECT [^{123}I]β-CIT	Resting (longitudinal) Prospective PD naïve	↓CN and right Put (PD-ICD < PD-nonICD) ↓Total striatum (PD-ICD < PD-nonICD)
Premi et al. (197)	PD-ICD		SPECT [^{123}I]FP-CIT	Resting	↓ Left Put and IFG (PD-ICD < PD-nonICD) Functional desconnection between basal ganglia and contralateral ACC (PD-ICD)
Navalpotro-Gomez et al. (198)	PD-ICD	QUIP QUIP-RS	SPECT [^{123}I]FP-CIT PET FDG	Resting	VS (PD-ICD < PD-nonICD) ↓DaT in VS associated to ↓metabolism in PFC and ACC (PD-ICD)
Hammes et al. (165)	PD	QUIP-RS BIS	^{18}F-DOPA-PET	Resting	↓ Dopamine synthesis capacity in the nucleus accumbens was associated with ICB
Hinkle et al. (199)	PD-ICD	QUIP	SPECT [^{123}I]FP-CIT VMAT2 PET (18F-AV133)	Resting	Right striatal VMAT2 ↑ (PD-ICD) Normalizing VMAT2 with DaT SBR strengthened bidirectional correlations with ICD (high VMAT2/DaT) in all striatal regions bilaterally
b) Studies with dopaminergic receptors					
Boileau et al. (200)	PD		PET [^{11}C]-raclopride [^{11}C]-(+)-PHNO	Resting	VS (PD<HC) GP (PD<HC) Putamen (PD>HC)
Payer et al. (201)	PD-ICD		PET [^{11}C]-(+)-PHNO	Resting	VS (ICD+ <ICD-) Dorsal striatum (ICD+ >ICD-) Negative correlation between VS with ICD severity (ICD+)
Stark et al. (202)	PD-ICD		PET [^{18}F] fallypride	Resting	VS (ICD+ <ICD-) Putamen (ICD+ <ICD-)
Task related studies					
a) Activation studies					
van Eimeren et al. (203)	PD-PG		PET H_2(15)O	Before and after 3 mg apomorphine Card selection game with probabilistic feedback	↓activity with DA in left OFC, amygdala and ACC (PG+)
Antonelli et al. (204)	PD		PET H_2(15)O	Before and after 1 mg PMX Delay discounting task, Go/ No Go Task	DA ↑medial PFC and PCC and ↓ in the VS in cognitive impulsivity tasks
a) Molecular studies focusing dopaminergic system with task					
Steeves et al. (205)	PD-PG		PET [^{11}C]-raclopride	Gambling task	PD-PG ↑ dopaminergic release in VS during gambling
O'Sullivan et al. (206)	PD-ICD/ICB		PET [^{11}C]-raclopride	Reward-related cues and L-dopa challenge	↑ Dopaminergic release in VS in ICD/ICB+ following reward-related cue exposure and L-Dopa challenge
Ray et al. (207)	PD-PG		PET [^{18}F] fallypride	Gambling task	↓ Dopamine in ACC during control task, not during gabling task in PD-PG ↑ Dopamine in SN and in the TVA

(Continued)

TABLE 3 | Continued

Wu et al. (208)	PD-ICD single or multiple	PET [^{11}C]-raclopride	Reward-related visual cues/neutral visual cues	↑ Dopamine release in VS in both single and multiple ICD patients in response to reward cues

PD-PG, PD patients with pathological gambling; G-SAS, Gambling Symptom Assessment Scale; BIS, Barratt Impulsiveness Scale 11; MRI, magnetic resonance imaging; VBM, voxel-based morphometry; SBA, Surface-based analysis; OFC, orbitofrontal cortex; PD-ICD, PD patients with impulse control disorder; MIDI, Minnesota impulse disorder inventory; QUIP, Questionnaire for Impulsive-Compulsive Disorders; CT, cortical thickness; ICB, impulse control behaviours; ACC, anterior cingulate cortex; IFG, inferior frontal gyrus; dlPFC, dorsolateral prefrontal cortex; TCI-R, Temperament and Character Inventory-Revised; DTI, diffusion tensor imaging; FA, fractional anisotropy; PRS, Punding Rating Scale; rs-fMRI, resting state-functional MRI; CF, functional connectivity; DMN, default-mode network; DA, dopaminergic agonists; PD-CB, PD patients with compulsive buying; VS, ventral striatum; PD-HS, PD patients with hypersexuality; MGS, Massachusetts Gambling Screen, DDS, dopaminergic dysregulation syndrome; PCC, posterior cingulate cortex; ASBPD, Ardouin Scale of Behaviour in Parkinson's disease; SPECT, single-photon emission computed tomography; PD-ICD, PD patients with impulse control disorder; OFC, orbitofrontal cortex; SOGS, South Oaks Gambling Scale; PFC, prefrontal cortex; ACC, Anterior cingulate cortex; PCC, posterior cingulate cortex; BIS, Barratt Impulsiveness Scale 11; PET, positron emission tomography; MIDI, Minnesota impulse disorder inventory; SRMI, Self-Report Manic Inventory; QUIP, Questionnaire for Impulsive-Compulsive Disorders; VS, ventral striatum; vmPFC, ventromedial prefrontal cortex; GP, Globus pallidus; SAST, Sexual Addiction Screening Test; G-SAS, Gambling Symptom Assessment Scale; DA, dopaminergic agonists; PMX, pramipexol; ICB, impulse control behaviors; DDS, dopaminergic dysregulation syndrome; SN, substantia nigra; VTA, ventral tegmental area.

In conclusion, altered patterns of resting FC in regions involved in cognitive control and inhibition of inappropriate behaviour are associated with ICD in PD, with an important putative effect of dopaminergic medication in the FC between areas of the limbic system and VS participating in the inhibitory-control in the reward circuitry.

Nuclear Imaging

Glucose Metabolism

Studies with ^{18}F-FDG PET in ICD show heterogeneous methodology, which can lead to some discrepant findings. Some of them have evidenced higher metabolic rates in the OFC, AAC, and insula in PD patients with higher impulsivity scores (189), with increased connectivity between the parahippocampus and the caudate (190) in patients with ICD respect to non-ICD. A recent systematic review stated that medicated PD-ICDs show increased metabolism in OFC and cingulate cortices, VS, amygdala, insula, temporal and supramarginal gyri (210). In the same line, a recent study suggests that brain metabolism is more preserved in PD-ICD patients than in patients without ICD, which could be related to ICD development (191). In contrast, a single study in PD-ICDs patients reported an association of lower DAT availability in the VS with lower FDG uptake in several cortical areas belonging to the limbic and associative circuits as well as in other regions involved in reward and inhibition processes (198). All these evidences can be matter of debate regarding metabolic studies in general population, which have largely demonstrated that, the hypometabolism of brain regions from "control networks" such as the PFC or the ACC could increase their vulnerability to relapse since it would interfere with cognitive inhibition.

Taken together, available data suggest that ICDs in PD patients are associated with functional alterations (with the influence of dopaminergic treatment) within the mesocorticolimbic network that could affect the control of impulse and lead to impaired inhibitory mechanisms. Although most studies show hypermetabolism in areas of mesocorticolimbic system involved with inhibition and cognitive control networks, one study looking at the relationship of cerebral metabolism and dopaminergic denervation found hypometabolic limbic and associative areas which in turn correlated with the severity of dopaminergic degeneration in the ventral striatum.

Dopamine

The most severe dopaminergic cell loss in PD patients occurs in the ventrolateral SNc, leading to dopaminergic deficits mostly in the posterior putamen, ultimately affecting the function of the motor circuit of the basal ganglia (211). However, molecular neuroimaging studies in PD-ICD patients, have revealed that patients also have decreased dopaminergic innervation in the ventral striatum (VS), as measured by DAT SPECT and PET (165, 192, 196–199, 212, 213). Nevertheless, not all studies reported previous finding (193). Moreover, reduced mesolimbic DAT availability has been reported even before the emergence of ICDs, indicating that it may be a predisposing factor for the development of these disorders (195, 196) once dopaminergic treatment is initiated.

Interpretation of altered DAT binding can sometimes be confusing because of two reasons. First, DAT availability may not correlate with dopaminergic neuron counts in PD patients (214). Second, its variation can reflect a functional downregulation in order to increase available dopamine in the synapse, given that the striatal dopamine synthesis capacity in PD-ICDs patients is not reduced, compared to matched PD-nonICDs (215).

On the other hand, functional molecular studies indicate that PD-ICDs patients have a higher release of dopamine in the VS during reward-related tasks (205, 206, 208). Moreover, there is also some evidence of a negative association between the VS dopamine synthesis capacity and ICD severity. Importantly, dopaminergic changes can be also measured outside the striatum. In fact, extrastriatal D2/D3 dopamine receptors can be measured using high-affinity radiotracers (such as [18F] fallypride or [11C] FLB-457). For example, one study in PD patients with pathological gambling showed a reduction in [11C] FLB-457 binding potential in the midbrain during gambling, where D2/D3 receptors are dominated by autoreceptors, along with low dopaminergic tone in the anterior cingulate cortex (ACC) (216).

Taken together, mounting evidence suggests that abnormal dopaminergic innervation or tone in the VS and possibly in the mesocortical circuit are key factors in the development of ICD in PD patients, and could potentially be used in the future as biomarkers for identifying patients at risk of developing

such abnormal behaviour when exposed to dopaminergic agents, especially DA.

CONCLUSION

In the current review, we highlighted the available and emerging MRI and radionuclide imaging (PET and SPECT studies) techniques used to assess cognitive impairment and ICD in PD. Although several limitations of the aforementioned studies are worth mentioning, including the literature review is not systematic, sample sizes are limited in some studies and different experimental designs and analysis techniques have been used, their findings still shed light on the potential usefulness of imaging for early diagnosing and monitoring the cognitive and neuropsychiatric symptoms of PD. Nevertheless, multimodal multimodal functional and structural longitudinal studies in early PD patients in large well-defined cohorts using advanced method of analysis are still needed in order to better predict the risk of dementia and ICD in PD patients, better understanding of pathophysiology as well as develop novel therapeutic interventions to improve patient care.

DATA AVAILABILITY STATEMENT

The original contributions presented in the study are included in the article/supplementary material, further inquiries can be directed to the corresponding author/s.

AUTHOR CONTRIBUTIONS

AM-B, MD-A, and IN-G: wrote up the original manuscript. MR-O: conception, supervision of the study, and reviewed the final manuscript. All authors contributed to the article and approved the submitted version.

REFERENCES

1. Gibb WRG, Lees AJ. Anatomy, pigmentation, ventral and dorsal subpopulations of the substantia nigra, and differential cell death in Parkinson's disease. *J Neurol Neurosurg Psychiatry.* (1991) 54:388–96. doi: 10.1136/jnnp.54.5.388
2. Mann DMA, Yates PO. Possible role of neuromelanin in the pathogenesis of Parkinson's disease. *Mech Ageing Dev.* (1983) 21:193–203. doi: 10.1016/0047-6374(83)90074-X
3. Aarsland D, Andersen K, Larsen JP, Lolk A, Kragh-Sørensen P. Prevalence and characteristics of dementia in Parkinson disease: an 8-year prospective study. *Arch Neurol.* (2003) 60:387–92. doi: 10.1001/archneur.60.3.387
4. Williams-Gray CH, Mason SL, Evans JR, Foltynie T, Brayne C, Robbins TW, et al. The CamPaIGN study of Parkinson's disease: 10-year outlook in an incident population-based cohort. *J Neurol Neurosurg Psychiatry.* (2013) 84:1258–64. doi: 10.1136/jnnp-2013-305277
5. Hely MA, Reid WGJ, Adena MA, Halliday GM, Morris JGL. The Sydney multicenter study of Parkinson's disease: the inevitability of dementia at 20 years. *Move Disord.* (2008) 23:837–44. doi: 10.1002/mds.21956
6. Broeders M, De Bie RMA, Velseboer DC, Speelman JD, Muslimovic D, Schmand B. Evolution of mild cognitive impairment in Parkinson disease. *Neurology.* (2013) 81:346–52. doi: 10.1212/WNL.0b013e31829c5c86
7. Gasca-Salas C, Estanga A, Clavero P, Aguilar-Palacio I, González-Redondo R, Obeso JA, et al. Longitudinal assessment of the pattern of cognitive decline in non-demented patients with advanced Parkinson's disease. *J Parkinsons Dis.* (2014) 4:677–86. doi: 10.3233/JPD-140398
8. Janvin CC, Larsen JP, Aarsland D, Hugdahl K. Subtypes of mild cognitive impairment in Parkinson's disease: progression to dementia. *Move Disord.* (2006) 21:1343–9. doi: 10.1002/mds.20974
9. Litvan I, Aarsland D, Adler CH, Goldman JG, Kulisevsky J, Mollenhauer B, et al. MDS task force on mild cognitive impairment in Parkinson's disease: critical review of PD-MCI. *Move Disord.* (2011) 26:1814-24. doi: 10.1002/mds.23823
10. Pigott K, Rick J, Xie SX, Hurtig H, Chen-Plotkin A, Duda JE, et al. Longitudinal study of normal cognition in Parkinson disease. *Neurology.* (2015) 85:1276–82. doi: 10.1212/WNL.0000000000002001
11. Pedersen KF, Larsen JP, Tysnes OB, Alves G. Prognosis of mild cognitive impairment in early Parkinson disease: the Norwegian ParkWest study. *JAMA Neurol.* (2013) 70:580–6. doi: 10.1001/jamaneurol.2013.2110
12. Hughes TA, Ross HF, Musa S, Bhattacherjee S, Nathan RN, Mindham RHS, et al. A 10-year study of the incidence of and factors predicting dementia in Parkinson's disease. *Neurology.* (2000) 54:1596–602. doi: 10.1212/WNL.54.8.1596
13. Rinne JO, Mlic JR, Paljärvi L, Rinne UK. Dementia in Parkinson's disease is related to neuronal loss in the medial substantia nigra. *Ann Neurol.* (1989) 26:47–50. doi: 10.1002/ana.410260107
14. Del Tredici K, Braak H. Dysfunction of the locus coeruleus-norepinephrine system and related circuitry in Parkinson's disease-related dementia. *J Neurol Neurosurg Psychiatry.* (2013) 84:774–83. doi: 10.1136/jnnp-2011-301817
15. Halliday GM, Blumbergs PC, Cotton RGH, Blessing WW, Geffen LB. Loss of brainstem serotonin- and substance P-containing neurons in Parkinson's disease. *Brain Res.* (1990) 510:104–7. doi: 10.1016/0006-8993(90)90733-R
16. Tagliavini F, Pilleri G, Bouras C, Constantinidis J. The basal nucleus of Meynert in idiopathic Parkinson's disease. *Acta Neurol Scand.* (1984) 70:20–8. doi: 10.1111/j.1600-0404.1984.tb00798.x
17. Compta Y, Parkkinen L, O'Sullivan SS, Vandrovcova J, Holton JL, Collins C, et al. Lewy- and Alzheimer-type pathologies in Parkinson's disease dementia: which is more important? *Brain.* (2011) 134:1493-505. doi: 10.1093/brain/awr031
18. Aarsland D, Marsh L, Schrag A. Neuropsychiatric symptoms in Parkinson's disease. *Move Disord.* (2009) 24:2175–86. doi: 10.1002/mds.22589
19. Weintraub D, Koester J, Potenza MN, Siderowf AD, Stacy M, Voon V, et al. Impulse control disorders in Parkinson disease: a cross-sectional study of 3090 patients. *Arch Neurol.* (2010) 67:589–95. doi: 10.1001/archneurol.2010.65
20. Bastiaens J, Dorfman BJ, Christos PJ, Nirenberg MJ. Prospective cohort study of impulse control disorders in Parkinson's disease. *Move Disord.* (2013) 28:327–33. doi: 10.1002/mds.25291
21. Samuel M, Rodriguez-Oroz M, Antonini A, Brotchie JM, Ray Chaudhuri K, Brown RG, et al. Management of impulse control disorders in Parkinson's disease: controversies and future approaches. *Move Disord.* (2015) 30:150–9. doi: 10.1002/mds.26099
22. Hutton C, Draganski B, Ashburner J, Weiskopf N. A comparison between voxel-based cortical thickness and voxel-based morphometry in normal aging. *NeuroImage.* (2009) 48:371–80. doi: 10.1016/j.neuroimage.2009.06.043
23. Camicioli R, Mooler M, Kinney A, Corbridge E, Glassberg K, Kaye J. Parkinson's disease is associated with hippocampal atrophy. *Mov Disord.* (2003) 18:784–90. doi: 10.1002/mds.10444
24. Brück A, Kurki T, Kaasinen V, Vahlberg T, Rinne JO. Hippocampal and prefrontal atrophy in patients with early non-demented Parkinson's disease is related to cognitive impairment. *J Neurol Neurosurg Psychiatry.* (2004) 75:1467–9. doi: 10.1136/jnnp.2003.031237
25. Song SK, Lee JE, Park HJ, Sohn YH, Lee JD, Lee PH. The pattern of cortical atrophy in patients with Parkinson's disease according to cognitive status. *Move Disord.* (2011) 26:289–96. doi: 10.1002/mds.23477

26. Choi SH, Jung TM, Lee JE, Lee SK, Sohn YH, Lee PH. Volumetric analysis of the substantia innominata in patients with Parkinson's disease according to cognitive status. *Neurobiol Aging.* (2012) 33:1265–72. doi: 10.1007/978-1-4614-1788-0
27. Beyer MK, Bronnick KS, Hwang KS, Bergsland N, Tysnes OB, Larsen JP, et al. Verbal memory is associated with structural hippocampal changes in newly diagnosed Parkinson's disease. *J Neurol Neurosurg Psychiatry.* (2013) 84:23–8. doi: 10.1136/jnnp-2012-303054
28. Pagonabarraga J, Corcuera-Solano I, Vives-Gilabert Y, Llebaria G, García-Sánchez C, Pascual-Sedano B, et al. Pattern of regional cortical thinning associated with cognitive deterioration in Parkinson's disease. *PLoS ONE.* (2013) 8:e54980. doi: 10.1371/journal.pone.0054980
29. Lee JE, Cho KH, Song SK, Kim HJ, Lee HS, Sohn YH, et al. Exploratory analysis of neuropsychological and neuroanatomical correlates of progressive mild cognitive impairment in Parkinson's disease. *J Neurol Neurosurg Psychiatry.* (2014) 85:7–16. doi: 10.1136/jnnp-2013-305062
30. Filoteo JV, Reed JD, Litvan I, Harrington DL. Volumetric correlates of cognitive functioning in nondemented patients with Parkinson's disease. *Move Disord.* (2014) 29:360–7. doi: 10.1002/mds.25633
31. Kandiah N, Zainal NH, Narasimhalu K, Chander RJ, Ng A, Mak E, et al. Hippocampal volume and white matter disease in the prediction of dementia in Parkinson's disease. *Parkinsonism Relat Disord.* (2014) 20:1203–8. doi: 10.1016/j.parkreldis.2014.08.024
32. Wen MC, Ng A, Chander RJ, Au WL, Tan LCS, Kandiah N. Longitudinal brain volumetric changes and their predictive effects on cognition among cognitively asymptomatic patients with Parkinson's disease. *Parkinsonism Relat Disord.* (2015) 21:483–8. doi: 10.1016/j.parkreldis.2015.02.014
33. Foo H, Mak E, Chander RJ, Ng A, Au WL, Sitoh YY, et al. Associations of hippocampal subfields in the progression of cognitive decline related to Parkinson's disease. *NeuroImage Clin.* (2016) 14:37–42. doi: 10.1016/j.nicl.2016.12.008
34. Low A, Foo H, Yong TT, Tan LCS, Kandiah N. Hippocampal subfield atrophy of CA1 and subicular structures predict progression to dementia in idiopathic Parkinson's disease. *J Neurol Neurosurg Psychiatry.* (2019) 90:681–7. doi: 10.1136/jnnp-2018-319592
35. Zheng D, Chen C, Song WC, Yi ZQ, Zhao PW, Zhong JG, et al. Regional gray matter reductions associated with mild cognitive impairment in Parkinson's disease: a meta-analysis of voxel-based morphometry studies. *Behav Brain Res.* (2019) 371:111973. doi: 10.1016/j.bbr.2019.111973
36. Gasca-Salas C, García-Lorenzo D, Garcia-Garcia D, Clavero P, Obeso JA, Lehericy S, et al. Parkinson's disease with mild cognitive impairment: severe cortical thinning antedates dementia. *Brain Imaging Behav.* (2019) 13:180–8. doi: 10.1007/s11682-017-9751-6
37. Chung SJ, Yoo HS, Lee YH, Lee HS, Ye BS, Sohn YH, et al. Frontal atrophy as a marker for dementia conversion in Parkinson's disease with mild cognitive impairment. *Hum Brain Mapp.* (2019) 40:3784–94. doi: 10.1002/hbm.24631
38. Xu R, Hu X, Jiang X, Zhang Y, Wang J, Zeng X. Longitudinal volume changes of hippocampal subfields and cognitive decline in Parkinson's disease. *Quant Imaging Med Surg.* (2020) 10:220–32. doi: 10.21037/qims.2019.10.17
39. Zhou C, Guan XJ, Guo T, Zeng QL, Gao T, Huang PY, et al. Progressive brain atrophy in Parkinson's disease patients who convert to mild cognitive impairment. *CNS Neurosci Ther.* (2020) 26:117–25. doi: 10.1111/cns.13188
40. Donzuso G, Monastero R, Cicero CE, Luca A, Mostile G, Giuliano L, et al. Neuroanatomical changes in early Parkinson's disease with mild cognitive impairment: a VBM study; the Parkinson's Disease Cognitive Impairment Study (PaCoS). *Neurol Sci.* (2021) 42:3723–31. doi: 10.1007/s10072-020-05034-9
41. Kamagata K, Motoi Y, Abe O, Shimoji K, Hori M, Nakanishi A, et al. White matter alteration of the cingulum in Parkinson disease with and without dementia: evaluation by diffusion tensor tract-specific analysis. *Am J Neuroradiol.* (2012) 33:890–5. doi: 10.3174/ajnr.A2860
42. Hattori T, Orimo S, Aoki S, Ito K, Abe O, Amano A, et al. Cognitive status correlates with white matter alteration in Parkinson's disease. *Hum Brain Mapp.* (2012) 33:727–39. doi: 10.1002/hbm.21245
43. Deng B, Zhang Y, Wang L, Peng K, Han L, Nie K, et al. Diffusion tensor imaging reveals white matter changes associated with cognitive status in patients with Parkinson's disease. *Am J Alzheimers Dis Other Dementias.* (2013) 28:154–64. doi: 10.1177/1533317512470207
44. Melzer TR, Watts R, Macaskill MR, Pitcher TL, Livingston L, Keenan RJ, et al. White matter microstructure deteriorates across cognitive stages in Parkinson disease. *Neurology.* (2013) 80:1841–9. doi: 10.1212/WNL.0b013e3182929f62
45. Agosta F, Canu E, Stefanova E, Sarro L, Tomić A, Špica V, et al. Mild cognitive impairment in Parkinson's disease is associated with a distributed pattern of brain white matter damage. *Hum Brain Mapp.* (2014) 35:1921–9. doi: 10.1002/hbm.22302
46. Auning E, Kjærvik VK, Selnes P, Aarsland D, Haram A, Bjørnerud A, et al. White matter integrity and cognition in Parkinson's disease: a cross-sectional study. *BMJ Open.* (2014) 4:e003976. doi: 10.1136/bmjopen-2013-003976
47. Chen B, Fan GG, Liu H, Wang S. Changes in anatomical and functional connectivity of Parkinson's disease patients according to cognitive status. *Eur J Radiol.* (2015) 84:1318–24. doi: 10.1016/j.ejrad.2015.04.014
48. Bledsoe IO, Stebbins GT, Merkitch D, Goldman JG. White matter abnormalities in the corpus callosum with cognitive impairment in Parkinson disease. *Neurology.* (2018) 91:E2244-55. doi: 10.1212/WNL.0000000000006646
49. Chondrogiorgi M, Astrakas LG, Zikou AK, Weis L, Xydis VG, Antonini A, et al. Multifocal alterations of white matter accompany the transition from normal cognition to dementia in Parkinson's disease patients. *Brain Imaging Behav.* (2019) 13:232–40. doi: 10.1007/s11682-018-9863-7
50. Beyer MK, Aarsland D, Greve OJ, Larsen JP. Visual rating of white matter hyperintensities in Parkinson's disease. *Move Disord.* (2006) 21:223–9. doi: 10.1002/mds.20704
51. Lee SJ, Kim JS, Yoo JY, Song IU, Kim BS, Jung SL, et al. Influence of white matter hyperintensities on the cognition of patients with parkinson disease. *Alzheimer Dis Assoc Disord.* (2010) 24:227–33. doi: 10.1097/WAD.0b013e3181d71a13
52. Joki H, Higashiyama Y, Nakae Y, Kugimoto C, Doi H, Kimura K, et al. White matter hyperintensities on MRI in dementia with Lewy bodies, Parkinson's disease with dementia, Alzheimer's disease. *J Neurol Sci.* (2018) 385:99–104. doi: 10.1016/j.jns.2017.12.018
53. Huang X, Wen MC, Ng SYE, Hartono S, Chia NSY, Choi X, et al. Periventricular white matter hyperintensity burden and cognitive impairment in early Parkinson's disease. *Eur J Neurol.* (2020) 27:959–66. doi: 10.1111/ene.14192
54. Lewis SJG, Dove A, Robbins TW, Barker RA, Owen AM. Cognitive impairments in early Parkinson's disease are accompanied by reductions in activity in frontostriatal neural circuitry. *J Neurosci.* (2003) 23:6351–6. doi: 10.1523/JNEUROSCI.23-15-06351.2003
55. Monchi O, Petrides M, Mejia-Constain B, Strafella AP. Cortical activity in Parkinson's disease during executive processing depends on striatal involvement. *Brain.* (2007) 130:233–44. doi: 10.1093/brain/awl326
56. Seibert T, Murphy E, Kaestner E, Brewer J. Interregional correlations in parkinson disease and parkinson-related dementia with resting functional MR imaging. *Radiology.* (2012) 236:226–34. doi: 10.1148/radiol.12111280
57. Baggio HC, Sala-Llonch R, Segura B, Marti MJ, Valldeoriola F, Compta Y, et al. Functional brain networks and cognitive deficits in Parkinson's disease. *Hum Brain Mapp.* (2014) 35:4620–34. doi: 10.1002/hbm.22499
58. Lebedev AV, Westman E, Simmons A, Lebedeva A, Siepel FJ, Pereira JB, et al. Large-scale resting state network correlates of cognitive impairment in Parkinson's disease and related dopaminergic deficits. *Front Syst Neurosci.* (2014) 8:45. doi: 10.3389/fnsys.2014.00045
59. Amboni M, Tessitore A, Esposito F, Santangelo G, Picillo M, Vitale C, et al. Resting-state functional connectivity associated with mild cognitive impairment in Parkinson's disease. *J Neurol.* (2015) 262:425–34. doi: 10.1007/s00415-014-7591-5
60. Baggio HC, Segura B, Sala-Llonch R, Marti MJ, Valldeoriola F, Compta Y, et al. Cognitive impairment and resting-state network connectivity in Parkinson's disease. *Hum Brain Mapp.* (2015) 36:199–212. doi: 10.1002/hbm.22622
61. Gorges M, Müller HP, Lulé D, Pinkhardt EH, Ludolph AC, Kassubek J. To rise and to fall: functional connectivity in cognitively normal and cognitively impaired patients with Parkinson's disease. *Neurobiol Aging.* (2015) 36:1727–35. doi: 10.1016/j.neurobiolaging.2014.12.026
62. Shin NY, Shin YS, Lee PH, Yoon U, Han S, Kim DJ, et al. Different functional and microstructural changes depending on duration of mild

cognitive impairment in Parkinson disease. *Am J Neuroradiol.* (2016) 37:897–903. doi: 10.3174/ajnr.A4626
63. Chen B, Wang S, Sun W, Shang X, Liu H, Liu G, et al. Functional and structural changes in gray matter of parkinson's disease patients with mild cognitive impairment. *Eur J Radiol.* (2017) 93:16–23. doi: 10.1016/j.ejrad.2017.05.018
64. Bezdicek O, Ballarini T, RuŽička F, Roth J, Mueller K, Jech R, et al. Mild cognitive impairment disrupts attention network connectivity in Parkinson's disease: a combined multimodal MRI and meta-analytical study. *Neuropsychologia.* (2018) 112:105–15. doi: 10.1016/j.neuropsychologia.2018.03.011
65. Díez-Cirarda M, Strafella AP, Kim J, Peña J, Ojeda N, Cabrera-Zubizarreta A, et al. Dynamic functional connectivity in Parkinson's disease patients with mild cognitive impairment and normal cognition. *NeuroImage Clin.* (2018) 17:847–55. doi: 10.1016/j.nicl.2017.12.013
66. Hou Y, Yang J, Luo C, Ou R, Zou Y, Song W, et al. Resting-state network connectivity in cognitively unimpaired drug-naïve patients with rigidity-dominant Parkinson's disease. *J Neurol Sci.* (2018) 395:147–52. doi: 10.1016/j.jns.2018.10.003
67. Wolters AF, van de Weijer SCF, Leentjens AFG, Duits AA, Jacobs HIL, Kuijf ML. Resting-state fMRI in Parkinson's disease patients with cognitive impairment: a meta-analysis. *Parkinsonism Relat Disord.* (2019) 62:16-27. doi: 10.1016/j.parkreldis.2018.12.016
68. Fathy YY, Hepp DH, de Jong FJ, Geurts JJG, Foncke EMJ, Berendse HW, et al. Anterior insular network disconnection and cognitive impairment in Parkinson's disease. *NeuroImage Clin.* (2020) 28:102364. doi: 10.1016/j.nicl.2020.102364
69. Pan C, Ren J, Li L, Li Y, Xu J, Xue C, et al. Differential functional connectivity of insular subdivisions in de novo Parkinson's disease with mild cognitive impairment. *Brain Imaging Behav*. (2021). doi: 10.1007/s11682-021-00471-2. [Epub ahead of print].
70. Delgado-Alvarado M, Gago B, Navalpotro-Gomez I, Jiménez-Urbieta H, Rodriguez-Oroz MC. Biomarkers for dementia and mild cognitive impairment in Parkinson's disease. *Move Disord.* (2016) 31:861–81. doi: 10.1002/mds.26662
71. Sarasso E, Agosta F, Piramide N, Filippi M. Progression of grey and white matter brain damage in Parkinson's disease: a critical review of structural MRI literature. *J Neurol.* (2020) 268:3144–79. doi: 10.1007/s00415-020-09863-8
72. Wu L, Liu FT, Ge JJ, Zhao J, Tang YL, Yu WB, et al. Clinical characteristics of cognitive impairment in patients with Parkinson's disease and its related pattern in 18F-FDG PET imaging. *Hum Brain Mapp.* (2018) 39:4652–62. doi: 10.1002/hbm.24311
73. Yoo HS, Yun HJ, Chung SJ, Sunwoo MK, Lee JM, Sohn YH, et al. Patterns of neuropsychological profile cortical thinning in Parkinson's disease with punding. *PLoS ONE.* (2015)10:e0134468. doi: 10.1371/journal.pone.0134468
74. Na Young S, Bang M, Yoo S-W, Kim JS, Yun E, Yoon U, et al. Cortical thickness from MRI to predict conversion from mild cognitive impairment to dementia in Parkinson disease: a machine learning-based model. *Radiology.* (2021) 300:390–9. doi: 10.1148/radiol.2021203383
75. Smith C, Malek N, Grosset K, Cullen B, Gentleman S, Grosset DG. Neuropathology of dementia in patients with Parkinson's disease: a systematic review of autopsy studies. *J Neurol Neurosurg Psychiatry.* (2019) 90:1234–43. doi: 10.1136/jnnp-2019-321111
76. Morales DA, Vives-Gilabert Y, Gómez-Ansón B, Bengoetxea E, Larrañaga P, Bielza C, et al. Predicting dementia development in Parkinson's disease using Bayesian network classifiers. *Psychiatry Res Neuroimaging.* (2013) 213:92–8. doi: 10.1016/j.pscychresns.2012.06.001
77. Leocadi M, Canu E, Donzuso G, Stojkovic T, Basaia S, Kresojević N, et al. Longitudinal clinical, cognitive, and neuroanatomical changes over 5 years in GBA-positive Parkinson's disease patients. *J Neurol.* (2021). doi: 10.1007/s00415-021-10713-4. [Epub ahead of print].
78. Sampedro F, Marín-Lahoz J, Martínez-Horta S, Pagonabarraga J, Kulisevsky J. Reduced gray matter volume in cognitively preserved COMT 158Val/Val Parkinson's disease patients and its association with cognitive decline. *Brain Imaging Behav.* (2020) 14:321–8. doi: 10.1007/s11682-018-0022-y
79. Sampedro F, Marín-Lahoz J, Martínez-Horta S, Pagonabarraga J, Kulisevsky J. Early gray matter volume loss in MAPT H1H1 de Novo PD patients: a possible association with cognitive decline. *Front Neurol.* (2018) 9:394. doi: 10.3389/fneur.2018.00394
80. Gorges M, Müller HP, Liepelt-Scarfone I, Storch A, Dodel R, Hilker-Roggendorf R, et al. Structural brain signature of cognitive decline in Parkinson's disease: DTI-based evidence from the LANDSCAPE study. *Ther Adv Neurol Disord.* (2019) 12:1756286419843447. doi: 10.1177/1756286419843447
81. Minett T, Su L, Mak E, Williams G, Firbank M, Lawson RA, et al. Longitudinal diffusion tensor imaging changes in early Parkinson's disease: ICICLE-PD study. *J Neurol.* (2018) 265:1528–39. doi: 10.1007/s00415-018-8873-0
82. Agosta F, Kostic VS, Davidovic K, Kresojević N, Sarro L, Svetel M, et al. White matter abnormalities in Parkinson's disease patients with glucocerebrosidase gene mutations. *Move Disord.* (2013) 28:772–8. doi: 10.1002/mds.25397
83. Kamagata K, Motoi Y, Tomiyama H, Abe O, Ito K, Shimoji K, et al. Relationship between cognitive impairment and white-matter alteration in Parkinson's disease with dementia: tract-based spatial statistics and tract-specific analysis. *Eur Radiol.* (2013) 23:1946–55. doi: 10.1007/s00330-013-2775-4
84. Duncan GW, Firbank MJ, Yarnall AJ, Khoo TK, Brooks DJ, Barker RA, et al. Gray and white matter imaging: a biomarker for cognitive impairment in early Parkinson's disease? *Move Disord.* (2016) 31:103–10. doi: 10.1002/mds.26312
85. Dalaker TO, Larsen JP, Bergsland N, Beyer MK, Alves G, Dwyer MG, et al. Brain atrophy and white matter hyperintensities in early Parkinson's disease. *Move Disord.* (2009) 24:2233–41. doi: 10.1002/mds.22754
86. González-Redondo R, Toledo J, Clavero P, Lamet I, García-García D, García-Eulate R, et al. The impact of silent vascular brain burden in cognitive impairment in Parkinson's disease. *Eur J Neurol.* (2012) 19:1100–7. doi: 10.1111/j.1468-1331.2012.03682.x
87. Raichle ME. The brain's default mode network. *Ann Rev Neurosci.* (2015) 38:433–47. doi: 10.1146/annurev-neuro-071013-014030
88. Tessitore A, Esposito F, Vitale C, Santangelo G, Amboni M, Russo A, et al. Default-mode network connectivity in cognitively unimpaired patients with Parkinson disease. *Neurology.* (2012) 79:2226–32. doi: 10.1212/WNL.0b013e31827689d6
89. Chen X, Liu M, Wu Z, Cheng H. Topological abnormalities of functional brain network in early-stage Parkinson's disease patients with mild cognitive impairment. *Front Neurosci.* (2020) 14:1298. doi: 10.3389/fnins.2020.616872
90. Hou Y, Yuan X, Wei Q, Ou R, Yang J, Gong Q, et al. Primary disruption of the default mode network subsystems in drug-naïve Parkinson's disease with mild cognitive impairments. *Neuroradiology.* (2020) 62:685–92. doi: 10.1007/s00234-020-02378-z
91. Guo W, Jin W, Li N, Gao J, Wang J, Chang Y, et al. Brain activity alterations in patients with Parkinson's disease with cognitive impairment based on resting-state functional MRI. *Neurosci Lett.* (2021) 747:135672. doi: 10.1016/j.neulet.2021.135672
92. Zarifkar P, Kim J, La C, Zhang K, YorkWilliams S, Levine TF, et al. Cognitive impairment in Parkinson's disease is associated with Default Mode Network subsystem connectivity and cerebrospinal fluid Aβ. *Parkinsonism Relat Disord.* (2021) 83:71–8. doi: 10.1016/j.parkreldis.2021.01.002
93. Disbrow EA, Carmichael O, He J, Lanni KE, Dressler EM, Zhang L, et al. Resting state functional connectivity is associated with cognitive dysfunction in non-demented people with Parkinson's disease. *J Parkinsons Dis.* (2014) 4:453–65. doi: 10.3233/JPD-130341
94. Peraza LR, Nesbitt D, Lawson RA, Duncan GW, Yarnall AJ, Khoo TK, et al. Intra- and inter-network functional alterations in Parkinson's disease with mild cognitive impairment. *Hum Brain Mapp.* (2017) 38:1702–15. doi: 10.1002/hbm.23499
95. Caminiti SP, Siri C, Guidi L, Antonini A, Perani D. The neural correlates of spatial and object working memory in elderly and Parkinson's disease subjects. *Behav Neurol.* (2015) 2015:10. doi: 10.1155/2015/123636
96. Giehl K, Tahmasian M, Eickhoff SB, van Eimeren T. Imaging executive functions in Parkinson's disease: an activation likelihood estimation meta-analysis. *Parkinsonism Relat Disord.* (2019) 63:137–42. doi: 10.1016/j.parkreldis.2019.02.015
97. Poston KL, Yorkwilliams S, Zhang K, Cai W, Everling D, Tayim FM, et al. Compensatory neural mechanisms in cognitively unimpaired Parkinson disease. *Ann Neurol.* (2016) 79:448–63. doi: 10.1002/ana.24585

98. Pagonabarraga J, Kulisevsky J. Cognitive impairment and dementia in Parkinson's disease. *Neurobiol Dis*. (2012) 46:590–6. doi: 10.1016/j.nbd.2012.03.029
99. Lucas-Jiménez O, Díez-Cirard M, Ojeda N, Peña J, Cabrera-Zubizarreta A, Ibarretxe-Bilbao N. Verbal memory in Parkinson's Disease: a combined DTI and fMRI study. *J Parkinsons Dis.* (2015) 5:793–804. doi: 10.3233/JPD-150623
100. Bohnen NI, Koeppe RA, Minoshima S, Giordani B, Albin RL, Frey KA, et al. Cerebral glucose metabolic features of Parkinson disease and incident dementia: longitudinal study. *J Nucl Med.* (2011) 52:848–55. doi: 10.2967/jnumed.111.089946
101. Garcia-Garcia D, Clavero P, Salas CG, Lamet I, Arbizu J, Gonzalez-Redondo R, et al. Posterior parietooccipital hypometabolism may differentiate mild cognitive impairment from dementia in Parkinson's disease. *Eur J Nucl Med Mol Imaging.* (2012) 39:1767–77. doi: 10.1007/s00259-012-2198-5
102. Hosokai Y, Nishio Y, Hirayama K, Takeda A, Ishioka T, Sawada Y, et al. Distinct patterns of regional cerebral glucose metabolism in Parkinson's disease with and without mild cognitive impairment. *Move Disord.* (2009) 24:854–62. doi: 10.1002/mds.22444
103. Huang C, Mattis P, Perrine K, Brown N, Dhawan V, Eidelberg D. Metabolic abnormalities associated with mild cognitive impairment in Parkinson disease. *Neurology.* (2008) 70:1470-7. doi: 10.1212/01.wnl.0000304050.05332.9c
104. Pappatá S, Santangelo G, Aarsland D, Vicidomini C, Longo K, Bronnick K, et al. Mild cognitive impairment in drug-naive patients with PD is associated with cerebral hypometabolism. *Neurology.* (2011) 77:1357–62. doi: 10.1212/WNL.0b013e3182315259
105. González-Redondo R, García-García D, Clavero P, Gasca-Salas C, García-Eulate R, García-Eulate R, et al. Grey matter hypometabolism and atrophy in Parkinson's disease with cognitive impairment: a two-step process. *Brain.* (2014) 137:2356-67. doi: 10.1093/brain/awu159
106. Huang C, Mattis P, Tang C, Perrine K, Carbon M, Eidelberg D, et al. Metabolic brain networks associated with cognitive function in Parkinson's disease. *NeuroImage.* (2007) 34:714–23. doi: 10.1016/j.neuroimage.2006.09.003
107. Tard C, Demailly F, Delval A, Semah F, Defebvre L, Dujardin K, et al. Hypometabolism in posterior and temporal areas of the brain is associated with cognitive decline in Parkinson's disease. *J Parkinsons Dis.* (2015) 5:569–74. doi: 10.3233/JPD-150583
108. Baba T, Hosokai Y, Nishio Y, Kikuchi A, Hirayama K, Suzuki K, et al. Longitudinal study of cognitive and cerebral metabolic changes in Parkinson's disease. *J Neurol Sci.* (2017) 15:288–93. doi: 10.1016/j.jns.2016.11.068
109. Rinne JO, Portin R, Ruottinen H, Nurmi E, Bergman J, Haaparanta M, et al. Cognitive impairment and the brain dopaminergic system in Parkinson disease. *Arch Neurol.* (2000) 57:470–5. doi: 10.1001/archneur.57.4.470
110. Walker Z, Costa DC, Walker RWH, Shaw K, Gacinovic S, Stevens T, et al. Differentiation of dementia with Lewy bodies from Alzheimer's disease using a dopaminergic presynaptic ligand. *J Neurol Neurosurg Psychiatry.* (2002) 73:134–40. doi: 10.1136/jnnp.73.2.134
111. Ito K, Nagano-Saito A, Kato T, Arahata Y, Nakamura A, Kawasumi Y, et al. Striatal and extrastriatal dysfunction in Parkinson's disease with dementia: a 6-[18F]fluoro-L-dopa PET study. *Brain.* (2002) 125:1358-65. doi: 10.1093/brain/awf134
112. Nagano-Saito A, Kato T, Arahata Y, Washimi Y, Nakamura A, Abe Y, et al. Cognitive- and motor-related regions in Parkinson's disease: FDOPA and FDG PET studies. *NeuroImage.* (2004) 22:553–61. doi: 10.1016/j.neuroimage.2004.01.030
113. van Beilen M, Portman AT, Kiers HAL, Maguire RP, Kaasinen V, Koning M, et al. Striatal FDOPA uptake and cognition in advanced non-demented Parkinson's disease: a clinical and FDOPA-PET study. *Parkinsonism Relat Disord.* (2008) 14:224–8. doi: 10.1016/j.parkreldis.2007.08.011
114. Nobili F, Campus C, Arnaldi D, De Carli F, Cabassi G, Brugnolo A, et al. Cognitive-nigrostriatal relationships in de novo, drug-naïve Parkinson's disease patients: a [I-123]FP-CIT SPECT Study. *Move Disord.* (2010) 25:35–43. doi: 10.1002/mds.22899
115. Polito C, Berti V, Ramat S, Vanzi E, De Cristofaro MT, Pellican,ò G, et al. Interaction of caudate dopamine depletion and brain metabolic changes with cognitive dysfunction in early Parkinson's disease. *Neurobiol Aging.* (2012) 33:206.e29-39. doi: 10.1016/j.neurobiolaging.2010.09.004
116. Niethammer M, Tang CC, Ma Y, Mattis PJ, Ko JH, Dhawan V, et al. Parkinson's disease cognitive network correlates with caudate dopamine. *NeuroImage.* (2013) 78:204–9. doi: 10.1016/j.neuroimage.2013.03.070
117. Sawamoto N, Piccini P, Hotton G, Pavese N, Thielemans K, Brooks DJ. Cognitive deficits and striato-frontal dopamine release in Parkinson's disease. *Brain.* (2008) 131:1294-302. doi: 10.1093/brain/awn054
118. Christopher L, Duff-Canning S, Koshimori Y, Segura B, Boileau I, Chen R, et al. Salience network and parahippocampal dopamine dysfunction in memory-impaired parkinson disease. *Ann Neurol.* (2015) 77:269–80. doi: 10.1002/ana.24323
119. Bohnen NI, Kaufer DI, Ivanco LS, Lopresti B, Koeppe RA, Davis JG, et al. Cortical cholinergic function is more severely affected in Parkinsonian dementia than in Alzheimer disease. *Arch Neurol.* (2003) 60:1745–8. doi: 10.1001/archneur.60.12.1745
120. Hilker R, Thomas AV, Klein JC, Weisenbach S, Kalbe E, Burghaus L, et al. Dementia in Parkinson disease: functional imaging of cholinergic and dopaminergic pathways. *Neurology.* (2005) 65:1716–22. doi: 10.1212/01.wnl.0000191154.78131.f6
121. Gilman S, Koeppe RA, Nan B, Wang CN, Wang X, Junck L, et al. Cerebral cortical and subcortical cholinergic deficits in parkinsonian syndromes. *Neurology.* (2010) 74:1416–23. doi: 10.1212/WNL.0b013e3181dc1a55
122. Klein JC, Eggers C, Kalbe E, Weisenbach S, Hohmann C, Vollmar S, et al. Neurotransmitter changes in dementia with Lewy bodies and Parkinson disease dementia *in vivo*. *Neurology.* (2010) 74:885–92. doi: 10.1212/WNL.0b013e3181d55f61
123. Kotagal V, Müller MLTM, Kaufer DI, Koeppe RA, Bohnen NI. Thalamic cholinergic innervation is spared in Alzheimer disease compared to parkinsonian disorders. *Neurosci Lett.* (2012) 514:169–72. doi: 10.1016/j.neulet.2012.02.083
124. Shimada H, Hirano S, Sinotoh H, Ota T, Tanaka N, Sato K, et al. Dementia with lewy bodies can be well-differentiated from Alzheimer's disease by measurement of brain acetylcholinesterase activity - a [11C]MP4A PET study. *Int J Geriatr Psychiatry.* (2015) 30:1105–13. doi: 10.1002/gps.4338
125. Meyer PM, Strecker K, Kendziorra K, Becker G, Hesse S, Woelpl D, et al. Reduced α4β2*-nicotinic acetylcholine receptor binding and its relationship to mild cognitive and depressive symptoms in Parkinson disease. *Arch Gen Psychiatry.* (2009) 66:866–77. doi: 10.1001/archgenpsychiatry.2009.106
126. Colloby S, Pery E, Pakrasi S, Pimlott S, Wyper D, McKeith I, et al. Nicotinic 123I-5IA-85380 single photon emission computed tomography as a predictor of cognitive progression in Alzheimer's disease and dementia with Lewy bodies. *Am J Geriatr Psychiatry.* (2010) 18:86–90. doi: 10.1097/JGP.0b013e3181b972aa
127. Edison P, Rowe CC, Rinne JO, Ng S, Ahmed I, Kemppainen N, et al. Amyloid load in Parkinson's disease dementia and Lewy body dementia measured with [11C]PIB positron emission tomography. *J Neurol Neurosurg Psychiatry.* (2008) 79:1331–8. doi: 10.1136/jnnp.2007.127878
128. Jokinen P, Scheinin N, Aalto S, Någren K, Savisto N, Parkkola R, et al. [11C]PIB-, [18F]FDG-PET and MRI imaging in patients with Parkinson's disease with and without dementia. *Parkinsonism Relat Disord.* (2010) 16:666–70. doi: 10.1016/j.parkreldis.2010.08.021
129. Gomperts SN, Locascio JJ, Rentz D, Santarlasci A, Marquie M, Johnson KA, et al. Amyloid is linked to cognitive decline in patients with Parkinson disease without dementia. *Neurology.* (2013) 80:85–91. doi: 10.1212/WNL.0b013e31827b1a07
130. Petrou M, Dwamena BA, Foerster BR, Maceachern MP, Bohnen NI, Müller ML, et al. Amyloid deposition in Parkinson's disease and cognitive impairment: a systematic review. *Move Disord.* (2015) 30:928–35. doi: 10.1002/mds.26191
131. Shah N, Frey KA, Müller MLTM, Petrou M, Kotagal V, Koeppe RA, et al. Striatal and cortical β-Amyloidopathy and cognition in Parkinson's disease. *Move Disord.* (2016) 31:111–7. doi: 10.1002/mds.26369
132. Ahktar R, Xie S, Chen Y, Rick J, Gross R, Nasrallah I, et al. Regional brain amyloid-β Accumulation associates with domain-specific cognitive performance in Parkinson disease without dementia. *PLoS ONE.* (2017) 12:e0177924. doi: 10.1371/journal.pone.0177924

133. Fiorenzato E, Biundo R, Cecchin D, Frigo AC, Kim J, Weis L, et al. Brain amyloid contribution to cognitive dysfunction in early-stage Parkinson's disease: the PPMI dataset. *J Alzheimers Dis.* (2018) 66:229–37. doi: 10.3233/JAD-180390
134. Melzer TR, Stark MR, Keenan RJ, Myall DJ, MacAskill MR, Pitcher TL, et al. Beta amyloid deposition is not associated with cognitive impairment in Parkinson's disease. *Front Neurol.* (2019) 10:391. doi: 10.3389/fneur.2019.00391
135. Na S, Jeong H, Park JS, Chung YA, Song IU. The impact of amyloid-beta positivity with 18f-florbetaben pet on neuropsychological aspects in parkinson's disease dementia. *Metabolites.* (2020) 10:380. doi: 10.3390/metabo10100380
136. Biundo R, Weis L, Fiorenzato E, Pistonesi F, Cagnin A, Bertoldo A, et al. The contribution of beta-amyloid to dementia in Lewy body diseases: a 1-year follow-up study. *Brain Commun.* (2021) 3:fcab180. doi: 10.1093/braincomms/fcab180
137. Gomperts SN, Locascio JJ, Makaretz SJ, Schultz A, Caso C, Vasdev N, et al. Tau positron emission tomographic imaging in the lewy body diseases. *JAMA Neurol.* (2016) 73:1334–41. doi: 10.1001/jamaneurol.2016.3338
138. Kantarci K, Lowe VJ, Boeve BF, Senjem ML, Tosakulwong N, Lesnick TG, et al. AV-1451 tau and β-amyloid positron emission tomography imaging in dementia with Lewy bodies. *Ann Neurol.* (2017) 81:58–67. doi: 10.1002/ana.24825
139. Buongiorno M, Antonelli F, Compta Y, Fernandez Y, Pavia J, Lomeña F, et al. Cross-sectional and longitudinal cognitive correlates of FDDNP PET and CSF amyloid-β and tau in Parkinson's disease. *J Alzheimers Dis.* (2017) 55:1261–72. doi: 10.3233/JAD-160698
140. Edison P, Ahmed I, Fan Z, Hinz R, Gelosa G, Ray Chaudhuri K, et al. Microglia, amyloid, and glucose metabolism in parkinson's disease with and without dementia. *Neuropsychopharmacology.* (2013) 38:938–49. doi: 10.1038/npp.2012.255
141. Fan Z, Aman Y, Ahmed I, Chetelat G, Landeau B, Ray Chaudhuri K, et al. Influence of microglial activation on neuronal function in Alzheimer's and Parkinson's disease dementia. *Alzheimers Dement.* (2015) 11:608–21.e7. doi: 10.1016/j.jalz.2014.06.016
142. Femminella GD, Ninan S, Atkinson R, Fan Z, Brooks DJ, Edison P. Does microglial activation influence hippocampal volume and neuronal function in Alzheimer's disease and Parkinson's disease dementia? *J Alzheimers Dis.* (2016) 51:1275–89. doi: 10.3233/JAD-150827
143. Wilson H, Dervenoulas G, Pagano G, Tyacke RJ, Polychronis S, Myers J, et al. Imidazoline 2 binding sites reflecting astroglia pathology in Parkinson's disease: an *in vivo* 11C-BU99008 PET study. *Brain.* (2019) 142:3116–28. doi: 10.1093/brain/awz260
144. Meyer PT, Frings L, Hellwig S. Update on SPECT and PET in parkinsonism - part 2: biomarker imaging of cognitive impairment in Lewy-body diseases. *Curr Opin Neurol.* (2014) 27:398–404. doi: 10.1097/WCO.0000000000000107
145. Gasca-Salas C, Clavero P, García-García D, Obeso JA, Rodríguez-Oroz MC. Significance of visual hallucinations and cerebral hypometabolism in the risk of dementia in Parkinson's disease patients with mild cognitive impairment. *Hum Brain Mapp.* (2016) 37:968–77. doi: 10.1002/hbm.23080
146. Tang CC, Poston KL, Dhawan V, Eidelberg D. Abnormalities in metabolic network activity precede the onset of motor symptoms in Parkinson's disease. *J Neurosci.* (2010) 30:1049–56. doi: 10.1523/JNEUROSCI.4188-09.2010
147. Meles SK, Renken RJ, Pagani M, Teune LK, Arnaldi D, Morbelli S, et al. Abnormal pattern of brain glucose metabolism in Parkinson's disease: replication in three European cohorts. *Eur J Nucl Med Mol Imaging.* (2020) 47:437–50. doi: 10.1007/s00259-019-04570-7
148. Schrag A, Siddiqui UF, Anastasiou Z, Weintraub D, Schott JM. Clinical variables and biomarkers in prediction of cognitive impairment in patients with newly diagnosed Parkinson's disease: a cohort study. *Lancet Neurol.* (2017) 16:66–75. doi: 10.1016/S1474-4422(16)30328-3
149. Sampedro F, Marín-Lahoz J, Martínez-Horta S, Pagonabarraga J, Kulisevsky J. Dopaminergic degeneration induces early posterior cortical thinning in Parkinson's disease. *Neurobiol Dis.* (2019) 124:29–35. doi: 10.1016/j.nbd.2018.11.001
150. Müller MLTM, Bohnen NI. Cholinergic dysfunction in parkinson's disease. *Curr Neurol Neurosci Rep.* (2013) 13:377. doi: 10.1007/s11910-013-0377-9
151. Bohnen NI, Kanel P, Müller MLTM. Molecular imaging of the cholinergic system in Parkinson's disease. *Int Rev Neurobiol.* (2018) 141:211–50. doi: 10.1016/bs.irn.2018.07.027
152. Bohnen NI, Albin RL, Müller MLTM, Petrou M, Kotagal V, Koeppe NI, et al. Frequency of cholinergic and caudate nucleus dopaminergic deficits across the predemented cognitive spectrum of parkinson disease and evidence of interaction effects. *JAMA Neurol.* (2015) 72:194–200. doi: 10.1001/jamaneurol.2014.2757
153. Pimlott SL, Piggott M, Owens J, Greally E, Court JA, Jaros E, et al. Nicotinic acetylcholine receptor distribution in Alzheimer's disease, dementia with lewy bodies, Parkinson's disease, and vascular dementia: *in vitro* binding study using 5-[125I]-A-85380. *Neuropsychopharmacology.* (2004) 29:108–16. doi: 10.1038/sj.npp.1300302
154. Kehagia AA, Barker RA, Robbins TW. Cognitive impairment in Parkinson's disease: the dual syndrome hypothesis. *Neurodegenerat Dis.* (2012) 11:79–92. doi: 10.1159/000341998
155. Winer JR, Maass A, Pressman P, Stiver J, Schonhaut DR, Baker SL, et al. Associations between Tau, β-amyloid, and cognition in Parkinson disease. *JAMA Neurol.* (2018) 75:227–35. doi: 10.1001/jamaneurol.2017.3713
156. Wang Q, Liu Y, Zhou J. Neuroinflammation in Parkinson's disease and its potential as therapeutic target. *Transl Neurodegenerat.* (2015) 4:19. doi: 10.1186/s40035-015-0042-0
157. Le W, Wu J, Tang Y. Protective microglia and their regulation in Parkinson's disease. *Front Mol Neurosci.* (2016) 9:89. doi: 10.3389/fnmol.2016.00089
158. McGeer PL, McGeer EG. Inflammation and neurodegeneration in Parkinson's disease. *Parkinsonism Relat Disord.* (2004) 10(Suppl 1):S3–7. doi: 10.1016/j.parkreldis.2004.01.005
159. Kouli A, Camacho M, Allinson K, Williams-Gray CH. Neuroinflammation and protein pathology in Parkinson's disease dementia. *Acta Neuropathol Commun.* (2020) 8:211. doi: 10.1186/s40478-020-01083-5
160. Best L, Ghadery C, Pavese N, Tai YF, Strafella AP. New and Old TSPO PET radioligands for imaging brain microglial activation in neurodegenerative disease. *Curr Neurol Neurosci Rep.* (2019) 19:24. doi: 10.1007/s11910-019-0934-y
161. Terada T, Yokokura M, Yoshikawa E, Futatsubashi M, Kono S, Konishi T, et al. Extrastriatal spreading of microglial activation in Parkinson's disease: a positron emission tomography study. *Annal Nucl Med.* (2016) 30:579–87. doi: 10.1007/s12149-016-1099-2
162. Volterra A, Meldolesi J. Astrocytes, from brain glue to communication elements: the revolution continues. *Nat Rev Neurosci.* (2005) 6:626–40. doi: 10.1038/nrn1722
163. Olmos G, Alemany R, Escriba PV, García-Sevilla JA. The effects of chronic imidazoline drug treatment on glial fibrillary acidic protein concentrations in rat brain. *Br J Pharmacol.* (1994) 111:997–1002. doi: 10.1111/j.1476-5381.1994.tb14842.x
164. Booth HDE, Hirst WD, Wade-Martins R. The role of astrocyte dysfunction in Parkinson's disease pathogenesis. *Trends Neurosci.* (2017) 40:358–70. doi: 10.1016/j.tins.2017.04.001
165. Hammes J, Theis H, Giehl K, Hoenig MC, Greuel A, Tittgemeyer M, et al. Dopamine metabolism of the nucleus accumbens and fronto-striatal connectivity modulate impulse control. *Brain.* (2019) 142:733–43. doi: 10.1093/brain/awz007
166. Pellicano C, Niccolini F, Wu K, O'Sullivan SS, Lawrence AD, Lees AJ, et al. Morphometric changes in the reward system of Parkinson's disease patients with impulse control disorders. *J Neurol.* (2015) 262:2653–61. doi: 10.1007/s00415-015-7892-3
167. Tessitore A, Santangelo G, De Micco R, Vitale C, Giordano A, Raimo S, et al. Cortical thickness changes in patients with Parkinson's disease and impulse control disorders. *Parkinsonism Relat Disord.* (2016) 24:119–25. doi: 10.1016/j.parkreldis.2015.10.013
168. Biundo R, Weis L, Facchini S, Formento-Dojot P, Vallelunga A, Pilleri M, et al. Patterns of cortical thickness associated with impulse control disorders in Parkinson's disease. *Move Disord.* (2015) 30:688–95. doi: 10.1002/mds.26154
169. Imperiale F, Agosta F, Canu E, Markovic V, Inuggi A, Jecmenica-Lukic M, et al. Brain structural and functional signatures of impulsive-compulsive behaviours in Parkinson's disease. *Mol Psychiatry.* (2018) 23:459–66. doi: 10.1038/mp.2017.18

170. Tessitore A, De Micco R, Giordano A, di Nardo F, Caiazzo G, Siciliano M, et al. Intrinsic brain connectivity predicts impulse control disorders in patients with Parkinson's disease. *Move Disord.* (2017) 32:1710–9. doi: 10.1002/mds.27139
171. Ye Z, Hammer A, Münte TF. Pramipexole modulates interregional connectivity within the sensorimotor network. *Brain Connect.* (2017) 7:258–63. doi: 10.1089/brain.2017.0484
172. Ricciardi L, Lambert C, De Micco R, Morgante F, Edwards M. Can we predict development of impulsive-compulsive behaviours in Parkinson's disease? *J Neurol Neurosurg Psychiatry.* (2018) 89:476–81. doi: 10.1136/jnnp-2017-317007
173. Yoo HB, Lee JY, Lee JS, Kang H, Kim YK, Song IC, et al. Whole-brain diffusion-tensor changes in parkinsonian patients with impulse control disorders. *J Clin Neurol.* (2015) 11:42–7. doi: 10.3988/jcn.2015.11.1.42
174. Canu E, Agosta F, Markovic V, Petrovic I, Stankovic I, Imperiale F, et al. White matter tract alterations in Parkinson's disease patients with punding. *Parkinsonism Relat Disord.* (2017) 43:85–91. doi: 10.1016/j.parkreldis.2017.07.025
175. Zadeh MM, Ashraf-Ganjouei A, Sherbaf FG, Haghshomar M, Aarabi MH. White matter tract alterations in drug-Naïve Parkinson's disease patients with impulse control disorders. *Front Neurol.* (2018) 9:163. doi: 10.3389/fneur.2018.00163
176. Carriere N, Lopes R, Defebvre L, Delmaire C, Dujardin K. Impaired corticostriatal connectivity in impulse control disorders in Parkinson disease. *Neurology.* (2015) 84:2116–23. doi: 10.1212/WNL.0000000000001619
177. Tessitore A, Santangelo G, De Micco R, Giordano A, Raimo S, Amboni M, et al. Resting-state brain networks in patients with Parkinson's disease and impulse control disorders. *Cortex.* (2017) 94:63–72. doi: 10.1016/j.cortex.2017.06.008
178. Petersen K, Van Wouwe N, Stark A, Lin YC, Kang H, Trujillo-Diaz P, et al. Ventral striatal network connectivity reflects reward learning and behavior in patients with Parkinson's disease. *Hum Brain Mapp.* (2018) 39:509–21. doi: 10.1002/hbm.23860
179. Navalpotro-Gomez I, Kim J, Paz-Alonso PM, Delgado-Alvarado M, Quiroga-Varela A, Jimenez-Urbieta H, et al. Disrupted salience network dynamics in Parkinson's disease patients with impulse control disorders. *Parkinsonism Relat Disord.* (2020) 70:74–81. doi: 10.1016/j.parkreldis.2019.12.009
180. Koh J, Kaneoke Y, Donishi T, Ishida T, Sakata M, Hiwatani Y, et al. Increased large-scale inter-network connectivity in relation to impulsivity in Parkinson's disease. *Sci Rep.* (2020) 10:11418. doi: 10.1038/s41598-020-68266-x
181. Mata-Marín D, Pineda-Pardo JÁ, Molina JA, Alonso-Frech F, Vela L, Obeso I. Aberrant salient and corticolimbic connectivity in hypersexual Parkinson's disease. *Brain Connect.* (2021). doi: 10.1089/brain.2020.0868. [Epub ahead of print].
182. Rao H, Mamikonyan E, Detre JA, Siderowf AD, Stern MB, Potenza MN, et al. Decreased ventral striatal activity with impulse control disorders in Parkinson's Disease. *Move Disord.* (2010) 25:1660–9. doi: 10.1002/mds.23147
183. Frosini D, Pesaresi I, Cosottini M, Belmonte G, Rossi C, Dell'Osso L, et al. Parkinson's disease and pathological gambling: results from a functional MRI study. *Move Disord.* (2010) 25:2449–53. doi: 10.1002/mds.23369
184. Voon V, Gao J, Brezing C, Symmonds M, Ekanayake V, Fernandez H, et al. Dopamine agonists and risk: Impulse control disorders in Parkinson's; Disease. *Brain.* (2011) 134:1438-46. doi: 10.1093/brain/awr080
185. Politis M, Loane C, Wu K, O'Sullivan SS, Woodhead Z, Kiferle L, et al. Neural response to visual sexual cues in dopamine treatment-linked hypersexuality in Parkinson's disease. *Brain.* (2013) 136:400-11. doi: 10.1093/brain/aws326
186. Girard R, Obeso I, Thobois S, Park SA, Vidal T, Favre E, et al. Wait and you shall see: sexual delay discounting in hypersexual Parkinson's disease. *Brain.* (2019) 142:146–62. doi: 10.1093/brain/awy298
187. Paz-Alonso PM, Navalpotro-Gomez I, Boddy P, Dacosta-Aguayo R, Delgado-Alvarado M, Quiroga-Varela A, et al. Functional inhibitory control dynamics in impulse control disorders in Parkinson's disease. *Move Disord.* (2020) 35:316–25. doi: 10.1002/mds.27885
188. Haagensen BN, Herz DM, Meder D, Madsen KH, Løkkegaard A, Siebner HR. Linking brain activity during sequential gambling to impulse control in Parkinson's disease. *NeuroImage Clin.* (2020) 27:102330. doi: 10.1016/j.nicl.2020.102330
189. Tahmasian M, Rochhausen L, Maier F, Williamson KL, Drzezga A, Timmermann L, et al. Impulsivity is associated with increased metabolism in the fronto-insular network in Parkinson's Disease. *Front Behav Neurosci.* (2015) 9:317. doi: 10.3389/fnbeh.2015.00317
190. Verger A, Klesse E, Chawki MB, Witjas T, Azulay JP, Eusebio A, et al. Brain PET substrate of impulse control disorders in Parkinson's disease: a metabolic connectivity study. *Hum Brain Mapp.* (2018) 39:3178–86. doi: 10.1002/hbm.24068
191. Marín-Lahoz J, Sampedro F, Horta-Barba A, Martínez-Horta S, Aracil-Bolaños I, Camacho V, et al. Preservation of brain metabolism in recently diagnosed Parkinson's impulse control disorders. *Eur J Nucl Med Mol Imaging.* (2020) 47:2165–74. doi: 10.1007/s00259-019-04664-2
192. Cilia R, Ko JH, Cho SS, van Eimeren T, Marotta G, Pellecchia G, et al. Reduced dopamine transporter density in the ventral striatum of patients with Parkinson's disease and pathological gambling. *Neurobiol Dis.* (2010) 39:98–104. doi: 10.1016/j.nbd.2010.03.013
193. Joutsa J, Martikainen K, Niemelä S, Johansson J, Forsback S, Rinne JO, et al. Increased medial orbitofrontal [18F]fluorodopa uptake in Parkinsonian impulse control disorders. *Move Disord.* (2012) 27:778–82. doi: 10.1002/mds.24941
194. Voon V, Rizos A, Chakravartty R, Hulholland N, Robinson S, Howell N, et al. Impulse control disorders in Parkinson's disease: decreased striatal dopamine transporter levels. *J Neurol Neurosurg Psychiatry.* (2014) 85:148–52.
195. Vriend C, Nordbeck AH, Booij J, van der Werf YD, Pattij T, Voorn P, et al. Reduced dopamine transporter binding predates impulse control disorders in Parkinson's disease. *Move Disord.* (2014) 29:904–11. doi: 10.1002/mds.25886
196. Smith KM, Xie SX, Weintraub D. Incident impulse control disorder symptoms and dopamine transporter imaging in Parkinson disease. *J Neurol Neurosurg Psychiatry.* (2016) 87:864–70. doi: 10.1136/jnnp-2015-311827
197. Premi E, Pilotto A, Garibotto V, Bigni B, Turrone R, Alberici A, et al. Impulse control disorder in PD: a lateralized monoaminergic frontostriatal disconnection syndrome? *Parkinsonism Relat Disord.* (2016) 30:62–6. doi: 10.1016/j.parkreldis.2016.05.028
198. Navalpotro-Gomez I, Dacosta-Aguayo R, Molinet-Dronda F, Martin-Bastida A, Botas-Peñin A, Jimenez-Urbieta H, et al. Nigrostriatal dopamine transporter availability, and its metabolic and clinical correlates in Parkinson's disease patients with impulse control disorders. *Eur J Nucl Med Mol Imaging.* (2019) 46:2065–76. doi: 10.1007/s00259-019-04396-3. [Epub ahead of print].
199. Hinkle JT, Mills KA, Perepezko K, Pontone GM. Bidirectional correlations between dopaminergic function and motivation in Parkinson's disease. *J Geriatr Psychiatry Neurol.* (2021) 891988721996802. doi: 10.1177/0891988721996802
200. Boileau I, Guttman M, Rusjan P, Adams J, Houle S, Tong J, et al. Decreased binding of the D3 dopamine receptor-preferring ligand [11C]-(+)-PHNO in drug-naive Parkinson's disease. *Brain.* (2009) 132(Pt 5):1366–75. doi: 10.1093/brain/awn337
201. Payer D, Guttman M, Kish S, Tong J, Strafella A, Zack M, et al. [^{11}C]-(+)-PHNO PET imaging of dopamine D(2/3) receptors in Parkinson's disease with impulse control disorders. *Mov Disord.* (2015) 30:160–6. doi: 10.1002/mds.26135
202. Stark AJ, Smith CT, Petersen KJ, Trujillo P, Van Wouwe NC, Donahue MJ, et al. [^{18}F]fallypride characterization of striatal and extrastriatal $D_{2/3}$ receptors in Parkinson's disease. *Neuroimage Clin.* (2018) 18:433–42. doi: 10.1016/j.nicl.2018.02.010
203. Van Eimeren T, Pellecchia G, Cilia R, Ballanger B, Steeves TDL, Houle S, et al. Drug-induced deactivation of inhibitory networks predicts pathological gambling in PD. *Neurology.* (2010) 75:1711-6. doi: 10.1212/WNL.0b013e3181fc27fa
204. Antonelli F, Ko J, Miyaski J, Lang A, Houle S, Valzania F, et al. Dopamine-agonists and impulsivity in Parkinson's disease: Impulsive choices vs. impulsive actions. *Hum Brain Mapp.* (2014) 35:2499–506. doi: 10.1002/hbm.22344
205. Steeves TDL, Miyasaki J, Zurowski M, Lang AE, Pellecchia G, Van Eimeren T, et al. Increased striatal dopamine release in Parkinsonian patients

with pathological gambling: a [11C] raclopride PET study. *Brain*. (2009) 132:1376-85. doi: 10.1093/brain/awp054

206. O'Sullivan SS, Wu K, Politis M, Lawrence AD, Evans AH, Bose SK, et al. Cue-induced striatal dopamine release in Parkinson's disease-associated impulsive-compulsive behaviours. *Brain*. (2011) 134:969-78. doi: 10.1093/brain/awr003
207. Ray N, Miyaski J, Zurowski M, Ko J, Choo S, Pellecchia G, Antonelli F, et al. Extrastriatal dopaminergic abnormalities of DA homeostasis in Parkinson's patients with medication-induced pathological gambling: A [11C] FLB-457 and PET study. *Neurobiol Dis*. (2012) 48:519–25. doi: 10.1016/j.nbd.2012.06.021
208. Wu K, Politis M, O'Sullivan SS, Lawrence AD, Warsi S, Bose S, et al. Single versus multiple impulse control disorders in Parkinson's disease: an 11C-raclopride positron emission tomography study of reward cue-evoked striatal dopamine release. *J Neurol.* (2015) 262:1504–14. doi: 10.1007/s00415-015-7722-7
209. Cilia R, Siri C, Marotta G, Isaias IU, De Gaspari D, Canesi M, et al. Functional abnormalities underlying pathological gambling in parkinson disease. *Arch Neurol.* (2008) 65:1604–11. doi: 10.1001/archneur.65.12.1604
210. Martini A, Tamburin S, Biundo R, Weis L, Antonini A, Pizzolo C, et al. Incentive-driven decision-making networks in de novo and drug-treated Parkinson's disease patients with impulsive-compulsive behaviors: a systematic review of neuroimaging studies. *Parkinsonism Relat Disord*. (2020) 78:165–77. doi: 10.1016/j.parkreldis.2020.07.020
211. Seibyl JP, Marchek KL, Quinlan D, Sheff K, Zoghbi S, Zea-Ponce Y, et al. Decreased single-photon emission computed tomographic {123I}β-CIT striatal uptake correlates with symptom severity in parkinson's disease. *Annal Neurol.* (1995) 38:589–98. doi: 10.1002/ana.410380407
212. Lee JY, Seo SH, Kim YK, Yoo HB, Kim YE, Song IC, et al. Extrastriatal dopaminergic changes in Parkinson's disease patients with impulse control disorders. *J Neurol Neurosurg Psychiatry*. (2014) 85:23–30. doi: 10.1136/jnnp-2013-305549
213. Voon V, Napier TC, Frank MJ, Sgambato-Faure V, Grace AA, Rodriguez-Oroz M, et al. Impulse control disorders and levodopa-induced dyskinesias in Parkinson's disease: an update. *Lancet Neurol.* (2017) 16:238–50. doi: 10.1016/S1474-4422(17)30004-2
214. Honkanen EA, Saari L, Orte K, Gardberg M, Noponen T, Joutsa J, et al. No link between striatal dopaminergic axons and dopamine transporter imaging in Parkinson's disease. *Move Disord.* (2019) 34:1562–6. doi: 10.1002/mds.27777
215. Majuri J, Joutsa J. Molecular imaging of impulse control disorders in Parkinson's disease. *Eur J Nucl Med Mol Imaging*. (2019) 46:2220–22. doi: 10.1007/s00259-019-04459-5
216. Brittain JS, Watkins KE, Joundi RA, Ray NJ, Holland P, Green AL, et al. A role for the subthalamic nucleus in response inhibition during conflict. *J Neurosci*. (2012) 32:13396-401. doi: 10.1523/JNEUROSCI.2259-12.2012

Conflict of Interest: AM-B, MD-A, and IN-G declare that the research was conducted in the absence of any commercial or financial relationships that could be construed as a potential conflict of interest. MR-O received financial support for her research from national and local government institutions in Spain (Carlos III Institute of Health, Navarra Government) and honoraria from Insightec, and Boston Scientific for lectures, travel and accommodation to attend scientific meetings.

Publisher's Note: All claims expressed in this article are solely those of the authors and do not necessarily represent those of their affiliated organizations, or those of the publisher, the editors and the reviewers. Any product that may be evaluated in this article, or claim that may be made by its manufacturer, is not guaranteed or endorsed by the publisher.

frontiers in Neurology

ORIGINAL RESEARCH
published: 01 March 2022
doi: 10.3389/fneur.2021.760518

Quantification of Brain β-Amyloid Load in Parkinson's Disease With Mild Cognitive Impairment: A PET/MRI Study

Michela Garon[1], Luca Weis[1], Eleonora Fiorenzato[2], Francesca Pistonesi[1], Annachiara Cagnin[3,4], Alessandra Bertoldo[4,5], Mariagiulia Anglani[6], Diego Cecchin[4,7], Angelo Antonini[1,4,8] and Roberta Biundo[2,8]*

[1] Parkinson and Movement Disorders Unit, Department of Neuroscience, University of Padua, Padua, Italy, [2] Department of General Psychology, University of Padua, Padua, Italy, [3] Department of Neuroscience, University of Padua, Padua, Italy, [4] Padova Neuroscience Center, University of Padua, Padua, Italy, [5] Department of Information Engineering, University of Padua, Padua, Italy, [6] Neuroradiology Unit, Padua University Hospital, Padua, Italy, [7] Nuclear Medicine Unit, Department of Medicine - DIMED, Padua University Hospital, Padua, Italy, [8] Study Center for Neurodegeneration, University of Padua, Padua, Italy

OPEN ACCESS

Edited by:
Frederic Sampedro,
Sant Pau Institute for Biomedical Research, Spain

Reviewed by:
Maria Salsone,
National Research Council (CNR), Italy
Arnau Puig-Davi,
Hospital de la Santa Creu i Sant Pau, Spain

***Correspondence:**
Angelo Antonini
angelo3000@yahoo.com
orcid.org/0000-0003-1040-2807

Specialty section:
This article was submitted to Applied Neuroimaging, a section of the journal Frontiers in Neurology

Received: 18 August 2021
Accepted: 24 December 2021
Published: 01 March 2022

Citation:
Garon M, Weis L, Fiorenzato E, Pistonesi F, Cagnin A, Bertoldo A, Anglani M, Cecchin D, Antonini A and Biundo R (2022) Quantification of Brain β-Amyloid Load in Parkinson's Disease With Mild Cognitive Impairment: A PET/MRI Study. Front. Neurol. 12:760518. doi: 10.3389/fneur.2021.760518

Background: Mild cognitive impairment in Parkinson's disease (PD-MCI) is associated with faster cognitive decline and conversion to dementia. There is uncertainty about the role of β-amyloid (Aβ) co-pathology and its contribution to the variability in PD-MCI profile and cognitive progression.

Objective: To study how presence of Aβ affects clinical and cognitive manifestations as well as regional brain volumes in PD-MCI.

Methods: Twenty-five PD-MCI patients underwent simultaneous PET/3T-MRI with [^{18}F]flutemetamol and a clinical and neuropsychological examination allowing level II diagnosis. We tested pairwise differences in motor, clinical, and cognitive features with Mann–Whitney U test. We calculated [^{18}F]flutemetamol (FMM) standardized uptake value ratios (SUVR) in striatal and cortical ROIs, and we performed a univariate linear regression analysis between the affected cognitive domains and the mean SUVR. Finally, we investigated differences in cortical and subcortical brain regional volumes with magnetic resonance imaging (MRI).

Results: There were 8 Aβ+ and 17 Aβ- PD-MCI. They did not differ for age, disease duration, clinical, motor, behavioral, and global cognition scores. PD-MCI-Aβ+ showed worse performance in the overall executive domain ($p = 0.037$). Subcortical ROIs analysis showed significant Aβ deposition in PD-MCI-Aβ+ patients in the right caudal and rostral middle frontal cortex, in precuneus, in left paracentral and pars triangularis ($p < 0.0001$), and bilaterally in the putamen ($p = 0.038$). Cortical regions with higher amyloid load correlated with worse executive performances ($p < 0.05$). Voxel-based morphometry (VBM) analyses showed no between groups differences.

Conclusions: Presence of cerebral Aβ worsens executive functions, but not motor and global cognitive abilities in PD-MCI, and it is not associated with middle-temporal cortex atrophy. These findings, together with the observation of significant proportion of PD-MCI-Aβ-, suggest that Aβ may not be the main pathogenetic determinant of cognitive deterioration in PD-MCI, but it would rather aggravate deficits in domains vulnerable to Parkinson primary pathology.

Keywords: Parkinson's disease, mild cognitive impairment, amyloid-β, atrophy, cognition, executive functions, dementia, PET

INTRODUCTION

Cognitive alterations in Parkinson's disease (PD) are among the most disabling non-motor symptoms, and they impact negatively on patient's and caregiver's quality of life and can be present already in early stages of disease. Parkinson's disease with mild cognitive impairment (PD-MCI) have up to six-fold higher risk to develop dementia (PDD) (1). However, the characteristics and the severity of the cognitive profile as well as the rate of progression to dementia are heterogenous (2, 3). Factors contributing to variability in PD cognitive performance are: (a) presence of specific genetic mutations or variants (4), (b) characteristics of phenotypic manifestations including dominant akinetic rigid form or early occurrence of postural instability and hallucinations, (c) variable expression of synuclein pathology, in particular presence of cortical Lewy bodies, (d) presence of misfolded β-amyloid (Aβ), and in some cases of tau neurofibrillary tangles, which are considered typical Alzheimer hallmarks. Magnetic resonance imaging (MRI) studies in PD-MCI have reported variable structural and functional patterns without clarifying the underlying mechanisms (5–7). Some studies have suggested contribution of Aβ cortical and subcortical depositions to cognitive decline in PD particularly in association with attentive and executive deficits, while others indicated an increased risk of dementia in the late disease stages (8–13). These differences may be related to the heterogeneous methodology adopted including variability in age and sex as well as poorly characterized cognitive diagnosis in relatively small cohorts (11, 14–17). In a recent PET/MRI study (18) in cognitively well-characterized Lewy Body disease (LBD) patients, we observed an integral role of brain amyloidosis in cognitive profile and progression, affecting mainly global cognition (MoCA, MMSE), attentive/executive, and semantic recall abilities. Our study also confirmed the Aβ contribution to cognitive dysfunction in a significant proportion of our Lewy body dementia subjects, although half of the demented patients were Aβ-. However, we did not explore whether and at which extent presence of amyloid deposition contributes specifically to MCI status in PD patients. Considering MCI established heterogeneity as well as its greater vulnerability to dementia, the purpose of this analysis is to investigate whether amyloidosis distinguishes a specific PD-MCI profile across the various and heterogeneous patterns and if so its contribution to dementia development. Hence, in the current study, we expanded previous analysis of PET/MRI data and focused specifically on the quantification of [^{18}F]flutemetamol (FMM) deposition in the PD-MCI cohort, and in their related cognitive, clinical, and brain structural correlates.

METHODS

Participants

Data of 25 PD-MCI were analyzed from the cohort recruited in the context of a previously published study (18). Patients were recruited at the Parkinson's Disease and Movement Disorders Unit of Neurology Clinic in Padua from 2016 to 2020. Parkinson's disease diagnosis was based on the most recent MDS clinical diagnostic criteria (19), confirmed by abnormal DaTscan SPECT imaging. Exclusion criteria included deep brain stimulation, atypical Parkinsonian disorders, severe psychiatric or neurological comorbidity, presence of pathogenic genetic mutations, and clinically relevant cerebrovascular disease on MRI. All participants underwent a complete neuropsychological evaluation, simultaneous PET/MRI with FMM, and a genetic assessment. A customized genetic panel (more than 90 genes associated to Movement Disorders) was used to analyze patients' DNA, and only individuals without genetic mutations were further included in this study. Regarding genetic variability as a possible confounding factor, we excluded from this study subjects carrying known PD genetic mutations and variants, but we did not screen for apolipoprotein E (APOE) ε4. In particular, mutations of the glucocerebrocidase (GBA) gene have been associated with more rapid cognitive decline in PD-MCI, with subsequent α-synuclein deposition enhancement as well as effects in proteins implicated in dopamine production, metabolism, and signaling (20).

The study was approved by the Ethic Committee of the University of Padua (4340/AO/17). All patients gave written informed consent according to the Declaration of Helsinki.

Clinical and Neuropsychological Examination

Demographic and clinical characteristics were collected by expert neurologists (AA, ACC). The severity of extrapyramidal symptoms was assessed with the motor Unified Parkinson's Disease Rating Scale (21) as well as with the Hoehn and Yahr score "on" medication. Levodopa Equivalent Daily Dose and Dopamine Agonist Equivalent Daily Dose were calculated for each patient (22). Patients' age at disease onset was defined as the age at which they noticed the first motor symptom suggestive of PD. All participants underwent a comprehensive

neuropsychological evaluation, in line with the MDS task force level II PD-MCI diagnostic criteria (23) [for further details on cognitive tests adopted, see Fiorenzato et al. (24)]. In all patients the evaluation of functional and instrumental activities of daily living was performed independently of the impairment ascribable to motor or autonomic symptoms. Regarding the behavioral evaluation, the Beck Depression Inventory (BDI-II), Starkstein Apathy Scale, and the State-Trait Anxiety Inventory (STAI-Y1 and Y2) were used to detect the presence of eventual depression, apathy, state and trait anxiety, respectively. Patients were evaluated in "on" medication state. The cognitive tests were administered by trained neuropsychologists, in the morning, on two separate occasions within 3–5 days.

PET/MRI Acquisition and PET/FMM Images Classification

Parkinson's disease patients in accordance with the amyloid imaging procedure guidelines (25) received an intravenous injection of about 185 MBq FMM (performed manually over 10 s and flushed with 30 ml of saline over about 15 ± 5 s) directly in an integrated 3T PET/MRI system (Biograph mMR; Siemens, Erlangen, Germany). Images were acquired between 0–10 and 90–110 min after injection according to Cecchin et al. (26). Anatomical volumetric data *via* T1-weighted-3D magnetization-prepared rapid acquisition gradient echo sequence (TR 1.900 ms, TE 2.53 ms, slice thickness 1 mm, matrix 256 × 256, FOV 250 mm) were simultaneously acquired. Additionally, a 1 mm-isotropic T2-weighted-3D, and Two-Dimensional Susceptibility-Weighted Imaging, were acquired for clinical evaluation, excluding secondary parkinsonisms, the presence of vascular brain damage, and allowing visual rating scales assessment.

Visual assessment of FMM images is a robust and reliable method for detection of brain neuritic Aβ plaques (25). A binary visual classification was performed by an expert nuclear medicine physician (DC, with both in-person and e-training), blinded to cognitive status and diagnosis, who rated each scan as amyloid-positive (Aβ+) or negative (Aβ-).

For further details about PET reconstruction and PET/FMM images classification procedures see Biundo et al. (18).

PET Quantification

The PET frames were realigned, averaged, and co-registered with their respective MRI scans with the Freesurfer v7.01 (http://surfer.nmr.mgh.harvard.edu/). Since realignment might bias standardized uptake value ratios (SUVRs) comparison and partial volume correction (PVC) estimation (27), in order to improve the reliability of the realignment process, both T1w3d and PET were first manually z-cropped including medulla and cerebellum and rigidly realigned to the anterior commissure-posterior commissure line (AC-PC line) using the Freeview Freesurfer tool. We performed voxel-based three-compartment PVC to the MRI coregistered PET images using the PETSurfer tool in FreeSurfer (28, 29). Standardized uptake value ratios were computed to address intersubject effects using cerebellar gray matter (GM) as the reference region.

PET SUVR Subcortical ROIs

Fourteen subcortical striatal and extra striatal regions ROIs (nucleus accumbens, caudate, putamen, amygdala, globus pallidus, thalamus, and hippocampus) were extracted in the native MRI space using Freesurfer v7.01 Desikan/Killiany atlas 11 segmentations (30). Standardized uptake value ratio maps were then projected to the subcortical regions to extract the mean value for each PD patient.

PET SUVR Cortical Surface-Based Analysis

Vertex-wise general linear model (GLM) (between group comparisons) comparing cerebral cortical SUVR of the PD-MCI Aβ+/– was run using Freesurfer. Standardized uptake value ratio maps of each subject were sampled onto the left and right surfaces *via* the individual subject's surface, and a surface-based smoothing of 8-mm full width at half maximum was applied. Surface areas of significant amyloid load, which survived a cluster-wise Monte Carlo correction for multiple comparisons after running 10,000 permutations, were considered for the following steps.

PET SUVR Subcortical Analysis

Mean subcortical SUVR values were compared between hemispheres using the Wilcoxon test and tested for Left-Right hemisphere correlation using the non-parametric Spearman test. Subcortical regions with an inter-hemisphere difference $p > 0.2$ and a correlation significance of $p < 0.001$ were averaged, to reduce the degrees of freedom in multiple comparisons testing as well as to increase the statistical power. The obtained values were compared between PD-MCI-Aβ+ and Aβ- with a non-parametric Mann–Whitney U test for amyloid load.

Voxel Based MRI Cortical Analyses

The Brain Anatomical Analysis using Diffeomorphic deformation (BAAD 4.31—http://www.shiga-med.ac.jp/$\sim$hqbioph/BAAD/Welcome_to_BAAD.html) (31) and Statistical Parametric Mapping tool (SPM12, https://www.fil.ion.ucl.ac.uk/spm/software/spm12/) were used to calculate the cortical alteration patterns. This tool includes a Computational Anatomy Toolbox (CAT12)-based (http://www.neuro.uni-jena.de/cat/), T1-weighted-3D diffeomorphic segmentation after inhomogeneity correction, T1-weighted-3D quality check assessment, and Total Intracranial Volume (TIV) estimation. T2-weighted-3D was included in the multimodal segmentation to correct brain atrophy estimation for the presence of white matter lesions. Brain Anatomical Analysis using Diffeomorphic deformation integrates CAT12 tool for the normalization to the standard MNI space (31). Moreover, it provides at subject level a voxel-wise non-parametric statistical map of GM and white matter alterations, comparing each participant's normalized and segmented brain MRI images to the age- and sex-matched normative data with the SnPM13 tool (http://warwick.ac.uk/snpm), as previously described (31). See first level maps comparison, PD-MCI subgroups vs. healthy population, in **Supplementary Figure 1**; in addition, further methodological details are reported in our previous work (18).

TABLE 1 | Demographical, clinical, motor, and behavioral characteristics of PD-MCI Aβ+ vs. Aβ-.

		PD-MCI Aβ+	PD-MCI Aβ−	Mann-Whitney U Test/Fisher Test
		Mean (SD)/Frequency	Mean (SD)/Frequency	
Demographics	Sex (male/female)	7/1	9/8	0.182
	Age (years)	72.75 (3.69)	68.82 (7.36)	0.074
	Education (years)	11.25 (3.95)	8.47 (3.60)	0.111
Clinical characteristics	Disease Duration (years)	8.63 (2.61)	10.58 (5.78)	0.578
	Age at motor symptoms' onset (years)	64.75 (4.26)	58.76 (9.42)	0.091
	LEDD (mg tot/die)	886.875 (405.80)	887.88 (429.60)	1.000
	DAED (mg tot/die)	115 (125.47)	124.27 (123.62)	0.816
Motor characteristics	MDS-UPDRS I	11	15.29 (10.77)	1.000
	MDS-UPDRS II	10	19.43 (7.76)	0.250
	MDS-UPDRS III	27.33 (15.70)	29.4 (15.27)	0.815
	MDS-UPDRS IV—fluctuation	2.4 (2.88)	3.91 (3.78)	0.600
	MDS-UPDRS IV—dyskinesia	0	1.18 (2.13)	0.245
	MDS-UPDRS total score	34	65.43 (23.07)	0.250
	H&Y	2.58 (0.91)	2.37 (1.00)	0.837
Functional independence and global cognitive status	ADL	5.4 (0.51)	5.52 (0.62)	0.447
	IADL	4.25 (1.40)	4.82 (2.30)	0.406
	PD-CFRS	5.875 (4.48)	7.31 (5.50)	0.538
	MMSE (corrected score)	24.71 (1.84)	24.67 (1.81)	0.884
	MoCA (corrected score)	19.18 (2.00)	20.31 (2.57)	0.391
Behavioral measures	PDQ-8	8.57 (7.63)	11 (5.81)	0.270
	APATHY	14.57 (2.44)	18.77 (6.44)	0.130
	STAI-Y1	35.25 (5.70)	41.13 (9.07)	0.154
	STAI-Y2	39.71 (10.24)	45.53 (8.60)	0.157
	BDI-II	11.00 (6.34)	9.93 (6.89)	0.657
	BIS-11	60.80 (10.60)	65.78 (10.43)	0.479
	QUIP-RS	8.14 (7.73)	6.33 (8.52)	0.590

Mann–Whitney U test was run to test between-group differences. Fisher Exact test was used for the sex variable. ADL, activities of daily living; BDI-II, Beck Depression Inventory-II; BIS-11, Barratt Impulsiveness Scale; DAED, dopamine agonist equivalent dose; HC, healthy controls; IADL, Instrumental activities of daily living; LEDD, levodopa equivalent daily dose; MDS-UPDRS, Movement Disorder Society Unified Parkinson's Disease Rating Scale; MMSE, Mini-Mental State Examination; MoCA, Montreal Cognitive Assessment; PD-CFRS, Parkinson's Disease -Cognitive Functional Rating Scale; PDQ-8, Parkinson's Disease Questionnaire; QUIP-RS, Questionnaire for Impulsive-Compulsive Disorders in Parkinson's Disease–Rating Scale; STAI (Y-1, Y-2), State-Trait Anxiety Inventory.

Statistical maps of GM alterations were then included in a second level GLM analysis comparing PD-MCI-Aβ+ vs. PD-MCI-Aβ- subgroups to assess for possible GM differences. Areas of shared alterations were tested with a conjunction analysis including the two subgroups as factors. To reduce false positives (32), a Bayesian Probabilistic Threshold-Free Cluster Enhancement (TFCE) method was used to define GM patterns differences in PD-MCI subgroups. A significant threshold family-wise error (FWE) corrected of $p < 0.001$ was adopted. The atlas (AAL3v1, http://www.gin.cnrs.fr/en/tools/aal/) provided with the automated anatomical parcellation tool was used for results.

Statistical Analyses

Pairwise differences between the two subgroups (PD-MCI-Aβ+ vs. PD-MCI-Aβ-) in demographic, motor, clinical, cognitive, and behavioral characteristics were assessed with Mann–Whitney U test or Fisher's exact test for categorical variables. Each cognitive raw score was converted to z-score using the Italian normative data, considering as pathologic a performance below the −1.5 SD cut-off. The z-compound (mean z-score among tests of each cognitive domain) was also calculated. Moreover, we tested the hypothesis that increased amyloid load might alter a cognitive domain performance, by running a univariate linear regression analysis between the significantly affected cognitive domains and the mean SUVR, extracted from each cluster/subcortical region with a marked amyloid deposition. Statistical analyses were run with "R software" (R version 3.6.2 (2019-12-12)—Copyright (C) 2019).

RESULTS

Clinical Characteristics

Seventeen out of 25 PD-MCI patients were classified as Aβ- and 8 Aβ+. The two groups did not differ in demographic, clinical,

TABLE 2 | Comparison of the neuropsychological scores between PD-MCI subgroups (Aβ+ vs. Aβ-).

		PD-MCI Aβ+		PD-MCI Aβ−		Mann Whitney *U* Test
Cognitive domains	**Cognitive tests**	**Median**	**IQR 25–75**	**Median**	**IQR 25–75**	***p*-values**
Attention/working memory	TMT A	42.50	35 to 69.8	72.50	54.3 to 91	0.076
	TMT B	355	229 to 367	248	198.5 to 330.3	0.542
	TMT B-A	314.50	188 to 336	174.50	130.5 to 238.3	0.553
	DSS (WAIS-IV)	8	8 to 10.5	9.50	8 to 11	0.635
	z-compound	−0.22	−0.6 to 0.1	−0.63	−1.4 to 0.1	0.124
Executive domain	Phonemic fluency	30.50	27.5 to 33.5	30	23 to 35	0.944
	Stroop/color task-Time	48.12	14.2 to 73	35.80	21.1 to 47.8	0.759
	Stroop/color task-Errors	4.40	1.7 to 8.1	0.38	0 to 2.3	0.092
	Similarities (WAIS-IV)	8	7.5 to 9	7.50	6.8 to 10	0.761
	CDT	11	10.5 to 12	12	10 to 13	0.797
	z-compound	−1.48	−1.9 to −1.1	−0.60	−1 to −0.5	**0.037**
Memory domain	Prose memory test	6	5 to 6.5	4.50	1.8 to 7.3	0.545
	Prose memory test delayed	8	5 to 10	6.50	4.5 to 9.25	0.500
	ROCF delayed	8.40	6.8 to 11.8	9.9	7.4 to 11.4	0.806
	WPAT	11.50	11.3 to 16.3	10.50	8 to 11.6	0.105
	z-compound	−1.07	−1.3 to 0.8	−1.60	−1.9 to −0.9	0.140
Visuospatial domain	ROCF copy	19.40	12.6 to 25	24.50	20.8 to 28.7	0.178
	VOSP—incomplete letters subtask	16.50	13 to 18	17	15 to 18	0.747
	Benton—JLO	18	16 to 22.5	19	9.5 to 22	0.806
	z-compound	−2.80	−3.4 to −2	−2.21	−2.6 to −1.6	0.344
Language domain	Category fluency	30	30 to 34.5	31	28 to 39	0.679
	Naming Task	28.30	27 to 29.2	29.50	28.4 to 30.4	0.211
	z-compound	−0.83	−1.1 to −0.6	−0.94	−1.5 to −0.3	1.000
Apraxia	Apraxia	19.25	19 to 20	19	17.8 to 19.8	0.253

IQR, interquartile range; WAIS IV, Wechsler Adult Intelligence Scale—Fourth Edition; VOSP, Visual Object and Space Perception; TMT, Trail Making Test; WPAT, Word paired associated task; JLO, Judgement of Line Orientation; ROCF, Rey-Osterrieth complex figure test; CDT, Clock drawing task; DSS, Digit Span Sequencing. Statistically significant results are in bold type.

motor, and behavioral variables including global cognition scales scores (MMSE and MoCA) (see **Table 1**).

Looking at the performances in each single cognitive test, the two cohorts showed no differences in any individual test of the five investigated cognitive domains. However, PD-MCI-Aβ+ showed worse performance (z-compound) in the overall executive domain than PD-MCI-Aβ- ($p = 0.037$, see **Table 2**).

Cortical and Subcortical β-Amyloid Distribution in PD-MCI-Aβ+

Cortical surface analysis showed significant (cluster-wise Monte Carlo corrected) bilateral amyloid depositions in the caudal and rostral middle frontal cortices, in the right precuneus and in left paracentral and pars triangularis areas, in PD-MCI-Aβ+ compared with Aβ- (see **Figure 1A** and **Table 3**). Given that values of FMM SUVR in subcortical regions (nucleus accumbens, caudate, putamen, amygdala, pallidum, thalamus, and hippocampus) were highly correlated between hemispheres ($p < 0.0001$), we analyzed the right-left averaged ROIs scores. The only subcortical region showing significant amyloid deposition was the putamen ($p = 0.038$), despite this result was no more significant following multiple comparisons correction (see **Table 4**).

Cortical Gray Matter in PD-MCI-Aβ+

Cortical voxel-based morphometry (VBM) analysis showed a similar pattern of brain atrophy in PD-MCIAβ+ and PD-MCIAβ-. Conjunction analysis showed that PD-MCI subgroups shared a similar pattern of atrophy in bilateral orbitofrontal, middle frontal, superior middle frontal regions, rostral and middle cingulate cortex, and fusiform regions and orbicular and superior temporal region on the right hemisphere (see **Figure 1B** and **Table 5**).

Association Between β-Amyloid Load and Cognitive Functions

Only the executive domain was affected by the amyloid presence (see **Table 2**), and therefore only this domain was considered for further analyses. There was a negative linear relationship between cortical regions with significant amyloid load and worsening in executive performance. Namely, we found a significant association with the following regions: in the right hemisphere, the caudal middle frontal gyrus ($r = -0.53$; $p = 0.01$), and the

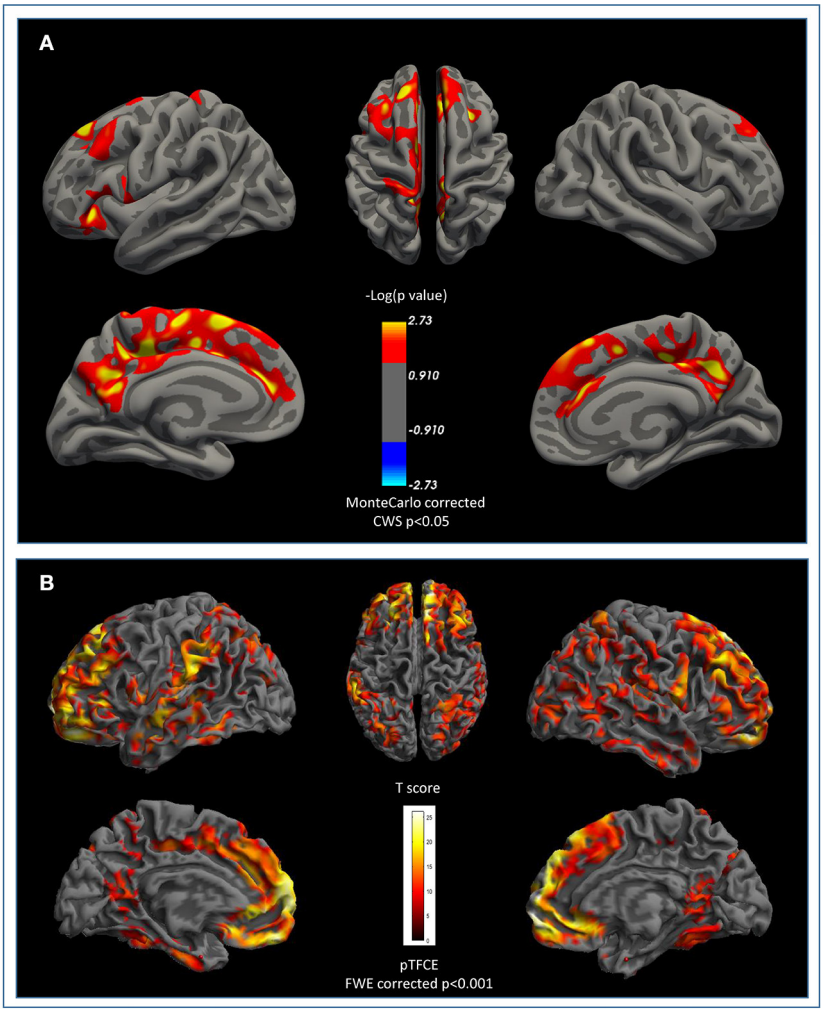

FIGURE 1 | β-Amyloid cortical deposition and brain atrophy in PD-MCI. **(A)** Surface based comparison between standardized uptake value ratios (SUVR) in PD-MCI-Aβ+ vs. Aβ-. Areas that survived a cluster-wise Monte-Carlo correction ($p < 0.05$) adjusted for two-hemispheres are displayed. Cerebellum cortex was used as reference region for partial volume correction. **(B)** Shared pattern of atrophy between PD-MCI-Aβ+ vs. Aβ- compared to healthy matched population at FWE pTFCE $p < 0.001$. No areas survived after β-amyloid +/– at TFCE uncorrected $p < 0.001$ threshold. FWE, family-wise error; TFCE, Threshold-Free Cluster Enhancement.

TABLE 3 | Pattern of β-amyloid cortical deposition in PD-MCI.

	Regions	MNI X	MNI Y	MNI Z	Cluster-wise MC *p*-value	N of vertices	Size (mm^2)	Max – log10(*p*)
Rh	Caudal middle frontal gyrus	26.5	18	41.8	0.0001	4,702	2429.8	3.408
	Precuneus	11	−55.7	38.4	0.0001	5,647	2383.4	3.625
Lh	Paracentral lobule	−12.9	−28.6	47.2	0.0001	15,206	7136.8	4.962
	Pars triangularis	−38.7	30.4	−6.7	0.0001	4,339	2041.4	3.301
	Rostral middle frontal gyrus	−30.4	26.1	38.6	0.0031	2,577	1494.8	2.951

Cortical surface-based comparison between SUVR in PD-MCI β-Amyloid +/–. Areas that survived a cluster-wise $p < 0.05$ Monte-Carlo corrected threshold adjusted for two-hemispheres values. Cerebellum cortex was used as reference region after partial volume correction in PETsurfer. Rh, right hemisphere; Lh, left hemisphere; MC, Monte Carlo correction. Coordinates were displayed in MNI space.

precuneus ($r = -0.56$; $p = 0.005$); while in left hemisphere, the rostral middle frontal ($r = -0.49$; $p = 0.017$), the paracentral ($r = -0.57$; $p = 0.005$), and the pars triangularis regions ($r = -0.53$; $p = 0.01$). By contrast, the subcortical L/R-putamen did not show any significant correlation with the executive domain dysfunctions ($r = -0.33$; $p = 0.130$) (see **Figure 2**).

TABLE 4 | Pattern of β-amyloid striatal and extra-striatal subcortical deposition.

	PD-MCI Aβ− (*n* = 16)		PD-MCI Aβ+ (*n* = 7)		Mann Whitney U test
Subcortical region (average L/R SUVR)	**Median**	**2.5 to 97.5 P**	**Median**	**2.5 to 97.5 P**	***p-value (uncorrected)***
Nucleus accumbens	−1.14	−3.32 to 1.72	−0.39	−2.63 to 1.51	0.423
Putamen	1.15	0.45 to 2.78	1.73	1.29 to 3.14	**0.038**
Caudate	0.38	0.08 to 3.03	0.98	0.56 to 2.14	0.161
Hippocampus	1.13	0.76 to 1.84	1.06	0.88 to 1.41	0.689
Globus pallidus	2.17	0.59 to 3.51	2.21	0.51 to 2.47	0.738
Amygdala	1.21	0.67 to 2.40	1.34	0.96 to 1.62	0.345
Thalamus	1.38	−0.06 to 1.89	1.7	0.32 to 2.16	0.204

Significant result (in bold) was not corrected for multiple comparison testing, following this correction, this difference was not statistically significant. Standardized uptake value ratios (SUVR); L/H, left-right; P, percentiles; PD-MCI, Parkinson's disease with mild cognitive impairment; Aβ, β-amyloid positive vs. negative.

TABLE 5 | Areas of gray matter atrophy in PD-MCI vs. controls.

AAL3 atlas				**Cluster**	**Cluster**	**Peak**	**Peak**	**Peak**
	MNI (X)	**MNI (Y)**	**MNI (Z)**	**N voxels**	**P (FWE-corr)**	**P (FWE-corr)**	**T**	**Z**
Medial OFC-L	−9	51	−21	64,435	0.0000	0.0000	Inf	Inf
Medial OFC-R	13.5	52.5	−18			0.0000	Inf	Inf
Medial OFC-R	−15	24	−16.5			0.0000	Inf	Inf
Frontal superior L	−26	38	44			0.0000	17.05	7.21
Frontal superior medial L	8	42	53			0.0000	14.19	6.75
Fusiform R	45	−37.5	−16.5	6,815	0.0000	0.0000	19.0372	7.4730
Fusiform R	40.5	−45	−15			0.0000	15.0621	6.9023
Temporal inferior R	54	−24	−21			0.0000	14.8525	6.8672
Precuenus R	7.5	−64.5	64.5	11	0.0001	0.0001	11.1572	6.1303
Precuenus L	−4.5	−49.5	42	392	0.0000	0.0001	10.8696	6.0611
Precuenus L	−6	−49.5	55.5			0.0002	10.6720	6.0124
Cingulate middle–L	−12	−39	36			0.0002	10.6214	5.9998
Precuenus R	16.5	−66	28.5	243	0.0000	0.0002	10.5749	5.9881
Fusiform R	34.5	−7.5	−36	29	0.0000	0.0006	9.7211	5.7626
Caudate L	−9	13.5	3	21	0.0000	0.0008	9.5086	5.7029

DISCUSSION

In the present study, we used simultaneous PET/MRI imaging study to investigate how Aβ burden affects cognitive performance in PD-MCI patients, diagnosed with a comprehensive neuropsychological assessment, allowing a level II diagnosis.

We found that in our PD-MCI cohort, 8/25 (31%) patients were Aβ+, corroborating previous data on brain amyloid prevalence in non-demented PD (20). While all demographic, clinical, behavioral, and motor variables did not differ, PD-MCI-Aβ+ showed a trend for higher age of motor's symptoms onset, suggesting that extracellular β-amyloid deposition is an age-related pathological marker (33).

From a neuropsychological point of view, PET amyloid positivity was associated with worse performance in the executive domain, supporting previous PD literature on the contribution of Aβ on attentive and executive dysfunctions (10, 34, 35).

Interestingly, brain Aβ did not impact other cognitive domains such as visuo-spatial and semantic memory, which are considered highly sensitive in detecting the deterioration and progression to severe impairment and dementia (1, 2, 18, 23, 36–38). These results seem to suggest that PD-MCI-Aβ+ cognitive pattern does not share the typical cognitive profile of MCI due to Alzheimer's disease (AD).

The observation of a significant proportion of PD-MCI-Aβ- can possibly suggest that Aβ is not the main pathogenetic cause of cognitive deterioration in PD (10, 11, 18, 34). Instead, amyloidosis may enhance early deficits in those cognitive domains already vulnerable to PD primary pathology (2, 18), possibly indicating that in PD concomitant conditions may aggravate cognition and herald dementia (39–41). In this regard, in a recent longitudinal study performed in a large PD *de novo* cohort, we concluded that amyloid burden together with asymmetric dopaminergic loss (in the left hemisphere) and aging exhibited independent and interactive contributions to

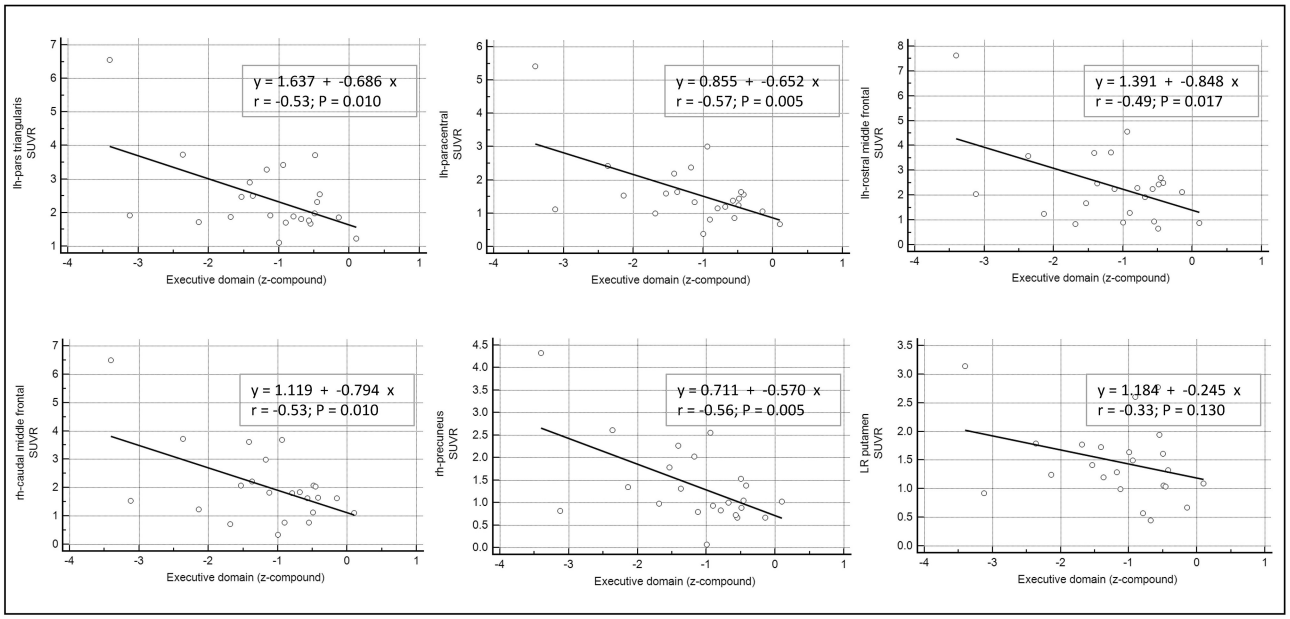

FIGURE 2 | Correlation between β-amyloid load in cortical and subcortical areas and cognitive performance. Univariate linear regression model between the executive domain (z-compound) and the mean standardized uptake value ratios (SUVR) of each significant cortical and subcortical ROIs.

PD-cognitive progression (namely, involving attentive/executive alterations) (42).

One of the strengths of our study is the quantification of cortical Aβ load using a surface-based approach and SUVR measures, not reported in our previous work (18).

We found increased Aβ uptake in the cortical areas, mostly located in the frontal (i.e., caudal and rostral middle frontal cortices and pars triangularis) as well as in the parietal regions (i.e., paracentral lobule and precuneus), which overall correlated with a poor executive performance.

From a cognitive perspective, the involvement of these areas as well as their key role within the fronto-striatal circuit is well-established. They subserve a wide range of cognitive tasks, such as executive functions and working-memory abilities, involving information monitoring and manipulation, planning and organization of complex behaviors, and attention shifting (43), with frontal striatal network alterations underlying early changes in PD, and predicting cognitive decline as well as dementia (44, 45). Noteworthy, the present findings corroborate our previous PET-amyloid evidence in a PD *de novo* cohort (10), showing that increased cortical and subcortical amyloid was associated with a worse performance in attentive/executive domains. Yet, this reinforces the concept of cortical and subcortical amyloid accumulation as an additional biomarker contributing to cognitive impairment in PD (10, 12, 46).

Increased FMM uptake in PD-MCI-Aβ+ was also present in the right precuneus, which is anatomically and functionally connected with subcortical striatal areas and implied in functional abnormalities in PD-MCI (47). Our findings support previous PET imaging studies in non-demented PD, despite the fact that different Aβ-tracers were used (46, 48), showing a greater amyloid burden particularly in the precuneus and frontal regions, as well as their inverse correlation with cognitive performance (46). Other evidence did not corroborate this pattern, reporting no differences between PD-MCI and PD with normal cognition, possibly due to the small sample size (34). Evidence of amyloid deposition in the parietal regions seems to be consistent across PET imaging studies (12, 48, 49). Of note, one reported an association with visuospatial impairments (49) but no significant correlations between amyloid and executive functions; however, the entire Lewy bodies spectrum was analyzed.

Overall, previous studies in PD population yielded mixed results, and as highlighted in the Petrous et al. review (13), there is only a few published evidence about the role of Aβ in PD-MCI, due to the heterogeneous nature of this clinical syndrome as well as the high variability in the MCI-assessment between studies.

Further, PD-MCI-Aβ+ presented increased FBB uptake in the putamen, but without significant correlation with executive functions. In a previous analysis of the PPMI dataset, we had reported a correlation between executive tests and putamen Aβ accumulation, but this included only early *de novo* PD with limited cognitive characterization, not allowing to diagnose MCI (10). Another study reported a correlation but using a different PET tracer and in a cohort with various cognitive alterations (50). It is possible that lack of correlation in our cohort was related to the limited number of PD-MCI-Aβ+, but future studies should focus on this specific marker of PD-related amyloidosis exploring also its relevance on the magnitude of levodopa response and on motor complications.

Finally, we also evaluated GM volumetric changes at MRI. Results showed similar atrophy patterns in right fronto-temporal regions in both PD-MCI subgroups, replicating previous

findings adopting different structural analysis methods (5, 7). Interestingly, cortical VBM patterns were similar in PD-MCI with and without Aβ deposition, and excluded the presence of middle-temporal atrophy, a characteristic of early AD (51). This supports our previous findings of absence of AD-atrophy pattern in the LBD patients with dementia (18).

Our current work has limitations. Each subgroup (Aβ+ and Aβ-) included a relatively small number of PD-MCI subjects, resulting in lower statistical power to detect differences. However, results are aligned with previous evidence (18) of an independent role of Aβ in shaping MCI-profile and accelerating cognitive deficits in PD. Moreover, regarding the neuroimaging analyses we acknowledge that the small sample size can possibly affect the results; however, to reduce the false positive, we adopted TFCE or Monte Carlo FWE corrections, while to reduce the false negative an explorative uncorrected $p < 0.001$ was adopted.

Greater numerosity is needed to further explore the relationship between Aβ deposition and increased dementia-risk profiles. In particular, it would be worth exploring if low concentration of Aβ, below AD-range thresholds, may also have clinical relevance (13) in presence of an ongoing multisystem neurodegenerative process like PD. In this regard, a further limitation is that we did not screen our PD-MCI for APOE genotype which is now considered the main risk factor for cognitive decline in elderly patients with PD and Dementia with Lewy Bodies (34, 52, 53).

Finally, we did not include a control group of healthy controls and PD without cognitive deficits to assess age-related brain amyloid distribution. However, a recent publication of elderly individuals without cognitive deficits demonstrated areas of cerebral amyloid deposition (i.e., prefrontal, precuneus) similar to those observed in our Aβ+PD-MCI patients, suggesting that PD-related amyloidosis somehow overlaps age-related amyloid accumulation (54).

In conclusion, our study suggests that amyloid burden in the fronto-striatal network may play a role in worsening executive abilities in PD-MCI patients. Furthermore, the observation of more than 60% Aβ- in our PD-MCI patients led us to speculate about the independent role of amyloid load for PD-MCI. Notably, amyloid accumulation in our cohort was not associated with typical AD cognitive and brain atrophy pattern nor with specific clinical features and demographic characteristics, highlighting its potential unspecific contribution. Considering that up to 80% of PD patients may ultimately develop dementia with negative consequences on life quality and expectancy, a better understanding of the involved predictors is of key importance. We believe clarifying Aβ role in cognitive impairment and progression is clinically relevant, especially in the context of emerging applicability of amyloid-related treatments.

DATA AVAILABILITY STATEMENT

The original contributions presented in the study are included in the article/**Supplementary Material**, further inquiries can be directed to the corresponding author.

ETHICS STATEMENT

The studies involving human participants were reviewed and approved by Azienda Ospedale Università di Padova. The patients/participants provided their written informed consent to participate in this study.

AUTHOR CONTRIBUTIONS

AA and RB contributed to conception and design of the study. FP and MG organized the database. LW performed the statistical analysis and wrote sections of the manuscript. MG wrote the first draft of the manuscript. All authors contributed to manuscript revision, read, and approved the submitted version.

FUNDING

We are grateful to GE-Healthcare for the liberal contribution of all doses of [^{18}F]flutemetamol used in the present work and for covering publication fees.

SUPPLEMENTARY MATERIAL

The Supplementary Material for this article can be found online at: https://www.frontiersin.org/articles/10.3389/fneur.2021.760518/full#supplementary-material

Supplementary Figure 1 | Cortical atrophy in PD-MCI subgroups as compared to healthy population. Nonparametric comparison of PD-MCI gray matter atrophy compared to age and sex matched normal control (NC). A TFCE $p < 0.05$ FWE corrected threshold was used. TFCE, threshold-free cluster enhancement; FWE, family-wise error.

REFERENCES

1. Biundo R, Weis L, Antonini A. Cognitive decline in Parkinson's disease: the complex picture. *npj Parkin Dis.* (2016) 2:16018. doi: 10.1038/npjparkd.2016.18
2. Biundo R, Weis L, Facchini S, Formento-Dojot P, Vallelunga A, Pilleri M, et al. Cognitive profiling of Parkinson disease patients with mild cognitive impairment and dementia. *Parkins Relat Disord.* (2014) 20:394–9. doi: 10.1016/j.parkreldis.2014.01.009
3. Pagonabarraga J, Kulisevsky J. Cognitive impairment and dementia in Parkinson's disease. *Neurobiol Dis.* (2012) 46:590–6. doi: 10.1016/j.nbd.2012.03.029
4. Delgado-Alvarado M, Gago B, Navalpotro-Gomez I, Jimenez-Urbieta H, Rodriguez-Oroz MC. Biomarkers for dementia and mild cognitive impairment in Parkinson's disease. *Mov Disord.* (2016) 31:861–81. doi: 10.1002/mds.26662
5. Biundo R, Calabrese M, Weis L, Facchini S, Ricchieri G, Gallo P, et al. Anatomical correlates of cognitive functions in early Parkinson's disease patients. *PLoS ONE.* (2013) 8:e64222. doi: 10.1371/journal.pone.0064222
6. Chen B, Wang S, Sun W, Shang X, Liu H, Liu G, et al. Functional and structural changes in gray matter of Parkinson's disease patients with mild cognitive impairment. *Eur J Radiol.* (2017) 93:16–23. doi: 10.1016/j.ejrad.2017.05.018

7. Hall JM, Lewis SJG. Neural correlates of cognitive impairment in parkinson's disease: a review of structural MRI findings. *Int Rev Neurobiol.* (2019) 144:1–28. doi: 10.1016/bs.irn.2018.09.009
8. Bellomo G, Paolini Paoletti F, Chipi E, Petricciuolo M, Simoni S, Tambasco N, et al. A/T/(N) profile in cerebrospinal fluid of Parkinson's disease with/without cognitive impairment and dementia with lewy bodies. *Diagnostics (Basel).* (2020) 10:E1015. doi: 10.3390/diagnostics10121015
9. Yoo HS, Lee S, Chung SJ, Lee YH, Lee PH, Sohn YH, et al. Dopaminergic depletion, β-amyloid burden, and cognition in Lewy body disease. *Ann Neurol.* (2020) 87:739–50. doi: 10.1002/ana.25707
10. Fiorenzato E, Biundo R, Cecchin D, Frigo AC, Kim J, Weis L, et al. Brain amyloid contribution to cognitive dysfunction in early-stage Parkinson's disease: the PPMI dataset. *J Alzheimers Dis.* (2018) 66:229–37. doi: 10.3233/JAD-180390
11. Melzer TR, Stark MR, Keenan RJ, Myall DJ, MacAskill MR, Pitcher TL, et al. Beta amyloid deposition is not associated with cognitive impairment in Parkinson's disease. *Front Neurol.* (2019) 10:391. doi: 10.3389/fneur.2019.00391
12. Ledbetter C, Larmeu L, Reekes T, Patterson J, Garg P, Zweig R, et al. Basal ganglia amyloid beta accumulation and cognitive dysfunction in Parkinson disease. *J Nucl Med.* (2021) 62:1063.
13. Petrou M, Dwamena BA, Foerster BR, MacEachern MP, Bohnen NI, Muller ML, et al. Amyloid deposition in Parkinson's disease and cognitive impairment: a systematic review. *Mov Disord.* (2015) 30:928–35. doi: 10.1002/mds.26191
14. Colom-Cadena M, Grau-Rivera O, Planellas L, Cerquera C, Morenas E, Helgueta S, et al. Regional overlap of pathologies in Lewy body disorders. *J Neuropathol Exp Neurol.* (2017) 76:216–24. doi: 10.1093/jnen/nlx002
15. Sierra M, Gelpi E, Martí MJ, Compta Y. Lewy- and Alzheimer-type pathologies in midbrain and cerebellum across the Lewy body disorders spectrum. *Neuropathol Appl Neurobiol.* (2016) 42:451–62. doi: 10.1111/nan.12308
16. Bougea A, Stefanis L, Emmanouilidou E, Vekrelis K, Kapaki E. High discriminatory ability of peripheral and CFSF biomarkers in Lewy body diseases. *J Neural Transm (Vienna).* (2020) 127:311–22. doi: 10.1007/s00702-019-02137-2
17. Coughlin DG, Hurtig HI, Irwin DJ. Pathological influences on clinical heterogeneity in Lewy body diseases. *Mov Disord.* (2020) 35:5–19. doi: 10.1002/mds.27867
18. Biundo R, Weis L, Fiorenzato E, Pistonesi F, Cagnin A, Bertoldo A, et al. The contribution of beta-amyloid to dementia in Lewy body diseases: a 1-year follow-up study. *Brain Commun.* (2021) 3:fcab180. doi: 10.1093/braincomms/fcab180
19. Postuma RB, Berg D, Stern M, Poewe W, Olanow CW, Oertel W, et al. MDS clinical diagnostic criteria for Parkinson's disease. *Mov Disord.* (2015) 30:1591–601. doi: 10.1002/mds.26424
20. Chia R, Sabir MS, Bandres-Ciga S, Saez-Atienzar S, Reynolds RH, Gustavsson E, et al. Genome sequencing analysis identifies new loci associated with Lewy body dementia and provides insights into its genetic architecture. *Nat Genet.* (2021) 53:294–303. doi: 10.1038/s41588-021-00785-3
21. Antonini A, Abbruzzese G, Ferini-Strambi L, Tilley B, Huang J, Stebbins GT, et al. Validation of the Italian version of the movement disorder society—unified Parkinson's disease rating scale. *Neurol Sci.* (2012) 34:683–7. doi: 10.1007/s10072-012-1112-z
22. Tomlinson CL, Stowe R, Patel S, Rick C, Gray R, Clarke CE. Systematic review of levodopa dose equivalency reporting in Parkinson's disease. *Mov Disord.* (2010) 25:2649–53. doi: 10.1002/mds.23429
23. Litvan I, Goldman JG, Tröster AI, Schmand BA, Weintraub D, Petersen RC, et al. Diagnostic criteria for mild cognitive impairment in Parkinson's disease: movement disorder society task force guidelines. *Mov Disord.* (2012) 27:349–56. doi: 10.1002/mds.24893
24. Fiorenzato E, Antonini A, Camparini V, Weis L, Semenza C, Biundo R. Characteristics and progression of cognitive deficits in progressive supranuclear palsy vs. multiple system atrophy and Parkinson's disease. *J Neural Transm (Vienna).* (2019) 126:1437–45. doi: 10.1007/s00702-019-02065-1
25. Seibyl J, Catafau AM, Barthel H, Ishii K, Rowe CC, Leverenz JB, et al. Impact of training method on the robustness of the visual assessment of 18F-florbetaben PET scans: results from a phase-3 study. *J Nucl Med.* (2016) 57:900–6. doi: 10.2967/jnumed.115.161927
26. Cecchin D, Barthel H, Poggiali D, Cagnin A, Tiepolt S, Zucchetta P, et al. A new integrated dual time-point amyloid PET/MRI data analysis method. *Eur J Nucl Med Mol Imaging.* (2017) 44:2060–72. doi: 10.1007/s00259-017-3750-0
27. Schwarz CG, Jones DT, Gunter JL, Lowe VJ, Vemuri P, Senjem ML, et al. Contributions of imprecision in PET-MRI rigid registration to imprecision in amyloid PET SUVR measurements. *Hum Brain Mapp.* (2017) 38:3323–36. doi: 10.1002/hbm.23622
28. Greve DN, Svarer C, Fisher PM, Feng L, Hansen AE, Baare W, et al. Cortical surface-based analysis reduces bias and variance in kinetic modeling of brain PET data. *Neuroimage.* (2014) 92:225–36. doi: 10.1016/j.neuroimage.2013.12.021
29. Greve DN, Salat DH, Bowen SL, Izquierdo-Garcia D, Schultz AP, Catana C, et al. Different partial volume correction methods lead to different conclusions: an (18)F-FDG-PET study of aging. *Neuroimage.* (2016) 132:334–43. doi: 10.1016/j.neuroimage.2016.02.042
30. Desikan RS, Segonne F, Fischl B, Quinn BT, Dickerson BC, Blacker D, et al. An automated labeling system for subdividing the human cerebral cortex on MRI scans into gyral based regions of interest. *Neuroimage.* (2006) 31:968–80. doi: 10.1016/j.neuroimage.2006.01.021
31. Syaifullah AH, Shiino A, Kitahara H, Ito R, Ishida M, Tanigaki K. Machine learning for diagnosis of AD and prediction of MCI progression from brain MRI using brain anatomical analysis using diffeomorphic deformation. *Front Neurol.* (2021) 11:1894. doi: 10.3389/fneur.2020.576029
32. Spisák T, Spisák Z, Zunhammer M, Bingel U, Smith S, Nichols T, et al. Probabilistic TFCE: a generalized combination of cluster size and voxel intensity to increase statistical power. *Neuroimage.* (2019) 185:12–26. doi: 10.1016/j.neuroimage.2018.09.078
33. Beach TG. Physiologic origins of age-related beta-amyloid deposition. *Neurodegener Dis.* (2008) 5:143–5. doi: 10.1159/000113685
34. Gomperts SN, Locascio JJ, Rentz D, Santarlasci A, Marquie M, Johnson KA, et al. Amyloid is linked to cognitive decline in patients with Parkinson disease without dementia. *Neurology.* (2013) 80:85–91. doi: 10.1212/WNL.0b013e31827b1a07
35. Smith C, Malek N, Grosset K, Cullen B, Gentleman S, Grosset DG. Neuropathology of dementia in patients with Parkinson's disease: a systematic review of autopsy studies. *J Neurol Neurosurg Psychiatry.* (2019) 90:1234–43. doi: 10.1136/jnnp-2019-321111
36. Janvin CC, Larsen JP, Aarsland D, Hugdahl K. Subtypes of mild cognitive impairment in Parkinson's disease: progression to dementia. *Mov Disord.* (2006) 21:1343–9. doi: 10.1002/mds.20974
37. Lawson RA, Yarnall AJ, Duncan GW, Breen DP, Khoo TK, Williams-Gray CH, et al. Stability of mild cognitive impairment in newly diagnosed Parkinson's disease. *J Neurol Neurosurg Psychiatry.* (2017) 88:648–52. doi: 10.1136/jnnp-2016-315099
38. Greenland JC, Williams-Gray CH, Barker RA. The clinical heterogeneity of Parkinson's disease and its therapeutic implications. *Eur J Neurosci.* (2019) 49:328–38. doi: 10.1111/ejn.14094
39. Compta Y, Parkkinen L, O'Sullivan SS, Vandrovcova J, Holton JL, Collins C, et al. Lewy- and Alzheimer-type pathologies in Parkinson's disease dementia: which is more important? *Brain.* (2011) 134:1493–505. doi: 10.1093/brain/awr031
40. Lim EW, Aarsland D, Ffytche D, Taddei RN, van Wamelen DJ, Wan Y-M, et al. Amyloid-β and Parkinson's disease. *J Neurol.* (2019) 266:2605–19. doi: 10.1007/s00415-018-9100-8
41. McMillan CT, Wolk DA. Presence of cerebral amyloid modulates phenotype and pattern of neurodegeneration in early Parkinson's disease. *J Neurol Neurosurg Psychiatry.* (2016) 87:1112–22. doi: 10.1136/jnnp-2015-312690
42. Fiorenzato E, Antonini A, Bisiacchi P, Weis L, Biundo R. Asymmetric dopamine transporter loss affects cognitive and motor progression in Parkinson's disease. *Mov Disord.* (2021) 36:2303–13. doi: 10.1002/mds.28682
43. Nagano-Saito A, Leyton M, Monchi O, Goldberg YK, He Y, Dagher A. Dopamine depletion impairs frontostriatal functional connectivity during a set-shifting task. *J Neurosci.* (2008) 28:3697–706. doi: 10.1523/JNEUROSCI.3921-07.2008

44. Kehagia AA, Barker RA, Robbins TW. Neuropsychological and clinical heterogeneity of cognitive impairment and dementia in patients with Parkinson's disease. *Lancet Neurol.* (2010) 9:1200–13. doi: 10.1016/S1474-4422(10)70212-X
45. Filoteo JV, Reed JD, Litvan I, Harrington DL. Volumetric correlates of cognitive functioning in nondemented patients with Parkinson's disease. *Mov Disord.* (2014) 29:360–7. doi: 10.1002/mds.25633
46. Akhtar RS, Xie SX, Chen YJ, Rick J, Gross RG, Nasrallah IM, et al. Regional brain amyloid-beta accumulation associates with domain-specific cognitive performance in Parkinson disease without dementia. *PLoS ONE.* (2017) 12:e0177924. doi: 10.1371/journal.pone.0177924
47. Jia X, Li Y, Li K, Liang P, Fu X. Precuneus dysfunction in Parkinson's disease with mild cognitive impairment. *Front Aging Neurosci.* (2018) 10:427. doi: 10.3389/fnagi.2018.00427
48. Ghadery C, Koshimori Y, Christopher L, Kim J, Rusjan P, Lang AE, et al. The interaction between neuroinflammation and β-amyloid in cognitive decline in Parkinson's disease. *Mol Neurobiol.* (2020) 57:492–501. doi: 10.1007/s12035-019-01714-6
49. Gomperts SN, Rentz DM, Moran E, Becker JA, Locascio JJ, Klunk WE, et al. Imaging amyloid deposition in Lewy body diseases. *Neurology.* (2008) 71:903–10. doi: 10.1212/01.wnl.0000326146.60732.d6
50. Gomperts SN, Locascio JJ, Marquie M, Santarlasci AL, Rentz DM, Maye J, et al. Brain amyloid and cognition in Lewy body diseases. *Mov Disord.* (2012) 27:965–73. doi: 10.1002/mds.25048
51. Zhang B, Lin L, Wu S, Al-Masqari ZHMA. Multiple subtypes of Alzheimer's disease base on brain atrophy pattern. *Brain Sci.* (2021) 11:278. doi: 10.3390/brainsci11020278
52. Pankratz N, Byder L, Halter C, Rudolph A, Shults CW, Conneally PM, et al. Presence of an APOE4 allele results in significantly earlier onset of Parkinson's disease and a higher risk with dementia. *Mov Disord.* (2006) 21:45–9. doi: 10.1002/mds.20663
53. Chung J, Ushakova A, Doitsidou M, Tzoulis C, Tysnes OB, Dalen I, et al. The impact of common genetic variants in cognitive decline in the first seven years of Parkinson's disease: a longitudinal observational study. *Neurosci Lett.* (2021) 764:136243. doi: 10.1016/j.neulet.2021.136243
54. Toppala S, Ekblad LL, Tuisku J, Helin S, Johansson JJ, Laine H, et al. Association of early β-amyloid accumulation and neuroinflammation measured with [11C]PBR28 in elderly individuals without dementia. *Neurology.* (2021) 96:e1608–19. doi: 10.1212/WNL.0000000000011612

Conflict of Interest: AA has received compensation for consultancy and speaker related activities from UCB, Boehringer Ingelheim, General Electric, Britannia, AbbVie, Kyowa Kirin, Zambon, Bial, Theravance Biopharma, Roche, Medscape, Ever Pharma; he receives research support from Bial, Lundbeck, Roche, Angelini Pharmaceuticals, Horizon 2020—Grant 825785, Horizon2020 Grant 101016902, Ministry of Education University and Research (MIUR) Grant ARS01_01081, Cariparo Foundation. He serves as consultant for Boehringer–Ingelheim for legal cases on pathological gambling.

The remaining authors declare that the research was conducted in the absence of any commercial or financial relationships that could be construed as a potential conflict of interest.

Advantages of publishing in Frontiers

OPEN ACCESS
Articles are free to read for greatest visibility and readership

FAST PUBLICATION
Around 90 days from submission to decision

HIGH QUALITY PEER-REVIEW
Rigorous, collaborative, and constructive peer-review

TRANSPARENT PEER-REVIEW
Editors and reviewers acknowledged by name on published articles

Frontiers
Avenue du Tribunal-Fédéral 34
1005 Lausanne | Switzerland

Visit us: www.frontiersin.org
Contact us: frontiersin.org/about/contact

REPRODUCIBILITY OF RESEARCH
Support open data and methods to enhance research reproducibility

DIGITAL PUBLISHING
Articles designed for optimal readership across devices

FOLLOW US
@frontiersin

IMPACT METRICS
Advanced article metrics track visibility across digital media

EXTENSIVE PROMOTION
Marketing and promotion of impactful research

LOOP RESEARCH NETWORK
Our network increases your article's readership